



UNIVERSITAT^{DE}
BARCELONA

Denitrification in mountain lakes

Desnitrificación en lagos de montaña

Carlos Palacín Lizarbe



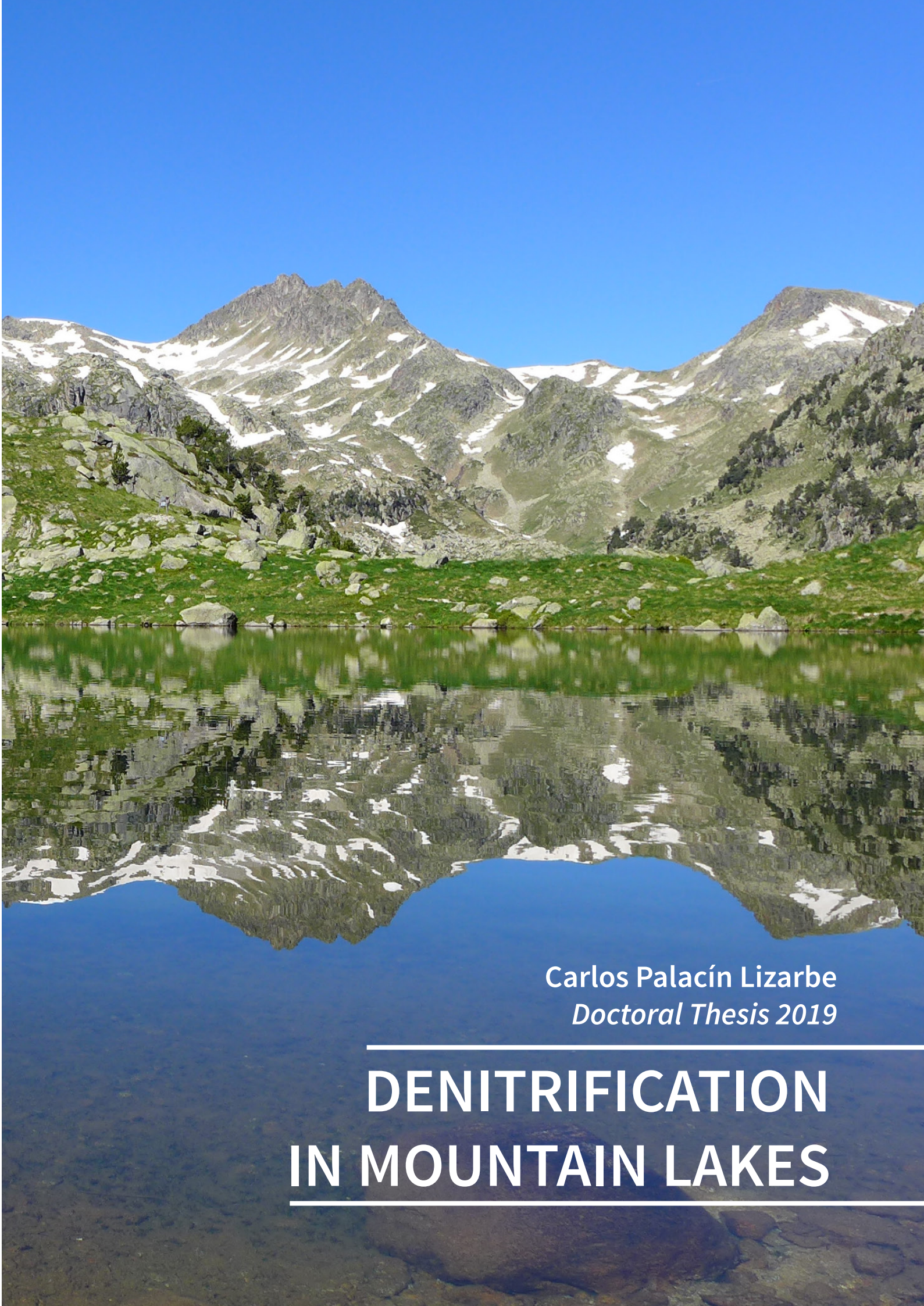
Aquesta tesi doctoral està subjecta a la llicència **Reconeixement 4.0. Espanya de Creative Commons.**

Esta tesis doctoral está sujeta a la licencia **Reconocimiento 4.0. España de Creative Commons.**

This doctoral thesis is licensed under the **Creative Commons Attribution 4.0. Spain License.**



DENITRIFICATION IN MOUNTAIN LAKES — Carlos Palacín Lizarbe — Doctoral Thesis 2019



Carlos Palacín Lizarbe
Doctoral Thesis 2019

DENITRIFICATION IN MOUNTAIN LAKES



UNIVERSITAT DE
BARCELONA



CSIC
CONSEJO SUPERIOR DE INVESTIGACIONES CIENTÍFICAS



CREAF

Tesis doctoral

Universitat de Barcelona
Facultat de Biologia
Departament de Biologia Evolutiva, Ecologia i Ciències Ambientals
Programa de doctorat en Ecologia, Ciències Ambientals i Fisiologia Vegetal

DENITRIFICATION IN MOUNTAIN LAKES

Desnitrificación en lagos de montaña

Memoria presentada por Carlos Palacín Lizarbe para
optar al título de Doctor por la Universitat de Barcelona.

Centre de Reserca Ecològica i Aplicacions Forestals (CREAF)
Consejo Superior de Investigaciones Científicas (CSIC)

Carlos Palacín Lizarbe
Barcelona, Junio 2019

El director de la tesis

Dr. Jordi Catalan Aguilà
Profesor de investigación, CSIC

La tutora de la tesis

Dra. Marisol Felip Benach
Profesora agregada, UB

Cover: Plan Lake. Photograph by Marc Sala Faig.

Dessing: Ana Palacín Lizarbe

Print & Layout: DESCONTROL Editorial i imprenta, SCCL.

Palacín Lizarbe, Carlos (2019) Denitrification in mountain lakes. PhD Thesis, Universitat de Barcelona.

159 pages.

A mi familia
y a ti, por leerme.

“El gran libro, siempre abierto y que hay que esforzarse en leer, es el de la naturaleza.”

Antoni Gaudí

Agradecimientos - Acknowledgments

Todo empezó en el 2011 cuando Pau me dijo que el grupo de investigación de los lagos del Pirineo estaba buscando un nuevo alumno de doctorado. Afortunadamente convencí a Jordi y me embarqué en este largo, intenso y complejo viaje que ha resultado ser esta Tesis, con una productiva estancia en Uppsala y pasando por distintos centros de Cataluña (CRAM-UB, CEAB-CSIC y CREAM).

Gracias Jordi por tu paciencia, y por compartir tu extensa sabiduría. Pau y Marc gracias por los consejos y por vuestra amistad, tengo muy gratos recuerdos en momentos de muestreo, en la caseta del Redó, o en el CRAM. Lluís, tú también me has enseñado mucho, sobretodo en la etapa inicial: cómo muestrear en montaña, cómo tener inventiva en el laboratorio... Al leer una cita de Ramón Margalef: *Un ecòleg ha de saber collar un cargol amb un martell i clavar un clau amb un tornavís*, siempre me acuerdo de tu inventiva, eres un auténtico crack. Sin ti no podría haber realizado las estimas de las tasas de desnitrificación. Continuando con la gente del CRAM, gracias Berta por los ratos en los descansos que amenizaban jornadas maratonianas... gracias Rober por tu ayuda en el campo, y por tus consejos de ski de montaña que mejoraron algo mi rudimentario estilo. Gracias Marisol por la ayuda tanto en el CRAM como en la UB. En general gracias por el magnífico ambiente de trabajo del CRAM. Gracias también a todos aquellos que me acompañaron, muchos de forma desinteresada, en los muestreos de campo. Gracias Rudu, Anahí, Chapas, Fran, Oscar, Aníbal, y un largo etcétera por los buenos momentos bajando Fallas, en los conciertos del local de Diablos, y en las salidas de ski.

Muchas gracias a los de Blanes (Sara, Rudi, Cèlia, Ibor, Magda, Vicente, Matheus, Carla) por las meriendas, las risas, y las birras... y a Xavi por las rutas de BTT. Gracias a la gente del grupo de eco microbiana por sus enseñanzas, llegué al CEAB siendo un incipiente limnólogo pero un completo ignorante de ecología molecular. María y Stefi gracias por vuestras enseñanzas en el laboratorio sobre extracción de DNA y qPCR. Joan gracias por tus enseñanzas sobre bioinformática. Y gracias a Carlos Ribera por las enseñanzas sobre LOI y R.

My stay at the SLU in Uppsala greatly improve the level of this Thesis, and also my molecular skills and my general knowledge about the nitrogen cycle. Sara and Chris, thank for giving me the opportunity to meet your group and for sharing your expert knowledge with me. In Uppsala, despite the intense lab work, I also have great memories with German, Caro, Lea, Louis, Jaanis and Tina drinking beers in the Nations, climbing in nature, dancing in the cultures carnival, and watching football.

El ambiente de trabajo en el CREAM también ha sido muy bueno. Nada más llegar, recuerdo el viaje a Urdiaín y a la sagardotegi, allí conocí a mucha gente del CREAM, Aitziber gracias por organizarlo. Gracias a la gente del despacho, Aitziber, Irene, Ferran por la compañía y afecto. Gracias a los futboleros tengo grandes recuerdos de las pachangas. Gracias a los de Cerdanyola Carlos Hernández, Xavi, Daijun, Jordi, por las birras en el irlandés y por las rutas en bici hasta la desembocadura del Besós. Victor gracias por tu ayuda impagable con el R.

Gracias a mi familia, Merche, Manuel, Ana y Carol, por el apoyo mas firme y continuado. Carol recuerdo cuando te conocí en Viu, sigues a mi lado y eso me hace ser muy feliz. Gracias también a Cari, a Miro y a Oscar por los buenos ratos en Mataró, en San Esteban y en Pont. Gracias Ana por maquetar la tesis.

Son muchas las personas que han hecho posible este trabajo, a todos ellos muchas gracias.

Barcelona, 3 de Junio de 2019

He tenido el apoyo económico de una Beca FPU del Ministerio de Educación, Cultura y Deporte (FPU12-00644) y de la prestación por desempleo del SEPE. Una beca de movilidad de la Asociación Ibérica de Limnología para asistir a un congreso. Agradezco a Marisol Felip el contrato de 2018. Parte de mi investigación ha sido financiada por proyectos del Ministerio de Economía y Competitividad: NitroPir (CGL2010-19737), Lacus (CGL2013-45348-P), Transfer (CGL2016-80124-C2-1-P).

Informe del director

El Dr. Jordi Catalán Aguilà, profesor de investigación del Consejo Superior de Investigaciones Científicas (CSIC), director de la Tesis Doctoral elaborada por Carlos Palacín Lizarbe y que tiene como título “Denitrification in mountain lakes”.

INFORMA

Que los trabajos de investigación llevados a cabo por Carlos Palacín Lizarbe como parte de su formación pre-doctoral e incluidos en su tesis doctoral han dado lugar a tres artículos publicados, y un manuscrito adicional a punto de ser enviado a una revista científica de ámbito internacional. A continuación se detalla la lista de artículos publicados, así como los índices de impacto (según el SCI y la ISI Web of Knowledge) de las revistas dónde han estado publicados los trabajos.

- I. Palacin-Lizarbe C, Camarero L, Hallin S, Jones CM, Cáliz J, Casamayor EO, and Catalan J (2019). The DNRA-denitrification dichotomy differentiates nitrogen transformation pathways in mountain lake benthic habitats. *Frontiers in Microbiology*. <https://doi.org/10.3389/fmicb.2019.01229>

El índice de impacto de la revista *Frontiers in Microbiology* en el 2017 fué de 4,019. Esta revista está situada en el primer cuartil de la categoría “Microbiology”.

- II. Palacin-Lizarbe, C., Camarero L., and Catalan J (2018). Estimating sediment denitrification rates using cores and N₂O microsensors. *Journal of Visualized Experiments* (142), e58553. <https://doi.org/10.3791/58553>

El índice de impacto de la revista *Journal of Visualized Experiments* en el 2017 fué de 1,184. Esta revista está situada en el segundo cuartil de la categoría “Multidisciplinary Sciences”.

- III. Palacin-Lizarbe C., Camarero L., and Catalan J. (2018). Denitrification temperature dependence in remote, cold, and N-poor lake sediments. *Water Resources Research* 54, 1161-1173. <https://doi.org/10.1002/2017WR021680>

El índice de impacto de la revista *Water Resources Research* en el 2017 fué de 4,361. Esta revista está situada en el primer cuartil de las categorías “Environmental Sciences”, “Limnology” y “Water Resources”.

Al mismo tiempo, el director CERTIFICA

Que el Sr. Carlos Palacín Lizarbe ha participado activamente en el desarrollo de los trabajos de investigación asociados a cada uno de estos artículos, así como en su elaboración. Concretamente, su participación en cada uno de los artículos ha sido la siguiente:

- Participación en el planteamiento inicial de los objetivos de cada uno de los artículos, los cuales han estado enmarcados en 2 proyectos nacionales (NITROPIR y LACUS).
- Participación en todas las campañas de recogida de muestras asociadas a cada artículo.
- Participación en el diseño y desarrollo de la parte experimental de cada estudio, y puesta a punto de los métodos de campo y de laboratorio asociados a todos los experimentos. Concretamente, parte de los análisis moleculares de los gremios transformadores de nitrógeno — PCR cuantitativas de distintos genes funcionales del metabolismo del Nitrógeno y secuenciación de las regiones V3-V4 del gen 16S rRNA — se realizaron durante una estancia de 4 meses en el laboratorio del “Soil Microbiology Group” liderado por de la catedrática Sara Hallin en la Universidad Sueca de Agronomía (SLU) en Uppsala, Suecia.
- Procesado y análisis de todas las muestras obtenidas, cálculo de resultados, análisis de datos y realización de modelos estadísticos asociados a cada artículo.
- Redacción de los artículos y seguimiento del proceso de revisión de todos los artículos publicados.

Finalmente, certifico que ningún coautor de los artículos anteriormente mencionados, y que forman parte de la Tesis Doctoral del Sr. Carlos Palacín Lizarbe han utilizado, ni tienen previsto utilizar, implícita o explícitamente estos trabajos para la elaboración de otra Tesis Doctoral.

Barcelona, 1 de Junio de 2019

Dr. Jordi Catalan Aguilà

Profesor de investigación, CSIC

List of publications

This thesis is based on the following articles referred in the text by Roman numerals:

- I. Palacin-Lizarbe C, Camarero L, Hallin S, Jones CM, Cáliz J, Casamayor EO, and Catalan J (2019). The DNRA-denitrification dichotomy differentiates nitrogen transformation pathways in mountain lake benthic habitats. *Frontiers in Microbiology*. <https://doi.org/10.3389/fmicb.2019.01229>
- II. Palacin-Lizarbe, C., Camarero L., and Catalan J (2018). Estimating sediment denitrification rates using cores and N₂O microsensors. *Journal of Visualized Experiments* (142), e58553. <https://doi.org/10.3791/58553>
- III. Palacin-Lizarbe C., Camarero L., and Catalan J. (2018). Denitrification temperature dependence in remote, cold, and N-poor lake sediments. *Water Resources Research* 54, 1161-1173. <https://doi.org/10.1002/2017WR021680>
- IV. Palacin-Lizarbe C, Camarero L, Hallin S, Jones CM, and Catalan J. Decoupling of denitrification rates and gene potentials in lake sediments of mountains affected by high atmospheric nitrogen deposition. (manuscript)

Abstract

The reservoir size and pathway rates of the nitrogen (N) cycle have been deeply modified by the human enhancement of N fixation, atmospheric emissions, and climate warming, doubling the reactive nitrogen (N_r) available in the biosphere. Denitrification transforms nitrate into nitrogenous gas and thus removes N_r back to the atmospheric reservoir. Across ecosystems, there is still rather limited knowledge of the denitrification rates and their relationships with environmental factors and the N-transforming guilds, particularly, for the abundant cold and N-poor freshwater systems.

The main goal of this thesis was to improve the current knowledge of denitrification in mountain lakes. In particular, we studied eleven pristine oligotrophic mountain lakes that have been affected by a high N deposition. The selected lakes showed a gradient of dissolved inorganic nitrogen in the water due to different lake productivity. We focused on spatial rather than in temporal variation, sampling during the ice-free period. Within lakes, we focused on the sediments because of their known higher denitrification rates than the water column. Specifically, we studied sediments near the deepest point of the lake, lithic biofilms from littoral cobbles, and littoral sediments from beds of isoetid and elodeid macrophytes, helophyte (*Carex rostrata*) belts, and rocky areas.

We aimed to measure the denitrification activity as similar as possible to *in situ* conditions, with this aim we used little disturbed sediment cores and *in situ* temperature for the denitrification rate measurements. We characterized the environment by including proximal (benthic) and more distal (lake) descriptors to capture potential drivers acting at different spatial scales. Denitrification is part of the N cycle, and other processes facilitate (e.g. nitrification) or compete (e.g. DNRA) with this pathway. Using molecular tools, we quantified the guilds involved in the main N-transformation pathways in benthic habitats (**article I**) and related them to the denitrification rates (**article IV**). We have also developed a method appropriate for estimating denitrification rates in any aquatic system with retrievable sediment cores (**article II**). Finally, we showed the interest of quantifying the temperature dependence of the process at different degrees of substrate limitation but within the range — or a beat above — the *in situ* substrate levels, instead of the typical quantification at substrate saturation (**article III**).

Following, there is a summary of the main findings. There is a complex N-transforming guild composition in benthic habitats of mountain lakes, which is deeply embedded in the overall prokaryotic community. These N-transforming guilds differ in the dominant pathway depending on the habitat and productivity of the lake, with the DNRA-denitrification dichotomy as the greatest differentiation (**article I**). The denitrification temperature dependence increases with nitrate limitation (**article III**). There is an average current denitrification rate of $1.5 \mu\text{mol N}_2\text{O m}^{-2} \text{h}^{-1}$ in the sediments of the Pyrenean lakes with higher activity in littoral than in the deep zones. The factors controlling current and potential denitrification rates differ. Current denitrification is controlled by the $\text{NO}_3^-/\text{NO}_2^-$ availability and secondarily by temperature; whereas potential denitrification is controlled by landscape productivity, the sulphate content, and the DNRA-denitrification (*nrfA-nirS*) competition (**article IV**).

The best candidate drivers, i.e. temperature, organic matter quantity and quality, and spatio-temporal redox conditions affecting the overall prokaryotic community and the N-transforming guilds are discussed. The estimated denitrification rates are compared to other mountain lake sediments, discussing the spatial variations, the controls, and the methods used. Finally, some unsolved questions of the N cycle in mountain lakes are discussed.

Overall this thesis contributes to increasing the knowledge of denitrification and other processes of the N cycle. The findings are probably not restricted only to mountain lakes encompassing other oligotrophic and remote ecosystems.

Keywords: Biogeochemistry, Nitrogen cycle, Limnology, Microbial ecology, Molecular ecology.

Resumen

El ciclo del nitrógeno (N) ha sido profundamente modificado por la fijación industrial de N, el aumento de emisiones, y el calentamiento global, doblando el nitrógeno reactivo (N_r) disponible en la biosfera. La desnitrificación transforma el nitrato en gases nitrogenados eliminando N_r del sistema. Hay un conocimiento muy limitado de las tasas de desnitrificación, así como de los gremios microbianos implicados en la transformación de N, especialmente en sistemas oligotróficos de aguadulce.

El principal objetivo de esta tesis es ampliar el conocimiento actual de la desnitrificación en lagos de montaña. Para ello, se estudiaron once lagos oligotróficos afectados por una alta deposición de N, que muestran un gradiente de nitrógeno inorgánico disuelto debido a una diferente productividad dentro de la oligotrofia. Concretamente se estudiaron los sedimentos del punto más profundo del lago, las bio-películas de las piedras litorales, y los sedimentos litorales de las áreas rocosas, de los cinturones de *Carex rostrata*, y de los lechos de macrófitas isoétidas y elodéidas.

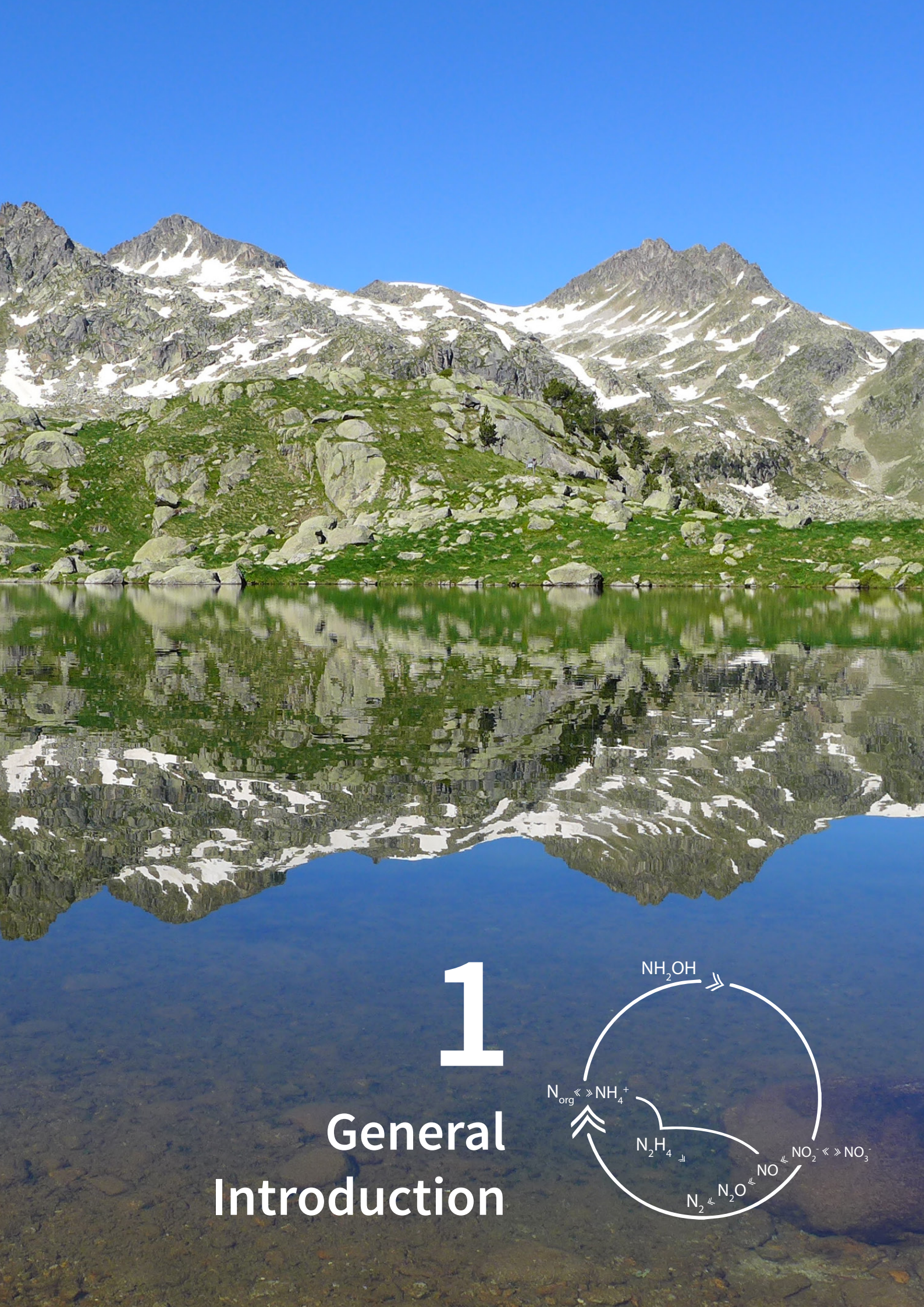
Se ha encontrado una compleja composición de gremios transformadores de N profundamente arraigada en la comunidad procariota general de los hábitats bentónicos. La ruta dominante de transformación de N cambia dependiendo del hábitat y la productividad del lago con la dicotomía DNRA-desnitrificación como mayor diferencia, con una dominancia de los desnitrificantes reductores de nitritos (*nirS*) en las capas superficiales de los sedimentos de los lagos someros, más cálidos y productivos. También una creciente dependencia de la temperatura en la desnitrificación al aumentar la limitación de nitratos. Se ha estimado una tasa promedio de desnitrificación de $1.5 \mu\text{mol N}_2\text{O m}^{-2} \text{h}^{-1}$ en los sedimentos de los lagos pirenaicos, con mayor actividad en la zona litoral que en la profunda. Diferentes variables controlan las tasas de desnitrificación actuales y potenciales; las primeras están controladas por la disponibilidad de nitratos y secundariamente por la temperatura, las potenciales están controladas por la productividad del sistema, el contenido de sulfatos y la competencia DNRA-desnitrificación (*nrfA-nirS*).

Esta tesis contribuye a aumentar el conocimiento del ciclo del N, y probablemente, los resultados obtenidos son extrapolables a otros ecosistemas oligotróficos y de áreas remotas.

Table of contents

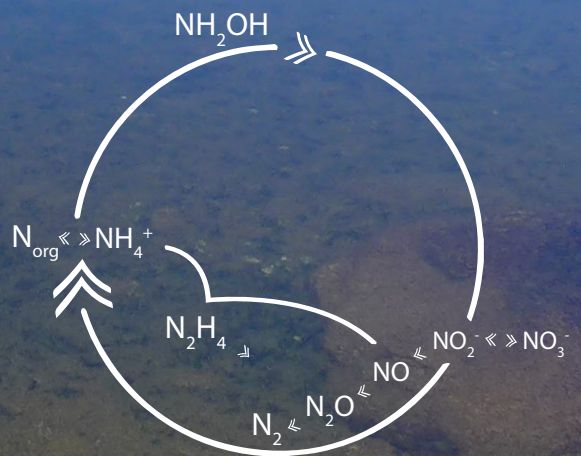
1. General introduction	25
1.1. Anthropogenic alteration of the nitrogen cycle	25
1.2. Mountain lakes as sensors of the global change.....	26
1.3. Denitrification types and steps.....	27
1.4. Nitrogen cycle processes that facilitate or compete with denitrification	29
1.5. Denitrification is a particularly difficult process to be measured	31
1.6. Denitrification in inland waters	33
2. Objectives	37
3. Article I	41
The DNRA-denitrification dichotomy differentiates nitrogen transformation pathways in mountain lake benthic habitats	
3.1. Abstract.....	41
3.2. Introduction	42
3.3. Materials and methods.....	44
3.4. Results	48
3.5. Discussion.....	55
3.6. Conclusions	58
4. Article II.....	63
Estimating sediment denitrification rates using cores and N ₂ O microsensors	
4.1. Short abstract	63
4.2. Long abstract	63
4.3. Introduction	64
4.4. Protocol.....	67
4.5. Representative results.....	74
4.6. Discussion.....	76
5. Article III.....	83
Denitrification temperature dependence in remote, cold and N-poor lake sediments	
5.1. Abstract.....	83
5.2. Introduction	84

5.3. Materials and methods.....	87
5.4. Results	91
5.5. Discussion.....	95
5.6. Conclusions	99
6. Article IV.....	103
Decoupling of current denitrification rates from gene potentials in lake sediments of mountains affected by high atmospheric nitrogen deposition	
6.1. Abstract.....	103
6.2. Introduction	104
6.3. Materials and methods.....	107
6.4. Results	111
6.5. Discussion.....	116
7. General discussion	121
7.1. Nitrogen cycle in mountain lakes: nitrogen-transforming guilds.....	121
7.2. Denitrification: spatial variation and drivers in mountain lake sediments	127
7.3. Unsolved questions of the nitrogen cycle in mountain lakes	130
8. Conclusions.....	135
References	139
Supplementary material	163
Appendix A. Table S.1. Sediments and water descriptors by sediment habitat	164
Appendix B. Publications of the present dissertation.....	167



1

General Introduction



1. General introduction

1.1. Anthropogenic alteration of the nitrogen cycle

In the last 150 years, nitrogen (N) has gone from being a limiting element in the biosphere to being an environmental problem due to its excess (Galloway *et al.* 2008). There is abundant N in the atmosphere, but in the form of N_2 , an inert gas unavailable for most organisms, except a few able to fix it into the so-called reactive nitrogen (N_r), which includes all the N compounds supporting biotic growth (Galloway *et al.* 2003). Human activities have at least doubled the levels of N_r available in the biosphere, largely as a result of the fertilizer production by chemical N_2 fixation, agricultural enhancement of plants with a symbiotic capacity of N_2 fixation, and fossil fuel burning (Erisman *et al.* 2011). According to the planetary boundaries framework (Rockstrom *et al.* 2009, Steffen *et al.* 2015), anthropogenic alteration of the N cycle is one of the major challenges facing the Earth system.

Naturally available N_r is produced mainly by lightning, wildfires and biological N_2 fixation (Fields 2004). The Haber-Bosch process is an artificial N_2 fixation process and is the main industrial procedure for the production of ammonia, mainly used for synthetic N_r fertilizers (Schlesinger 2013). The process converts N_2 to ammonia (NH_3) by a reaction with hydrogen (H_2) using a metal catalyst under high temperature and pressure (Smil 2001). Around half of the world's population is fed with food produced through the use of synthetic fertilizers (Erisman *et al.* 2008). Additionally, farmers increasingly introduced leguminous crops in their crop rotations, thereby enhancing N_r input to agricultural systems via biological N_2 fixation (Graham and Vance 2003). Ammonia dominates the N_r emissions from agriculture (Galloway *et al.* 2008). Furthermore, humans create N_r accidentally through fossil-fuel combustion emitting nitrogen oxides by industry, transport and energy sectors (Erisman *et al.* 2011).

The anthropogenic excess of N_r results in serious environmental problems, e.g. eutrophication and climate change (Erisman *et al.* 2011). Circulation of anthropogenic N_r in Earth's atmosphere, hydrosphere, and biosphere has a wide variety of consequences, which may be magnified with time as N_r moves through its biogeochemical cycle. The same N_r atom can cause multiple effects across Earth ecosystems and on human health until it is converted back to nonreactive N_2 , the so-called *Nitrogen Cascade* (Galloway *et al.* 2003).

1.2. Mountain lakes as sensors of the Global Change

In the context of Global Change, remote ecosystems — defined as being mainly affected by atmospheric processes rather than the direct human activity in the catchment — can be particularly informative about potential large-scale changes in the Earth system (Catalan *et al.* 2013), being considered informative sensors of Global Change (Smol 2012). The excess of N_r has atmospherically reached remote ecosystems. As a consequence of the increased N_r emissions, atmospheric transport and subsequent deposition has become the dominant distribution process of N_r on the Earth (Galloway *et al.* 2008). N_r deposition to ecosystems has increased from $\sim 0.5 \text{ kg N ha}^{-1} \text{ year}^{-1}$ — or even less in pristine conditions — to rates that are greater than one order of magnitude nowadays, exceeding $10 \text{ kg N ha}^{-1} \text{ year}^{-1}$ on average in large areas of the world (Camarero 2017). Alpine lakes of the Northern hemisphere and subarctic regions are examples of remote ecosystems that have been exposed to increased N_r deposition during the last decades (Holtgrieve *et al.* 2011, Camarero 2017), triggering a nutrient imbalance in these freshwater systems which are otherwise known to have low nutrient availability (Catalan *et al.* 2006). Overall, mountain lakes are good sites to study the effects of large-scale increasing N_r availability in pristine freshwater N-poor ecosystems.

The Pyrenean Lake district with 1062 lakes ($>0.5 \text{ ha}$) in a relatively small area, $\sim 270 \text{ km}$ in a straight line separates the westernmost lake near the Mesa de los tres reyes peak and the easternmost lake near the Canigou peak, being a “natural laboratory” that allows for the study of the effects of several environmental gradients (e.g. altitude, bedrock type, lake size, productivity) in relatively pristine mountain lakes (Catalan *et al.* 2006). Most of the lakes have a glacial origin and are dimictic, i.e. have two longer periods of water-column stratification in summer and winter with two faster periods of mixing between them (Catalan *et al.* 2006). The low rock weathering and limited soil development result in highly diluted waters, both in major salt components and nutrients (Catalan *et al.* 2006). The Pyrenean Lakes shows different productivity within the general oligotrophy: simplifying, smaller lakes at lower altitudes are the more productive ones (Catalan and Fee 1994). In general, more productive oligotrophic mountain lakes exhibit low dissolved inorganic nitrogen (DIN) concentrations due to higher consumption of N excess of the atmospheric loading by primary producers (Camarero and Catalan 2012). According to the total phosphorus (TP) more than 70 % of the lakes are ultraoligotrophic ($TP < 4.7 \mu\text{g L}^{-1}$), 22 % oligotrophic ($4.7 < TP < 9.3 \mu\text{g L}^{-1}$) and 6 % mesotrophic ($9.3 < TP < 31 \mu\text{g L}^{-1}$) (Catalan *et al.* 2006). Despite the general oligotrophy, warming (Catalan *et al.* 2002a, Catalan *et al.* 2014) and the increased N_r and phosphorus (P) deposition are causing incipient eutrophication of Pyrenean Lakes (Camarero 2017).

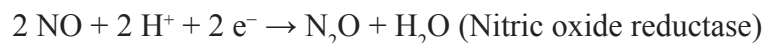
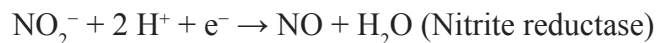
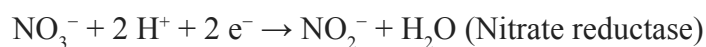
In this thesis, eleven lakes were sampled in the central Pyrenees near or within the Aigüestortes and Estany de Sant Maurici National Park. The studied lakes are ultraoligotrophic except Bassa de les Granotes, which is classified as oligotrophic (Catalan *et al.* 1993), with a circumneutral pH (~ 7) (Vila-Costa *et al.* 2014). The studied lake basins are on granodioritic bedrock of the Maladeta batholiths; however, those lakes located in large catchments, especially the Llebreta Lake, receive some runoff influence from other lithologies (Zwart 1979, Arranz 1997). The atmospheric N load from bulk deposition in the central Pyrenees in 2010 was c. $10 \text{ kg N ha}^{-1} \text{ year}^{-1}$, matching the global average (Camarero 2017). The N deposition in the Pyrenees consists of ammonium and nitrate in similar proportion (Camarero and Catalan 1993, 1996).

1.3. Denitrification types and steps

Denitrification is the microbial activity by which nitrogenous oxides, mainly nitrate and nitrite, are reduced to dinitrogen gasses, N_2O and N_2 (Tiedje 1988). Denitrification originally described a phenomenon, i.e., the loss of N_r from the viewpoint of the N balance (Zumft 1997). This *sensu lato* denitrification is nowadays used in the literature as nitrate removal, including denitrification (*sensu stricto*), nitrate assimilation, dissimilatory nitrate reduction to ammonium (DNRA), and anaerobic ammonium oxidation (anammox). Hereafter, I refer to denitrification with the *sensu stricto* meaning.

Even denitrification *sensu stricto* includes several types of mechanisms that convert nitrogen oxides to dinitrogen gases (Tiedje 1988). Respiratory denitrification is the microbial oxidation of organic matter in which nitrogenous oxides are the terminal electron acceptor (Seitzinger *et al.* 2006), a heterotrophic anaerobic process, and is the classical mechanisms that microbiologist typically refer to as denitrification (Tiedje 1988). Autotrophic denitrification includes the microbial nitrate reduction coupled to sulfur or iron oxidation (Zopfi *et al.* 2001, Weber *et al.* 2006, Burgin and Hamilton 2007). Codenitrification produces N_2O and N_2 through the reduction of nitrite (NO_2^-) by other nitrogen compounds, including azide, ammonium (NH_4^-), salicylhydroxamic acid, and hydroxylamine (H_3NO) (Tanimoto *et al.* 1992, Spott and Florian Stange 2011). Fungi (Tanimoto *et al.* 1992) and bacteria (Kumon *et al.* 2002) perform this process, being relevant in soils (Laughlin and Stevens 2002, Long *et al.* 2013). The term chemodenitrification is used to describe some N-gas-generating reactions catalyzed by abiotic agents (Tiedje 1988, Zhu-Barker *et al.* 2015). Since nitric oxide (NO) is a minor product of biological denitrification, its occurrence can be used as a preliminary indication of chemodenitrification (Tiedje 1988).

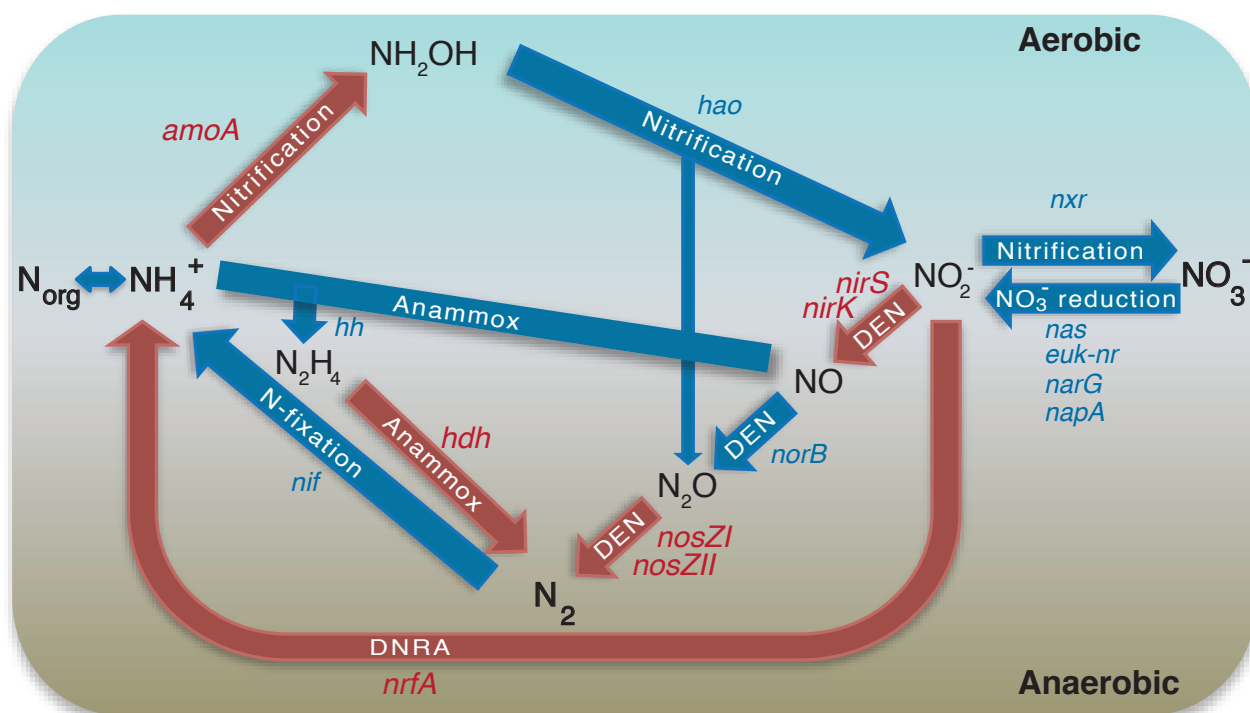
The complete denitrification (pathway) consists of four redox reactions (steps). These are the following half-reactions, with the enzyme catalysing the reaction in parentheses:



The complete process can be expressed as a net balanced redox reaction:



In the last decades, the use of molecular tools has enabled to assess the density and diversity of denitrifying bacteria (Philippot 2002, Philippot and Hallin 2005). Especially studying the genes encoding the catalytic subunit of the denitrifying reductases, e.g. *narG*, *napA*, *nirS*, *nirK*, *norB* and *nosZ* (Fig. 1.1). Different organisms perform nitrate reduction to nitrite. It can be part of the dissimilatory metabolism, e.g. denitrification, and then the reaction is catalyzed by enzymes with different cellular location, in the membrane or in the periplasm (encoded by the genes *narG* or *napA*, respectively), or be part of the assimilatory metabolism of prokaryotes or eukaryotes (Canfield *et al.* 2010).



<i>Genes</i> Enzymes		
<i>amo</i>	ammonium monooxygenase	
<i>hao</i>	hydroxylamine oxidoreductase	
<i>nxr</i>	nitrite oxidoreductase	
<i>hdh</i>	hydrazine dehydrogenase	
<i>hh</i>	hydrazine hydrolase	
<i>nif</i>	nitrogenase, various kinds	
<i>nas</i>	cytoplasmic, prokaryote-assimilatory	nitrite reductases:
<i>euk-nr</i>	cytoplasmic, eukaryote-assimilatory	<i>nirS</i> cytochrome- <i>cd1</i>
<i>narG</i>	membrane bound-dissimilatory	<i>nirK</i> copper-based
<i>napA</i>	periplasmic-dissimilatory	<i>nrf</i> formate-dependent
		<i>norB</i> nitric oxide reductase
		<i>nosZ</i> nitrous oxide reductase

Figure 1.1. Major biological nitrogen transformation pathways and genes that encode the enzymes catalysing the reaction [adapted from (Canfield *et al.* 2010)]. In red, the genes and related reactions accounted for in this thesis.

The next denitrification step, the reduction of NO_2^- to NO is catalysed by either a copper- or haem-dependent dissimilatory nitrite reductase, encoded by the *nirK* or *nirS* genes, respectively (Zumft 1997). These two nitrate reductases were long considered mutually exclusive and functionally redundant, although recent findings challenge this assumption. Both nitrite reductases are not always exclusive as both were found in 10 of 652 denitrifiers' genomes (Graf *et al.* 2014), and its joint expression has been demonstrated in *Pseudomonas stutzeri* (Wittorf *et al.* 2018). The two NO -forming nitrite reductases show different expression patterns and denitrification activity phenotypes suggesting functional differences (Wittorf *et al.* 2018), which is consistent with results of different habitat preferences and niche partitioning between organisms harbouring either *nirS* or *nirK* in various environments (e.g. (Desnues *et al.* 2007, Enwall *et al.* 2010, Yuan *et al.* 2012)).

Several nitric oxide reductases catalyse the NO reduction to nitrous oxide (N_2O). There is a fungal enzyme encoded by the gene *p450nor* (Higgins *et al.* 2016) and several prokaryotic enzymes (Hendriks *et al.* 2000, Zumft 2005). In bacteria, the reaction could serve to bioenergetic purposes (e.g. denitrification) or to detoxifying (e.g. found in non-denitrifying pathogens (Hendriks *et al.* 2000)).

The last step of denitrification is the N_2O reduction to di-nitrogen (N_2). It is catalysed by the nitrous oxide reductase, which is encoded by the *nosZ* gene (Zumft 1997), and is the only known sink for N_2O . The *nosZ* clade 2 (also called atypical *nosZ*, and hereafter, *nosZII*), recently discovered (Sanford *et al.* 2012, Jones *et al.* 2013), enhanced the taxonomic diversity of N_2O reducers, being important in determining the soil N_2O sink capacity (Jones *et al.* 2014).

Intergenomic comparisons highlight the modularity of the denitrification pathway (Graf *et al.* 2014). A large part of the *nirK* organisms has a truncated pathway lacking the *nor* gene, and a majority do not have *nosZ*. By contrast, most of the *nirS*-type denitrifiers also have the *nosZ* gene and, even more, also have *nor* gene. Furthermore, an important fraction of *nosZII* prokaryotes does not have any other denitrification gene (Graf *et al.* 2014), while some also harbour the *nrfA* gene encoding the gene catalysing the DNRA nitrite reduction (Fig. 1.1, (Sanford *et al.* 2012)). Some authors have introduced the term chemodenitrifier for organisms that perform complete denitrification through the combination of biotic and abiotic reactions (Onley *et al.* 2018). It remains unknown the relative contribution of these organisms to the entire N_r removal. Overall, it is worth to remark the modularity of the denitrification pathway.

1.4. Nitrogen cycle processes that facilitate or compete with denitrification

Nitrogen has up to nine oxidation states enabling a high diversity of N-compounds (Table 1.1). The degree of anoxia determines the abundance of these compounds, the electron availability (Stein and Klotz 2016), and eventually determine which processes of the N cycle occur (e.g. nitrification only occur in aerobic conditions, Fig. 1.1).

Table 1.1. Nitrogen compounds

Molecule	Name	Oxidation state
C-NH ₂	Organic-N	
NH ₃ , NH ₄ ⁺	Ammonia, Ammonium	-3
N ₂ H ₄	Hydrazine	-2
NH ₂ OH	Hydroxylamine	-1
N ₂	Dinitrogen	0
N ₂ O	Nitrous oxide	+1
NO	Nitric Oxide	+2
HNO ₂ , NO ₂ ⁻	Nitrous acid, Nitrite	+3
NO ₂	Nitrogen dioxide	+4
HNO ₃ , NO ₃ ⁻	Nitric acid, Nitrate	+5

Nitrification is an oxidation process including three reactions (Fig. 1.1): 1) The ammonia oxidation to hydroxylamine, 2) the conversion of hydroxylamine to nitrite, and 3) the nitrite oxidation to nitrate. The first two reactions are performed by bacteria and archaea – hereafter, ammonia oxidizer bacteria (AOB) and archaea (AOA) –, while the third is only performed by bacteria – hereafter, nitrite oxidizer bacteria (NOB). The complete process in a single organism (complete ammonia oxidation; comammox) has been recently demonstrated, being a capacity restricted to members of the genus *Nitrospira* (Daims *et al.* 2015, Van Kessel *et al.* 2015). Ammonia oxidation to hydroxylamine is the rate-limiting step process, and the gene encoding for the subunit A of the ammonia monooxygenase (*amoA*) catalysing this reaction has been the most used molecular marker for nitrification (e.g. (Rotthauwe *et al.* 1997, Tourna *et al.* 2008)).

Nitrification is an important source of NO₃⁻/NO₂⁻ to denitrification, especially in oligotrophic aquatic ecosystems with steep redox gradients (Seitzinger *et al.* 2006). The coupling between the two processes can occur within the same nitrifier organism or between distinct microorganisms. Nitrifier denitrification is a process carried out by ammonia oxidizers while in the canonical coupled nitrification-denitrification the denitrifiers use the nitrifier products (Wrage-Mönnig *et al.* 2018).

N₂O is a greenhouse gas with a global warming potential 310 times greater than that of the equivalent amount of CO₂ (Lashof and Ahuja 1990) and promotes ozone destruction in the stratosphere (Ravishankara *et al.* 2009). Several processes generate N₂O. However, denitrification and ammonia oxidation to nitrate (the first step of nitrification) are the primary N₂O generator processes (Butterbach-Bahl *et al.* 2013, Hallin *et al.* 2018). Denitrifiers may not always perform complete denitrification, resulting in the formation of N₂O as terminal product either because they lack the genetic capacity for N₂O reduction (e.g. fungi (Maeda *et al.* 2015)) or because environmental factors suppress the reaction (Firestone *et al.* 1980, Hallin *et al.* 2018). In a recently discovered denitrification, a methanotrophic bacterium, *Candidatus Methyloirabilis oxyfera*, consumes methane (another greenhouse gas) as a source of energy, reducing agent and carbon (C), and reduces NO₂⁻ to N₂ by

expressing a nitric oxide dismutase (Ettwig *et al.* 2010). This enzyme dismutates two NO molecules to O₂ and N₂ without producing N₂O; the O₂ produced is then used by this bacterium to oxidize methane to methanol, being a “denitrifying intra-oxygenic methanotroph”.

Some processes compete with denitrification using the same N compounds. The dissimilatory nitrate reduction to ammonium (DNRA, Fig. 1.1) is a fermentative anaerobic process that uses nitrate/nitrite as electron acceptor competing with denitrification (Tiedje 1988). The C/N ratio, pH, nitrite versus nitrate concentration, availability of fermentable C compounds, temperature and sulfide concentration, are potentially important environmental controls on this competition, with the former supposed to be the most important control (Tiedje 1988, Kraft *et al.* 2014). Yoon *et al.* (2015) investigated the switch between the two processes in a single microbial model, *Shewanella loihica*, capable of performing the two pathways. They found an equal contribution of the two processes at a C/N of 7.5, and warm temperatures favouring DNRA. The dissimilatory pathway (DNRA) is regulated by oxygen and is unaffected by ammonium, while the opposite is true of assimilatory reduction. DNRA prokaryotes are generally strictly anaerobes while denitrifiers are mainly facultative, so denitrifiers are more competitive in environments with fluctuating oxygen levels (Brunel *et al.* 1992, Wittorf *et al.* 2016, Chen *et al.* 2017a). In more constant anaerobic environments where the limitation of electron acceptors (e.g. NO₃⁻/NO₂⁻) often restricts metabolism, DNRA consumes more electrons than denitrification (8 vs 5) per mol of NO₃⁻, and slightly more energy is gained (Strohm *et al.* 2007). Probably the DNRA dominance at higher temperatures is related to higher reducing conditions.

Until recently, it was generally believed that ammonium could be activated only with molecular oxygen and that N_r could be lost only as N₂ through denitrification (Kuypers *et al.* 2018). The discovery of anaerobic ammonium oxidation (anammox, Fig. 1.1) to N₂ with nitrite as the terminal electron acceptor overturned both of these dogmas (Mulder *et al.* 1995, Strous *et al.* 1999). Anammox, as DNRA, compete with denitrification due to the use of nitrite as an electron acceptor.

1.5. Denitrification is a particularly difficult process to be measured

Despite the importance of the N cycle in the Earth, there are still large uncertainties regarding how the global N cycle is evaluated. A few flux estimates have been quantified with less than ±20% error, and many have uncertainties of ±50% and larger (Gruber and Galloway 2008). These uncertainties indicate the need for accurate estimations of denitrification rates across ecosystems and an understanding of the underlying mechanisms of variation. The pathway is highly relevant to the biosphere availability of N_r because it is the primary process of removal (Seitzinger *et al.* 2006).

Denitrification is particularly difficult to measure (Groffman *et al.* 2006). There are several alternative approaches and methods, each with advantages and disadvantages. Drawbacks to available methods

include their use of expensive resources, insufficient sensitivity, and the need to modify the substrate levels or alter the physical configuration of the process using disturbed samples (Groffman *et al.* 2006). There exist strictly methodological issues, e.g. the main challenge is to measure N_2 due to its elevated background levels in the environment (Groffman *et al.* 2006). The acetylene (C_2H_2) inhibition is the most commonly applied method to measure denitrification (Groffman *et al.* 2006), is based in the ability of C_2H_2 to inhibit the reduction of N_2O to N_2 (Yoshinari and Knowles 1976, Hynes and Knowles 1978). Thus, denitrification can be quantified by measuring the accumulated N_2O in the presence of C_2H_2 , which is feasible due to low environmental N_2O levels. The most critical problem of the method is that C_2H_2 partially inhibits the production of NO_3^- via nitrification (Hynes and Knowles 1978, Wrage *et al.* 2004), underestimating the denitrification rates (Mengis *et al.* 1997b), especially in oligotrophic ecosystems with small and/or dynamic NO_3^- pools (Seitzinger *et al.* 1993).

Denitrification dynamics is another challenge; the process can be episodic and spatially heterogeneous with hot spots and hot moments (Parkin 1987, Groffman *et al.* 2009) because of the fluctuations in resources (e.g., nitrate) and conditions (e.g., temperature), but also because it is a facultative microbial process, alternative to the more energetically beneficial heterotrophic aerobic respiration.

As mentioned before the use of molecular tools has enabled to assess the density and diversity of denitrifying bacteria (Philippot 2002, Philippot and Hallin 2005). However, protein-encoding gene abundance and community structure failed frequently to predict the corresponding process activity (Rocca *et al.* 2015), especially when assessing denitrification (Bowen *et al.* 2014, Graham *et al.* 2016), despite bias amplification does not seem a big problem (at least for *nirS* and *nirK* (Bonilla-Rosso *et al.* 2016)). Similarly, taxonomic classification does not necessarily predict functioning, as different prokaryotic traits may be conserved at different phylogenetic depths (Martiny *et al.* 2015). While ammonia oxidation and anammox capacities are restricted to only a few lineages, denitrification and DNRA are widely distributed across the phylogeny (Graf *et al.*, 2014; Welsh *et al.*, 2014). Denitrifiers are found among bacteria, archaea and eukaryotes (fungi (Kobayashi and Shoun 1995) and foraminifer (Risgaard-Petersen *et al.* 2006)). Although foraminifer denitrification mechanism and genes are unknown, and the process could be performed by its endobiont bacteria (Bernhard *et al.* 2012). Furthermore, the facultative character of most prokaryotic denitrifiers it is an extra difficulty to use taxonomic classification or functional gene abundance as proxies of denitrification activity (Graham *et al.* 2016).

Overall explain the high uncertainties in the denitrification rates; also what controls the rates *in situ* is only moderately understood because the abundance and function of denitrifying organisms are difficult to determine (Philippot and Hallin 2005), largely because of the wide array of microorganisms capable of this function, and environmental conditions that influence rates are not well defined (Wallenstein *et al.* 2006, Graham *et al.* 2010).

1.6. Denitrification in inland waters

Reactive nitrogen does not accumulate equally in all Earth's compartments (Galloway *et al.* 2003). Denitrification in freshwaters decreases N_r transfers originating from land-based and marine sources throughout the terrestrial–freshwater–marine continuum (Seitzinger *et al.* 2006). Denitrifying bacteria and primary producers (mainly algae and plants) consume most of the nitrate that goes into freshwater ecosystems, but as the excess influx goes up and up, the efficiency of removal goes down and down (Seitzinger 2008). Freshwater systems account for about 20% of global denitrification; they are hot spots of activity; e.g. soils average ~10% of the freshwater activity per area (Seitzinger *et al.* 2006). Numerous studies about denitrification were done in ecosystems affected by punctual N_r inputs, such as agricultural soils (e.g. (Enwall *et al.* 2005)) and adjacent streams (e.g. (Inwood *et al.* 2007)). Fewer studies explore the regional effects of N_r deposition (e.g. in mountain lakes (McCrackin and Elser 2010, 2011, 2012) and in forests (Dendooven *et al.* 1996, Freedman *et al.* 2013, Xu *et al.* 2017)).

Denitrification in lakes has been studied at least since Andersen (1974) with several posterior studies, which have been revised together with other aquatic ecosystems (Seitzinger 1988, Piña-Ochoa and Alvarez-Cobelas 2006, Seitzinger *et al.* 2006). Annual denitrification rates in lakes and streams are higher than in estuaries and coastal ecosystems (Piña-Ochoa and Alvarez-Cobelas 2006). Lakes have been identified as the aquatic ecosystems with the highest seasonal and site variation in denitrification rates (Piña-Ochoa and Alvarez-Cobelas 2006). Usually, denitrification rates correlate positively with nitrate and negatively with oxygen in the water of aquatic ecosystems (Piña-Ochoa and Alvarez-Cobelas 2006). N inputs influence denitrification rates whereas hydrology and geomorphology influence the proportion of N inputs that are denitrified, with remarkably similar relationships between denitrification and water residence time and N load across lakes, the river reaches, estuaries, and continental shelves (Seitzinger *et al.* 2006). In lakes where denitrification rates in both the water and sediments have been measured, denitrification is greater in the sediments (Seitzinger 1988). However, the denitrification variation in different sediment types is still poorly understood, e. g. Piña-Ochoa and Alvarez-Cobelas (2006) emphasized that space heterogeneity should be addressed more thoroughly. Few studies have compared denitrification rates between deep and littoral lake zones (Ahlgren 1994, Saunders and Kalff 2001, Rissanen *et al.* 2011, Bruesewitz *et al.* 2012, Nizzoli *et al.* 2018, Zhao *et al.* 2018) and, in the latter, between vegetated and nude sediments (Eriksson and Weisner 1999, Veraart *et al.* 2011a, Nizzoli *et al.* 2014, Vila-Costa *et al.* 2016).

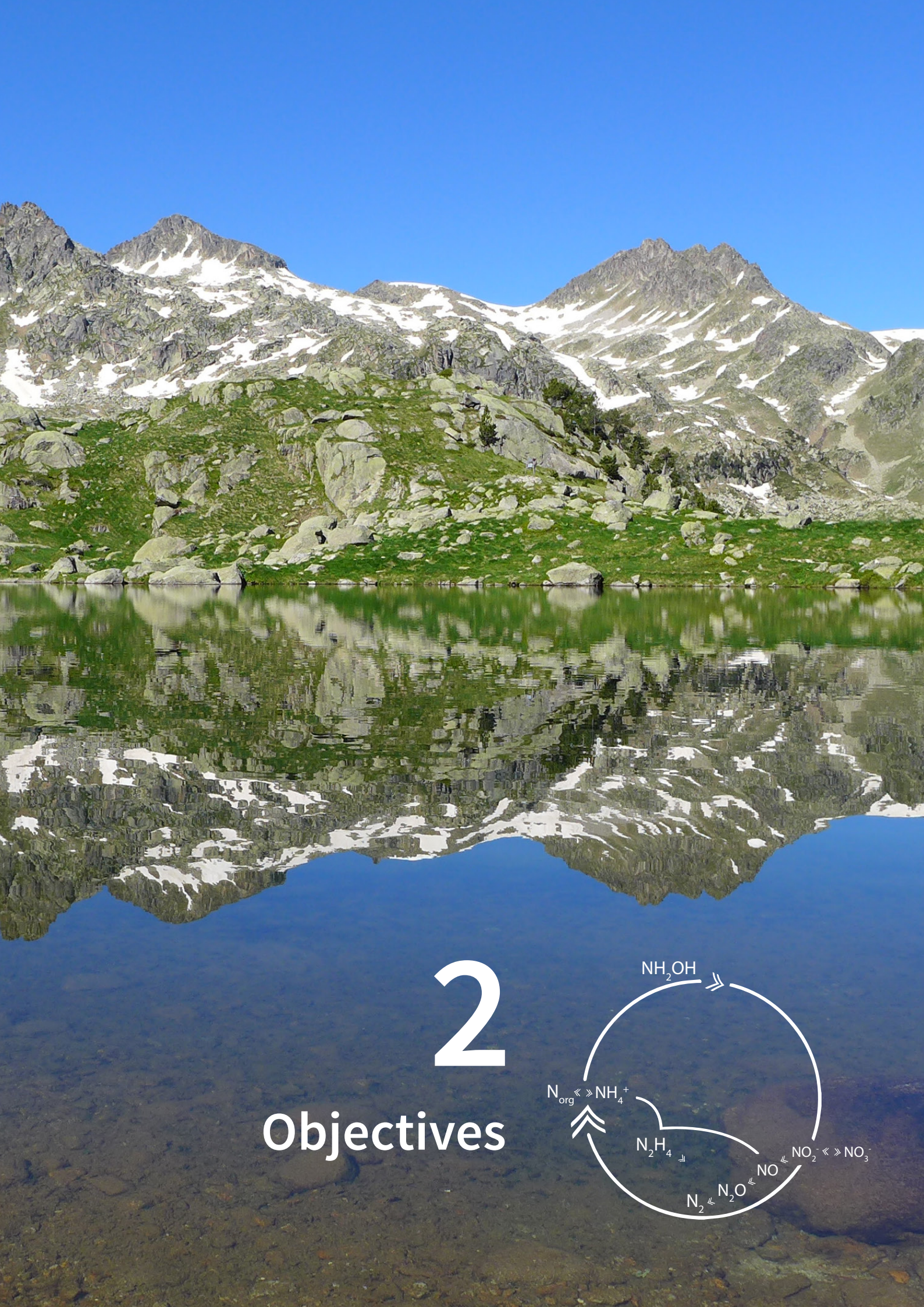
Information about denitrification rates in mountain lake sediments, despite its key role as N_r sink, is extremely limited and always using sediment slurries (McCrackin and Elser 2010, 2011, 2012, Vila-Costa *et al.* 2016, Castellano-Hinojosa *et al.* 2017). Slurries modify the sediment structure measuring higher rates compared to cores due to the enhancement of substrate diffusion when disturbing the sediment (Ambus 1993). N deposition affects mountain lakes denitrification rates of the sediment (McCrackin and Elser 2010), and N_2O concentration and saturation of the water (McCrackin and Elser 2011). However, N deposition has not saturated the sediment denitrification capacity (McCrackin and Elser 2012). In any case, nitrate availability is statistically the main driver

of denitrification rates (and N_2O concentration), independently of whether nitrate is measured in the epilimnion (McCrackin and Elser 2010) or in the water overlying the sediment (McCrackin and Elser 2012). Denitrification rates in mountain lake sediments show high variability, even in similar benthic habitat, e.g. ~10 m deep sediments or at the maximum lake depth if the lake was <10 m, always without macrophytes (McCrackin and Elser 2012).

The presence and composition of macrophytes influence the biogeochemistry of the mountain lake sediments (Gacia *et al.* 2009). In particular, isoetid species oxygenate the sediment (Sand-Jensen *et al.* 1982) and may promote coupled nitrification-denitrification (Vila-Costa *et al.* 2016). Usually sediment porewater show minimal levels of nitrate restricted to a thin surface layer of few millimetres (Bartrons *et al.* 2010, Melton *et al.* 2014), but in sediments with isoetids the intensive nitrification would result in high NO_3^- accumulation in the sediment porewater (max. 2 mM; (Catalan *et al.* 1994)). Sediments of oligotrophic lakes are known as hotspots of N cycling due to steep redox gradients (Melton *et al.* 2014), the more unknown epilithic biofilms growing in the littoral cobbles of mountain lakes also present denitrification genes (Vila-Costa *et al.* 2014), which suggests the existence of anaerobic layers. DNRA has been studied only once in mountain lakes, specifically in the water column of a tropical Mexican lake; the genetic potential showed the highest abundances in the hypolimnion with anoxic conditions during late stratification (Pajares *et al.* 2017).

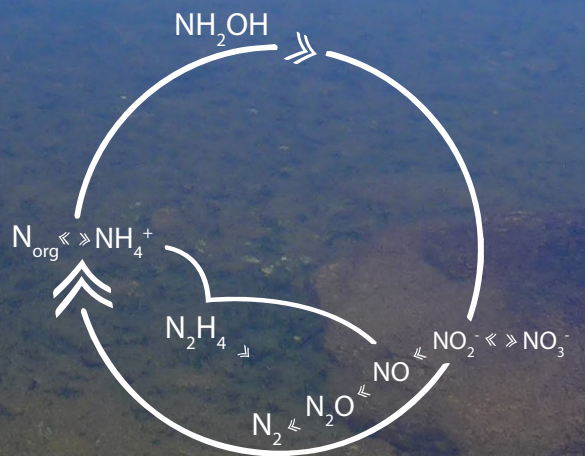
Recently, Castellano-Hinojosa *et al.* (2017) and Myrstener *et al.* (2016) report high proportions (13-83%) of N_2O respect the entire N-gas in the water and sediment slurries of a shallow warm Mediterranean mountain lake and in sediment slurries of a shallow boreal lake, respectively. These studies challenge the dominant view that N_2O emissions constitute a low proportion (0-6%) of total N emissions in freshwater ecosystems (Seitzinger 1988, McCrackin and Elser 2010, Rissanen *et al.* 2011, Saarenheimo *et al.* 2015a).

N deposition had not altered the abundance of denitrifiers in mountain lakes (McCrackin and Elser 2012), at least when it was measured using the most probable number technique (Staley and Griffin 1981). Light (PAR) and organic matter (OM), and C/N ratio, are the most influential variables explaining the abundance of nitrate and nitrite reducers, respectively (McCrackin and Elser 2012). Benthic habitat type, e.g. epilithic biofilms, nude or vegetated sediments, influence the abundances of the gene-encoding NO-forming nitrite reductases (Vila-Costa *et al.* 2014, Vila-Costa *et al.* 2016). While just one study explores the *nosZ* abundance and cultured (isolated) the N_2O -reducing bacteria from nude sediments of one mountain lake (Castellano-Hinojosa *et al.* 2017).



2

Objectives



2. Objectives

The main goal of this thesis was to study the denitrification process in mountain lakes. In particular, we studied eleven pristine oligotrophic mountain lakes that have been affected by a high N deposition. The selected lakes showed a gradient of dissolved inorganic nitrogen (DIN) in the water due to different lake productivity; more productive oligotrophic mountain lakes exhibit low DIN concentrations due to higher consumption by primary producers. Within lakes, we focused on sediments because they show higher denitrification rates than water (Seitzinger 1988). Specifically, we studied sediments near the deepest point of the lake, lithic biofilms from littoral cobbles, and littoral sediments from beds of isoetid and elodeid macrophytes, helophyte (*Carex rostrata*) belts, and rocky areas.

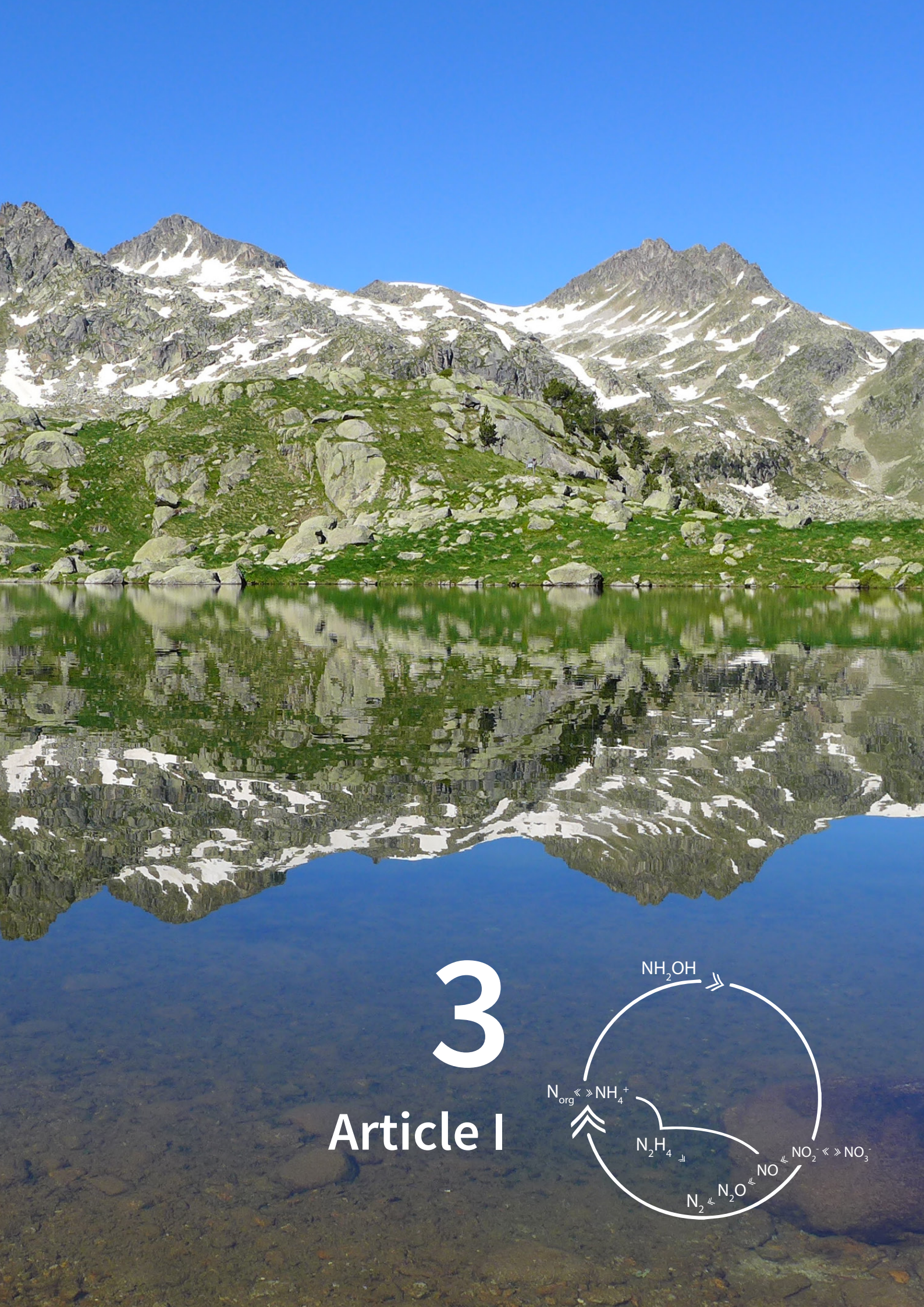
We used an approach based on the combination of concepts and techniques from biogeochemistry and microbial ecology. This combined view required the use of a diverse and interdisciplinary set of methods and approaches. We aimed to measure the denitrification activity as similar as possible to *in situ* conditions; therefore, we used little disturbed sediment cores and *in situ* temperature for denitrification rate measurements. We characterized the environment by including proximal (benthic) and more distal (lake) descriptors to capture potential drivers acting at different spatial scales.

In **article I**, we quantified guilds in the main N-transformation pathways in benthic habitats. The genes involved in denitrification (*nirS*, *nirK*, *nosZ*), nitrification (archaeal and bacterial *amoA*), DNRA (*nrfA*) and anammox (*hdh*) were quantified (Fig. 1), and the bacterial V3-V4 region of the 16S rRNA gene was sequenced. We related the functional guilds to the environmental data, and determined the bacterial community composition and linked these to the functional guilds using a multivariate approach combined with indicator species analyses. The overall aim was to describe the variation of the N transforming pathways in the mountain lake sediments.

In **article II**, we described the method developed during the thesis for estimating denitrification rates using sediment cores that combined the acetylene inhibition and microsensors measurements of the accumulated N₂O. This method was applied in articles III and IV.

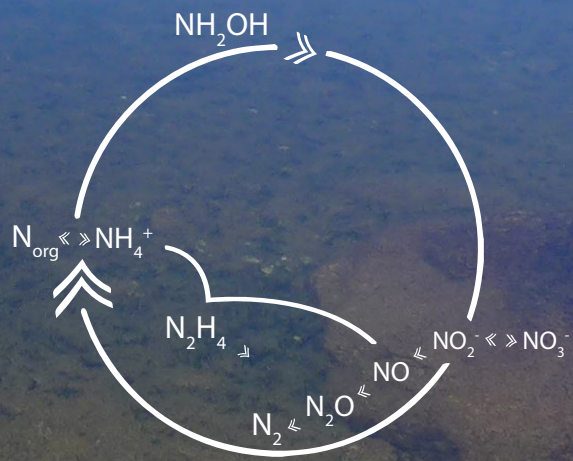
In **article III**, we experimentally investigated the denitrification rates of mountain lake sediments by manipulating nitrate concentration and temperature on field collected cores. The goal was to determine the activation energy (E_a) for denitrification in mountain lakes and check the effects of nitrate limitation on the activation energy.

In **article IV**, we measured current and potential denitrification rates (i.e. without and with nitrate added, respectively) in the main sediment habitats (vegetated littoral, non-vegetated deep and littoral) of eleven mountain lakes, and investigated the relationship of the rates with nitrogen functional gene potentials, sediment, water, and lake features. The aim was to investigate the relationship between current and potential (nitrate enhanced) denitrification rates with N-cycle gene potentials.



3

Article I



3. Article I

The DNRA-denitrification dichotomy differentiates nitrogen transformation pathways in mountain lake benthic habitats

3.1. ABSTRACT

Effects of nitrogen (N) deposition on microbially-driven processes in oligotrophic freshwater ecosystems are poorly understood. We quantified guilds in the main N-transformation pathways in benthic habitats of 11 mountain lakes along a dissolved inorganic nitrogen gradient. The genes involved in denitrification (*nirS*, *nirK*, *nosZ*), nitrification (archaeal and bacterial *amoA*), dissimilatory nitrate reduction to ammonium (DNRA, *nrfA*) and anaerobic ammonium oxidation (anammox, *hdh*) were quantified, and the bacterial 16S rRNA gene was sequenced. The dominant pathways and associated bacterial communities defined four main N-transforming clusters that differed across habitat types. DNRA dominated in the sediments, except in the upper layers of more productive lakes where *nirS* denitrifiers prevailed with potential N₂O release. Loss as N₂ was more likely in lithic biofilms, as indicated by the higher *hdh* and *nosZ* abundances. Archaeal ammonia oxidisers predominated in the isoetid rhizosphere and rocky littoral sediments, suggesting nitrifying hotspots. Overall, we observed a change in potential for reactive N recycling via DNRA to N losses via denitrification as lake productivity increases in oligotrophic mountain lakes. Thus, N deposition results in a shift in genetic potential from an internal N accumulation to an atmospheric release in the respective lake systems, with increased risk for N₂O emissions from productive lakes.

Original work: Palacin-Lizarbe C, Camarero L, Hallin S, Jones CM, Cáliz J, Casamayor EO, and Catalan J (2019). The DNRA-denitrification dichotomy differentiates nitrogen transformation pathways in mountain lake benthic habitats. *Frontiers in Microbiology*. <https://doi.org/10.3389/fmicb.2019.01229>

3.2. INTRODUCTION

According to the planetary boundaries framework (Rockstrom et al. 2009), anthropogenic alteration of the nitrogen (N) cycle is one of the major challenges facing the Earth system. Human activities have at least doubled the levels of reactive N (N_r) available in the biosphere (Erisman et al. 2011), resulting in deposition of N_r in or near heavily populated areas as well as remote ecosystems (Catalan et al. 2013). In the context of global change, remote ecosystems — defined here as being affected by atmospheric processes rather than direct human action in catchment areas — can be particularly informative about potential large-scale changes in the Earth system (Catalan et al. 2013). Alpine lakes of the Northern hemisphere and subarctic regions are examples of remote ecosystems that have been exposed to increased N_r deposition during the last decades (Holtgrieve et al. 2011, Camarero 2017), triggering a nutrient imbalance in these freshwater systems which are otherwise known to have low nutrient availability (Catalan et al. 2006). While alpine and subarctic lakes are often considered important sensors of global change (Smol 2012), there is minimal understanding of how increased N_r availability affects microbially-driven N-cycle pathways in these ecosystems (McCrackin and Elser (2010); **article III**).

The N cycle is best described as a modular and complex network of biological N-transformation reactions carried out by metabolically versatile communities of microorganisms (Graf et al. 2014, Kuypers et al. 2018), whose overall composition largely determines whether N_r is lost, via denitrification or anammox, or retained in the system via dissimilatory nitrate reduction to ammonium (DNRA). Within lakes, benthic habitats are known as hotspots of N cycling due to steep redox gradients in the sediments and biofilms (Melton et al. 2014). Furthermore, the presence and composition of macrophytes also influence the biogeochemistry of the sediment (Gacia et al. 2009). In particular, isoetid species oxygenate the sediment and may promote coupled nitrification-denitrification (Vila-Costa et al. 2016). However, the effect of increased N deposition on the N-cycling microbial communities, and the factors controlling their distribution are poorly understood in mountain lakes.

Our study aims to investigate how the distribution of microbial communities in general and those that drive different N-transformation pathways changes across a range of different benthic habitats in mountain lakes that have been affected by enhanced N deposition in the absence of significant acidification (Camarero and Catalan 1998). We hypothesise that benthic habitat type and lake productivity together determines the fate of deposited N and that increased productivity will promote pathways resulting in N_r loss. Lakes at lower altitudes tend to be more productive, particularly if they are small since the productive period is longer (Catalan et al. 2009) and phosphorus loading to the lake increases as the catchment is more vegetated (Kopáček et al. 2011). In the Pyrenees, more than 70 % of the lakes are considered ultraoligotrophic based on total phosphorus (TP; < 150 nM), whereas 22 % and 6 % are oligotrophic and mesotrophic, respectively (Catalan et al. 2006). In general, more productive oligotrophic mountain lakes exhibit low dissolved inorganic nitrogen (DIN) concentrations due to higher consumption of excess N from atmospheric loading by primary producers (Camarero and Catalan 2012). We therefore selected lakes to establish a DIN gradient and sampled lithic biofilms, sediments with elodeid, isoetid and helophyte macrophytes, and littoral and deep non-vegetated sediments (Fig. 3.1). We then characterised the N-functional pathways by quantifying the abundances of key N-functional genes involved in denitrification, nitrification, DNRA and anammox pathways (Table 3.1). We also determined the bacterial

community composition in the benthic habitats and linked these to the functional guilds using a multivariate approach combined with indicator species analyses. The environment was characterised by including proximal (benthic) and more distal (lake) descriptors to capture potential drivers acting at different spatial scales (Wallenstein et al. 2006, Battin et al. 2016).

Table 3.1. Nitrogen-functional genes accounted for in this study.

Gene	Enzyme	Pathway	Reaction	Process type
<i>amoA</i>	Ammonium monooxygenase	Nitrification	Ammonium oxidation to hydroxylamine	Aerobic
<i>nirS</i>	Nitrite reductase (cytochrome-cd1)	Denitrification	Nitrite reduction to nitric oxide	Anaerobic
<i>nirK</i>	Nitrite reductase (copper-based)			
<i>nosZ</i>	Nitrous oxide reductase	Denitrification	Nitrous oxide reduction to dinitrogen	Anaerobic
<i>nrfA</i>	Nitrite reductase (formate-dependent)	DNRA	Nitrite reduction to ammonium	Anaerobic
<i>hdh</i>	Hydrazine dehydrogenase	Anammox	Hydrazine oxidation to dinitrogen	Anaerobic

3.3. MATERIALS AND METHODS

Sampling location and habitat description

The lakes are located in the central region of the Pyrenees mountain range within the Aigüestortes i Estany de Sant Maurici National Park (Table 3.2; Fig. 3.1). All lakes are dimictic and ultra-oligotrophic (TP < 150 nM) except for Bassa de les Granotes, which is classified as oligotrophic (150 < TP < 300 nM; Catalan et al. (1993)) with a circumneutral pH (~7; Vila-Costa et al. (2014)). All main benthic habitats in the lakes were considered (Fig. 3.1), although certain habitats were present in only a few lakes (Tables 2 and S1). Plan Lake is particularly rich in macrophytes, including isoetids

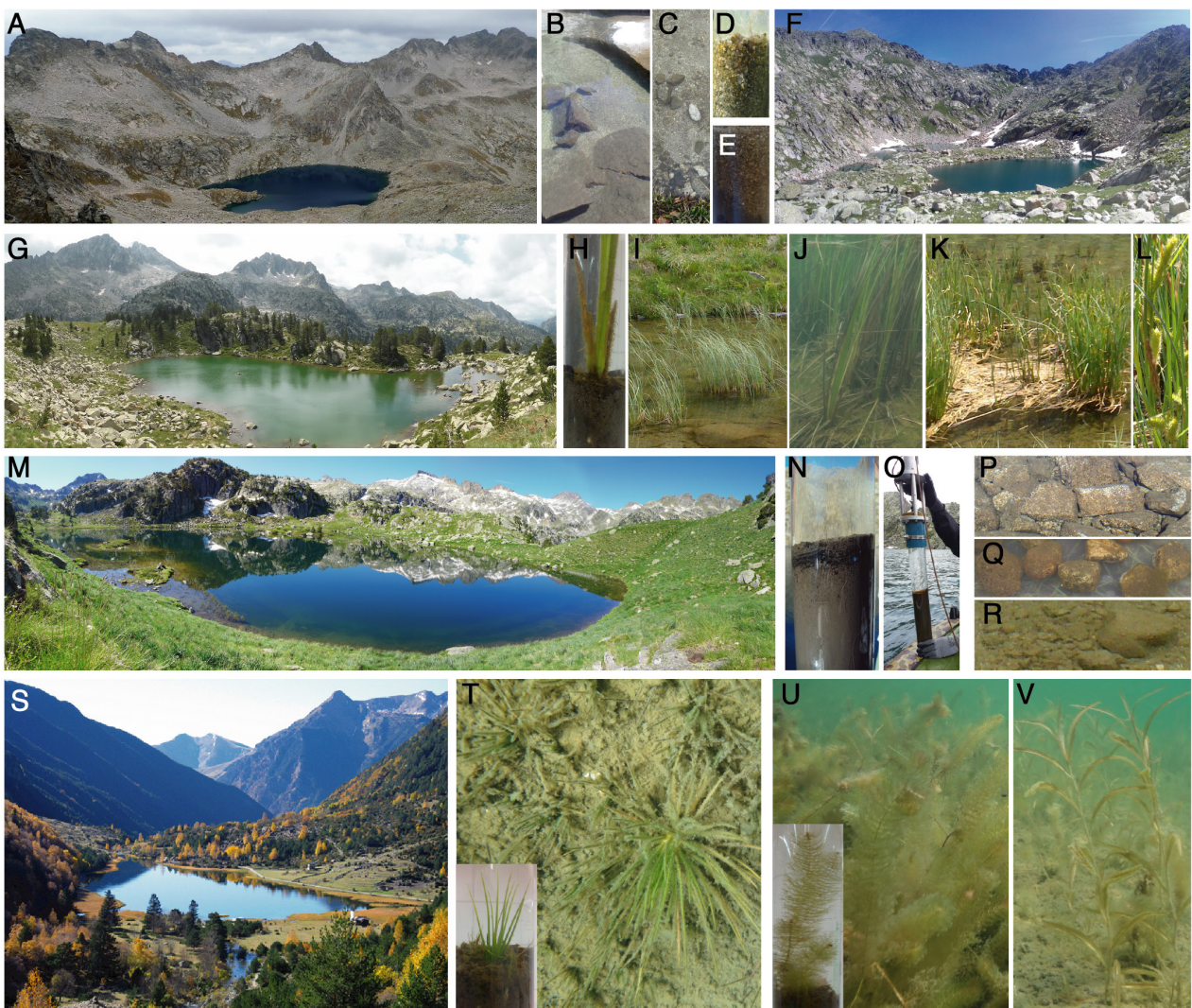


Figure 3.1. Examples of the lakes and habitats studied. Lakes: Contraix (A), Gelats de Bergús (F), Bassa de les Granotes (G), Plan (M), and Llebreta (S). Benthic habitats: sediments near the deepest point of the lake (non-vegetated) (N, O); littoral sediments from beds of isoetids (*Isoetes lacustris* (T)) and elodeids (*Myriophyllum alterniflorum* (U), *Potamogeton alpinus* (V)) macrophytes, helophyte (*Carex rostrata*) belts (H-L) and rocky areas (B-E); and lithic biofilms from littoral cobbles (P-R).

(*Isoetes setacea*, *I. palustris* and *Subularia aquatica*), elodeids (*Myriophyllum alterniflorum*, *Potamogeton alpinus* and *P. berchtoldii*) and the helophyte *Carex rostrata* (Gacia et al. 1994). Sampling was carried out during the ice-free period (June-November) of 2013 and 2014, with a total of 30 sites and 226 samples analysed.

Water, lithic biofilm, and sediment characterisation

The overlying water, sediments and lithic biofilms were characterised using physical, chemical and biological variables (Table S1). The temperature of the overlying water was measured at the time of sampling. For chemical analyses, water samples were filtered through a pre-combusted (4 h at 450°C) GF/F glass fibre filter. Nitrate and sulphate were determined by capillary electrophoresis using a Quanta 4000 (Waters) instrument. Ammonium and nitrite were determined by colourimetric methods in a segmented-flow autoanalyser (AA3HR, Seal), using the Berthelot reaction for ammonium (Bran+Luebbe method G-171-96) and the Griess reaction for nitrite (Bran+Luebbe method G-173-96). Dissolved organic carbon (DOC) was measured by catalytic combustion to CO₂ and detection by IR spectroscopy in a TOC5000 (Shimadzu) analyser.

Lithic biofilms were sampled collecting several cobbles ($\varnothing \sim 10$ cm) from different sites of the lake. Cobbles were scraped entirely (upper and lower sides) with clean metal brushes and washed with deionized water and pooling together the collected material. Biofilm subsamples were collected on 0.2- μ m pore polycarbonate membranes for DNA analysis, and triplicate volumes were filtered through a pre-combusted and pre-weighted GF/F glass fibre filters for chemical and physical analyses. Sediment cores ($\varnothing 6.35$ cm) were collected with a gravity corer (Glew 1991) around the deepest point of each lake or manually by scuba diving for the littoral sediments. The cores were sliced in three sections (0-0.5, 0.5-2 and 2-4 cm) to capture the oxic and the nitrate reduction zones (Melton et al. 2014).

For total carbon (C) and N and isotopic composition, ca. 5 mg of the freeze-dried sample was placed with a catalyst (V₂O₅) in tin capsules, and the analyses were performed by the University of California Davis Stable Isotope Facility. Organic matter (OM) content was determined using the loss on ignition (LOI) procedure (Heiri et al. 2001). The median grain size of the sediment was determined by laser diffraction (Mastersizer 2000, Malvern Instruments Ltd, UK), using freeze-dried sediment rehydrated in distilled water and introduced into the sample dispersion unit (Hydro 2000 G, Malvern Instruments Ltd, UK) after adding hexametaphosphate and sonicating to avoid aggregates. Laser obscuration was between 10-20 % and the measuring range between 0.02 and 2000 μ m.

DNA extraction and quantitative PCR of 16S rRNA and N cycle genes

DNA was extracted from 0.33 ± 0.06 g of sediment or lithic biofilm using the FastDNA® Spin Kit for Soil (MP Biomedical) following the manufacturer's instructions. The extracted DNA was quantified using the Qubit® fluorometer (Thermo Fisher Scientific Inc.).

Quantitative real-time PCR (qPCR) was used to quantify functional genes encoding enzyme involved in N-cycle pathways (Table 3.1 and S2), as well as the bacterial 16S rRNA gene. All qPCR reactions were performed in duplicate in a total reaction volume of 20 μ L using DyNAmo Flash SYBR Green qPCR kit (Thermo Fisher Scientific Inc.), 0.1% Bovine Serum Albumin, 0.5-1.0 μ M of each primer and 15 ng DNA on the Biorad CFX Connect Real-Time System. Primers, amplifica-

Table 3.2. Site location, habitats studied and characteristics sorted by the dissolved inorganic nitrogen (DIN) concentration.

Lake (Abbreviation)	Vegetation belt	Habitats Studied ^a	Latitude (N)	Longitude (E)	Altitude (m a.s.l.)	Area (ha)	Catchment (ha)	Depth ^b (m)	Renewal time (months)	TP ^c (nM)	DIN ^d (µM)
Redon de Vilamòs (R)	Alpine	I	42.78078	0.76233	2209	0.6	12	5	1.7	NA	1.2
Plan (P)	Subalpine	D, I, E, C, L	42.62248	0.9307	2188	5	23	9	15.1	102	1.7 ± 0.9
Bassa de les Granotes (G)	Alpine	D, L	42.5733	0.97124	2330	0.7	3	5	9.9	292	2.4 ± 0.7
Redó Aigüestortes (RA)	Subalpine	D, L	42.58216	0.95949	2117	6.3	325	11	1.6	76	8.5 ± 0.9
Gelat de Bergús (GB)	Alpine	D, R, L	42.59106	0.96331	2493	1.4	24	8	2.3	42	8.8 ± 3.3
Llong (Lo)	Montane	D, R, L	42.57431	0.95063	2000	7.1	1111	13	0.6	89	10.3 ± 11.6
Bergús (B)	Alpine	D, L	42.58947	0.95717	2449	6.2	126	50	3.9	44	17.1 ± 11.3
Llebreta (Le)	Montane	D, C, R, L	42.55083	0.89031	1620	8	5438	12	0.1	89	17.9 ± 2.7
Contraix (C)	Alpine	D, R, L	42.58874	0.91861	2572	9.3	100	59	9.9	49	18.0 ± 1.3
Redon (RC)	Alpine	D, R, L	42.64208	0.77951	2235	24.1	153	73	36	58	23.5 ± 19.6
Pòdo (Po)	Alpine	D, L	42.60307	0.93906	2450	4.6	33	25	9.4	75	25.2 ± 14.7

^a D, sediments in the deepest point of the lake; I, isoetid littoral sediments; E, elodeid littoral sediments; C, *Carex rostrata* belts littoral sediments; R, rocky areas littoral sediments, L, lithic biofilms from littoral cobbles.

^b Max. water column depth.

^c Total phosphorus (Camarero and Catalan 2012).

^d DIN concentration (sum of nitrate, nitrite and ammonium) in the overlying water.

tion protocols and resulting efficiencies for each assay are listed in Table S3. Potential inhibition of the PCR reactions was checked by amplifying a known amount of the pGEM-T plasmid (Promega) with the plasmid-specific T7 and SP6 primers added to the DNA extracts and non-template controls. No inhibition of the amplification reactions was detected with the amount of template DNA used. Standard curves for each assay were generated by serial dilutions of linearized plasmids with cloned fragments of the respective gene. Standard curves were linear ($R^2 = 0.997 \pm 0.003$) in the range used, and amplification efficiency was 90% for the 16S rRNA gene and 65-88 % for the functional genes (Table S3). Melting curve profiles were inspected, and final products were run on an agarose gel to confirm amplicon size. Non-template controls resulted in negligible values.

Sequencing of the 16S rRNA gene, sequence processing and OTU clustering

The diversity and structure of total bacterial and archaeal communities were determined by targeting the V3-V4 region of the 16S rRNA gene (Takahashi et al. 2014). Amplicon libraries for each sample were generated using a two-step protocol (Berry et al. 2011). First, PCR products were generated in duplicate 20 μ L reactions per sample using 16S rRNA primer constructs that included Nextera adapter sequences, with reactions consisting of Phusion PCR mastermix (ThermoFisher Scientific), 0.5 μ g μ L⁻¹ BSA, 0.25 μ M of each primer and 10 ng extracted DNA. Thermal cycling was performed for 25 cycles, and cycling conditions and primer sequences are listed in Table S3. The resulting PCR products were pooled and purified using the AMPure bead purification kit, and 3 μ L of the purified product was used as template in the second PCR using barcodes. Duplicate 30 μ L reactions were performed for each sample, with similar reagent concentrations as in the first step except for the use of 0.2 μ M final primer concentrations. PCR was performed according to Table S3. Products were pooled, bead purified, followed by equimolar pooling and sequencing performed by Microsynth AG (Balgach, Sweden) using the Illumina MiSeq platform with v3 chemistry (2 \times 300 bp paired-end reads).

Paired-end reads were merged using PEAR (Zhang et al. 2013) and dereplicated and clustered into operational taxonomic units (OTUs) at a cut-off of 3% identity using UPARSE (Edgar 2013). The final dataset comprised 13069 OTUs after removal of chimaeras and singletons, with 83 % of the quality filtered sequence pool mapped back to OTUs. Taxonomic assignment was carried out with the RDP classifier (Wang et al. 2007) against the SILVA reference database (release 119) (Quast et al. 2013). Sequences classified as mitochondria or chloroplasts were excluded. The original OTU table was rarefied (100 random subsampling) to 10660 sequences per sample. The sequences are available in the NCBI Sequence Read Archive (PRJNA494630).

Statistical methods

All multivariate, clustering and correlation analyses were performed using R (R Core Team 2019). Comparisons of gene abundances between habitat types were performed using Kruskal Wallis (KW) and Wilcoxon-Mann Whitney (WMW) tests. Principal component analysis (PCA) and Redundancy analysis (RDA) using Hellinger distances (Borcard et al. 2011) were used to investigate the unconstrained ordination of the relative abundances of the N-functional genes studied (PCA) and of the bacterial community composition (PCA), and the relationship between the relative abundance of the N-functional genes and the environmental conditions (RDA), as well as between the overall bacterial community composition and the relative abundance of the N-functional genes (RDA). Hereafter, we refer to the PCAs as gene-PCA (gen-PCA) and community-PCA (com-PCA), and to

the RDAs as gene-environment-RDA (gen-env-RDA) and community-gene-RDA (com-gen-RDA), respectively. In the analyses, functional gene abundances were standardised to total 16S rRNA gene copy numbers. Taxa < 5 % occurrence (3453 of the total 13069 OTUs) were excluded from the bacterial community composition analysis (com-PCA and com-gen-RDA), and values for nitrate, nitrite, ammonium and sulphate were log-transformed in the gen-env-RDA. In the RDAs, forward selection was used to identify a minimum set of significant explanatory variables ($p < 0.05$; Blanchet et al. (2008)), which exhibited low collinearity (variance inflation factors well below 10). Permutation tests of the resulting ordinations showed significant pseudo-F values ($p < 0.05$, $n = 1000$) for the main explanatory axes in each ordination — first to third axes in the gen-env-RDA, and first to fifth axes in the com-gen-RDA.

A structure of four sample clusters was present in both RDAs. Consequently, we used the samples scores of the three main axes of the com-gen-RDA as coordinates in four-group k-means clustering. We looked for indicative OTUs of each cluster performing a multi-level pattern analysis using the *multipatt* function from the *indicpecies* R package (Cáceres and Legendre 2009), considering site group combinations, and the entire OTU set (13069) as the community data table. For each OTU, the method provides an indicator value (IndVal) of each cluster or a joint set of them. We accepted as significant indicator taxa those with adjusted p-value < 0.001, using the false discovery rate method to calculate the adjusted p-value (Storey et al. 2004).

3.4. RESULTS

Genetic potentials

The sum of the N-functional gene copies per dry weight of sediment increased with organic matter (OM; $r = 0.42$ $p < 0.001$, Fig. 3.2A) but with a large scattering. Individual gene abundances were highly positively correlated among them (Fig. 3.2B). However, the correlation structure markedly simplified when standardizing by the 16S rRNA copy number in each sample (Fig. 3.2C), showing that the *nrfA* pool was weakly related to the rest of N-functional gene pools. The sum of the N-functional gene copies accounted for an average of 15 ± 8 % (mean \pm SD) of bacterial 16S rRNA gene copies across all samples (Fig. S1). Maximum values of 52 % were found in the lower sediment layer (2–4 cm) near the isoetid rhizosphere, while minimum values of 2 % were observed in lithic biofilms. Hereafter, unless otherwise indicated, we report the N-functional gene abundance standardised to total bacterial 16S rRNA gene copies.

The *nirS* and *nrfA* genes showed the highest relative abundances, up to 33 % and 31 % of total 16S gene copies, respectively. The abundance of *nirS* was approximately 50-fold greater than *nirK* across all lakes, with the highest numbers detected in the more productive lakes (R, P and G, Table 3.2; Fig. 3.3A-B). The abundance of *nirK* genes exhibited an overall trend of increasing abundance with lake DIN levels (Fig 3B), opposed to that observed for *nirS*. Higher *nrfA* abundance was observed in the

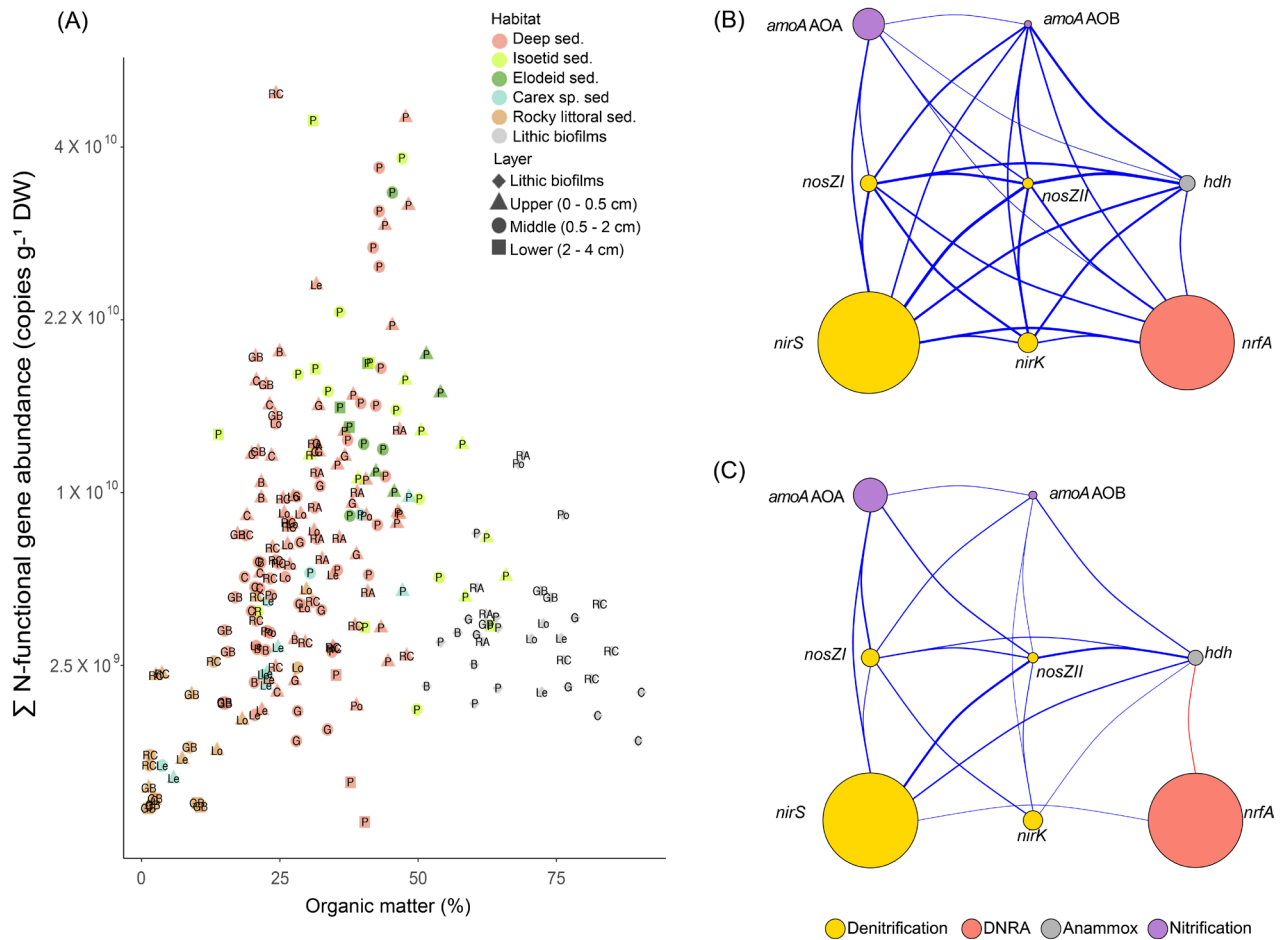


Figure 3.2. A) Sum of the accounted N-functional gene copies g⁻¹ of dry weight (DW) against the percentage of organic matter (OM). Labels are the Lake abbreviations (see Table 3.2). Note that Y-axis has a square root scale. B-C) Correlation structure of N-transforming gene abundances in mountain lake benthic habitats. N-functional gene abundances are in gene copies g⁻¹ DW (B) or standardised to the 16S rRNA gene copies (C) (Table S2). The nodes symbolise the genes whose colour and size indicate their associated pathway and abundance, respectively. Link width is proportional to the coefficient values of significant associations ($p < 0.05$), and blue and red colours indicate positive and negative Spearman's correlations, respectively.

sediments of the deepest part of the lakes (Fig. 3.3E), while abundances in the elodeid sediments were significantly higher than those of the isoetids (KW test, $p = 0.028$). Closer inspection of the macrophyte sediment profiles showed a significant *nrfA* increase deeper in the elodeid sediments ($r = 0.85$, $p < 0.001$; Fig. S2A), while no trend was observed in the isoetid sediments.

The *amoA* gene of ammonia-oxidising archaea (AOA) was more abundant than the bacterial (AOB) counterpart. No obvious trend was observed for either AOA or AOB abundance across the lake DIN gradient. Although the average total abundance of ammonia oxidisers across all lakes was low relative to those of 16S rRNA genes ($0.87 \pm 2.66\%$ and $0.05 \pm 0.14\%$ for AOA and AOB, respectively), several lakes showed AOA and AOB proportions of 57 and 23 % of the total N-functional gene

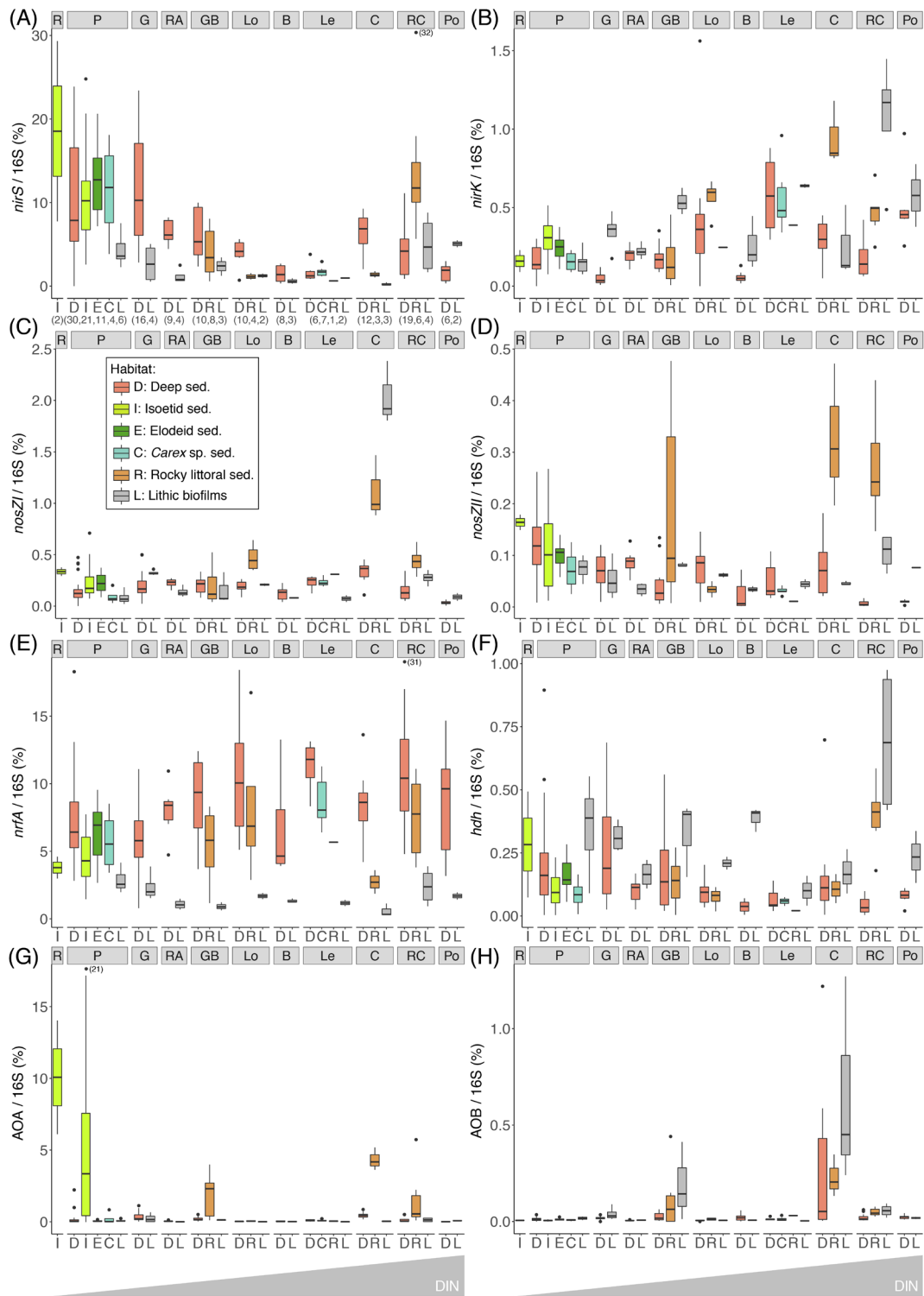


Figure 3.3. Abundances of *nirS* (A), *nirK* (B), *nosZI* (C), *nosZII* (D), *nrfA* (E), *hdh* (F), archaeal *amoA* (G) and bacterial *amoA* (H) standardised to the 16S rRNA gene copies in different lakes and habitats. Numbers in brackets in the X-axis indicated the samples analysed. Boxplots depict the interquartile range (box), median value (line), 1.5 x interquartile (whiskers), and outliers (points). Lakes are arranged from left to right by increasing water-column DIN level (see Table 3.2 for lake abbreviations and characteristics).

abundance. The highest AOA abundance was observed in the lower sediment layers of the isoetid rhizosphere and rocky littoral sediments of high-altitude lakes in the alpine belt, that is, those located above treeline (Fig. 3.3G). Abundances of AOA were significantly higher in isoetid than elodeid sediments (KW test, $p < 0.001$), and increased with depth in the former ($r = 0.64$, $p = 0.001$; Fig. S2B). All habitats of the highest altitude lakes (GB and C lakes, Table 3.2, Fig. 3.3H) showed a relatively high abundance of AOB copies compared to the same habitats in lakes at lower elevations.

The gene variants of the nitrous oxide reductase, *nosZ* clade I and II, as well as the *hdh* gene associated with the anammox pathway, exhibited low relative abundances (Fig. 3.3C-D and F). The abundance of clade I *nosZ* genes was typically higher (~7-fold on average) than that of clade II *nosZ* across all lakes and habitats. The lithic biofilm habitats of Contraix, the most elevated lake, showed the highest abundance of *nosZ* clade I genes (Fig. 3.3C), while *nosZ* clade II abundances were higher in the rocky littoral sediments of alpine lakes (Fig. 3.3D). Relative abundances of *hdh* were higher in the lithic biofilms (Fig. 3.3F), with no obvious relationship with DIN levels across the lakes.

N-functional genes and the environment

The constrained ordination of N-functional gene abundances identified three distinct gradients explaining 54 % of the total variation across habitats and lakes (Fig. 3.4). A similar result was obtained in a non-constrained analysis (Fig. S3), indicating that the main environmental drivers were captured by the constrained analysis. The main variation of benthic N-cycling genetic potentials was across a *nirS* vs *nrfA* abundance gradient (Fig. 3.4). The *nirS*-rich samples corresponded to those from shallow and productive lakes (R, P and G, Table 3.2; Fig. S4A-B), specifically the upper sediments in all habitats and sediments near the roots of isoetids. These sites were associated with higher temperature, DNA content, isotopic signatures, DOC content, and C and N content, as well as coarser granulometry (Fig. S5) and lower C/N and nitrate/nitrite ratios (Fig. 3.4). In contrast, *nrfA* rich environments occurred in the deep parts of the deep lakes, the lower layers of all sediments (except the isoetid rhizosphere) and the littoral sediments of the montane belt lakes (Table 3.2; Fig. S4A-B). Sulphate, ammonium, nitrate and nitrite concentrations were higher in these sites compared to those associated with *nirS*. The same *nirS*-*nrfA* main axis was also found if only samples from the deep habitat were included in the analysis.

The gen-env-RDA second axis of variation discriminated between sediments and lithic biofilms. The latter characterised by higher abundances of *nirK*, *nosZI*, *nosZII*, *hdh* and AOB (Fig. 3.4A). The rocky littoral sediments of Lake Contraix separated from the other sediment samples (Fig. S4A). These sites shared relatively high concentrations of nitrate, nitrite and sulphate in the overlying water, high OM content, and particular isotopic signatures (high $\delta^{13}\text{C}$ and low $\delta^{15}\text{N}$). Finally, the third axis of variation was associated with the AOA abundance (Fig. 3.4B) and resulted in the segregation of the majority of the isoetid sediments from the other habitats. The sites with the highest abundance of AOA were located close to the isoetid rhizosphere and in the rocky littoral sediments of the alpine lakes (Fig. S4B, Table 3.2). These samples showed high $\delta^{15}\text{N}$ values and likely corresponded to more oxygenated sediments (Fig. 3.4B).

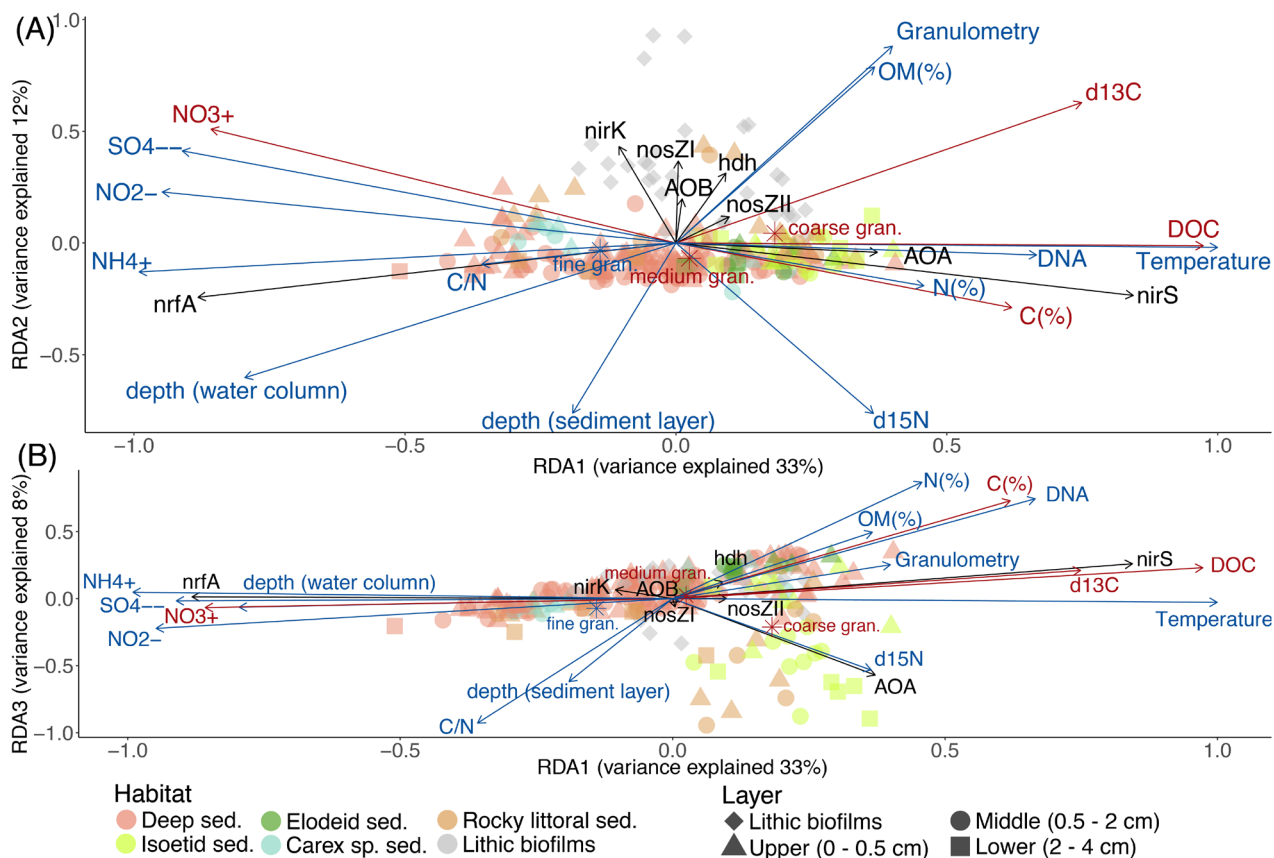


Figure 3.4. RDA based on N-functional gene abundances (response variables, black arrows) and the environmental variables (explanatory variables, blue arrows). Red arrows represent the unselected environmental variables in the previous forward selection. Triplots of the 1st and 2nd (A) or of the 1st and 3rd (B) main gradients. See figure S4A and B for samples scores. The axes sizes are proportional to the explained variation.

N-functional genes and the associated microbial community

The ordination of the OTU composition constrained by the N-functional gene abundances resulted in a pattern of four distinct sample clusters (Fig. 3.5), similar to that obtained in an unconstrained ordination (Fig. S6). The four clusters consisted of samples associated with a high relative abundance of *nrfA*, *nirS*, AOA, or a combination of the rest of the targeted genes. Classification of samples into the four clusters using k-means followed by indicator species analysis resulted in approximately 29 % of OTUs being identified as exclusively associated with samples from a single cluster (Fig. 3.6; Table S4-S5). Approximately 12 % of OTUs were significant indicators of the AOA sample cluster and found across a wide range of different bacterial taxa. By contrast, 6 % of OTUs were significant indicators of the mixed N-transformation cluster, with large numbers of indicators concentrated within the phyla Cyanobacteria, Bacteroidetes and Planctomycetes, as well as Alpha- and Betaproteobacteria classes. Similarly, 6 % of OTUs were associated with samples in the *nrfA* cluster and were classified into Firmicutes, Bacteroidetes, Actinobacteria and Chloroflexi phyla, and Epsilon- and Deltaproteobacterial classes. Finally, 4 % of OTUs were exclusive indicators of samples in the *nirS* cluster and were found across a large number of bacterial taxa, similar to the AOA sample cluster.

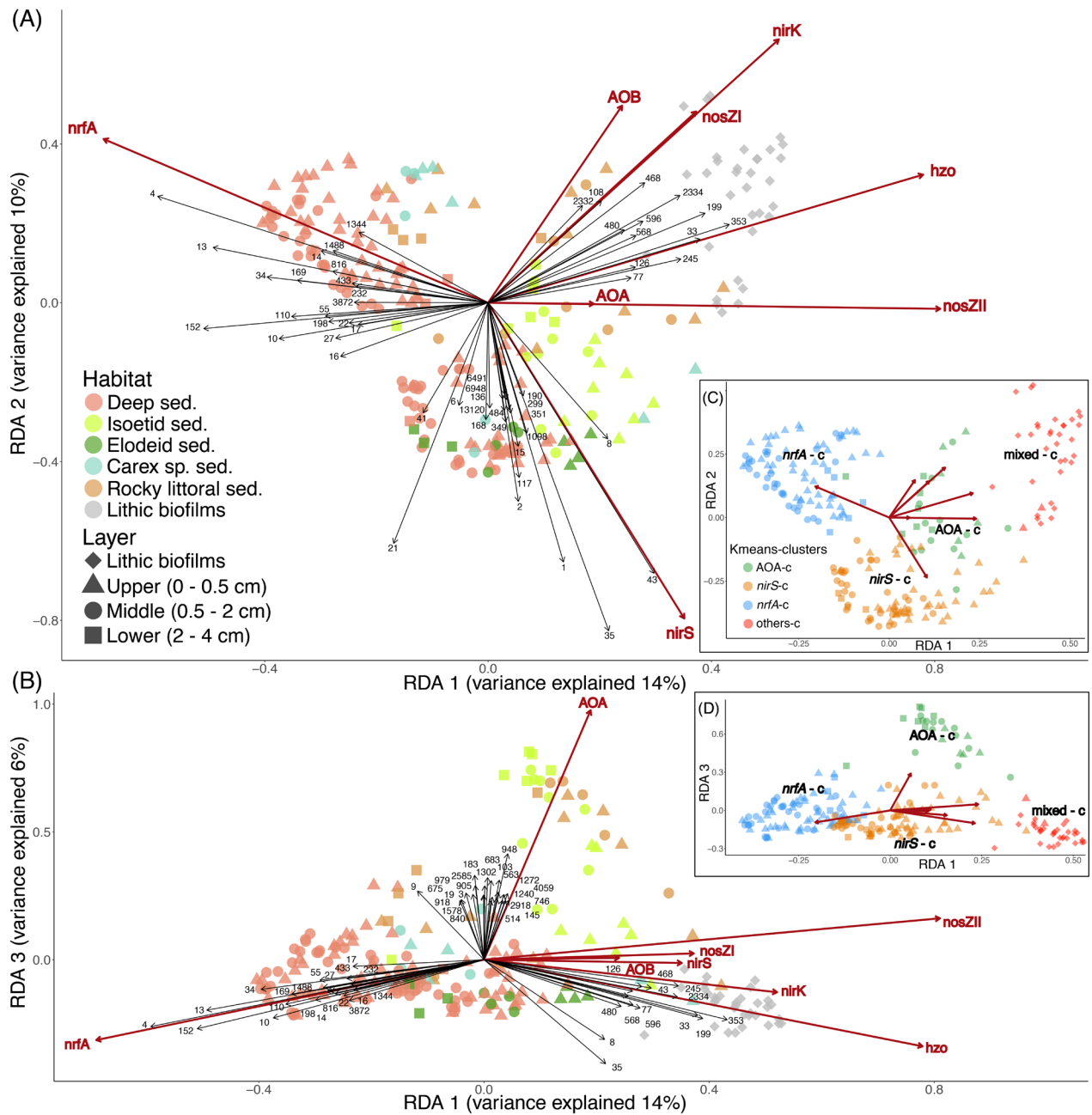
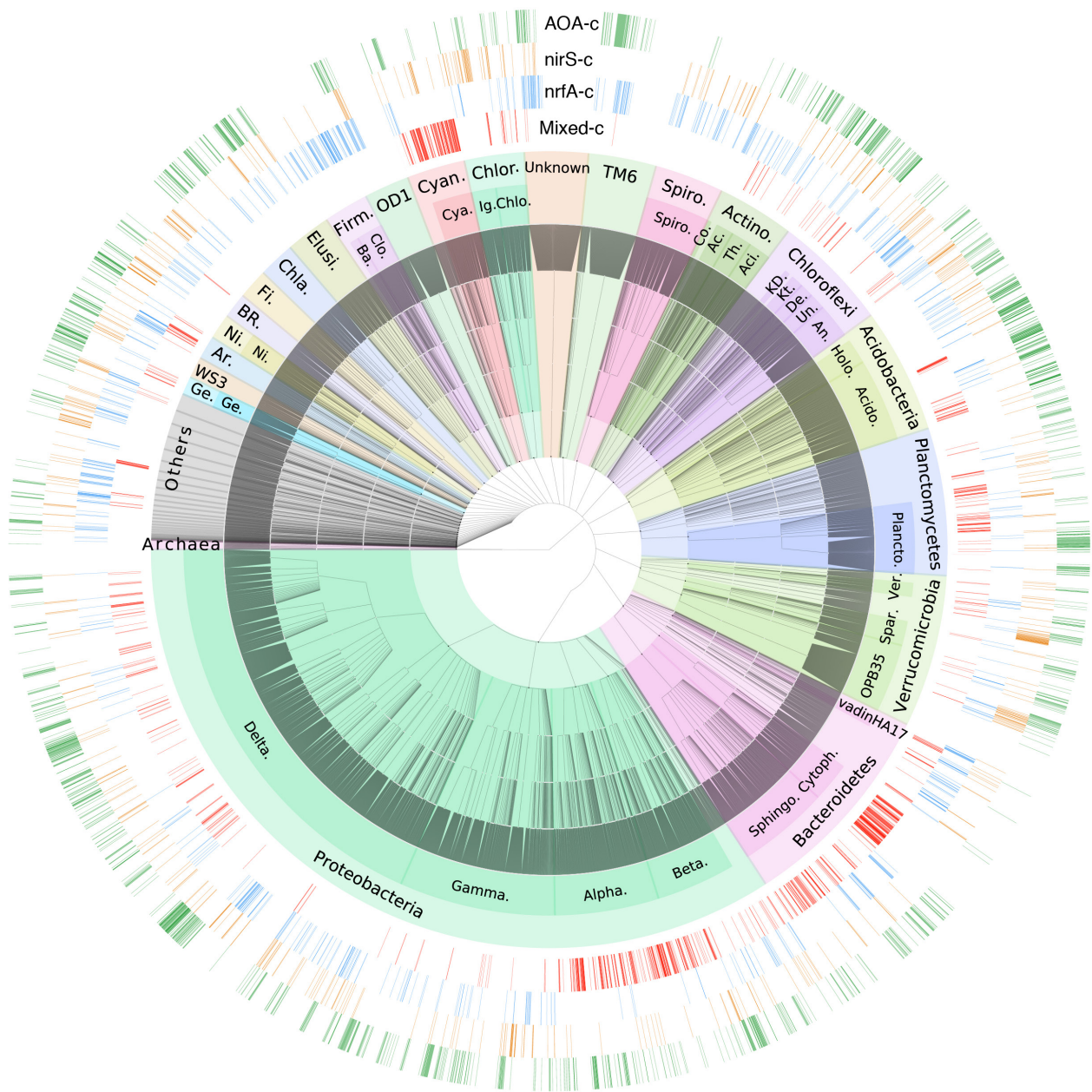


Figure 3.5. RDA with the OTUs abundance (response variables) and the abundance of the N-functional genes (explanatory variables, red arrows). Triplots of the 1st and 2nd (A) or the 1st and 3rd (B) main gradients. Only the most influential OTUs for each gradient are shown (black arrows and ID, Table S6). Clusters are resulting from the k-means analysis with the sample scores of the three main RDA gradients (Subplots C and D). See figure S4C and D for samples scores. The axes sizes are proportional to the explained variation.

Figure 3.6. Hierarchical taxonomic classification of OTUs found in all surveyed lakes. Major bacterial phyla are indicated by shaded areas, while dominant classes within each phylum are labelled. External rings show OTUs that are exclusive indicators (adjusted-p. < 0.001) of each of the four N-transformation functional sample clusters, as delimited by the dominant N-functional gene abundances. (Next page).



Phylum Abbreviations

Actino.: Actinobacteria	Spiro.: Spirochaetae	TM6.: Cand. division TM6	Chlor.: Chlorobi
Cyano.: Cyanobacteria	OD1.: Cand. division OD1	Firmi.: Firmicutes	Elusi.: Elusimicrobia
Chla.: Chlamydiae	Fi.: Fibrobacteres	BR.: Cand. division BRC1	Ni.: Nitrospirae
Ar.: Armatimonadetes	WS3.: Cand. division WS3	Ge.: Gemmatimonadetes	

Class Abbreviations

Delta.: Deltaproteobacteria	Gamma.: Gammaproteobacteria	Alpha.: Alphaproteobacteria	Beta.: Betaproteobacteria
Spingo.: Spingobacteriia	Cytoph.: Cytophagia	OPB35.: OPB35 soil group	Sparto.: Spartobacteria
Ver.: Verrucomicrobiae	Plancto.: Planctomycetacia	Acido.: Acidobacteria	Holo.: Holophagae
An.: Anaerolineae	Un.: Uncultured	De.: Dehalococcidia	Kt.: Ktedonobacteria
KD.: KD4.96	Ac.: Acidimicrobiia	Th.: Thermoleophilia	Ac.: Actinobacteria
Co.: Coriobacteriia	Spiro.: Spirochaetes	Chlo.: Chlorobia	Ig.: Ignavibacteria
Cya.: Cyanobacteria	Clo.: Clostridia	Ba.: Bacilli	Ni.: Nitrospira
Ge.: Gemmatimonadetes			

3.5. DISCUSSION

The DNRA-Denitrification gradient

The gradient of *nrfA* to *nirS* dominance was the main pattern of variation in the N-transforming microbial communities of the benthic habitats. From an ecosystem perspective, this gradient indicates a shift from habitats with a higher potential for internal N_r cycling via DNRA, and thus retention of N_r in the system, to those in which loss of N_r from the lake is more likely through denitrification. The environments with the lowest ratios of denitrifying to DNRA nitrite reductase genes were characterised by variables indicating refractory organic matter with high C/N, lower oxygen diffusion and lower redox potentials. This was particularly the case in the deepest part of the deep lakes (maximum depth ≥ 25 m) and in the deeper regions of the reduced elodeid sediments. In agreement with our result, previous work in a tropical high-altitude oligotrophic lake has shown *nrfA* abundance to be highest in the deepest part of the hypolimnion with anoxic conditions during late stratification (Pajares et al. 2017), and more reduced conditions favoured DNRA over denitrification in Australian estuaries (Kessler et al. 2018). Increased C/N ratio may favour DNRA over denitrification (Kraft et al. 2014).

The highest genetic potential for denitrification, based on *nirS* abundance, was detected in shallower and less oligotrophic lakes, where DIN levels were lower in the water column due to higher primary productivity. These lakes also have lower C/N ratios (Table S1). Generally, lake autochthonous OM is fresher and of higher quality (e.g. lower C/N), and is a substantial proportion of total OM in lakes with a lower ratio of the catchment to the lake area. This fresh OM can be used as electron donors for denitrifiers, as demonstrated in several aquatic ecosystems (eutrophic lakes (Chen et al. 2012, Gardner et al. 2017), streams (Barnes et al. 2012, Stelzer et al. 2014), wetlands (Dodla et al. 2008), and oceans (Van Mooy et al. 2002)). Oxygen levels in upper sediments of shallow and productive lakes likely fluctuate to a greater degree than those observed in habitats dominated by DNRA, thereby favouring organisms with facultative anaerobic respiration pathways such as denitrification (Wittorf et al. 2016, Chen et al. 2017a). The *nirS* denitrifiers along the DNRA-denitrification gradient were associated with *nosZ* clade II N_2O reduction and AOA communities involved in ammonia oxidation, whereas denitrifier communities present in lithic biofilms dominated by *nirK*-types were associated with *nosZ* clade I N_2O reduction and AOB. These patterns indicate that different N transformation networks developed in these habitats even when in both cases exhibited potential for linked nitrification and denitrification.

The overall high proportion of denitrifying nitrite versus nitrous oxide reductase genes (~ 30 *nir:nosZ* ratio on average) suggests a dominance of partial denitrification, especially in productive habitats dominated by *nirS* denitrifier communities (i.e., *nirS*-cluster showed *nir:nosZ* higher ratios compared to the other clusters, WMW test, $p < 0.01$). This observation agrees with Castellano-Hinojosa et al. (2017) who found high N_2O/N_2 emissions in a productive, shallow warm Mediterranean mountain lake, as well as Myrstener et al. (2016) who demonstrated that addition of nitrate, phosphorus and labile C to sediments from a boreal lake resulted in higher relative N_2O production compared to addition of nitrate alone. Other studies have shown that higher *nir:nosZ1* ratios in the sediments of boreal lakes were associated with hypolimnion N_2O excess, as well as increased phosphate and nitrate concentrations (Saarenheimo et al. 2015a). Thus, productive sites could favour partial

denitrifiers that survive anoxic periods. Before arriving to the atmosphere, N₂O might be consumed in the hypolimnion of deep lakes. *NosZ*-harbouring bacteria have been found in the hypolimnion of boreal lakes (Peura et al. 2018). However, in the sediments studied, the higher *nir:nosZ* ratios were found in shallower lakes in which N₂O may easily reach the atmosphere (Dore et al. 1998). Further studies accounting for real N₂O emissions could corroborate our conjecture.

Nitrite-dependent anaerobic methane oxidation (N-DAMO, (Simon and Klotz 2013)) is a potential alternative to DNRA, denitrification and anammox nitrite consumption. N-DAMO has been found as a key driver of methane oxidation in nitrate-rich lakes (Deutzmann et al. 2014) and reduced sandy riverbeds (Shen et al. 2018). In these habitats, bacteria related to Candidatus *Methyloirabilis oxyfera*, known to perform this pathway, were abundant. In our study, we detected only two OTUs of low relative abundance (0.02 %) classified as Candidatus *Methyloirabilis*. Nonetheless, OTUs belonging to the genus *Methylocaldum* were more abundant (~ 0.3 %), and were significant indicators of the '*nirS*' cluster. These findings are similar to those of a survey of methane oxidation in Indian reservoirs (Naqvi et al. 2018), where low relative abundance of NC10 bacteria capable of N-DAMO (0.003-0.022 %) was found; whereas Type I aerobic methanotrophs, which include *Methylocaldum* and other members of the Methylococcaceae family, were predominant and co-occurred with a diverse community of potential *nirS* type denitrifiers. Other Methylococcaceae are partial denitrifying aerobic methanotrophs with N₂O as the end product (Kits et al. 2015a, Kits et al. 2015b). Overall, these results, added to the high ratio of *nir* to *nosZ* gene abundance, suggest that N₂O emissions are the most likely endpoint of nitrite reduction in *nirS*-cluster sediments, independent of the pathway. Further studies are required to elucidate the importance and distribution of methane dependent processes in mountain lakes and to evaluate their role as a bypass of partial denitrification.

The idiosyncratic lithic biofilms

Microbial N-transforming guilds in the lithic biofilms differentiate from those in the sediments. Gene abundance results indicate a complex N-transformation structure in this habitat, consisting of processes demanding both oxic and anoxic conditions, which suggest highly structured microbial communities in relatively short spatial distances. The idiosyncratic nature of the guild composition (*e.g.* *nosZI*, *hdh*, *nirK*) declines as the productivity of the lake increases; *nirS* becomes more prominent compared to *nirK*, and the N-transforming communities are more similar to the upper sediments. The high abundance of *nirS* differs from the dominance of *nirK* previously found in another study of epilithic biofilms from a subset of the same lakes. A main difference between the two studies is that in Vila-Costa et al. (2014) only sampled the upper side of the cobbles, whereas we sampled both sides. Differences in ammonia oxidisers between the upper (light-side) and lower (dark-side) sides of cobbles have been previously reported (Merbt et al. 2017). The higher relative abundance of *hdh* and *nosZ* genes indicates that N loss in the form of N₂ could be higher in the lithic biofilms compared to the other benthic habitats in the studied lakes.

Archaeal nitrification hotspots

The positive $\delta^{15}\text{N}$ signals observed in samples from the lower sediment layers of the isoetid rhizosphere and the rocky littoral sediments of the alpine lakes support the view of them as nitrification hotspots (Mariotti et al. 1981), likely performed by AOA as suggested by the *amoA* gene abundance. Nitrification in rocky littoral sediments could be quantitatively more relevant than the isoetid rhizosphere given that rocky littorals occupy large areas in alpine lakes. Nevertheless, the archaeal *amoA* densities observed in the lower isoetid sediment layer were nearly 100-fold higher than in the rocky sediment samples with the highest AOA abundance. Sediments close to the roots of isoetids are episodically well-oxygenated due to the release of oxygen through roots during photosynthetic periods (Sand-Jensen et al. 1982), which increases the interface between oxidised and reduced sediments where the NH_4^+ oxidation occurs. Intensive nitrification would result in high NO_3^- accumulation in the sediment porewater (max. 2 mM; (Catalan et al. 1994)). However, this is likely transient as the NO_3^- concentration in the overlying water column was negligible, suggesting a close coupling of nitrification and denitrification in this habitat (Vila-Costa et al. 2016). Indeed, there was a positive correlation ($r = 0.68$, $p < 0.001$) between nitrification and denitrification gene abundances in the isoetid sediments of Plan lake. Lakes at a higher altitude, Contraix and Gelats de Bergús, also showed significant correlations between nitrification and denitrification gene abundances for deep and littoral habitats ($r = 0.48$, $p = 0.02$ and $r = 0.44$, $p = 0.08$, respectively), suggesting that nitrification and denitrification are also linked in the nitrification hotspots.

Linking the taxonomic distribution and functional potential

Each of the four main N-transforming communities consists of a highly diverse and distinct consortium of co-occurring bacterial taxa, based on the large number of indicator OTUs detected. However, taxonomic classification does not necessarily predict functioning, as different prokaryotic traits may be conserved at different phylogenetic depths (Martiny et al. 2015). While ammonia oxidation and anammox capacities are restricted to only a few lineages, denitrification and DNRA are widely distributed across the phylogeny (Graf et al. 2014, Welsh et al. 2014). Thus, many of the indicator OTUs identified are likely not directly involved in each N-transformation pathway. However, the high degree of similarity observed between unconstrained and functional gene-constrained OTU-based ordinations indicates that shifts in the genetic potential of different N-transformation processes are tightly linked to changes in the overall prokaryotic community structure, which itself is shaped by differences in environmental conditions across habitats.

Links between taxonomic composition and functional potential has been observed in previous works in lakes based on metagenomes or sequencing of functional genes. The occurrence of several proteobacterial families, in particular, Rhodobacteraceae (Alphaproteobacteria), Methylococcaceae (Gammaproteobacteria), and Burkholderiales, Comamonadaceae and Rhodocyclaceae (Betaproteobacteria) has been shown to be strongly associated with denitrification gene presence or abundance (Vila-Costa et al. 2014, Peura et al. 2015, Saarenheimo et al. 2015b, Castellano-Hinojosa et al. 2017, Chen et al. 2017b). These taxa were also highly abundant in samples within the *nirS*-denitrifier and mixed functional gene communities, which included *nirK*-type denitrifiers. Moreover, metagenomic studies of boreal lakes water columns have identified *nosZ* sequences originating from Myxococcales (Deltaproteobacteria) and Sphingobacteriaceae (Bacteroidetes) in the hypolimnion near the oxycline (Peura et al. 2015, Peura et al. 2018). Many organisms within these families are known to possess the clade II variant of the *nosZ* gene (Hallin et al. 2018). Accordingly, a large proportion

of indicator OTUs for the mixed N-cycling communities, which includes the clade II *nosZ* variant, were also classified as belonging to these families. The 4th most abundant genus in the studied lakes is *Anaeromyxobacter*, one member of this Deltaproteobacteria genus is *A. dehalogenans* a chemodenitrifier, an organism that combines chemical chemodenitrification reactions and enzymatic reaction(s) to reduce NO₃⁻ to N₂O or N₂, without having denitrifying nitrite reductases codified by *nirS* or *nirK*, also performs DNRA and Fe-reduction (Onley et al. 2018). *Rhodoferax* (Beta-) and *Desulfomonile* (Delta-) possible chemodenitrifiers (Onley et al. 2018) were also common genus present. There are other eubacteria non-proteobacteria taxa also carrying denitrifying genes (Graf et al. 2014) present in our samples (e.g. Actinobacteria).

OTUs associated with samples in the *nrfA* cluster were classified as Firmicutes, Epsilon- and Deltaproteobacteria (Campylobacterales and *Anaeromyxobacter*, *Desulfovibrio* and *Geobacter*, respectively), Bacteroidetes (Bacteroidia), Actinobacteria (Coriobacterales and Corynebacterales) and Chloroflexi (Anaerolineaceae), all these taxa include microbes that are known to carry *nrfA* (Welsh et al. 2014).

Regarding the ammonia oxidisers, the primers used in the 16S rRNA sequencing mainly target bacteria, but also pick up Euryarchaeota (Takahashi et al. 2014). Therefore, OTUs assigned to Thaumarchaeota were not detected, although AOA hotspots could be identified based on qPCR data. Nitrosomonadaceae was the most common AOB, with 89 OTUs classified as being similar to uncultured members of this family. Nitrospirae was the only identified nitrite oxidising bacteria (NOB) in our samples. There was a likely coupling between AOA and NOB, as suggested by the correlation between archaeal *amoA* genes and the relative abundance of Nitrospirae members in general, and *Nitrospira* in particular, in the AOA-cluster samples ($r = 0.65$ $p = 0.0005$, $r = 0.47$ $p = 0.02$, respectively). This coupling has previously also been found in grasslands (Simonin et al. 2015), agricultural soils (Jones and Hallin 2019), and sediments of an Andean mountain lake (Parro et al. 2019). Comammox *Nitrospira* could be important in the nitrifying hotspots found in the present study, as suggested by previous studies in other surface-attached oligotrophic habitats (Kits et al. 2017, Pjevac et al. 2017, Fowler et al. 2018). For anaerobic ammonia oxidation, OTUs belonging to the “*Candidatus Anammoximicrobium*” (Khramenkov et al. 2013) was the only taxa present with demonstrated anammox capacity. However, more bacteria within the numerous uncultured Planctomycetes detected in our samples could potentially perform anammox.

3.6. CONCLUSIONS

The N-transforming guild composition in benthic habitats of mountain lakes is complex and deeply embedded in the overall prokaryotic community. There is a high positive correlation among all the genes, and they all generally increase with OM. The dominant pathways change depending on the habitat and productivity of the lake (Fig. 3.7). The fate of nitrite is the main diverging point differentiating the N-transforming guilds. The genetic potential for DNRA dominate in the deep

part of the lakes and the lower sediment layers, which indicates recycling of the N_r . By contrast, the denitrifying *nirS* nitrite reduction potential prevails in the upper layer of the sediments in the shallow, warmer and more productive lakes, which indicates a loss of N_r . Emissions of N_2O and N_2 are likely spatially segregated within lakes, with lithic biofilms being candidates for preferential N loss as N_2 as they show a more balanced gene abundance of nitrous oxide reductases (*nosZI+II*) and anammox (*hdh*) in relation to NO-forming nitrite reductases (*nirS+nirK*). The more productive and *nirS*-dominated habitats may be a main source of N_2O because of the striking excess of this gene over the ones of the final steps of complete denitrification unless another bypass process is relevant (e.g. N-DAMO). There may be two types of nitrifying-denitrifying coupled community types in the benthic habitats of mountain lakes. The first is based on nitrification by AOA coupled to Nitrospirae (NOB) and denitrification by *nirS*-denitrifiers, with hotspots in the rocky littoral sediments of the lakes above treeline and the sediments near the isoetid rhizosphere. The second includes AOB coupled to *nirK*-type denitrifiers reducing nitrite and *nosZI*- N_2O reduction in the lithic biofilms. Overall, our results point out two types of potential response to high atmospheric N deposition in these lakes. In highly oligotrophic lakes, there will be an accumulation of N_r because of the predominance of internal N_r recycling via DNRA. In less oligotrophic lakes, generally with macrophyte growth, the N_r deposition loads may be more effectively directed towards N gas release to the atmosphere via denitrification.

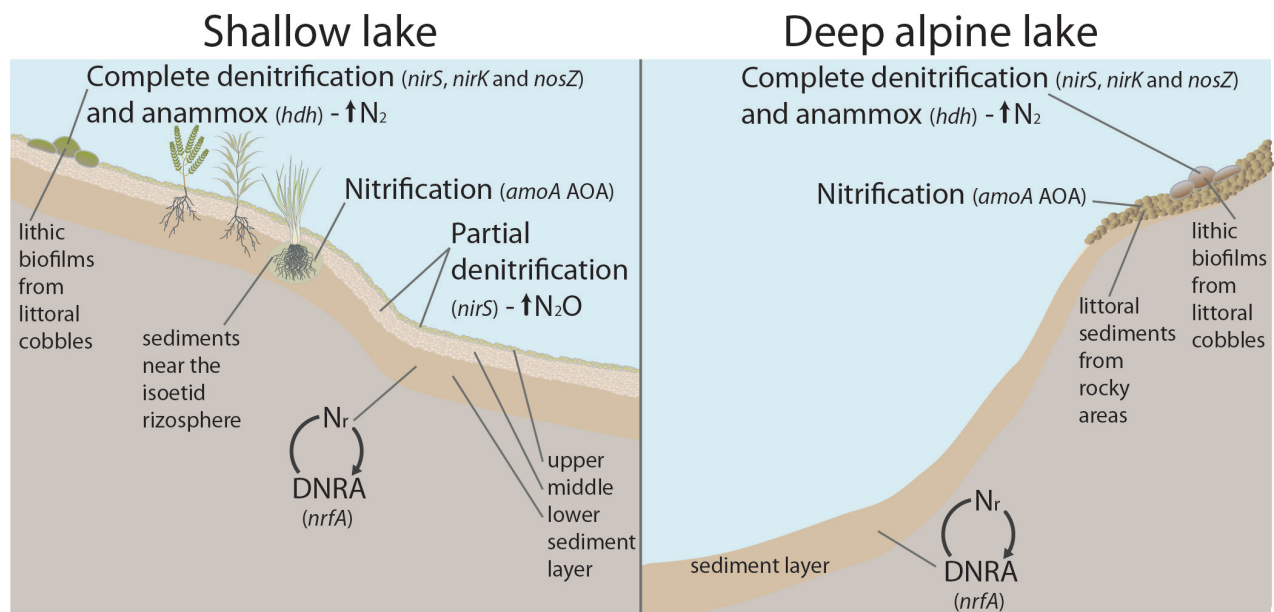


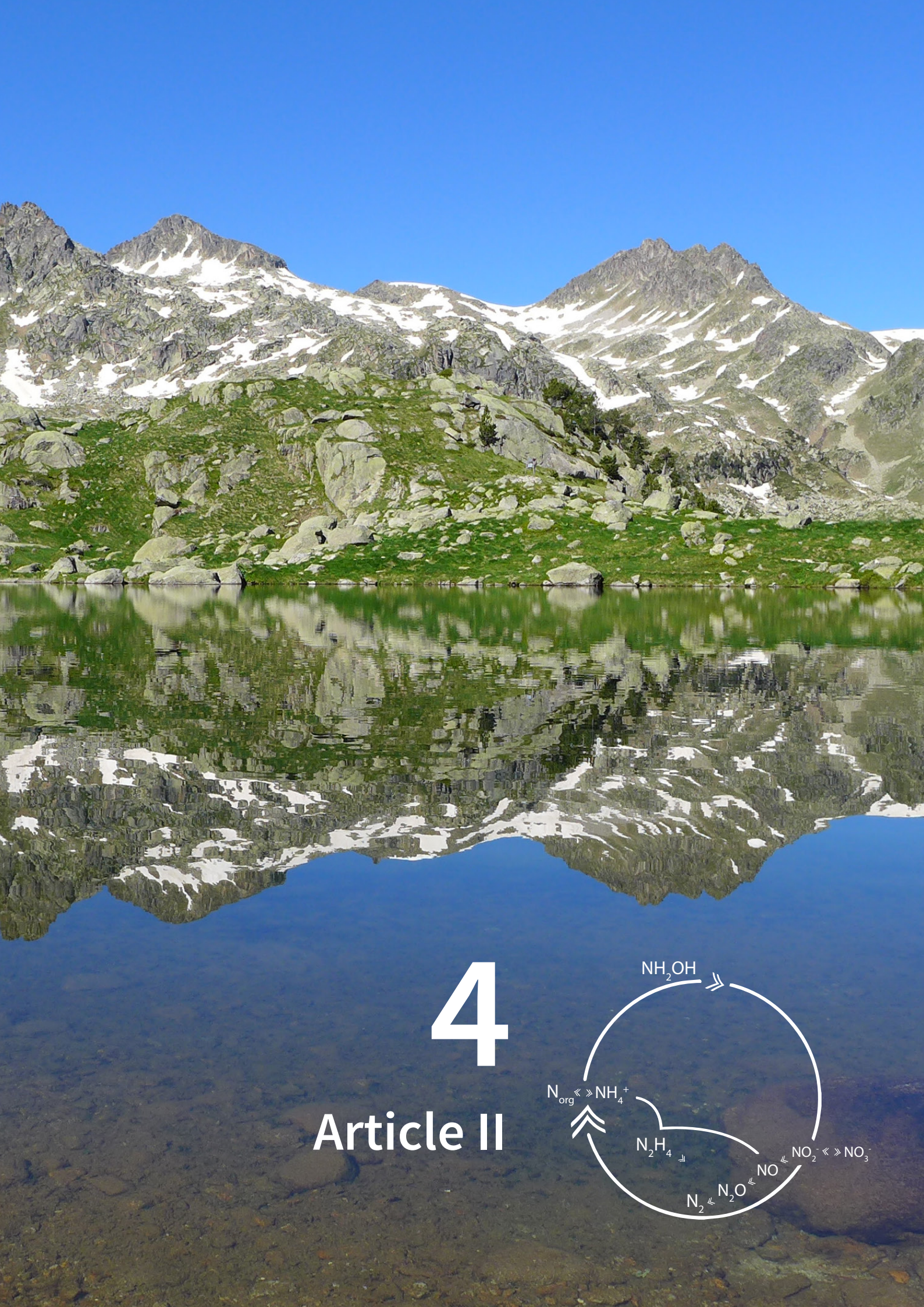
Figure 3.7. Conceptual sketch of a shallow, mountain lake with macrophytes (left), and a deep alpine lake (right). The benthic habitats with the genetic potential for the dominant N-cycling process(es) and fate of N (N_r recycling, or N_2 and N_2O emission) are indicated. The dominant N functional gene(s) in each habitat are shown in italics. Abbreviations: N_r , reactive nitrogen; AOA, ammonia-oxidizing archaea; anammox, anaerobic ammonium oxidation; DNRA, dissimilatory nitrate reduction to ammonium.

FUNDING

The Spanish Government provided funds through the Ministerio de Educación as a predoctoral fellowship to CPL (FPU12–00644) and research grants of the Ministerio de Economía y Competitividad: NitroPir (CGL2010–19737), DARKNESS (CGL2012-32747), LACUS (CGL2013–45348-P), TRANSFER (CGL2016–80124-C2-1-P). The REPLIM grant (INRE - INTERREG Programme. EUUN – European Union. EFA056/15) and the ALTER-NET Mobility Scheme supported the final writing.

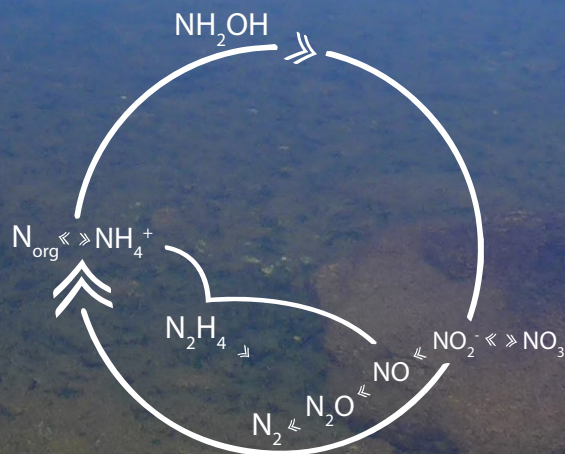
ACKNOWLEDGMENTS

We thank the authorities of the Aigüestortes and Estany de Sant Maurici National Park for sampling facilities in protected areas and support.



4

Article II



4. Article II

Estimating sediment denitrification rates using cores and N₂O microsensors

4.1. SHORT ABSTRACT

This method estimates sediment denitrification rates in sediment cores using the acetylene inhibition technique and microsensor measurements of the accumulated N₂O. The protocol describes procedures for collecting the cores, calibrating the sensors, performing the acetylene inhibition, measuring the N₂O accumulation, and calculating the denitrification rate.

4.2. LONG ABSTRACT

Denitrification is the primary biogeochemical process removing reactive nitrogen from the biosphere. The quantitative evaluation of this process has become particularly relevant for assessing the anthropogenic-altered global nitrogen cycle and the emission of greenhouse gases (i.e., N₂O). Several methods are available for measuring denitrification, but none of them are completely satisfactory. Problems with existing methods include their insufficient sensitivity, and the need to modify the substrate levels or alter the physical configuration of the process using disturbed samples. This work describes a method for estimating sediment denitrification rates that combines coring, acetylene inhibition, and microsensor measurements of the accumulated N₂O. The main advantages of this method are a low disturbance of the sediment structure and the collection of a continuous record of N₂O accumulation; these enable estimates of reliable denitrification rates with minimum values up to 0.4–1 μmol N₂O m⁻² h⁻¹. The ability to manipulate key factors is an additional advantage for obtaining experimental insights. The protocol describes procedures for collecting the cores, calibrating the sensors, performing the acetylene inhibition, measuring the N₂O accumulation, and calculating the denitrification rate. The method is appropriate for estimating denitrification rates in any aquatic system with retrievable sediment cores. If the N₂O concentration is above the detection limit of the sensor, the acetylene inhibition step can be omitted to estimate the N₂O emission instead of denitrification. We show how to estimate both actual and potential denitrification rates by increasing nitrate availability as well as the temperature dependence of the process. We illustrate the procedure using mountain lake sediments and discuss the advantages and weaknesses of the technique compared to other methods. This method can be modified for particular purposes; for instance, it can be combined with ¹⁵N tracers to assess nitrification and denitrification or field *in situ* measurements of denitrification rates.

Original Work: Palacin-Lizarbe, C., Camarero L., and Catalan J (2018). Estimating sediment denitrification rates using cores and N₂O microsensors. *Journal of Visualized Experiments* (142), e58553. <https://doi.org/10.3791/58553>.

4.3. INTRODUCTION

Anthropogenic alteration of the nitrogen cycle is one of the most challenging problems for the Earth system (Rockstrom et al. 2009). Human activity has at least doubled the levels of reactive nitrogen available to the biosphere (Erismann et al. 2011). However, there remain large uncertainties regarding how the global N cycle is evaluated. A few flux estimates have been quantified with less than $\pm 20\%$ error, and many have uncertainties of $\pm 50\%$ and larger (Gruber and Galloway 2008). These uncertainties indicate the need for accurate estimations of denitrification rates across ecosystems and an understanding of the underlying mechanisms of variation. Denitrification is a microbial activity through which nitrogenous oxides, mainly nitrate and nitrite, are reduced to dinitrogen gases, N_2O and N_2 (Tiedje 1988). The pathway is highly relevant to the biosphere availability of reactive nitrogen because it is the primary process of removal (Seitzinger et al. 2006). N_2O is a greenhouse gas with a warming potential nearly 300 times that of CO_2 over 100 years, and it is the current major cause of stratospheric ozone depletion due to the large quantities being emitted (Ravishankara et al. 2009, IPCC 2013).

In the following, we present a protocol for estimating sediment denitrification rates using cores and N_2O microsensors experimentally (Figure 4.1). Denitrification rates are estimated using the acetylene inhibition method (Balderston et al. 1976, Yoshinari and Knowles 1976) and measurements of the accumulation of N_2O during a defined period (Figures 2, 3). We demonstrate the method by applying it to mountain lake sediments. This case study highlights the performance of the method for detecting relatively low rates with minimal disturbance to the physical structure of the sediments.

Denitrification is particularly difficult to measure (Groffman et al. 2006). There are several alternative approaches and methods, each with advantages and disadvantages. Drawbacks to available methods include their use of expensive resources, insufficient sensitivity, and the need to modify the substrate levels or alter the physical configuration of the process using disturbed samples (Groffman et al. 2006). An even more fundamental challenge to measuring N_2 is its elevated background levels in the environment (Groffman et al. 2006). The reduction of N_2O to N_2 is inhibited by acetylene (C_2H_2) (Balderston et al. 1976, Yoshinari and Knowles 1976). Thus, denitrification can be quantified by measuring the accumulated N_2O in the presence of C_2H_2 , which is feasible due to low environmental N_2O levels.

The use of C_2H_2 to measure denitrification rates in sediments was developed about 40 years ago (Sørensen 1978), and the incorporation of N_2O sensors occurred about 10 years later (Revsbech et al. 1988). The most widely applied acetylene-based approach is the “static core.” The accumulated N_2O is measured during an incubation period of up to 24 h after the C_2H_2 is added to the headspace of the sealed sediment core (Groffman et al. 2006). The method described here follows this procedure with some innovations. We add the C_2H_2 by bubbling the gas in the water phase of the core for some minutes, and we fill all the headspace with sample water before measuring the accumulation of N_2O with a microsensor. We also include a stirring system that prevents the stratification of the water without resuspending the sediment. The procedure quantifies the denitrification rate per sediment surface area (e.g., $\mu\text{mol } N_2O \text{ m}^{-2} \text{ h}^{-1}$).

The high spatial and temporal variation of denitrification presents another difficulty in its accurate quantification (Groffman et al. 2006). Usually, N_2O accumulation is measured sequentially by gas chromatography of headspace samples that are collected during the incubation. The method described provides improved monitoring of the temporal variation of the N_2O accumulation, because the microsensor provides a continuous signal. The microsensor multimeter is a digital microsensor amplifier (picoammeter) that interfaces with the sensor(s) and the computer (Figure 4.1a). The multimeter allows several N_2O microsensors to be used at the same time. For instance, up to four sediment cores from the same study site can be measured simultaneously to account for the spatial variability.

The core approach barely disturbs the sediment structure compared to some other methods (e.g., slurries). If the integrity of the sediments is altered, this leads to unrealistic denitrification rates (Jørgensen 1989) that are only adequate for relative comparisons. Higher rates are always obtained with slurry methods compared to core methods (Laverman et al. 2006), because the latter preserves the limitation of denitrification by substrate diffusion (Ambus 1993). Slurry measures cannot be considered representative of *in situ* rates (Christensen et al. 2000); they provide relative measures for comparisons made with the exact same procedure.

The method described is appropriate for estimating denitrification rates in any sediment type that can be cored. We particularly recommend the method for performing experimental manipulations of some of the driving factors. Examples are experiments that modify nitrate availability and temperature as needed for estimating the energy activation (E_a) of denitrification (**article III**) (Figure 4.2).



Figure 4.1: Experimental setup. (a) General experimental setup to estimate sediment denitrification rates using cores and N_2O microsensors. The incubation chamber ensures darkness and controlled-temperature (± 0.3 °C) conditions. Five intact sediment cores can be processed simultaneously using their respective N_2O sensors. (b) N_2O sensor calibration chamber. We adapted it with rubber stoppers and syringes to mix the N_2O water (see protocol step 3.4.3). There is a thermometer to control the water temperature. (c) Detail of a sediment core sample with the sensor inserted into the central hole of the PVC cover and the joints sealed with adhesive tape. The stirrer is hanging in the water, and the electromagnet is close to it and fixed to the external part of the acrylic tube. (d) Detail of the N_2O microsensors tip protected by a metal piece. (e) A sediment core just recovered. It was sampled from a boat in a deep lake; the acrylic tube with the core is still fixed to the messenger-adapted gravity corer (Glew 1991). See the Table of Materials with all the items needed to perform this method.

4.4. PROTOCOL

1. Preparation

NOTE: begin this on the day before the measurements are taken.

1.1. Assemble the measurement setup (Figure 4.1a, see the Table of Materials).

NOTE: To ensure a constant and high-quality power supply, the measurement device is connected to the grip via an uninterruptible power supply (UPS) that can also act as a backup. In the case of a long-duration power failure, a car battery can provide an extra power source.

1.2. Start the sensor's software and apply a -0.8 V voltage to polarize the N₂O microsensors. The signal shows a rapid descent and a subsequent rise, and then it finally decreases until it is low and stable.

NOTE: The microsensor manufacturer recommends polarization at least overnight (or longer) to ensure the stability of the sensor's signal. Another recommendation is to keep the sensor polarized if measurements are planned for multiple or consecutive days (Unisense S/A 2011).

1.2. Switch on the incubation chamber and adjust the experimental conditions (e.g., selected light off and temperature set to be similar to that expected in the field). Place a container with deionized water inside the chamber so that water is available later at the measurement temperature for calibration of the sensors.

NOTE: This step can be done the same day of the planned measurements, before the departure to collect the cores. For standard measurements, it is advisable to use dark conditions.

1.3. Pack the field core collection materials: corer device, sampling tubes, rubber stoppers, polyvinyl chloride (PVC) taps, screwdriver, GPS, thermometer, handheld sounder, wader, and inflatable boat (see the Table of Materials). Use a checklist to ensure all materials are included.

2. Sediment core collection

2.1. Depending on water depth, follow 2.1.1 or 2.1.2.

2.1.1. For deep water bodies

2.1.1.1. Use a messenger-adapted gravity corer (Glew 1991) from a boat or a platform (Figure 4.1e).

2.1.1.2. Fix the sampling tube (acrylic, \varnothing 6.35 cm, length \geq 50 cm) to the corer with a screwdriver.

- 2.1.1.3. Select the sampling point according to the investigation aims. Take note of the position (e.g., using GPS coordinates) and measurement depth (e.g., using a handheld sounder). If you sample from a boat, use an anchor (e.g., a bag with stones) to avoid drifting during core collection.
 - 2.1.1.4. Deploy the coring system until the sampling tube is ~1 m from the sediment. Use a rope with regular marks (e.g., intervals of 1 m) to control the depth position of the sampling equipment.
 - 2.1.1.5. Stabilize the sampling equipment for 60 s to minimize the movement of the boat. This will ensure the correct sediment penetration and recovery of a scarcely disturbed sediment core.
 - 2.1.1.6. Release ~1 m more rope so that the sampling tube penetrates the sediment. Be aware that if the sampling tube penetrates too much, it can disturb the water/sediment interface.
 - 2.1.1.7. Release the messenger while trying to keep tension in the rope so that the corer remains fixed and in a vertical position. When the messenger impacts the corer, a small difference can be felt in the tension of the rope. At that time, the corer should be closed to generate the vacuum that allows for recovery of the sediment core.
 - 2.1.1.8. Recover the corer by pulling the rope constantly and gently.
 - 2.1.1.9. Once the core is close to the surface but still entirely submerged (including the rubber part of the corer that ensures the vacuum), place a rubber stopper at the bottom of the sampling tube. Inspect the water/sediment interface; it should be clear and not visibly disturbed (Figure 4.1e). If this is not the case, discard the core, clean the tube, and repeat steps 2.1.1.4–9.
 - 2.1.1.10. Uplift the entire coring system from the water. Release the sampling tube from the corer and place a PVC cover on the top. Seal it with adhesive tape. Avoid the formation of air space.
- 2.1.2. For littoral habitats and shallow water bodies
- 2.1.2.1. Dress in a wader for sampling in very shallow waters (< 0.6 m).
 - 2.1.2.2. Use snorkeling or scuba diving for deeper sampling (up to 3 m).
 - 2.1.2.3. Select the sampling point according to the investigation aims. Take note of the position (e.g., GPS coordinates). Manually, deepen the sampling tube (e.g., acrylic, \varnothing 6.35 cm) into the sediment.

2.1.2.4. Place a rubber stopper in the top side of the sampling tube to obtain a vacuum.

2.1.2.5. Remove the core from the sediment and quickly introduce another rubber stopper at the tube bottom.

Note: It is necessary to work at all times with the tube underwater, so in very shallow sites, a recommendation is to shorten the tube up to 20 cm. Sometimes the sediment has a high water content and drains when the tube is removed from the sediment bed. In this case, it is necessary to introduce the bottom stopper without uplifting the core outside the sediment. To do this, manually immerse the stopper in the sediment around the tube and place it carefully to close the bottom of the tube.

2.1.2.6. Out of the water, substitute the topside rubber stopper with a PVC cover and seal the junction with adhesive tape.

2.2. Protect the core during its transfer to the laboratory by minimizing rotations and shaking.

3. Calibration of the nitrous oxide (N₂O) microsensors

3.1. Using the computer (strip chart, sensor software), check that the sensor's signal is stable and low (<20 mV).

3.2. Create a new file (e.g., with the date and the sampling site (130903_Redon_Lake)) to record the calibration values and sensor signals.

NOTE: The sensor signals are sensitive to temperature (Figure 4.4). Use the same temperature for the measurements and the sensor calibration. The sensor responds linearly between 0%–2.5% N₂O (Andersen et al. 2001). Therefore, a two-point calibration is sufficient (Unisense S/A 2011).

3.3. For the calibration value with zero nitrous oxide, read the sensor signal keeping the sensor tip submersed in N₂O-free water (deionized).

3.4. Calibrate with N₂O water at the desired concentration.

NOTE: Prepare water with a defined N₂O concentration, which will slightly exceed the maximum concentration expected during incubation. We use ~25 μM N₂O as the calibration value. Be aware of not exceeding the maximum sensor range concentration of 500 N₂O μM.

3.4.1. Obtain N₂O-saturated water by bubbling N₂O in deionized water for a few minutes.

NOTE: The N₂O water solubility depends on temperature and salinity (Weiss and Price 1980); see the table in the appendix of the sensor manual (Unisense S/A 2011).

3.4.2. Dilute the N₂O saturated water by adding a certain volume of saturated N₂O water to a volume of deionized water. For example, at 20 °C, adding 0.3 ml of saturated N₂O water, which has a concentration of 28.7 mM N₂O, to a total of 375 ml of water results in 22.9 μM N₂O water. Note that 375 ml is the total volume of the calibration chamber (Figure 4.1b).

3.4.3. After gently mixing the N₂O saturated water with deionized water in the calibration vessel to dilute it to the desired concentration, read the sensor signal when it is constant. This reading is the calibration value with X μM N₂O water. When mixing the solution, be careful not to generate bubbles, as this would eliminate N₂O from the calibration solution.

NOTE: Be aware that the N₂O in the water will slowly escape into the air; thus, the prepared calibration solution can only be used for a few minutes.

4. Core preparation and acetylene inhibition

4.1. Change the PVC cover located at the top of each sediment core by another cover with a hole in the center and a hanging magnetic stirrer. Re-seal the junction with adhesive tape.

4.2. Reduce the water phase of each sample to an approximate height of 12 cm (volume ≈ 380 mL). For this, first, insert a silicone tube in the central hole. Then, put the sediment core in a cylinder and push the bottom stopper to create pressure. The stopper and sediment sample go up, and the excess water passes through the tube. Collect the water in a recipient vessel.

NOTE: Samples with coarse granularity can be problematic during this step. Sediment particles placed between the stopper and the tube can deform the stopper and open a hole through which air bubbles can pass and disturb the sample. To avoid this problem, put the cylinder in the center of the bottom stopper and try to push with a constant force. The joint between the silicone tube used to evacuate the excess water and the PVC cover consists of a solid part (e.g., a 5 ml pipette tip without its narrowest end) inserted in the silicone tube.

4.3. Perform the acetylene inhibition by bubbling with acetylene gas in the water phase of the core for approximately 10 min. Avoid resuspending the sediment.

NOTE: As a possible modification of the method, add a substrate (nitrate) through a concentrated liquid medium before bubbling acetylene for potential denitrification measurements (e.g., as in Figure 4.3b, c).

5. Denitrification (N₂O accumulation measure)

5.1. Place the sensor in the sediment core through the central hole of the topside PVC cover. The tip of the sensor should be located in the water phase above the stirrer (Figure 4.1c). Fill all

the air space with the previous leftover water before sealing the junction sensor PVC cover.

NOTE: All the joints of the acrylic sampling tube must be sealed to avoid gas and water leaks during the measurement (Figure 4.1a, c). In the bottom part of the tube, the rubber stopper is sufficient for this. Sealing the topside part is more difficult. The PVC cover must be tuned. It must be heated with a torch; then, when the material becomes flexible but is not scorched, the cover is placed in the tube so that its shape can be molded. After cooling, the cover needs more modifications (with the exception of the cover used to transport the samples to the laboratory in steps 2.1.1.10 or 2.1.2.6). The central hole where the sensor is inserted must be drilled. The stirrer can be held with fishing line, which in turn is adhered with glue to the inside of the cover so that the stirrer hangs on the fishing line in the water (Figure 4.1c). Also, all the joints (PVC cover tube and PVC cover sensor) are sealed with adhesive tape. Place elastic adhesive tape to adjust the diameter of the sensor in order to seal the contact surface between the central hole of the PVC cover and the sensor (Figure 4.1c).

5.2. Switch on the electromagnetic pulse circuit that is part of the stirring system.

NOTE: The stirring system prevents the stratification of the water phase without disturbing (resuspending) the sediment. The stirring system consists of a circuit that switches on/off the electromagnet that attracts/releases the magnetic stirrer (see the Table of Materials for a detailed description).

5.3. Move the electromagnet around the external part of the acrylic tube until the stirrer moves continuously, and then fix it in place using adhesive tape (Figure 4.1c).

5.4. Close the incubation chamber to ensure a constant temperature (e.g., ± 0.3 °C).

5.5. Press the record button (sensor software) to start recording the sensor signal. Readings are typically recorded every 5 min.

5.6. Press the stop button at the end of the measurement period.

6. Final measurement steps

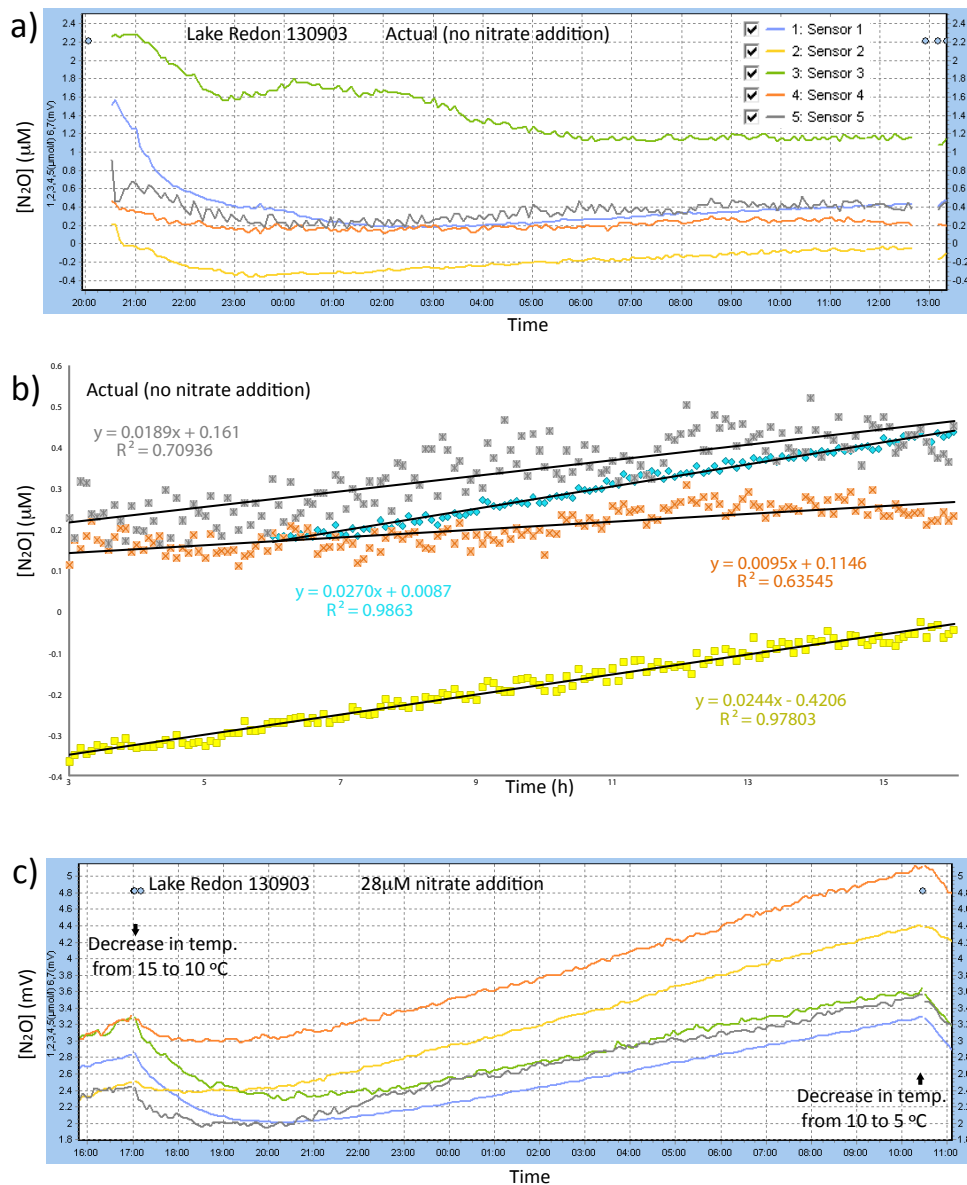
6.1. Wait at least ~10 min with the sensor's tip submerged in free-N₂O water (deionized) before reading the signal of the zero N₂O calibration measure.

6.2. Perform a final sensor calibration. For this, repeat the sensor calibration, following Section 3 but starting with step 3.3.

6.3. Save the file (sensor software).

7. Denitrification rate calculations

- 7.1. Start with the Excel output file generated by the sensor software that contains the record of the sensor's signal in mV and $\mu\text{M N}_2\text{O}$ and the calibration data.
- 7.2. Plot the sensor signal against time to visualize the N_2O accumulation trend (e.g., Figure 4.2a).
- 7.3. Use only the time range with a **linear accumulation**, excluding the initial acclimation period of the sample and a possible final saturation due to substrate limitation (e.g., Figure 4.2b). Create a linear model of the sensor signal (μM) over time (h). The slope is the denitrification rate ($\mu\text{M N}_2\text{O core}^{-1} \text{ h}^{-1}$), which, if divided by the area of the core (πr^2), transforms into the rate in $\mu\text{M N}_2\text{O m}^{-2} \text{ h}^{-1}$, and multiplied by the water volume ($h \pi r^2$, where h is the height of the water phase and r is the inner radius of the acrylic tube, in this case 0.12 m and 0.03175 m, respectively), it transforms into the rate in $\mu\text{mol N}_2\text{O m}^{-2} \text{ h}^{-1}$.



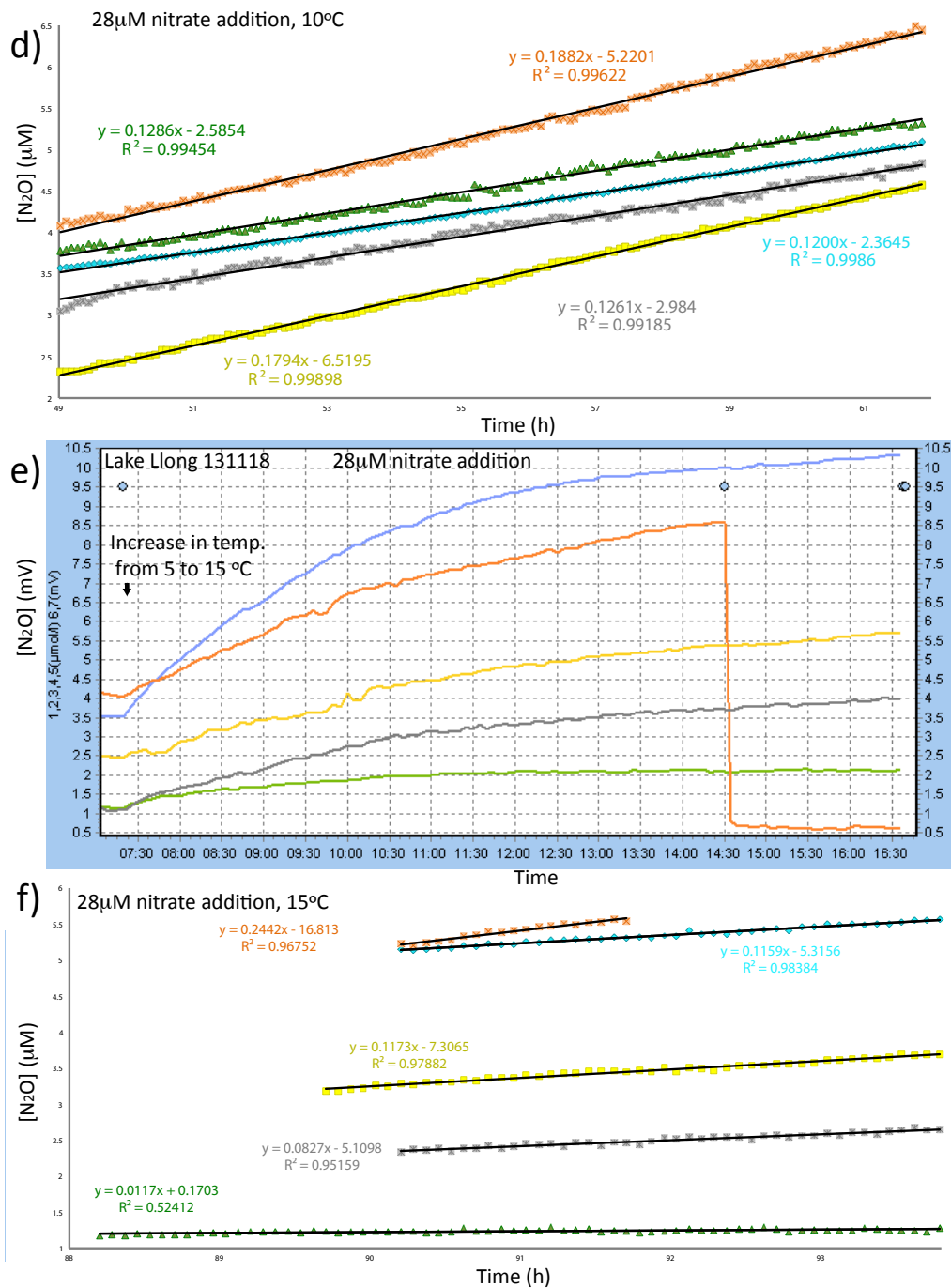


Figure 4.2: Denitrification rate calculations in a temperature dependence experiment. We show actual (panels a and b) and potential denitrification measurements (panels c–f). When we decrease the temperature of the measurement (c), at first the sample cools and the sensor signal, which is temperature dependent, declines. (a) A similar event occurs at the start of the incubation in the actual denitrification measurement; the warmer laboratory environment with respect to the incubation conditions produces a cooling of the sample, again accompanied by a decline in the sensor signal. (e) When we increase the temperature, at first the samples warm and the sensor signal increases exponentially instead of linearly. When the samples reach a constant temperature, the sensor signal increases linearly as usual. In all cases, it is possible to calculate the denitrification rates just by using the period of linear N_2O accumulation (b, d, and f). (b) Inactive sample 3 is not shown.

4.5. REPRESENTATIVE RESULTS

A total of 468 denitrification rates were estimated using the protocol above in sediments from Pyrenean mountain lakes over the period 2013–2014. We show some of these results to illustrate the procedure (Figures 2 and 3). In general, the linear model between the N_2O concentration and time has good correlation ($R^2 \geq 0.9$). The slope of the relationship provides an estimate of the denitrification rate (step 7.3; e.g., Figure 4.2d). If the denitrification activity is very low, the sensor's electronic noise becomes more important and the goodness of fit declines (e.g., sensors 4 and 5 in Figures 2b and 3a). Although the baseline detection limit of N_2O is $\sim 0.1 \mu\text{M}$ in water (Unisense S/A 2018), which is an intermediate value concerning alternative methods (Koike 1990), the possibility of accumulating thousands of continuous measurements to filter the noise permits estimates at relatively low denitrification rates, up to $\sim 1 \mu\text{mol N}_2\text{O m}^{-2} \text{ h}^{-1}$ (Figures 2, 3). Lower rates (i.e., $\sim 0.4 \mu\text{mol N}_2\text{O m}^{-2} \text{ h}^{-1}$) can be estimated by narrowing the water phase of the core sample to a height of 8 cm (see protocol step 4.2).

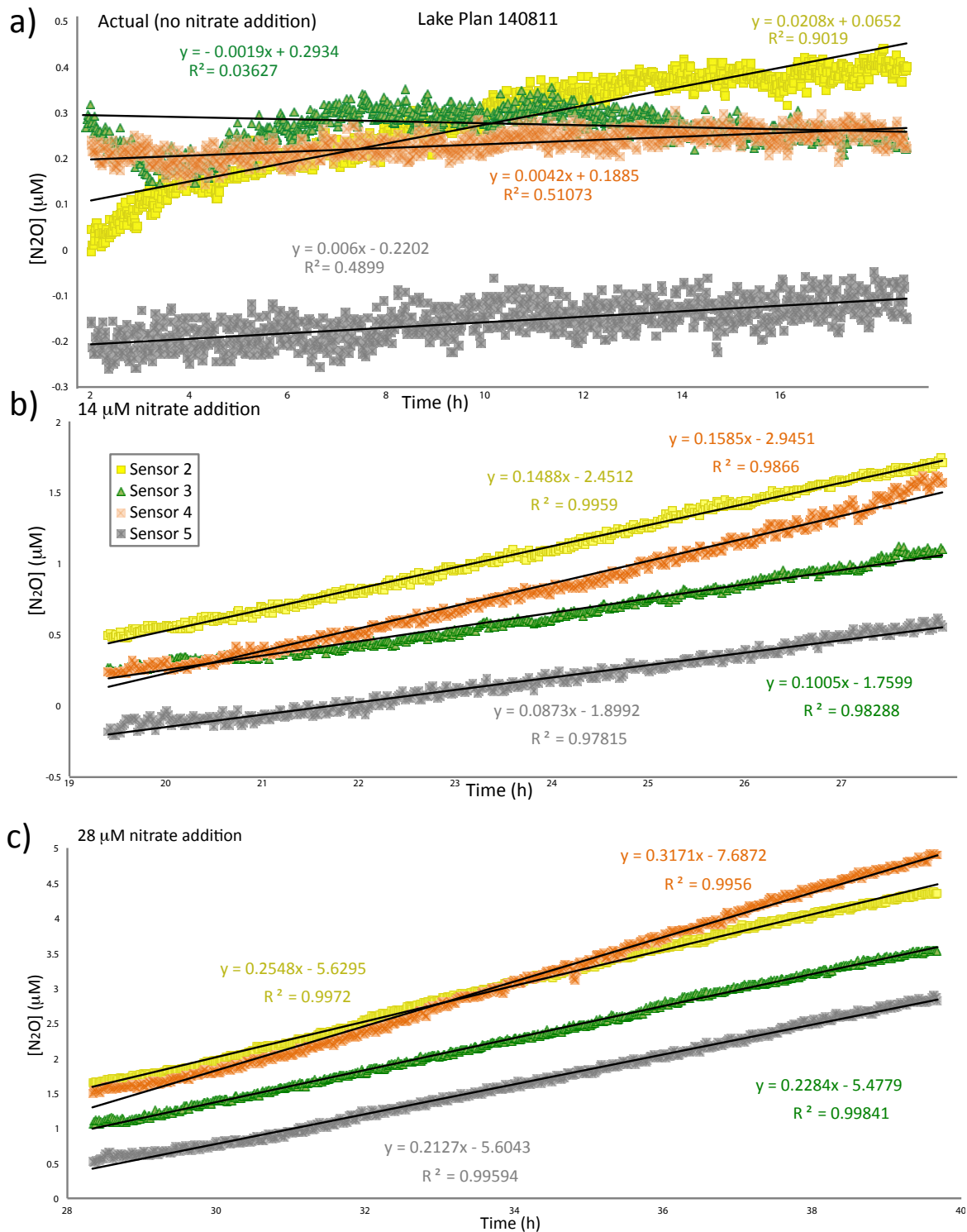


Figure 4.3: Examples of denitrification rate calculations. Actual (panel a) and potential (panels b and c) denitrification rates were estimated. We only used the time range with a linear N_2O accumulation to calculate the denitrification rate (slope of the linear model). However, in (a), for educational purposes, we show all the measurements (models) with more and less success; we would discard sample 3 due to the high instability of the sensor and sample 2 due to saturation in the N_2O accumulation. (a) Samples 4 and 5 with rates of 0.5 and 0.7 $\mu mol N_2O m^{-2} h^{-1}$, respectively, are cases of measurements near the detection limit of the method.

4.6. DISCUSSION

The main advantages of the described method are the use of minimally disturbed sediment core samples and the continuous recording of the N_2O accumulation. These allow estimates of relatively low denitrification rates that are likely similar to those occurring *in situ*. Nonetheless, there are some aspects to discuss concerning the coring, sensor performance, and potential improvements.

An apparently simple but critical step of the method is good core recovery. The sediment/water interface must satisfy three criteria: (1) no modification in its chemical or constituent composition, (2) no alteration in the water content or void ratio, and (3) no structure perturbation (Hvorslev 1949). The fewer disturbances suffered by the sample during the entire protocol, the more realistic and closer to *in situ* conditions will be the measured denitrification rate. There are several devices/techniques for the sediment core collection (Glew et al. 2001), and their selection depends on the water depth. We use a messenger-adapted gravity corer (Glew 1991) for deep samples (Figure 4.1e) because it is a reasonably light device and can rapidly recover short cores (Glew et al. 2001) (a core sediment of ≥ 10 cm length is more than enough to encompass the oxic and denitrifying layer in sediments (Laverman et al. 2007, Behrendt et al. 2013, Melton et al. 2014)). In coring jargon, “feel” is often referred to as the ability to know the location of the corer (whether it is still in the water column or already in the sediment) and whether it is open or closed (Glew et al. 2001). For intermediate water depths (5–50 m), usually there are no difficulties with feeling. A loss of feeling occurs in deeper water (>50 m) because the movements of the water column may mask the location of the corer (Glew et al. 2001). Feeling may also be lost in shallow water (<3 m) due to lateral drift and wave action (Glew et al. 2001); this is why we use a different method in shallow water, either direct manual coring by scuba diving or dressing in a wader. With this system, the person sampling can see the sediment and choose the exact place before coring; this allows, e.g., the sampling of a sediment core that contains a macrophyte. After sampling, the researcher must continue to work carefully to minimally disturb the sediment core sample during the rest of the protocol, especially when performing acetylene inhibition by bubbling.

Some details must be considered when using N_2O microsensors. The sensor software provides a continuous visualization (strip chart) of the sensor signal (background frequency of 1000 Hz) (Unisense S/A 2010). These raw data and the strip chart (e.g., Figure 4.2a) can be saved. It is necessary to check the correct behavior of the sensor after its polarization (e.g., when returning from field collection before step 4). In particular, a low (<20 mV) and constant base signal is expected when it is submerged in N_2O -free water. Recalibrate the sensor shortly (~ 2 h) after you start using it; if it has already been used for some days, the interval can be extended (~ 24 h) (Unisense S/A 2011). To minimize recalibrations, keep the sensor polarized unless it is not used for several days (Unisense S/A 2011). Over time, a change in the sensor signal may occur, up to 50% in months, which is due to a different permeability of its membrane (Unisense S/A 2011). The lower the electronic interference in the laboratory, the more constant and stable will be the sensor signal. In that sense, using a UPS improves the quality of the electrical energy that reaches the measurement device by filtering the voltage fluctuations. The sampling interval, selected in the Logger tab, is different from the background frequency. Each registered point is generated from the average of many measurements. The sampling interval (up to 10 s) indicates the frequency with which a data point is recorded. The number of measurements per unit of time used in the average is defined by the background frequency (Unisense S/A 2010). For instance, if we set a sampling frequency of 5 s and a background frequen-

cy of 500 measurements per second, then the data points are recorded every 5 s and the average of the 500 samples per second is measured during the previous 5 s. We record the sensor signal every 5 minutes (sampling interval) and set the background frequency to 1000 measurements per second. The study system must be known to select the correct sampling interval without “averaging” expected fluctuations. In highly active systems, short sampling intervals are recommended, while longer intervals allow optimizing the computer’s memory (Unisense S/A 2010). Some possible interfering substances (H_2S , NO , and CO_2) can affect the N_2O sensor’s signal (Unisense S/A 2018). The sensor is calibrated with deionized water, but the samples can contain interfering substances and modify the sensor’s reference signal. This situation could explain why negative values appear in samples 2 and 5 in Figures 2b and 3a, respectively. However, when the objective is to estimate the denitrification rate, the exact level of N_2O is not the key parameter. What is key is the slope of the linear model (evidencing a linear accumulation of N_2O). Finally, it is necessary to work with a fixed temperature because the response of the N_2O sensor changes with temperature (Figure 4.4).

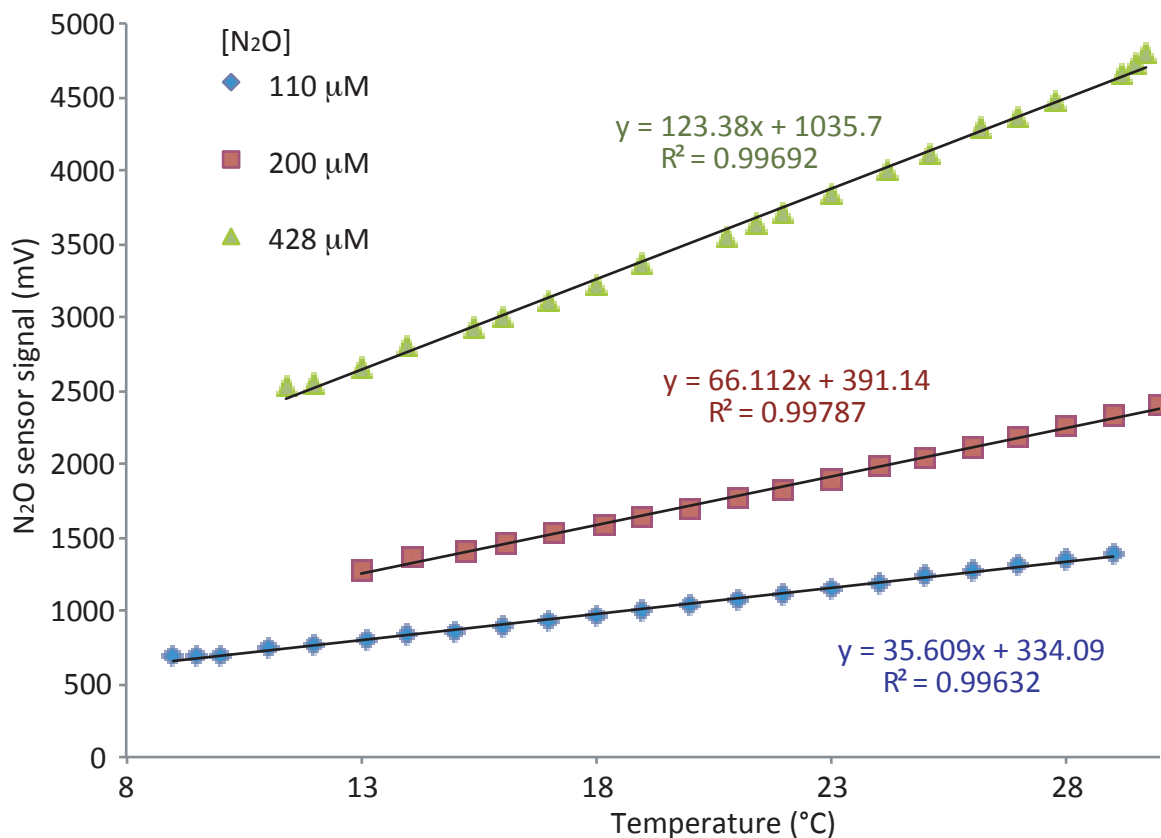


Figure 4.4: Temperature dependence of the N_2O microsensor response. The different slope of the linear model of the sensor signal versus the temperature at each N_2O concentration shows the temperature effect on the sensor’s signal.

Simple modifications or additions to the protocol also enable (1) characterization of the environmental conditions controlling the measured denitrification rates, (2) estimates of the potential denitrification rates by simulating the response to a driving gradient (e.g., nitrate), and (3) estimates of the sediment N_2O emission rates by skipping the C_2H_2 inhibition.

Depending on the study aims, several complementary measurements can be made: (1) just after recovering the core, *in situ* conditions, e.g., temperature; (2) before the measurement, samples of the water phase, e.g., $[NO_3^-]$; and (3) after the measurement, extrusions and slices of the core at different resolutions (mm-cm) (Glew et al. 2001, Schwing et al. 2016), following the procedures explained in Schwing et al. (2016).

To measure the potential denitrification rates, add nitrate to the water-phase of the core (e.g., Figure 4.2, 3) as described in (**article III**). If doing so, add the nitrate before the C_2H_2 inhibition (step 4.3). Also, if nitrate is added, it is advisable to also add carbon (C; e.g., acetate) and phosphorus (P) to maintain the *in situ* stoichiometric proportions of C, N, and P (e.g., in the surface sediment). This will prevent the limitation of denitrification by these elements (Bernhardt 2013, Finlay et al. 2013), and will also keep the C/N ratio that can influence the dominance of the nitrate consumption process (i.e., denitrification vs. dissimilatory nitrate reduction to ammonium (DNRA)) (Tiedje 1988). Anoxia can be fixed by bubbling an N_2 - CO_2 mixture for a few minutes, after the nitrate addition, to prevent oxygen interference with denitrification; however, note that this leads to a blockage of nitrification. To calculate sediment N_2O emission rates, omit the C_2H_2 inhibition (step 4.3). However, keep in mind that, as far as it is currently known in aquatic ecosystems, N_2O emissions are proportionally low compared to N_2 emissions (0%–4.3%) (Seitzinger 1988), so it is possible that the accumulated N_2O will be below the detection limit. If this is the case, an option is to add nitrate to increase the emitted N_2O , calculating potential N_2O emissions.

The main weakness of the method is the inhibition of nitrification by C_2H_2 (Seitzinger et al. 1993, Groffman et al. 2006). During the incubation, this inhibition of nitrification and the incomplete inhibition of N_2O reduction may become apparent, as both are very time dependent. For instance, the starting N_2O accumulation rate must reveal the real denitrification rate and progressively decay as the nitrate availability drops and N_2O diffuses into the nitrate free zone, where it is reduced (Christensen et al. 1989). Therefore, an estimated denitrification rate can be considered valid only if the readings show a linear accumulation of N_2O (Groffman et al. 2006).

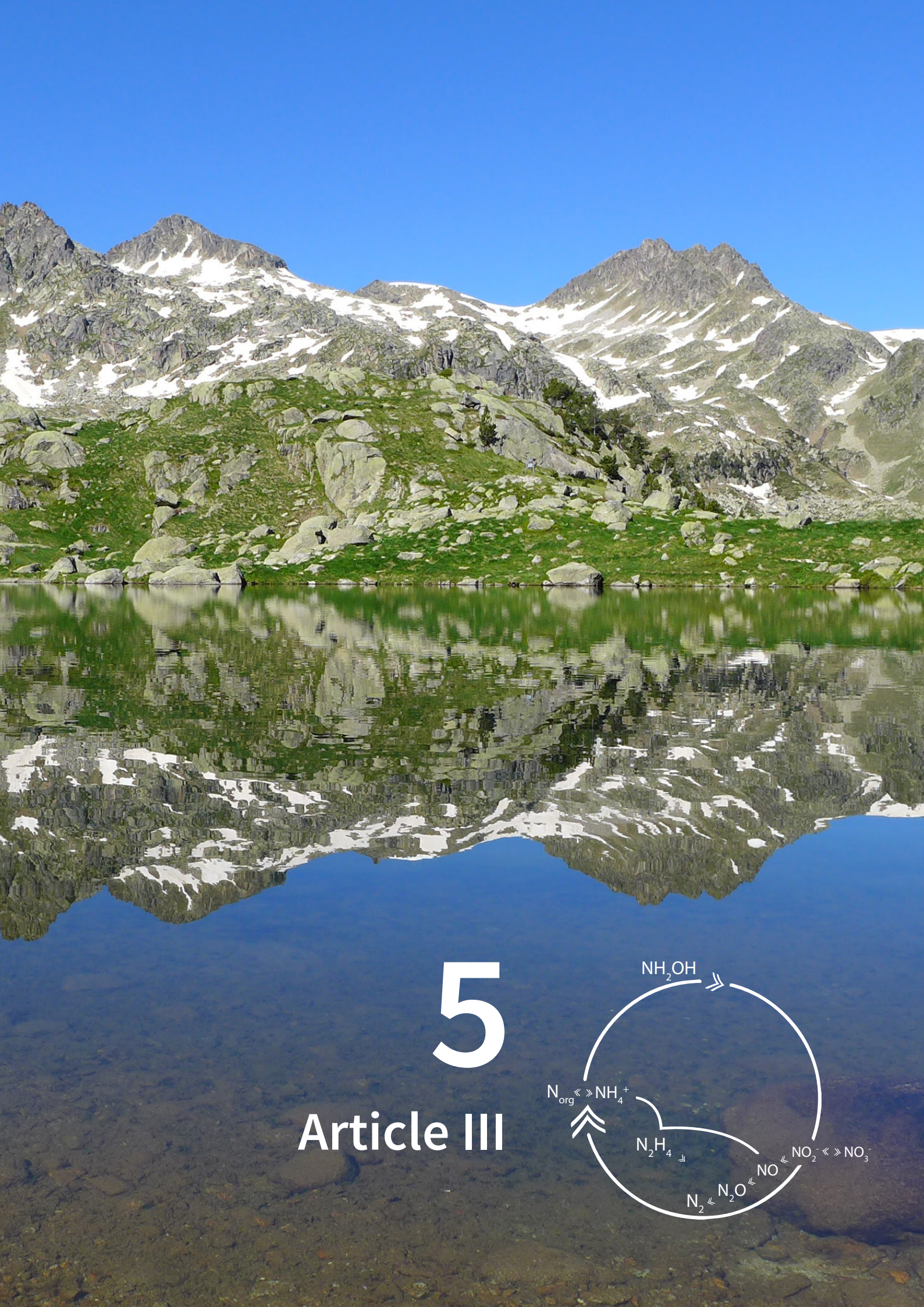
The method described estimates a denitrification rate per area that integrates the entire sediment activity. In this respect, there is some uncertainty about the radius of action of the acetylene inhibition when bubbling the gas in the aqueous phase of the sample. It is assumed that, at least, inhibition of the surficial layer of the sediment occurs, which is the one with the highest denitrification rates (Laverman et al. 2007, Behrendt et al. 2013).

Possible improvements to the method are its combined use with ^{15}N tracers and modifications that could allow the measurement of denitrification *in situ*. ^{15}N tracer methods can be used to determine the proportion of nitrification-denitrification coupling occurring in the samples (Peter 1992), and it can also account for other N flux processes besides denitrification (e.g., anammox and DNRA) (Jørgensen 1989, Risgaard-Petersen et al. 2003). However, these methods have the drawback of changing the substrate concentration (Groffman et al. 2006). Behrendt et al. (2013) use a method combining N_2O microsensors, C_2H_2 inhibition, and ^{15}N tracers to analyse the vertical activity

distribution of dissimilatory nitrate reduction processes (denitrification and DNRA) in sediments. They made vertical profiles in the sediment by penetrating the sediment with the sensors. The main difficulty in measuring denitrification *in situ* is the ability to handle a nonconstant temperature environment. It is necessary to record the N₂O accumulation and temperature simultaneously and then correct the N₂O sensor's signal by the temperature dependence during the denitrification rate calculations. This correction requires a previous analysis of the temperature dependence of the N₂O signal for each sensor. The sensors are handmade, and each one responds differently to temperature (e.g., sensor 1 shows a higher temperature dependence than the others in Figure 4.2c, e).

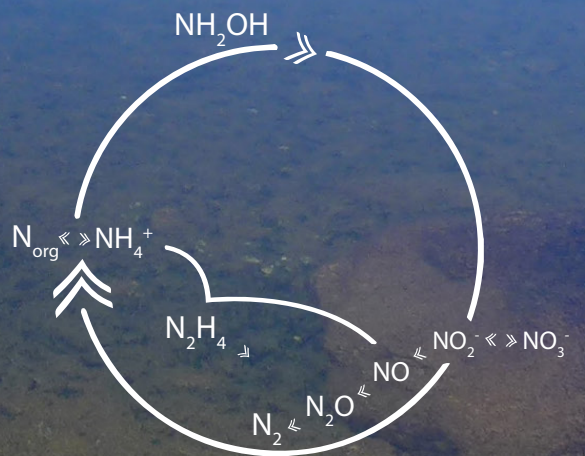
ACKNOWLEDGMENTS

The Spanish Government provided funds through the Ministerio de Educación as a predoctoral fellowship to C.P-L. (FPU12–00644) and research grants of the Ministerio de Economía y Competitividad: NitroPir (CGL2010–19737), Lacus (CGL2013–45348-P), Transfer (CGL2016–80124-C2-1-P). The REPLIM project (INRE - INTERREG Programme. EUUN – European Union. EFA056/15) supported the final writing of the protocol.



5

Article III



5. Article III

Denitrification temperature dependence in remote, cold and N-poor lake sediments

5.1. Abstract

The reservoir size and pathway rates of the nitrogen (N) cycle have been deeply modified by the human enhancement of N fixation, atmospheric emissions, and climate warming. Denitrification (DEN) transforms nitrate into nitrogenous gas and thus removes reactive nitrogen (N_r) back to the atmospheric reservoir. There is still a rather limited knowledge of the denitrification rates and their temperature dependence across ecosystems; particularly, for the abundant cold and N-poor freshwater systems (e.g., Arctic and mountain lakes). We experimentally investigated the denitrification rates of mountain lake sediments by manipulating nitrate concentration and temperature on field collected cores. DEN rates were nitrate limited in field conditions and showed a large potential for an immediate DEN increase with both warming and higher N_r load. The estimated activation energy (E_a) for denitrification at nitrate saturation was 46 ± 7 kJ mol⁻¹ (Q_{10} 1.7 \pm 0.4). The apparent E_a increased with nitrate (μ M) limitation as $E_a = 46 + 419 [\text{NO}_3^-]^{-1}$. Accordingly, we suggest that climate warming may have a synergistic effect with N emission reduction to readjusting the N cycle. Changes of nitrate availability might be more relevant than direct temperature effects on denitrification.

Key Points

- Denitrification rates in mountain lakes are both nitrate and temperature limited.
- The apparent activation energy (E_a , kJ mol⁻¹) for denitrification depends on nitrate (μ M) as $E_a = 46 + 419 [\text{NO}_3^-]^{-1}$.
- The impact of nitrogen emission reductions on the adjustment of the nitrogen cycle may be enhanced by climate warming.

Original Work: Palacin-Lizarbe C., Camarero L., and Catalan J. (2018). Denitrification temperature dependence in remote, cold, and N-poor lake sediments. *Water Resources Research* 54, 1161-1173.

5.2. INTRODUCTION

The anthropogenic alteration of the nitrogen (N) cycle is one of the most challenging problems for the Earth system (Rockstrom et al. 2009). Human activity has at least doubled the levels of reactive nitrogen (N_r) available to the biosphere, largely as a result of the industrial N fixation for fertilizer productions and the burning of fossil fuels (Erisman et al. 2011). The global N cycle is still evaluated with high uncertainty. A few flux estimates are quantified with less than $\pm 20\%$ error and many have uncertainties of $\pm 50\%$ and larger (Gruber and Galloway 2008). The transient situation of the planet with many factors that influence the N cycle changing simultaneously, demands a deeper understanding of the factors controlling the rates of the N cycle pathways (Baron et al. 2013, Greaver et al. 2016). The temperature dependence of the rates of the distinct pathways is of particular interest for evaluating potential synergistic effects of climate warming and nitrogen emissions on N global cycle.

Denitrification (DEN) is the microbial activity by which nitrogenous oxides, mainly nitrate and nitrite, are reduced to dinitrogen gasses, N_2O and N_2 (Tiedje 1988). DEN is the primary process removing N_r from the biosphere (Seitzinger et al. 2006). The DEN dynamics is typically episodic; driven by the fluctuating coexistence of primary resources, favorable conditions, and the microbial agents. Consequently, DEN rates are difficult to measure, model and upscale. Existing methods are problematic for different reasons (Groffman et al. 2006). Much of the challenges arise from the fact that small areas (hot spots) and brief periods (hot moments) account for a high percentage of the denitrification activity both in terrestrial and aquatic ecosystems (Parkin 1987, McClain et al. 2003, Groffman et al. 2009). A substantial proportion of denitrification occurs in the upper part of the sediments, where necessary resources (e.g. N-oxides, fresh organic matter) meet anaerobic conditions. Lakes have been identified as the aquatic ecosystems with the highest seasonal and site variation in DEN rates (Piña-Ochoa and Alvarez-Cobelas 2006), although part of the observed variability could be due to the methods applied. Particularly, the alteration of the integrity of the samples markedly affects the DEN rate (r_d) measured. Higher values in slurries are obtained compared to undisturbed core sediments (Ambus 1993). The former cannot be considered representing *in situ* rates. They only provide relative measures for comparisons, if applied in the same way. However, if the target is to integrate DEN rates in the evaluation of the nitrogen cycle, there is an urgent demand of measurements in conditions as close as possible to the natural ones to reduce the uncertainty of the estimates and provide the elements for a reliable upscaling of the measurements (Galloway 2004, Gruber and Galloway 2008).

The temperature dependence of an enzymatic process can be described by its activation energy (E_a), which reflects the increase in the rate with temperature (Arrhenius 1915) when there is no resource limitation. However, the biogeochemical E_a includes also temperature effects on molecular kinetics, physiological acclimation by microbial strains and microbial assemblage changes (Hall et al. 2010, Crowther and Bradford 2013). In natural conditions, the E_a values reflect a multi-step process and thus can vary with the substrate availability (Brezonik 1994) and may depend on the particular assemblage of organisms performing the biogeochemical reaction (Hall et al. 2008). Each of these DEN control levels has a longer characteristic time, from instantaneous to a few days.

In lakes, sediment DEN rates at timescales below a few days are more likely to be constrained by the substrate supply than temperature fluctuations. Nitrate declines by the same DEN activity and their supply depend on other microbial activities (e.g., nitrification) and physical transport. When measuring DEN E_a , experimentally, some environmental conditions may depart easily from those *in situ*, either because of the use of an unrealistic temperature range (Boulétreau et al. 2012), very high nitrate addition (Holmes et al. 1996) or both. Alternatively, some observational approaches to estimate DEN E_a use activities (r_d) measured at periods of the year with contrasting temperature (Bachand and Horne 2000, Sheibley et al. 2003). In this case, the substrate availability may change but also the assemblage of microorganisms present.

Consequently, there are a number of aspects to consider in an assessment of the biogeochemical DEN E_a for a certain type of ecosystems (Fig. 5.1). They include 1) the general methodological approach; fundamentally, whether the approach is experimental, controlling the temperature change, or observational, using spatial or temporal natural temperature variation. 2) How the substrates (i.e., organic carbon, nitrogen) are considered; particularly, whether they are artificially saturated or maintained within natural conditions. And, 3) which are the biogeochemical processes that could be a source of added uncertainty in the assessment provided their competition for nitrate or nitrite or their release of nitrous oxide.

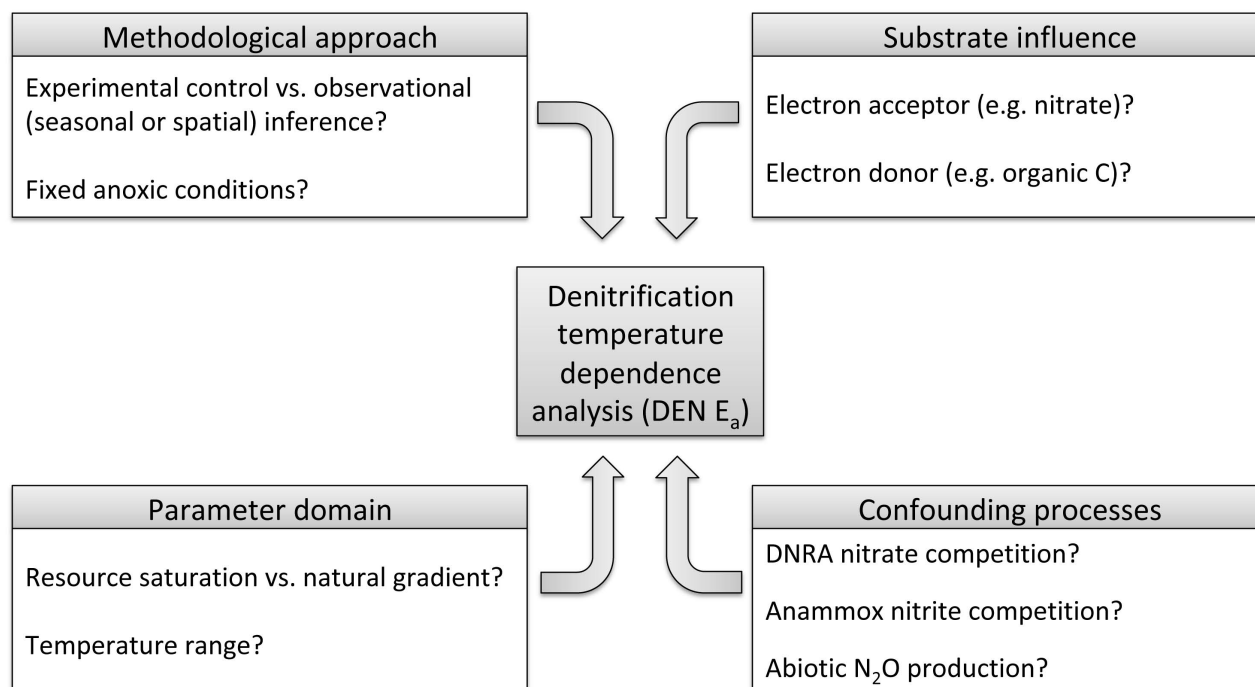


Figure 5.1. Main processes and aspects that affect the assessment of the denitrification temperature dependence.

There are few studies of the DEN E_a in oligotrophic systems (Holmes et al. 1996) and most are marine (Rysgaard et al. 2004, Canion et al. 2014b). In the current situation of Global Change, the case of remote ecosystems, those that are mostly influenced by atmospheric processes rather than direct human action in the watershed, are of particular interest. Many of these sites (e.g., alpine and subarctic regions) have, are or would experience increased N_r deposition (Holtgrieve et al. 2011) and warming (Smol 2012). Therefore, they are key sites for studying the interaction between temperature and the N cycle (Catalan et al. 2013).

The increase of N_r deposition is eventually reflected in the stream and lake loads depending on the degree of N saturation in the soil and vegetation (Stoddard 1994). Long-term sustained high N_r deposition results in a watershed quasi-steady-state so that N_r deposition and streams show similar temporal trends and fluctuations. One may expect that lakes would follow streams mid-term temporal patterns. However, recently, Camarero and Catalan (2012) have found an opposite trend during the last decades in the Pyrenees between lakes and streams. The latter follows the still N_r increasing tendency in the deposition, but lakes show a decline. The authors have attributed the opposed trends to an increase in lake productivity related to a higher phosphorus deposition. However, they were not able to evaluate whether an enhancement of denitrification could be an alternative explanation due to the lack of empirical information. The difficulty of the measuring DEN rates at low N_r concentrations may justify why remote systems have been overlooked with a few exceptions (McCrackin and Elser 2010, 2012, Vila-Costa et al. 2016, Castellano-Hinojosa et al. 2017). Indeed, it has been only one attempt to estimate DEN E_a in these systems (Myrstener et al. 2016). Consequently with this gap in knowledge, the aim of this study was to assess the DEN temperature dependence (E_a) in remote, cold and relatively N-poor lakes. From the several options above introduced (Fig. 5.1), our approach was thought as one that could be useful for an evaluation of the actual *in situ* rates in the area studied, the potential upscaling of DEN estimations over large sets of oligotrophic lakes, and projections of future scenarios of air temperature and nitrate deposition. Therefore, DEN measurements were conducted using intact core sediments, the acetylene inhibition method combined with sensors for nitrous oxide and experimental control of temperature and nitrate availability within the natural range found in these lakes. For complementarity, we compiled the existing data on DEN temperature dependence in aquatic ecosystems across the literature and evaluated the results according to the framework introduced in Fig. 5.1, emphasizing the likely reasons for the large variation in the estimations and, if so, the discrepancies with our results.

5.3. MATERIALS AND METHODS

General methodological approach

Three lakes with contrasting morphology and carbon flow characteristics (Table 5.1) were sampled to consider potential different microbial communities. In each sampling date, we collected five core sediments in the field, which were immediately transported to the lab to control for temperature and nitrate availability within the ranges that can be found in these mountain lakes. We used sensors for nitrous oxide combined with the acetylene inhibition method and anoxic conditions to minimize the disturbance of the sediment structure. For each core, we performed sequential estimations of the DEN rates (r_d) at several temperature values and nitrate concentrations. This procedure reduces the noise that the sediment spatial heterogeneity can introduce in the estimations but may introduce autocorrelation effects. To overcome the latter constraint, we did not follow the same experimental sequence in each trial, so we could statistically evaluate the autocorrelation influence and distinguish it from other sources of variation (e.g., nitrate concentration, lake, sensors). Although the experiment was planned for the same number of cores per lake (5), finally, we also included in the data set two preliminary tests - performed using only a part of the nitrate gradient in some Lake Redon cores - as they fitted in the general results obtained and thus increased the statistical robustness of the final model.

Sampling and experimental design

The selected three lakes are representative of the lake district of the Pyrenees (Table 5.1). They cover a broad range of maximum depth (9-73 m) and seasonal thermal variability (Catalan *et al.* 2002b). The experimental temperature (5-15°C) and the nitrate added levels (7-14-28 μM) covered the natural variability in the region and possible future scenarios. A total of 25 sediment cores (methacrylate, \varnothing 6.35 cm) were assessed (15 from Redon, 5 from Plan and 5 from Llong, Table S1). They were collected with a gravity corer (Glew 1991) at midday around the deepest point of each lake (Table 5.1). Only undisturbed cores with clear overlying water and interface were used. The experimental setup included an incubation chamber that ensured dark conditions and controlled temperature ($\pm 1^\circ\text{C}$) (Fig. 5.2). Nitrate was measured at the beginning of the incubations (Table S1). As a precautionary action, glucose was added in excess (1.5 g L⁻¹) to avoid carbon limitation (Vila-Costa *et al.* 2016) despite that some previous tests did not show conclusive evidence of such limitation. DEN measurements at different nitrate concentrations and temperatures started the next morning and were conducted sequentially, commonly: Step 1: First 7 μM nitrate addition at 5°C (0-12h); 2: 15°C (12-24h); 3: Second 7 μM nitrate addition at 15°C (24-36h); 4: 5°C (36-48h). 5: 14 μM nitrate addition at 5°C (48-60h); and 6: 15°C (60-72h).

Table 5.1. Study sites location and characteristics.

Lake	Redon	Plan	Llong
Latitude (N)	42.64208	42.62248	42.57431
Longitude (E)	0.77951	0.9307	0.95063
Altitude (m a.s.l.)	2235	2188	2000
Area (ha)	24	5	7
Maximum depth, (m)	73	9	12
Temperature ^a (°C)	4	5	3
NO₃^{-a} (µM)	5 (4-6)	1 (1-2)	8 (7-9)
NO₂^{-a} (µM)	0.17 (0.13-0.21)	0.05 (0.05-0.05)	0.15 (0.13-0.18)
NH₄^{+a} (µM)	9 (6-14)	3 (2-5)	25 (19-31)
DOC ^a (mg L-1)	52 (2-88)	74 (6-99)	15 (2-70)
LOI ^b (%)	25 (18-35)	44 (40-48)	27 (24-31)
Carbon ^b (% dry weight)	12 (10-18)	20 (17-24)	13 (11-14)
Nitrogen ^b (% dry weight)	1.2 (0.9-2.1)	1.9 (1.6-2.3)	1.2 (1.0-1.5)
Sediment grain size (median - µm) ^b	252 (166-351)	333 (205-465)	174 (130-223)

^a Characteristics of the water overlying the sediment. Ice-free season average, minimum, and maximum values.

^b Characteristics of the surface sediment (0-2 cm layer): Loss on ignition (LOI), as a proxy of organic matter (carbonates < 2%, not shown).

Denitrification measurement

DEN measurements were performed using the acetylene inhibition method combined with sensors for nitrous oxide (N₂O). Anoxia, first, and acetylene inhibition, after, were achieved by bubbling N₂ and C₂H₂ sequentially, respectively, during 10 minutes in the water phase of the core before each DEN measurement. Acetylene inhibits the reduction of N₂O to N₂ (Balderston *et al.* 1976, Yoshinari and Knowles 1976). The accumulated N₂O was measured using a modified Clark electrode probe (N₂O-R microsensor, Unisense A/S, Denmark) (detection limit = 0.1µM), in the water phase. A gentle magnet stirring was applied to avoid stratification but without resuspension of the sediment. Readings were taken every 5 minutes via a picoammeter logged to a laptop. The response of the electrochemical sensor is linear in the range of 0–1.2 mM (Andersen *et al.* 2001). The instrument

was kept polarized during all the measurement period. It was calibrated at each temperature using a calibration chamber (CAL300, Unisense A/S, Denmark), zero gas water (Milli-Q) and a freshly prepared $\sim 50 \mu\text{M}$ N_2O solution. The latter was obtained adding a certain volume of N_2O saturated water (Weiss and Price 1980) to the zero gas water following manufacturer's instructions as described in Foley *et al.* (2010).



Figure 5.2. Experimental setup. The incubation chamber ensured dark and controlled temperature ($\pm 1^\circ\text{C}$) conditions. Five intact lake sediment cores could be processed at once using their respective N_2O sensors.

Water and sediment characterization

Immediately after collection, we measured the temperature ($^\circ\text{C}$) of water overlying the sediment core (Table 5.1). For chemical analyses, water samples were filtered through a pre-combusted (4 h at 450°C) GF/F glass fiber filter. Nitrate was determined by capillary electrophoresis using a Quanta 4000 (Waters) instrument. Ammonium and nitrite were determined by colorimetric methods in a segmented-flow autoanalyzer (AA3HR, Seal), using the Berthelot reaction for ammonium (Bran+Luebbe method G-171-96) and the Griess reaction for nitrite (Bran+Luebbe method G-173-96). Dissolved organic carbon (DOC) was measured by catalytic combustion to CO_2 and detection by IR spectroscopy in a TOC5000 (Shimadzu) analyzer. The water column of the lakes sampled show a circumneutral pH (~ 7) (Vila-Costa *et al.* 2014).

After DEN measurements, the surface sediment was sliced (2 cm) and freeze-dried for 72 h. Around 5 mg of the dried sample was encapsulated together with a catalyst (Va_2O_5) in tin capsules for the determination of C and N using a C-H-N-S (Carlo-Erba) analyzer. The dry weight percentage of organic matter content in the sediments was determined by loss on ignition (LOI) following Heiri *et al.* (2001). In all cases, the samples were equilibrated to room temperature in a desiccator before weighing them. The median grain size of the sediment was determined by laser diffraction (Mastersizer 2000, Malvern Instruments Ltd, UK). Freeze dried sediment was rehydrated in distilled water and introduced into the sample dispersion unit (Hydro 2000 G, Malvern Instruments Ltd, UK) adding hexametaphosphate and sonicating to avoid aggregates. Laser obscuration was between 10-20 % and the measuring range between 0.02 and 2000 μm .

Numerical methods

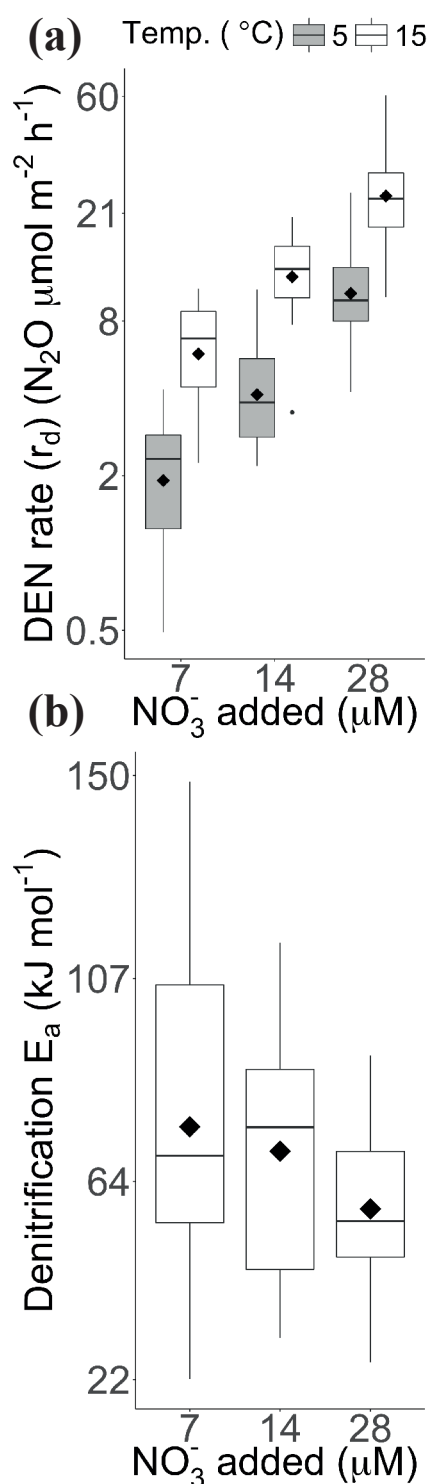
Denitrification activity rates (r_d) (N=107) were calculated by linear regression from the sequential readings of the N_2O sensors ($r = 0.89 \pm 0.02$ (mean \pm standard error), with an average of 66 point measurements). Raw r_d values in $\mu\text{M } N_2O \text{ core}^{-1} \text{ h}^{-1}$ were transformed to $\mu\text{mol } N_2O \text{ m}^{-2} \text{ h}^{-1}$ using the inner core section area. The apparent activation energy (E_a ; kJ mol^{-1}) of the denitrification process was estimated according to the Arrhenius equation: $r_{d_j}/r_{d_i} = \exp [E_a/R (1/T_i - 1/T_j)]$ where R is the gas constant ($8.314 \text{ J K}^{-1} \text{ mol}^{-1}$); T, the absolute temperature ($^{\circ}\text{K}$); and r_d , the denitrification activity rate. The subscripts (i, j) indicate two different thermal conditions. Statistics were conducted using R version 3.3.0 (R Development Core Team 2016). Linear mixed-effects models were performed using the *lme* and *lmer* functions within the nlme and lme4 R packages, respectively (Pinheiro *et al.* 2007, Bates *et al.* 2015). Functions *ANOVA* of the R core package stats (R Development Core Team 2016), *AICc* (Akaike Information Criterion for a small sample size) of the package AICcmodavg (Mazerolle 2016) and fixed, global explained variance and *r.squaredGLMM* of MuMIn (Bartoń 2016) were used to select the best fitting model.

Compiled data of DEN E_a in aquatic ecosystems

For comparison, we compiled data about the denitrification temperature dependence in aquatic ecosystems across literature (Table S2). For each study, the apparent activation energy (E_a ; kJ mol^{-1}) of the denitrification process was estimated by the Arrhenius equation above or by the slope of an Arrhenius plot of $\ln(r_d)$ as a function of T^{-1} when more than two temperature data were available.

5.4. RESULTS

Denitrification temperature dependence in mountain lakes sediments



The denitrification activity rates (r_d) measured ranged from 0.5 to 60.5 $\mu\text{mol N}_2\text{O m}^{-2} \text{h}^{-1}$ (Table S1). The rates increased with the experimental temperature, and nitrate addition levels (Fig. 5.3a). Rates (mean \pm standard error) for 7, 14 and 28 μM nitrate added were at 5°C 2.2 \pm 0.3, 4.6 \pm 0.5, 11.3 \pm 1.2 $\mu\text{mol N}_2\text{O m}^{-2} \text{h}^{-1}$, respectively, and at 15°C 6.6 \pm 0.8, 12.7 \pm 0.9, 27.0 \pm 2.9 $\mu\text{mol N}_2\text{O m}^{-2} \text{h}^{-1}$, respectively.

From the measured rates, the apparent activation energy was estimated for each nitrate level (Table S1, average $E_a = 67 \pm 4 \text{ kJ mol}^{-1}$). DEN r_d at 5°C had a larger influence on the E_a values than those at 15°C as shown by a significant negative correlation ($r = -0.51$, $p = 0.0001$) between E_a and $\ln(r_d)$ at 5°C and not significant at 15°C.

E_a values and their variation declined when the nitrate added increased (Fig. 5.3b). E_a negatively correlated ($r = -0.33$, $p = 0.01$) with the initial experimental nitrate (water phase plus added) concentrations. E_a at nitrate saturation was estimated by fitting a linear relationship between the inverse of nitrate concentration and E_a (model 0 in Table 5.2). In this model, the intercept indicates the value of E_a when the influence of nitrate concentration tends to zero.

Figure 5.3. (a) Denitrification rates (r_d) at the two experimental temperatures and the three nitrate enrichments. Note the natural logarithm scale in Y-axis. (b) Apparent activation energy (E_a) at the three nitrate enrichments. The number of observations of DEN E_a was 12, 20 and 19, respectively for each level of nitrate added (7, 14 and 28 μM). Note that the actual experimental nitrate concentrations in each enrichment class varied according to the initial field concentration (Table S1).

Table 5.2. Alternative regression models relating the DEN E_a (kJ mol^{-1}) to the inverse of the nitrate concentration ($[\text{NO}_3^-]^{-1}$) (μM) in the overlying water of the lake sediments.

Regression model	Random part	Formula	E_a at nitrate saturation (Intercept \pm se)	p-value	Coefficient \pm se	p-value	AICc	Fixed R^2	Global R^2
0	Lm model, no random part	mod0=lme($E_a \sim [\text{NO}_3^-]^{-1}$)	50 \pm 8	<0.00001	315 \pm 141	0.0303	481	0.09	0.09
1	GLS model, no random part	mod1=gls($E_a \sim [\text{NO}_3^-]^{-1}$)	50 \pm 8	<0.00001	315 \pm 141	0.0303	465	0.09	0.09
2	GLS model, no random part	mod2=gls($E_a \sim [\text{NO}_3^-]^{-1}$, correlation=corAR1(form= \sim Add phase Core))	50 \pm 8	<0.00001	324 \pm 139	0.0239	467	0.09	0.09
3	Sensor effect	mod3=lme($E_a \sim [\text{NO}_3^-]^{-1}$, random= \sim 1+ $[\text{NO}_3^-]^{-1}$ Sensor)	44 \pm 8	<0.00001	451 \pm 227	0.0529	464	0.15	0.47
4	Sensor effect (just slope)	mod4=lme($E_a \sim [\text{NO}_3^-]^{-1}$, random= \sim 0+ $[\text{NO}_3^-]^{-1}$ Sensor)	46 \pm 7	<0.00001	419 \pm 175	0.0207	460	0.13	0.42
5	Sensor (with nested core effect)	mod5=lme($E_a \sim [\text{NO}_3^-]^{-1}$, random= \sim 1+ $[\text{NO}_3^-]^{-1}$ Sensor/Core)	45 \pm 8	<0.00001	438 \pm 228	0.0666	473	0.14	0.49
6	Core effect	mod6=lme($E_a \sim [\text{NO}_3^-]^{-1}$, random= \sim 1+ $[\text{NO}_3^-]^{-1}$ Core)	48 \pm 9	<0.00001	365 \pm 177	0.0505	469	0.11	0.34
7	Core effect (just slope)	mod7=lme($E_a \sim [\text{NO}_3^-]^{-1}$, random= \sim 0+ $[\text{NO}_3^-]^{-1}$ Core)	49 \pm 8	<0.00001	339 \pm 153	0.0368	465	0.1	0.29
8	Nitrate added effect	mod8=lme($E_a \sim [\text{NO}_3^-]^{-1}$, random= \sim 1+ $[\text{NO}_3^-]^{-1}$ Nitrate added)	42 \pm 15	0.0068	495 \pm 298	0.1038	472	0.18	0.3
9	Nitrate addition phase effect	mod9=lme($E_a \sim [\text{NO}_3^-]^{-1}$, random= \sim 1+ $[\text{NO}_3^-]^{-1}$ Add phase)	48 \pm 10	<0.00001	366 \pm 200	0.0732	472	0.11	0.15
10	Lake effect	mod10=lme($E_a \sim [\text{NO}_3^-]^{-1}$, random= \sim 1+ $[\text{NO}_3^-]^{-1}$ Lake)	50 \pm 8	<0.00001	315 \pm 141	0.0307	472	0.09	0.09

Note. All the regression models have the same fixed part, that is the inverse of the nitrate concentration ($[\text{NO}_3^-]^{-1}$). Thus the models differ in the random part. The coefficient is the slope of the model and shows the influence of the inverse of nitrate concentration in the E_a . AICc is the second-order Akaike's information criterion for a small sample size (Mazerolle 2016). Fixed R^2 represents the variance explained by the fixed factor ($[\text{NO}_3^-]^{-1}$), and global R^2 represents the total variance explained by both fixed and random factors (i.e., the entire model) (Bartoń 2016). Model 2 takes into account the temporal autocorrelation. Models 3, 4 and 5 take into account the sensor (#1, #2, #3, #4 or #5) effect, thus correcting for differences in sensor performance. Models 5 (nested in the sensor), 6 and 7 consider the core (sample) effect. Model 8 takes into account the three nitrate enrichment levels, and model 9 the addition order (first, second and third). Model 10 takes into account the lake effect. Models with more than one factor crossed in the random part (not shown) were also built with the *lmer* function within the *lme4* R package (Bates *et al.* 2015), these models did not improve model 1, 3 or 4 ($p > 0.05$) in ANOVAs and showed higher AICc values). *Abbreviations:* lm (linear model), gls (linear model fitted using generalized least squares), lme (linear mixed-effects model) and se (standard error).

The variation of the rates measured under the same conditions of temperature and nitrate concentration was markedly high. Therefore, we investigated whether the estimation of the E_a dependency on nitrate concentration could be improved by taking into account other experimental issues and the lake idiosyncrasy (Table 5.2). We developed alternative mixed regression models including different factors in the random part and maintaining the inverse of nitrate concentration as the only factor in the fixed part (see supporting information for details). The alternative models took into account: the five sensor performance; the autocorrelation intrinsic to subsequent experimental additions; the nitrate addition level; the order of the addition level (not all the experiments followed the complete sequence from 7 to 28 $\mu\text{M NO}_3^-$) and the lake of the core. The only models that significantly improved the initial model 1 were those accounting for the sensor effects (model 3 and 4 in Table 5.2). They showed the lower AICc values and explained more variance (ANOVA p-values of 0.047 and 0.008 for model 3 and 4, respectively). When we considered core, lake, autocorrelation or nitrate addition features did not improve the E_a estimation. We eventually selected model 4 as the best estimation because it is simpler than model 3. Consequently, the denitrification E_a at nitrate saturation is estimated to be $46 \pm 7 \text{ kJ mol}^{-1}$ (i.e., $Q_{10} = 1.7 \pm 0.4$) and the apparent E_a to vary according to nitrate concentration as:

$$E_a = 46 + 419 [\text{NO}_3^-]^{-1} \quad (1)$$

Comparison with other aquatic ecosystems

We identified a total of 21 previous studies (Table S2) to compare our results with estimations from other sites and methods. They included lakes (Cavari and Phelps 1977, Messer and Brezonik 1984, Myrstener *et al.* 2016), ponds (Veraart *et al.* 2011b), streams (Holmes *et al.* 1996, Boulétreau *et al.* 2012), rivers (Pfenning and McMahon 1997, Pattinson *et al.* 1998, Silvennoinen *et al.* 2008), denitrification beds (i.e., carbon supply to promote denitrification in eutrophic rivers, (Cameron and Schipper 2010, Warneke *et al.* 2011)), hyporheic (Sheibley *et al.* 2003) and riparian (Ambus 1993) zones, groundwaters (Jørgensen *et al.* 2009), swamps (Westermann and Ahring 1987), wetlands (King and Nedwell 1984), estuaries (Brin *et al.* 2017) and marine environments (Rysgaard *et al.* 2004, Canion *et al.* 2014a, Canion *et al.* 2014b, Kraft *et al.* 2014, Brin *et al.* 2017). There is a large scattering in the E_a values estimated. However, the most similar sites to those in our study (Rysgaard *et al.* 2004, Myrstener *et al.* 2016) were also from remote, cold and N-poor areas, and showed similar E_a values plotted against the inverse of nitrate (Fig. 5.4).

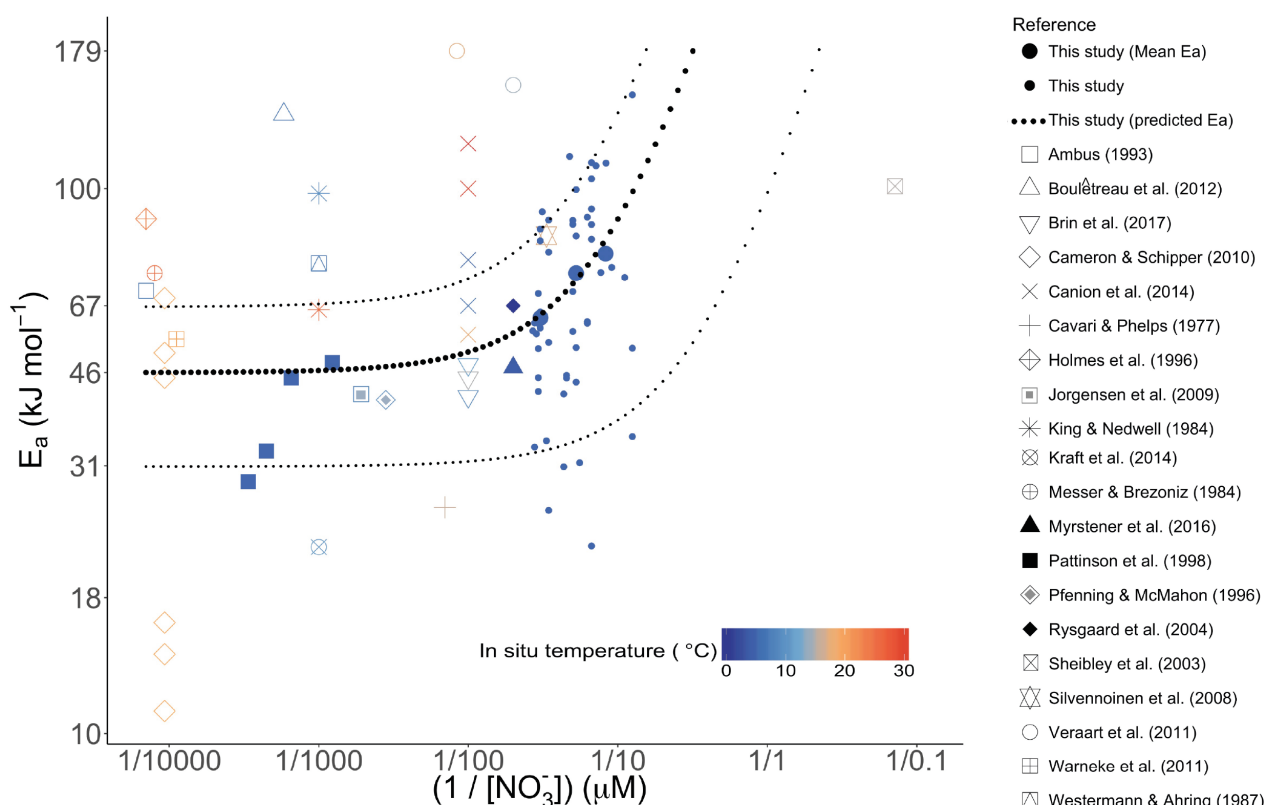


Figure 5.4. Denitrification temperature dependence (E_a) against the inverse of the nitrate concentration in compiled data from aquatic ecosystems. The solid circles are data from this study. The small circles are the E_a values resulting from each experiment ($N = 51$) and the large circles correspond to the average E_a values for each three nitrate enrichment levels. The black dotted line indicates the model $E_a = 46 + 419 [\text{NO}_3^-]^{-1}$. The thin dotted lines indicate the 95% confidence intervals (see model 4 in Table 2). Note that X- and Y-axis are on a \log_{10} scale.

5.5. DISCUSSION

Denitrification rates, nitrate, and temperature

The denitrification rates (r_d) obtained were similar to the few other measurements in mountain lake sediments (McCrackin and Elser 2012, Vila-Costa *et al.* 2016). The values are in the low range of freshwater sediments (Seitzinger 1988, Piña-Ochoa and Alvarez-Cobelas 2006) as expected from cold and oligotrophic environments. However, despite the apparent harsh conditions, the denitrification activity intensifies with increasing nitrate and temperature without becoming saturated (Fig. 5.3a) within the range of values currently found in the Pyrenees (Camarero and Catalan 2012). Therefore, the current denitrification potential of these systems can respond to warming or increased N_r deposition (or watershed loading) without any time lag.

It could be argued that the experimental sequential procedure of 72h incubations could facilitate an enrichment of denitrifiers in our experiment. We used the shortest time to obtain reliable measurements of the activity rate without disturbing the sediment interface. An alternative experimental design, based on pseudo-replicates of several cores from the same site incubated at the various levels of nitrate and temperature, would notably increase the sample-related heterogeneity due to the patchy nature of any sediment. We think that the cold and oligotrophic conditions of the studied system prevent any significant enrichment in denitrifiers during the experimental development.

In the compiled DEN E_a studies, there are variable values for similar NO_3^- enrichments (Fig. 5.4), which may be attributed to changing assemblages of denitrifiers. A case of a latitudinal gradient in coastal marine sediments, with higher values for subtropical locations (121 and 100 kJ mol^{-1}) (Canion *et al.* 2014a). A case of cultures with a different nitrate reducing dominant species, *Pseudomonas* sp. or *Vibrio* sp., with 98 and 60 kJ mol^{-1} E_a values, respectively, isolated at 10 and 25°C from a salt-marsh sediment (King and Nedwell 1984). And cases of seasonal variability, with E_a ranges of 70 to 76, 36 to 53 and 38 to 60 kJ mol^{-1} in swamp, estuary and continental shelf sediments from temperate ecosystems, respectively (Westermann and Ahring 1987, Brin *et al.* 2017). Beyond the sequential experimental issue, different denitrifier assemblages between lakes could also be a source of variation in our data. However, models including the lake site as a source of random variation did not improve the fitting (Table 5.2). Only the use of molecular techniques to characterize the microbial assemblages (i.e., 16S rRNA) will settle discussions about this issue and clarify the relative influence of physicochemical and biological constraints.

To our knowledge, only another study measured DEN activities experimentally controlling both temperature and nitrate gradients close to the *in situ* conditions (Pattinson *et al.* 1998). In this study, E_a values also declined with increasing nitrate. Provided the difference of about three orders of magnitude in nitrate concentrations between the two studies, one has to conclude that DEN saturation by nitrate is achieved at different concentrations in eutrophic and oligotrophic ecosystems. Even so, the range of E_a estimated in the eutrophic experiment fell within the 95% confidence limit of our model (Fig. 5.4).

The higher E_a values (155-179 kJ mol^{-1}) have been found in eutrophic ponds (Veraart *et al.* 2011b). In this case, there was not an experimental forcing of the anoxia, so the authors attribute the high

effect of warming on denitrification rates to a decline in the oxygen interference due to a synergic effect of lowering both the oxygen solubility and the production/respiration ratio when the temperature increases. Boulétreau *et al.* 2012 also found a high E_a (137 kJ mol⁻¹): they were using a wide, and high experimental temperature range (1-40°C) compared to the *in situ* temperature (7.2±1.7 °C) of their sites. The same experimental set, indicate a lower E_a (43 kJ mol⁻¹) when calculated only for a narrower temperature range (1-12°C) closer to that *in situ* (Table S2). The lowest E_a values (<20 kJ mol⁻¹) were found by Cameron and Schipper (2010).

Coupled nitrification could also interfere the DEN experiments if ammonium levels are high. Sheibley *et al.* (2003) performed the only study of DEN E_a at markedly low nitrate concentrations without any addition. Their E_a estimates depart from our model (Fig. 5.4). In that case, there was an intense nitrification, also highly dependent on temperature and ammonium concentrations (22 µM), and DEN E_a was estimated using activity rates at different seasons as a surrogate for temperature control.

In our compiled data, including our study, we did not find any significant correlation between DEN E_a values and any statistical temperature descriptor (T max, T min, T mean, T *in situ* or annual T mean, Table S2). Canion *et al.* (2014a) found a higher DEN E_a value for warmer (subtropical) than colder (temperate or polar) environments. They suggested an adaptation of denitrifiers to *in situ* temperature, supported by a previous study in the polar region (Canion *et al.* 2013). Although not universally, there are trade-offs between genetic adaptation to low and high temperature (Bennett and Lenski 2007). In a salt-march study, culture isolates at 10, and 25°C from the same sediment sample resulted in different nitrate-reducing dominant species, *Pseudomonas* sp. and *Vibrio* sp., and showed different E_a (98 and 60 kJ mol⁻¹, respectively). The highest E_a was in the culture isolated at the closer temperature to *in situ* (15°C) (King and Nedwell 1984). Recurrently, DEN E_a values are higher when obtained from temperatures around *in situ*. In the literature data, a mean increase of 42±11% (±se) is achieved when E_a is calculated with a narrow temperature range close to the *in situ* one compared with the result using the complete temperature range of the experiment (Table S2). We found a similar increase (51%) when the temperature range was reduced to values close to the *in situ* temperature in the samples of Lake Redon (Table S2). Consequently, we highlight the convenience of measuring DEN temperature dependence as close as possible to *in situ* conditions of temperature.

In the current context of results (Fig. 5.4), it seems necessary to recommend experiments following a common procedure including an experimental nitrate gradient and temperatures no more than 15 °C beyond the *in situ* values. The spatial or temporal distribution of the samples should not be a surrogate for these gradients.

Carbon limitation, nitrate supply and competing process

There were two aspects with potential influence on DEN temperature dependence (Fig. 5.1) that we did not explicitly consider, carbon limitation and competing processes. We did not expect a denitrification limitation by carbon in the Pyrenean mountain lakes. There is a higher ratio of primary production to respiration in both the water column and the surface sediments, resulting in an elevated

fresh carbon stock for bacterial activity (Camarero *et al.* 1999). All in all, our experimental measurements were made with the addition of glucose. In fact, one can expect a C availability influence on the denitrification-temperature dependence mostly in warm and eutrophic (nitrate-rich) aquatic ecosystems. The lowest DEN E_a values ($<20 \text{ kJ mol}^{-1}$) in the compiled data were found by Cameron and Schipper (2010) in an extended 10-months incubation experiment. The low E_a values could be due to a C-limitation in the warmer treatments using labile C sources (green waste, maize cobs, and wheat straw). C deficiency could also cause the low E_a (26 kJ mol^{-1}) assessed in a *Pseudomonas aeruginosa* culture isolated from Lake Kinneret as there was no addition of any C source (Cavari and Phelps 1977, Gal *et al.* 2003).

In the method that we applied, the experimental assumption is that nitrification is not acting because of the induced anoxic conditions and the inhibition of the ammonium monooxygenase by acetylene (Hynes and Knowles 1978). Consequently, sources of NO_3^- supply variation restrict to diffusive transport and uptake by alternative biogeochemical pathways. Nitrate diffusion aspects appear to have had no significant influence in our experiment as core and lake factors, which implicitly account for differences in sediment particle size, did not improve the models (Table 5.2).

Nitrate uptake, anammox and dissimilatory nitrate reduction to ammonium (DNRA) are the biogeochemical processes that can compete with DEN for nitrate. We may assume that nitrate assimilation should not be relevant because of the high abundance of ammonium — the preferred N source (Luque-Almagro *et al.* 2011) — and the common low rates of nitrogen uptake in dark conditions (Lorenzen *et al.* 1998).

Anammox competes with DEN for nitrite. To our knowledge, there is no evidence of the dominance of anammox or DEN depending on the nitrate concentration. Anammox seems more sensitive to nitrate fluctuations than DEN (Rysgaard *et al.* 2004). The highest anammox activity respect to DEN has been found at 5°C in Arctic marine sediments (Rysgaard *et al.* 2004). Canion *et al.* (2014b) found similar results in Arctic fjord sediments with anammox bacteria being more specialized for psychrophilic activity than denitrification. Recently, Brin *et al.* (2017) in a warmer habitat, temperate marine sediments, did not find differences in temperature responses for the two processes.

The ratio of electron acceptor (i.e., NO_3^-) to electron donor (i.e., organic C) is the most frequently mentioned partitioning factor between DEN and DNRA (Tiedje *et al.* 1982). DNRA is the dominant pathway under nitrate-limited conditions, while DEN is the favored pathway under nitrate-replete conditions (Smith *et al.* 1982, King and Nedwell 1985, 1987, Herbert and Nedwell 1990, Laverman *et al.* 2006, Dong *et al.* 2009, Mania *et al.* 2014, Nogaro and Burgin 2014). Slightly more energy is obtained per mol of NO_3^- by DNRA than by DEN (Strohm *et al.* 2007) and, additionally, DNRA consumes more electrons (8 vs. 5) during the reduction of NO_3^- to NH_4^+ (Burgin and Hamilton 2007). Low NO_3^- and high organic C availability can thus create more favorable conditions for DNRA than DEN (MacFarlane and Herbert 1982, Tiedje *et al.* 1982). The *in situ* C/N ratios of the sediment (Table 5.1) were always higher than 10 in our samples, in the range of values more favorable to DNRA. A C/N ratio for an equal contribution of the two processes of nitrate reduction is ~ 7.5 (Yoon *et al.* 2015)). In all our experimental treatments, the DOC/nitrate ratio was above 100 (a/a), thus with similar conditions favoring DNRA as in field conditions.

Some studies have also shown a dominance of DNRA over DEN at higher temperatures (Ogilvie *et al.* 1997, Yoon *et al.* 2015). This dominance could be temporal during summer periods (King and

Nedwell 1984, Jørgensen 1989) or spatial as occurs in some warm tropical ecosystems (Dong *et al.* 2011). Nonetheless, this apparent temperature effect may mask the true influence of the co-occurring higher reducing conditions and lower nitrate concentrations at higher temperatures that eventually determine a low ratio of electron acceptor to electron donor (Jørgensen 1989, Gardner *et al.* 2006, Gardner and McCarthy 2009, Gross-Wittke *et al.* 2010, Nizzoli *et al.* 2010, Zhu-Barker *et al.* 2015). The only two studies with data of temperature dependence for the two nitrate reduction processes are at a high nitrate concentration (1 mM). Kraft *et al.* (2014) shows E_a values of 22 and 40 kJ mol⁻¹, for DEN and DNRA respectively, in the complete experimental range of temperatures (10 to 30°C), and 26 and 79 kJ mol⁻¹, respectively, in a narrow segment of temperature (10 to 15°C) – based on E_a values calculated from Fig. S8A. Yoon *et al.* (2015) investigated the switch between the two processes in a single microbial model, *Shewanella loihica*, a species capable of performing the two pathways. They found a dominance of DNRA at warmer temperatures, with DEN showing a decline from 21 to 30 °C and a null activity at 37°C. Temperature does not appear to be an issue in our experiment concerning DNRA and DEN partition. Using slurry incubations overestimate DNRA by enhancing nitrate availability to deeper layers of the sediments, where ammonifiers dominate over denitrifiers (Behrendt *et al.* 2013). This procedure could have affected other DEN estimates in mountain lakes (Vila-Costa *et al.* 2016) but their results do not differ markedly from our ones.

The generation of N₂O due to abiotic processes could let to an overestimation of the denitrification activity. At the current stage of knowledge, it is hard to infer any contribution of chemical processes to the overall NO and N₂O production (Schreiber *et al.* 2012). There are two major abiotic N₂O production pathways. The NH₂OH decomposition to N₂O at circumneutral pH is favored by high Mn (IV), temperature and salinity, and low organic carbon. The chemodenitrification of NO and NO₂⁻ to N₂O is favored by high pH, low O₂ and solid Fe (III) or Cu (II) catalysts (Zhu-Barker *et al.* 2015). Few of these favorable conditions are present in the studied lakes (e.g., the granitic nature of the bedrock in the studied lakes confers low levels of iron to the sediments (Catalan *et al.* 2014)). However, these processes may be relevant in watersheds of metamorphic rocks rich in metals, which are common in some parts of the Pyrenees and other mountain ranges (Catalan *et al.* 1993).

We can conclude that DNRA, at nitrate limiting conditions and high temperature, and anammox, at low temperature and C/N, are the most like processes influencing DEN yield in mountain lakes. Future experiments on the temperature dependence of DEN, Anammox, and DNRA across gradients of nitrate, C/N and temperature are necessary to clarify these interactions.

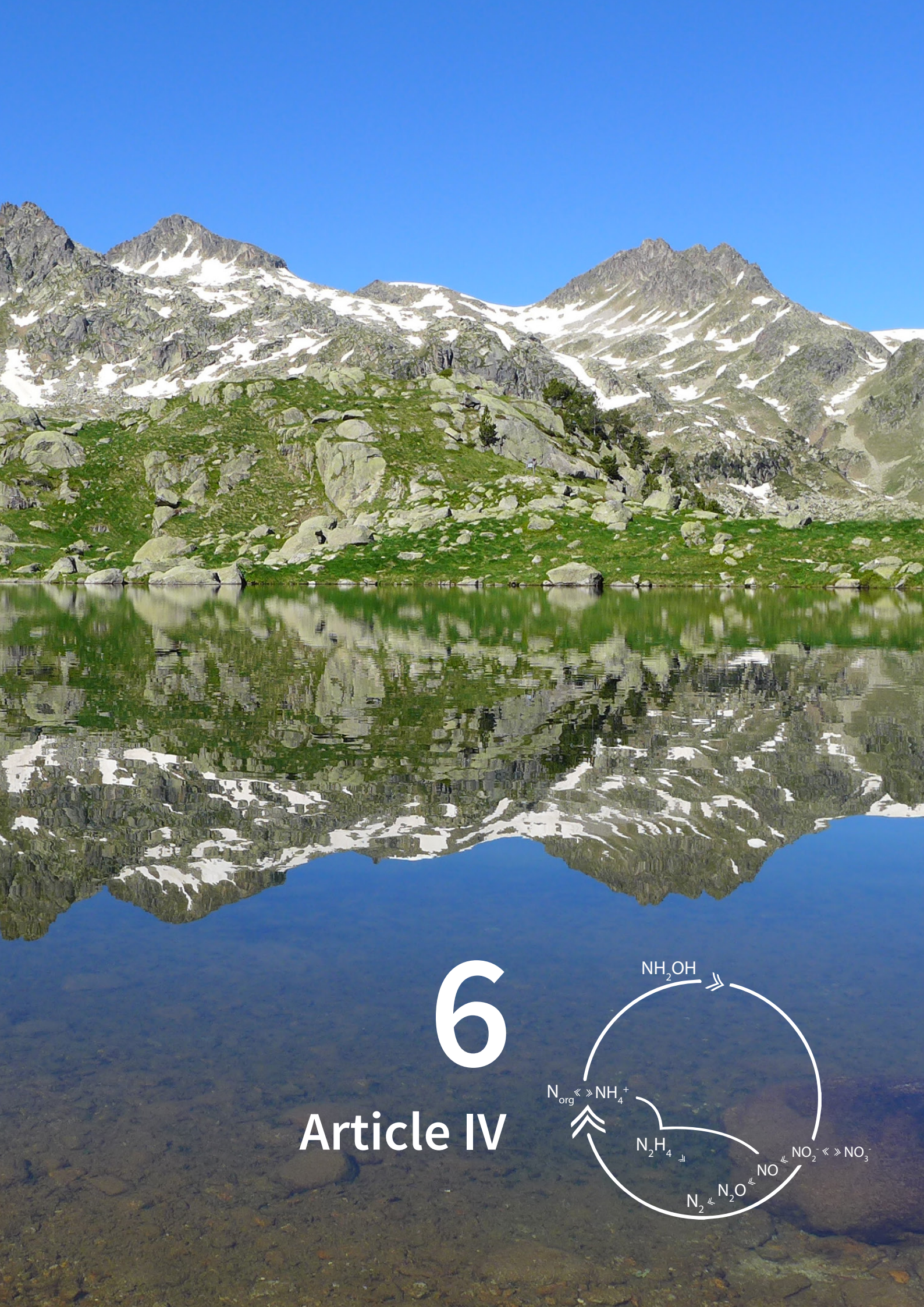
5.6. CONCLUSIONS

There is still a limited knowledge about denitrification rates and their temperature dependence in general and, particularly, for cold and N-poor systems, despite that the latter cover a high percentage of the continental aquatic ecosystems. Our study shows that the low rates of denitrification observed are not nitrate saturated and the system can respond to warming and increased N_r loadings, either from deposition or the watershed. The case-by-case estimation of DEN E_a present much variability, but there is a robust statistical behavior that can be applied to modeling, upscaling and as a benchmark for actual measurements. Three main conclusions derive from our results:

1. Under nitrate saturation conditions (e.g., $> 100\mu\text{M}$) a DEN E_a significantly different from 46 kJ mol^{-1} (e.g., > 67 or < 31) would suggest that there is another factor interfering (e.g., C quality or quantity limitation; or very distinct microbial assemblage related to other features of the system).
2. Below saturation and not at extremely low nitrate levels ($> 3\mu\text{M}$), equation (1) can be applied for modeling the temperature influence on DEN rates, accounting for nitrate levels.
3. In the natural environments of remote areas, *in situ* nitrate values are still far from DEN saturation. Currently, this feature leads to very high apparent DEN E_a values but this does not mean that with warming higher DEN rates could be sustained. In case of temperature increase, a short transitory period of high DEN would lead to a rapid depletion of nitrate unless nitrate supply rates would proportionally increase. Therefore, in a warmer scenario, variation in denitrification rates will continue mostly depending on nitrate supply processes that include proximal (e. g., sediment-related nitrification), local (e. g., N_r leaching from soils) and regional (e. g., atmospheric N_r deposition) components (Wallenstein *et al.* 2006).

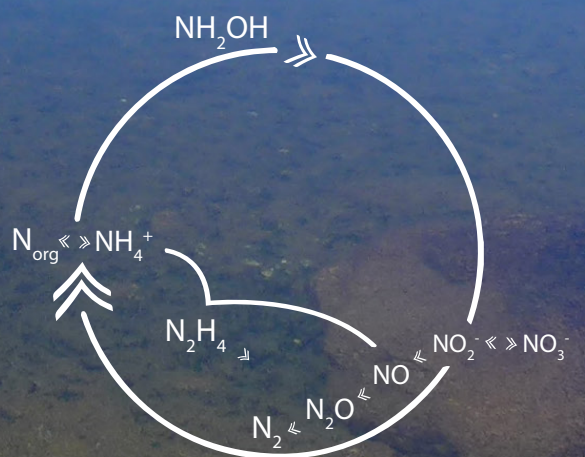
ACKNOWLEDGMENTS

Thanks to Berta Fueyo, Marc Sala-Faig, Rober Sánchez and Pau Giménez-Grau for help in the laboratory and field sampling. The Spanish Government provided funds through the research grants of the Ministerio de Economía y Competitividad: NitroPir (CGL2010-19737), Lacus (CGL2013-45348-P) and Transfer (CGL2016-80124-C2-1-P) and a predoctoral fellowship to CPL (FPU12-00644). All the experimental and compiled data is available in the supporting material (Appendix B).



6

Article IV



6. Article IV

Decoupling of current denitrification rates from gene potentials in lake sediments of mountains affected by high atmospheric nitrogen deposition

6.1. ABSTRACT

During the last decades, the atmospheric nitrogen load in mountain ranges of the Northern Hemisphere has increased several folds. Lake nitrate concentrations reflect the atmospheric shift, but little is known about how the new situation may have modified denitrification rates. We measured current and potential (nitrate-added) denitrification rates in several lake types and across benthic habitats in the Pyrenees. Current denitrification rates ranged from 0 to 9 $\mu\text{mol N}_2\text{O m}^{-2} \text{h}^{-1}$ (mean, 1.5 ± 1.6 SD). However, gene potentials were not correlated current rates but to potential rates. Littoral habitats showed higher rates than deep sediments. The high current rates occurred in warmer sediments with more substrate availability, via coupling with archaeal nitrification or using the nitrate in the water overlying the sediment. The high denitrification potentials occur in *nirS* gene-rich and *nrfA* gene-poor sediments from lakes at low altitude, small catchments and more productive with sulphate rich and nitrate poor overlying water. In these lakes, the water-sediment interface experiments more fluctuating redox conditions that may favour denitrifiers because of their facultative nature able to use alternative electron acceptors. We conclude that the increase in nitrogen deposition has enhanced the denitrification activity by raising the substrate availability but not at a sufficient rate to compensate for the nitrate load in the most oligotrophic sites because nitrate supply is not the primary driver stimulating denitrifier populations.

With permission of: Ll. Camarero, S. Hallin, C.M. Jones and J. Catalan, who are co-authors of this study.

6.2. INTRODUCTION

Nitrogen directly available to the biosphere (i.e., reactive nitrogen, N_r) has at least doubled due to human activities since preindustrial times (Erisman *et al.* 2011). This anthropogenic alteration is one of the major problems facing the Earth (Rockstrom *et al.* 2009). The same atom of N_r can cause multiple effects across Earth ecosystems until it is converted back to nonreactive N_2 (Galloway *et al.* 2003). Denitrification is the primary process of N_r removal (Seitzinger *et al.* 2006, Kuypers *et al.* 2018); microbial activity reduces nitrogenous oxides, mainly nitrate and nitrite, to dinitrogen gases, N_2O and N_2 (Tiedje 1988) (Fig. 6.1). Many mountain areas of the Northern Hemisphere have received large atmospheric loadings of N_r during the last decades (Bergstrom and Jansson 2006, Baron *et al.* 2011, Catalan *et al.* 2013, Camarero 2017). Freshwater systems account for about 20% of global denitrification; they are hotspots of activity; e.g. soils only average ~10% of the freshwater denitrification activity per area (Seitzinger *et al.* 2006). In mountain areas affected by high nitrogen (N) deposition, streams and lakes show elevated nitrate concentrations (Bergstrom and Jansson 2006). Waters are poor in phosphorus (P) and, therefore, N supply usually exceeds the uptake capacity of algae (Bergstrom and Jansson 2006). The accumulation of nitrate in these systems is an indication of an alteration of the N cycle since preindustrial times. However, little is still known about how the rates of the nitrogen pathways have been modified. In particular, information about denitrification in mountain lake sediments is minimal despite its crucial role as N_r sink (McCrackin and Elser 2010, 2012, Vila-Costa *et al.* 2016, Castellano-Hinojosa *et al.* 2017, **article III**). Sediments show higher denitrification rates than the water column (Seitzinger 1988). However, the denitrification variation in different sediment types is still poorly understood (Piña-Ochoa and Alvarez-Cobelas 2006). Few studies have compared denitrification rates between deep and littoral lake zones (Ahlgren 1994, Saunders and Kalff 2001, Rissanen *et al.* 2011, Bruesewitz *et al.* 2012, Nizzoli *et al.* 2018, Zhao *et al.* 2018) and, in the latter, between vegetated and nude sediments (Eriksson and Weisner 1999, Veraart *et al.* 2011a, Nizzoli *et al.* 2014, Vila-Costa *et al.* 2016).

Evaluating the denitrification rates occurring in the field is particularly challenging and still, involve large uncertainties (Galloway 2004). There are strictly methodological issues (Groffman *et al.* 2006). For instance, the substrate diffusion can be easily modified depending on the method; higher rates are measured in mixed slurries compared to cores (Ambus 1993). Except (**article III**), the previous studies of denitrification activity in mountain lake sediments have used sediment slurries (McCrackin and Elser 2010, 2012, Vila-Costa *et al.* 2016, Castellano-Hinojosa *et al.* 2017). On the other hand, denitrification dynamics can be episodic and spatially heterogeneous with hot spots and temporal peaks (Parkin 1987, Groffman *et al.* 2009). The variation occurs because of the fluctuations in resources (e.g., nitrate) and conditions (e.g., temperature), but also because denitrification has a facultative character for denitrifiers as an alternative to the more energetically beneficial heterotrophic aerobic respiration. A recent study of the N-functional gene abundances in mountain lakes has shown microbial assemblages structured according to the habitat and lake conditions (**article I**), with denitrification genes favoured in some of them. However, it is unknown whether the observed gene potentials are related to the high availability of nitrate from external sources (eventually atmospheric deposition) or to other factors related to the facultative metabolism of denitrifiers.

As in many aquatic ecosystems, one of the primary sources of N to the sediments in mountain lakes

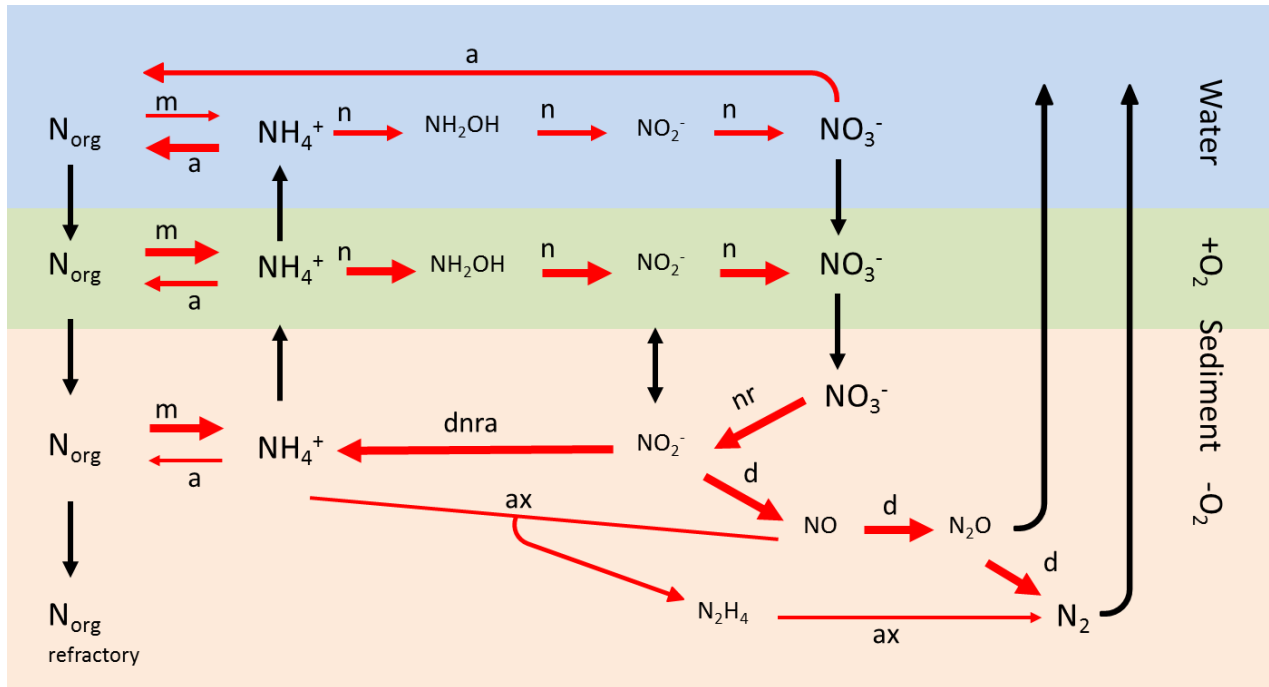


Figure 6.1. Scheme of the nitrogen cycle in mountain lakes. Black and red arrows indicate transport and reactions, respectively. Abbreviations: a, assimilation; ax, anaerobic ammonium oxidation (anammox); d, denitrification; dnra, dissimilatory nitrate reduction to ammonium; n, nitrification; nr, nitrate reduction; m, mineralization.

is the depositional flux of organic detritus. On the other hand, sediments may also uptake dissolved nitrogen compounds from the overlying water. In fact, a large proportion of mountain lake sediments are located within the photic zone, and benthic microalgal communities develop on their surface, modifying the exchange of nitrogen compounds with the water column. The growth of algae and macrophytes influences the nitrification, and denitrification processes by oxygen release, carbon (C) exudates, and N_r assimilation, (Sand-Jensen *et al.* 1982, Peterson *et al.* 2011, Veraart *et al.* 2011a, Chen *et al.* 2012, Mezzari *et al.* 2013, Nizzoli *et al.* 2014, Vila-Costa *et al.* 2016, Gardner *et al.* 2017). In mountain lakes affected by high N deposition, phytoplankton and benthic algae growth are limited by P (Axler *et al.* 1994, Bergstrom and Jansson 2006). Therefore, despite the general oligotrophy in these lakes, we can expect an increasing availability of organic C and nitrogen (N_{org}) to the sediments with increasing P-driven productivity. Productivity is usually higher, the smaller the lake, and at the lower the altitude where it is located because the growth season expands and nutrient and organic matter (OM) from the surroundings increases. As a result of these general tendencies, the trophic gradient in mountain lakes characterises by opposed changes of nitrate and total P (or dissolved organic carbon). In which way denitrification is responding to this pattern? Do higher nitrate concentrations promote higher denitrification rates? Are rates and gene potentials correlated? Does the facultative character of denitrifiers determine their abundance rather than the substrate for denitrification? Could have the enhanced N_r deposition substantially changed

the patterns of denitrifier's distribution in mountain lakes? Provided the facultative character of the denitrifier prokaryotes, and the energetic advantage of aerobic respiration upon denitrification, we hypothesised that denitrification at *in situ* conditions would not necessarily correlate with the genetic potential but to nitrate availability. Conversely, submitting the samples to nitrate concentrations above the *in situ* values would tend to saturate the gene pool activity, and thus denitrification measurements will better correlate with the gene potential. Accordingly, the potential denitrification rates should be markedly higher than the current rates.

To test our hypothesis, we measured current denitrification rates (r_c) using little-disturbed sediment cores from several lakes and habitats and potential denitrification rates (r_p) using the same cores and conditions but with the addition of nitrate up to the highest value observed in the lakes of the mountain range. Then, we investigated the relationship of both sets of results with descriptors of the gene potentials, sediment features, water column physical and chemical conditions and lake characteristics (Wallenstein *et al.* 2006, Graham *et al.* 2016). In fact, gene potentials related better to the potential denitrification rates than the current rates and, also, the environmental descriptors, in general, accounted for about twice of the variation found in potential rates than current rates. Although denitrification rates may have changed with the increased nitrogen deposition in mountain ranges of the Northern Hemisphere, the driver of the denitrification potential, i.e., denitrifier density, may not have shifted if they are more related to the organic matter fluxes (e.g., N_{org}) to the sediments or other environmental features that favour their facultative character.

6.3. MATERIALS AND METHODS

Sites and sampling

The lakes studied are situated in the central area of the Pyrenees within or nearby the Aigüestortes i Estany de Sant Maurici National Park (Table 6.1). The atmospheric nitrogen load from bulk deposition (rain and the fine fraction of dry deposition) in this area in 2010 was c. 10 kg N ha⁻¹ matching the global average (Camarero 2017). The lakes are dimictic, with a snow-ice cover during about half of the year, and ultra-oligotrophic (total phosphorus [TP] < 150 nM, except Bassa de les Granotes, which is oligotrophic (TP < 300 nM) (Catalan *et al.* 1993)) with a circumneutral pH (~7) (Vila-Costa *et al.* 2014).

Table 6.1. Lakes studied sorted by water nitrate concentration and their characteristics.

Lake (Abbreviation)	Sediment habitat ^a	Latitude (N)	Longitude (E)	Altitude ^b (m a.s.l.)	Lake area ^b (ha)	Catchment area ^b (ha)	Renewal time ^b (months)	Depth ^c (m)	TP ^d (nM)	NO ₃ ⁻ (µM)
Contraix (C)	R, D	42.58874	0.91861	2,572	9.3	100	9.9	59	49	15.5 ± 0.9
Bergús (B)	D	42.58947	0.95717	2,449	6.2	126	3.9	50	44	11.3 ± 0.6
Llebreta (Le)	C, R, D	42.55083	0.89031	1,620	8	5,438	0.1	12	89	10.6 ± 2.3
Redó Aigüestortes (RA)	D	42.58216	0.95949	2,117	6.3	325	1.6	11	76	7.0 ± 1.0
Llong (Lo)	R, D	42.57431	0.95063	2,000	7.1	1,111	0.6	13	89	6.3 ± 3.8
Gelat de Bergús (GB)	R, D	42.59106	0.96331	2,493	1.4	24	2.3	8	42	5.0 ± 1.0
Redon (R)	R, D	42.64208	0.77951	2,235	24.1	153	36	73	58	4.8 ± 1.3
Pòdo (Po)	D	42.60307	0.93906	2,450	4.6	33	9.4	25	75	1.0 ± 0.0
Bassa de les Granotes (G)	D	42.5733	0.97124	2,330	0.7	3	9.9	5	292	0.2 ± 0.4
Plan (P)	E, I, C, D	42.62248	0.9307	2,188	5	23	15.1	9	102	0.1 ± 0.4
Redon de Vilamòs (RV)	I	42.78078	0.76233	2,209	0.6	12	1.7	5	NA	0

^a Studied habitat: littoral sediments from rocky areas (R), helophyte (*Carex rostrata*) belts (C), beds of isoetids (I) and elodeid (E) macrophytes, and non-vegetated deep (D) sediments.

^b Lake descriptors used for modelling denitrification rates.

^c Maximum water column depth.

^d Total phosphorus (Camarero and Catalan, 2012).

All main sediment habitats in the lakes were considered: vegetated littoral sediments with elodeid (E), isoetid (I) or helophyte macrophytes (*Carex rostrata*, C), and non-vegetated rocky littoral (R) and deep sediments (D). Some habitats were present in only a few lakes (Table 6.1). Plan Lake was exceptionally rich in macrophytes, including isoetids (*Isoetes palustris*, *I. setacea* and *Subularia aquatica*), elodeids (*Potamogeton alpinus*, *P. berchtoldii* and *Myriophyllum alterniflorum*) and the helophyte *Carex rostrata* (Gacia *et al.* 1994). During the ice-free period (June-November) of 2013 and 2014, a total of 146 sediment cores from 20 sites and 37 times were sampled. Different techniques were used for coring depending on the habitat, only barely disturbed sediment cores (>10 cm of sediment height, acrylic sampling tube, ø 6.35 cm) with clear overlying water and interface were used. We sampled the sediments around the deepest zone of the lake from an inflatable boat using a messenger-adapted gravity corer (Glew 1991), while we sampled manually, dressing a wader or by snorkelling, the littoral habitats (**article II**).

Denitrification rate measurements

The acetylene inhibition method, combined with sensors for nitrous oxide (N_2O), was used for the denitrification measurements. This method enables estimates of reliable denitrification rates of at least $0.4 - 1 \mu\text{mol N}_2\text{O m}^{-2} \text{h}^{-1}$ (**article II**). Measurements were performed in an incubation chamber ensuring darkness and constant temperature ($\pm 1 \text{ }^\circ\text{C}$) of 5, 10 or 15 $^\circ\text{C}$, using the nearest temperature to the one measured *in situ*. Acetylene inhibition was achieved by bubbling C_2H_2 for 10 min in the water phase of the core before each denitrification measurement. Acetylene inhibits the reduction of N_2O to N_2 (Balderston *et al.* 1976, Yoshinari and Knowles 1976). The accumulated N_2O was measured using a modified Clark electrode probe (N_2O -R microsensor, Unisense A/S, Denmark; detection limit $\sim 0.1 \mu\text{M}$), in the water phase. A gentle magnet stirring was applied to prevent water stratification but avoiding sediment resuspension. Readings were taken every 5 min via a picoammeter logged to a laptop. The response of the electrochemical sensor is linear in the range of 0–1.2 mM (Andersen *et al.* 2001). The instrument was kept polarised during the measurement period. It was calibrated at the measuring temperature using a calibration chamber, zero gas water (deionised) and a freshly prepared $\sim 20 \mu\text{M N}_2\text{O}$ solution. The latter was obtained by adding a certain volume of N_2O saturated water (Weiss and Price 1980) to the zero gas water following manufacturer's instructions. Further details about the method are provided in **article II**.

A total of 314 denitrification rates were estimated. 104 current denitrification rates (r_c) were measured within less than ~ 4 h after sediment core sampling without any substrate addition (Fig. 6.2a). Denitrification potential rates were performed adding nitrate (7, 14 or 28 μM) and glucose (1.5 g/L) to the water phase of the core, a total of 39, 64, and 85 rates were measured for each treatment, respectively (Fig. 6.3a). These amounts of nitrate added were within, or slightly above, the *in situ* nitrate availability conditions found in the lakes within the Pyrenean range (Camarero and Catalan 2012). In a few cases (9), highly exaggerated nitrate concentrations (i.e. $>300 \mu\text{M}$) were added to check for the upper rate limits.

Water and sediment characterisation

The overlying water and sediments were characterised using physical, chemical and biological variables (Table S1). The temperature of the water overlying the sediment core was measured during sampling. For chemical analyses, water samples were filtered through a pre-combusted (4 h at 450 $^\circ\text{C}$) GF/F glass fibre filter. Nitrate and sulphate were determined by capillary electrophoresis using a Quanta 4000 (Waters) instrument. Ammonium and nitrite were determined by colourimetric methods in a segmented-flow autoanalyser (AA3HR, Seal), using the Berthelot reaction for ammonium (Bran+Luebbe method G-171-96) and the Griess reaction for nitrite (Bran+Luebbe method G-173-96). Dissolved organic carbon was measured by catalytic combustion to CO_2 and detection by IR spectroscopy in a TOC5000 (Shimadzu) analyser.

The upper sediment layer (0 – 0.5 cm depth) always showed the higher current and potential denitrification activities in slurries of sliced sediment core incubations. Sediment microprofiles in

non-vegetated marine and estuarine sediments also show the N₂O maximum peak above the 0.5 cm depth (Laverman *et al.* 2007, Behrendt *et al.* 2013). Therefore, only sediment descriptors from this layer were considered in the analysis of the denitrification variation (Table 6.3).

Around 5 mg of the freeze-dried sediment was encapsulated together with a catalyst (V₂O₅) in tin capsules for determination of C and N content and isotopic composition, performed at the University of California Davis Stable Isotope Facility. The dry weight percentage of OM content in the samples was determined using the loss on ignition (LOI) procedure following Heiri *et al.* (2001). The sediment density was determined using a pycnometer and rehydrating a known amount of freeze-dried sediment (previously weighted). The median grain size of the sediment was determined by laser diffraction (Mastersizer 2000, Malvern Instruments Ltd, UK). Freeze dried sediment was rehydrated in distilled water and introduced into the sample dispersion unit (Hydro 2000 G, Malvern Instruments Ltd, UK) adding hexametaphosphate and sonicating to avoid aggregates. Laser obscuration was between 10-20 % and the measuring range between 0.02 and 2000 µm.

DNA was extracted from 0.35 ± 0.02 g of sediment using the MP Biomedical FastDNA® Spin Kit for Soil. The extracted DNA was quantified using the Qubit® fluorometer (Life Technologies Corporation). Quantitative real-time PCR (qPCR) was used to quantify several N-functional genes: the denitrification genes *nirS* and *nirK*, encoding for two different nitrite reductases; *nosZI* and *nosZII*, encoding the nitrous oxide reductase from clade I and II, respectively; *nrfA*, encoding the formate-dependent nitrite reductase involved in the dissimilatory nitrate reduction to ammonium (DNRA); the anammox gene *hdh*, encoding for the hydrazine dehydrogenase; and the respective archaeal and bacterial ammonia oxidizer *amoA* genes coding for the ammonia monooxygenase. Also, the bacterial 16S rRNA gene was quantified as a proxy for the abundance of the total bacterial community. Further details about the molecular methods (e.g. primers (Rotthauwe *et al.* 1997, Hallin and Lindgren 1999, Lopez-Gutierrez *et al.* 2004, Mohan *et al.* 2004, Throbäck *et al.* 2004, Henry *et al.* 2006, Schmid *et al.* 2008, Tourna *et al.* 2008, Jones *et al.* 2013, Welsh *et al.* 2014) and amplification protocols) are provided in **article I**.

Statistical methods

Multiple linear regression models were developed to investigate the relationship of current and potential rates with descriptors of the gene potentials, sediment, water and lake features (Table 6.3). First, models were built for each type of descriptor and, after that, an overall model potentially including any descriptor was also fitted. In this way, the explanatory capacity of the environment could be investigated at different spatial scales (Wallenstein *et al.* 2006). Tables 1 and S1 list all measured descriptors included in the modelling. Only the descriptors that were selected in the models built with each type of descriptor (models 1-4 and 6-9) were included in the general models (models 5 and 10-12). All models selected show $p < 0.001$, and all variables $p < 0.05$. To select the best fitting models we used values of the Akaike's information criterion for small sample size (AICc) and adjusted R₂, and the *anova* function of the R core package stats (R Core Team, 2019).

All variables were standardised to z-scores that is subtracting the mean and dividing by the standard deviation. In this way, the values of the regression coefficients are proportional to the influence of each explanatory variable in the modelled variable (Table 6.3) and their relative importance can be immediately evaluated. Before being scaled, some variables were \log_{10} transformed to reduce the influence of extreme values: sediment dry weight / wet weight, archaeal and bacterial *amoA*, *nosZ1*, *nosZ2*, *nrfA* and *hdh* gene abundances, water ammonium and sulphate concentrations, lake and catchment area, and lake renewal time. To avoid overfitting, we selected the explanatory variables included in the models using the *dredge* function of MuMIn package (Bartoń 2016). Because not all descriptors were available for each sample, the number of final r_c estimations was reduced from the initial 104 in the complete dataset (Fig 1) to 69 in the models (Table 6.3). Kruskal-Wallis (KW) and Mann-Whitney (MW) tests were used for sample set comparisons. All calculations were performed using R version 3.4.3 (R Core Team, 2019).

6.4. RESULTS

Current denitrification rates

Current denitrification rates (r_c) ranged from 0 to 9 $\mu\text{mol N}_2\text{O m}^{-2} \text{h}^{-1}$ (Fig. 6.2), with a mean of $1.5 \pm 1.6 \mu\text{mol N}_2\text{O m}^{-2} \text{h}^{-1}$ (mean \pm SD). The rates differed among habitats ($R \approx C \approx I \gg D \approx E$, KW $p < 0.001$, Table 6.2). Sediments from all littoral habitats, except elodeids, showed higher (2.8-fold on average) r_c than the rest sediments (Fig. 6.2b, MW $p < 0.05$). In the sediments with isoetids, the rates correlated with the density of plants ($R = 0.83$ $p < 0.01$).

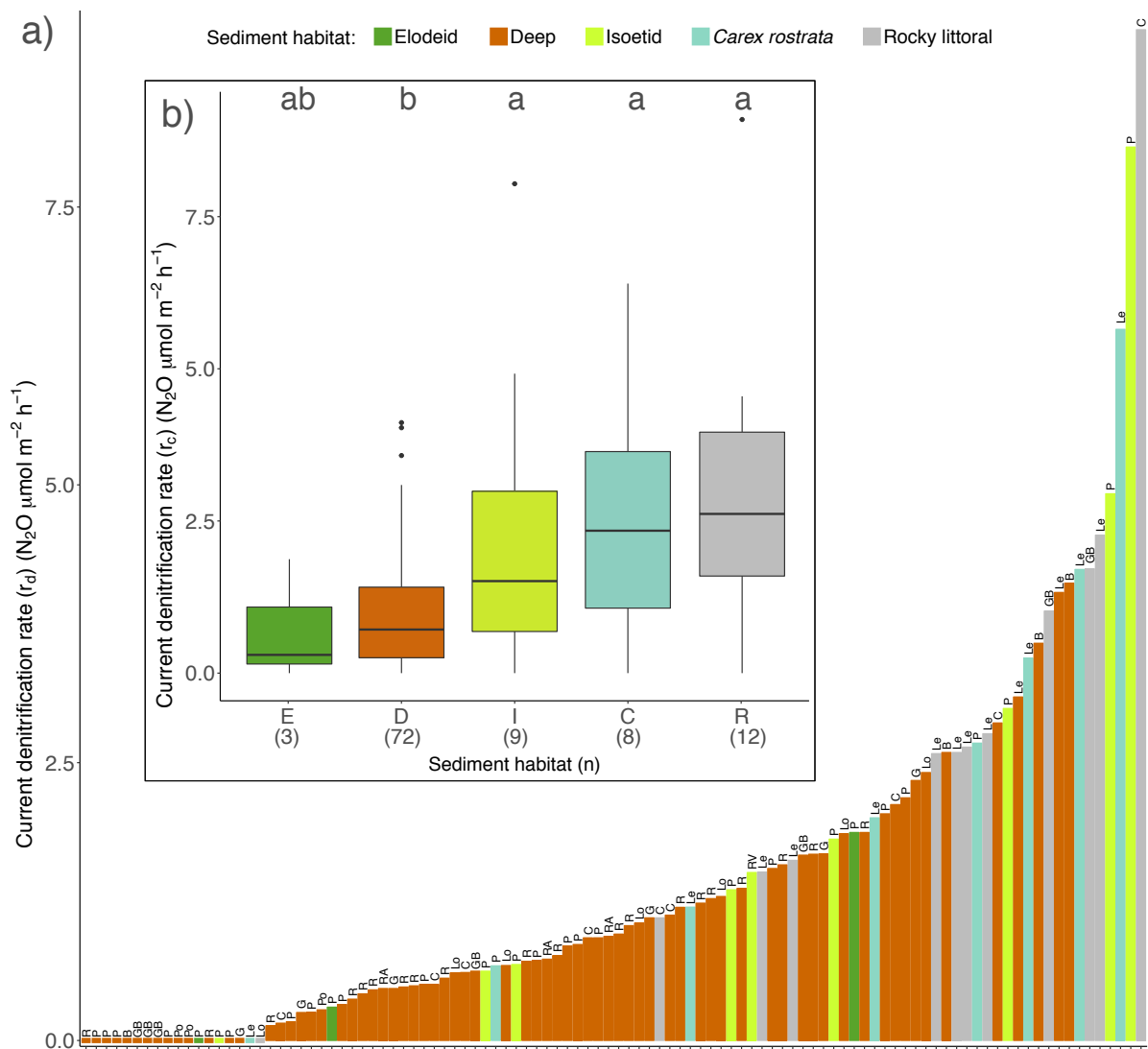


Figure 6.2. Current denitrification rates (r_c) in mountain lake sediments by (a) sample or (b) habitat. Colours indicate the studied habitats. In (a), barplot labels are the lake abbreviations (Table 6.1). Note that r_c differed between sediment habitats (KW $p < 0.001$, followed by an MW test $p < 0.05$), differences are indicated in (b) by characters over each box.

Potential denitrification rates

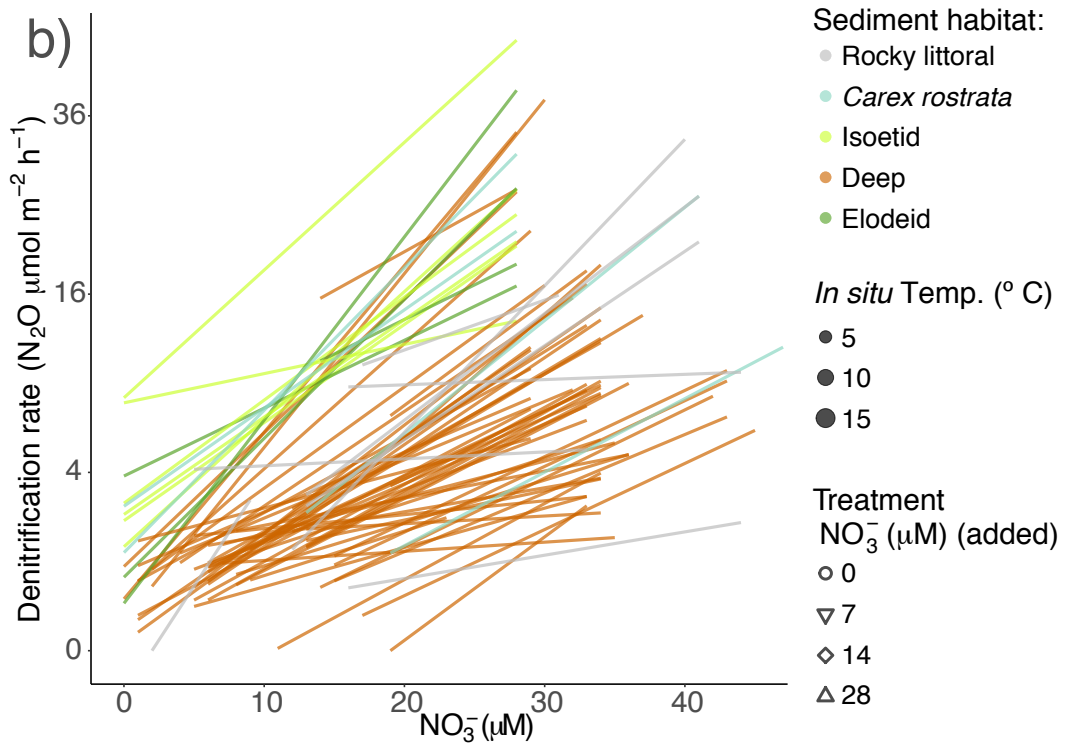
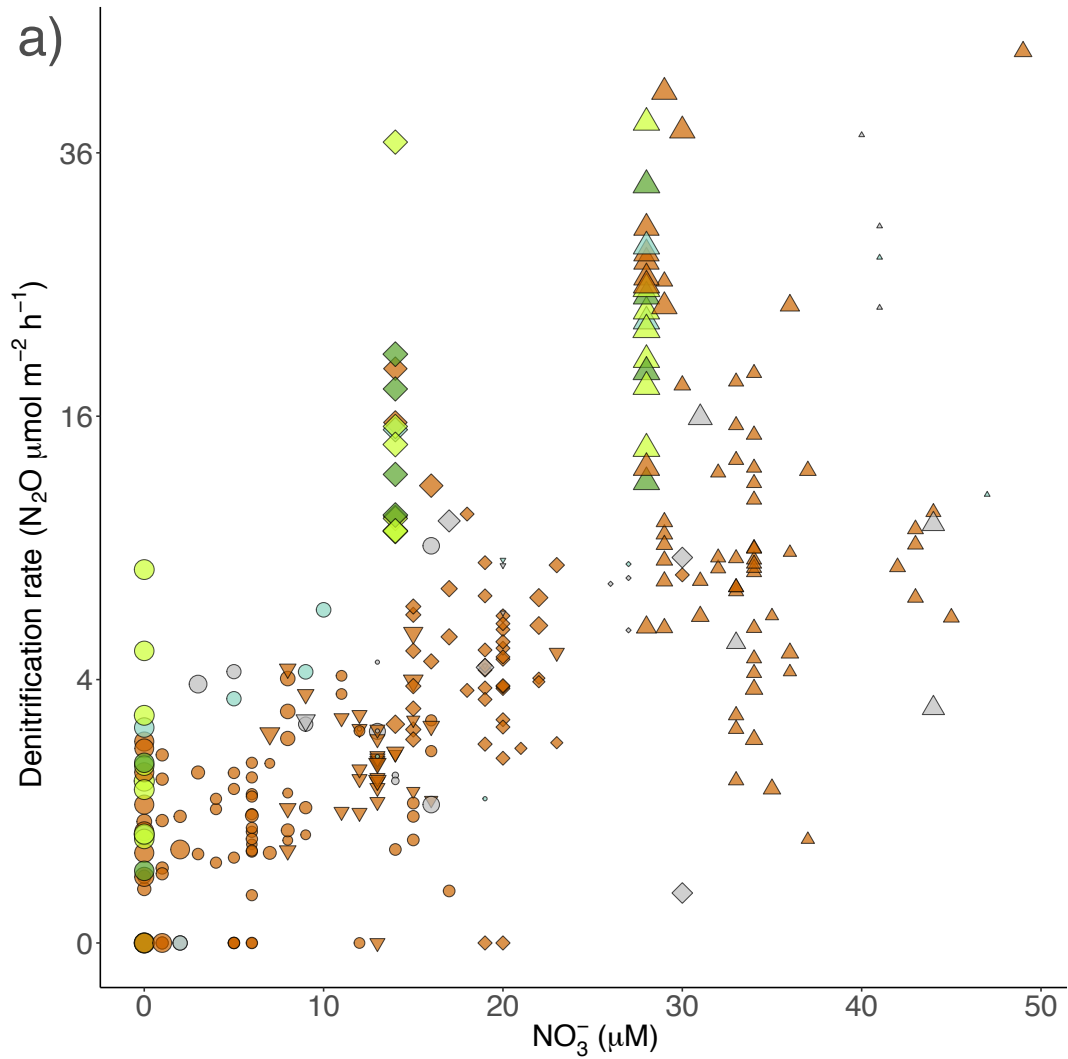
The higher denitrification rates achievable exaggerating the nitrate concentration (i.e. >300 μM), ranged from 11 to 186 $\mu\text{mol N}_2\text{O m}^{-2} \text{h}^{-1}$. More realistic, lower nitrate additions of 7, 14 and 28 μM , showed increasing denitrification rates (r_p) with the nitrate added (Fig. 6.3b). The increase was highly linear on average (2.7 ± 1.9 , 7.2 ± 5.8 , and 14.6 ± 10.2 $\mu\text{mol N}_2\text{O m}^{-2} \text{h}^{-1}$, respectively, for each treatment). However, r_p (28 μM nitrate added) values were still below the rates achieved with the extreme nitrate additions when comparing samples from the same lake and habitat. This result indicates a general over-dimensioned capacity for denitrification. The potential rates (28 μM nitrate added) also differed among habitat but differently than the current rates ($C \approx I \approx E > R > D$, KW $p < 0.001$, Table 6.2). In fact, there was no correlation between current and potential rates ($R = 0.20$, $p = 0.13$, Fig. 6.4).

Table 6.2. Current (r_c , no nitrate added) and potential (r_p , 28 μM nitrate added) denitrification rates in mountain lake sediments.

		Sediment habitat ^a					
		All	R	C	I	D	E
Current denitrification rates (r_c) ($\mu\text{mol N}_2\text{O m}^{-2} \text{h}^{-1}$)	mean	1.5	3.0	2.6	2.4	1.0	0.7
	SD	1.6	2.3	2.1	2.6	1.0	1.0
	min	0.0	0.0	0.0	0.0	0.0	0.0
	max	9.1	9.1	6.4	8.0	4.1	1.9
Potential denitrification rates (r_p) ($\mu\text{mol N}_2\text{O m}^{-2} \text{h}^{-1}$)	mean	14.6	17.9	22.2	22.8	12.3	22.1
	SD	10.2	12.9	7.5	7.9	9.6	8.8
	min	1.4	3.2	11.6	14.1	1.4	12.3
	max	45.8	37.6	28.0	38.8	45.8	33.1

^a Studied sediment habitat sorted by the mean r_c : littoral sediments from rocky areas (R), helophyte (*Carex rostrata*) belts (C), beds of isoetids (I) and elodeid (E) macrophytes, and non-vegetated deep (D) sediments.

Figure 6.3. Denitrification rates against the nitrate concentration in the water phase (initial plus added). Note the square root scale in the y-axis. Colours indicate the studied habitats. In (a), the symbol size is proportional to *in situ* temperature, and shape indicates the treatment (0, 7, 14 and 28 μM nitrate added, respectively). In (b), lines are the linear models for each sample. (Next page).



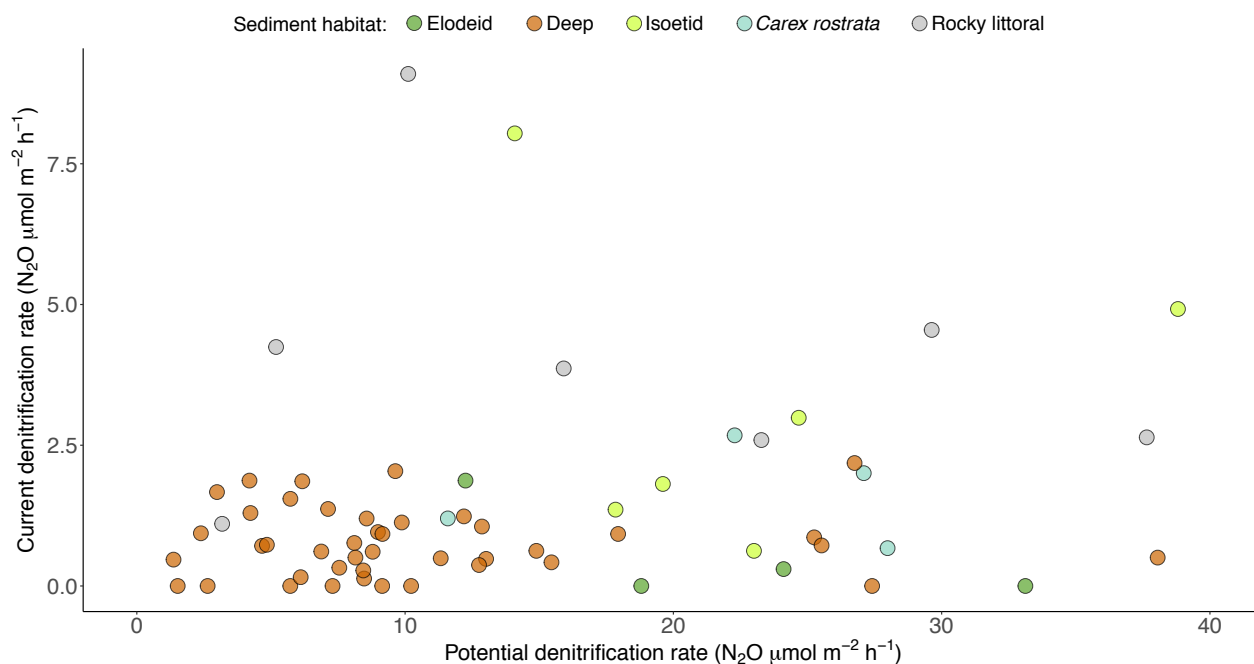


Figure 6.4. Current (no nitrate added) denitrification rates against potential (28 μM nitrate added) denitrification rates. Colours indicate the studied habitats.

Descriptors of the denitrification activity

Descriptors of the denitrification rates, both r_c and r_p , were assessed first individually from proximal (sediment) to distal (whole lake) compartments and, after that, considering an all-embracing minimum model (Table 6.3). The statistical explanation of r_c was generally low, particularly by the lake and molecular features. The general model (5), which included all the sediment and water descriptors selected in the respective individual models, indicated that both compartments show independent explicative capacity. The regression coefficients in the model indicated that sediment features have more influence than water column ones on determining rates. Only about 30% of the variation in r_c was explained.

The potential rates were better explained; about 70% of the r_p variation by the general model (10) and always more than 40% for any of the individual compartment models (Table 6.3). Building general models without either the molecular (11) or the lake descriptors (12) explained about 60% of the variations. One of the main difference between r_c and r_p was the role of lake features. For r_c the models with lake variables showed the lowest explicative capacity among compartments; in contrast, it was the highest for r_p and also, altitude and catchment size were the factors with higher influence in the general r_p model (10). These lake factors captured all the explicative value of descriptors directly linked with denitrification (model 11), such as nitrate and temperature; which showed a remarkable explicative capacity when considered alone (model 8).

Concerning the molecular descriptors in the sediments, better regression models of both r_c and r_p were obtained using N-functional gene abundances standardised by the 16S rRNA than using gene abundances by g^{-1} dry weight or by area. Molecular descriptors explained better the denitrification potential rates than the current rates (Table 6.3). *NirS* was the only gene pool selected in r_c and r_p models, but with an opposed contribution, positive in r_p and negative in r_c . Other significant gene potentials with similar relative influence were *amoA AOA*, for r_c and *nrfA* and *amoA AOB* for r_p , the latter two with negative regression coefficients (models 6, 10, 11).

The N and C sediment contents were the more influent descriptors within all r_c models, showing the higher coefficients and being selected in the general model 5. Interestingly, the absolute content of both elements was more explicative than the stoichiometric ratio. C/N ratio was included in the modelling but not selected. More specifically, N showed a greater negative effect than the positive effect of C. Regarding the denitrification potential rates, N was selected again (model 7) but in this case, with a positive effect, and the $\delta^{15}N$ signature as the complementary factor. $\delta^{15}N$ is not strictly an *in situ* factor because it was measured at the end of the experiment and could be modified during the incubation (Sebilo *et al.* 2003). None of these descriptors was included in the general r_p model 10.

Table 6.3. Multiple linear regression models relating the current (r_c , models 1-5) and potential (r_p , 28 μ M nitrate added, models 6-12) denitrification rates to several types of explanatory variables.

Model	Explanatory variables	Formula	AICc	Adj. R ²
Current denitrification rates (n = 69)				
1	Sediment (molecular)	$r_c = 0.36 * \log_{10} (amoA AOA) - 0.28 * nirS$	190	0.15
2	Sediment (rest)	$r_c = - 1.51 * N + 1.20 * C$	179	0.27
3	Water	$r_c = 0.56 * NO_3^- + 0.38 * Temperature - 0.31 * z + 0.27 * NO_2^-$	185	0.24
4	Lake	$r_c = 0.27 * \log_{10} (Catchment)$	196	0.06
5	All	$r_c = - 1.29 * N + 1.08 * C + 0.37 * NO_3^- + 0.31 * Temperature$	176	0.34
Denitrification potential rates (n = 52)				
6	Sediment (molecular)	$r_p = 0.43 * nirS - 0.33 * \log_{10} (nrfa) - 0.31 * \log_{10} (amoA AOB)$	121	0.48
7	Sediment (rest)	$r_p = 0.49 * \delta^{15}N + 0.48 * N$	124	0.43
8	Water	$r_p = 0.48 * Temperature + 0.40 * \log_{10} (SO_4^{2-}) - 0.39 * NO_3^-$	121	0.47
9	Lake	$r_p = - 0.76 * Altitude - 0.67 * \log_{10} (Catchment)$	115	0.52
10	All	$r_p = - 0.63 * Altitude - 0.58 * \log_{10} (Catchment) + 0.33 * \log_{10} (SO_4^{2-}) - 0.25 * \log_{10} (nrfa) + 0.23 * nirS$	100	0.67
11	All (but molecular)	$r_p = - 0.95 * \log_{10} (Catchment) - 0.77 * Altitude + 0.43 * \log_{10} (SO_4^{2-})$	104	0.62
12	All (but lake)	$r_p = - 0.49 * NO_3^- + 0.48 * \log_{10} (SO_4^{2-}) + 0.39 * nirS - 0.34 * \log_{10} (nrfa)$	112	0.57

Note: In all models, the intercept (not shown) was not significant ($p=1$) with negligible values ($< 1 \times 10^{-15}$). Residuals from models 5 and 10 do not show differences by habitat or lake (MW test, $p>0.05$).

Temperature was the common positive descriptor for current and potential rates in the models that included only the physicochemical descriptors of the water overlying the sediment (models 3 and 8, respectively). Nitrate and nitrite concentrations were positively related to current activities; while nitrate concentration showed a negative relationship with r_p . Sulphate concentration was positively related to r_p and was the only water factor selected in the general model 10. Finally, water depth was negatively related to r_c , indicating higher current activities in littoral habitats.

In summary, different factors described current and potential denitrification rates. Higher current activities occurred in warmer sediments with substrate availability, with nitrification performed by AOA and coupled to denitrification or using the nitrate in the water overlying the sediment. In contrast, higher denitrification potentials were found in *nirS*-rich sediments from productive lakes with warmer conditions (lower altitude) and small catchments where nitrate in the overlying water was depleted. Therefore, the availability of the nitrate controls the current activities, while the gene pool (*nirS*) controls the potential.

6.5. DISCUSSION

Control on denitrifier's density

If nitrate respiration governed the abundance of denitrifiers, we would find a correlation between current and potential denitrification rates. This was not the case. Therefore, denitrifier density should respond to other factors that may be related to their facultative metabolism, particularly their capacity for aerobic respiration. Others results agree with this interpretation: 1) *nirS* abundance correlates negatively with r_c but positively with r_p , 2) organic matter (OM) correlates with r_c and r_p , 3) *in situ* nitrate concentration correlates negatively with r_p and 4) landscape productivity correlates with r_p . The same negative nitrate- r_p relation was found in sediments of the Laurentian great lakes (Small *et al.* 2016), while in the rocky mountains r_p correlates with phosphorous (P), specifically with the P/C sediment ratio, a surrogate of productivity (McCrackin and Elser 2012). N and not C correlates with r_p , suggesting that denitrifiers are heterotrophic bacteria feeding on proteins (Van Mooy *et al.* 2002, Mrkonjic Fuka *et al.* 2007, Barnes *et al.* 2012) or other N_{org} compounds, overall on labile OM.

Denitrifiers have an advantage over other (strict) aerobic respirators in an oxygen fluctuating environment. This advantage comes from its ability to use N-oxides if oxygen is scarce (Trevors and Starodub 1987, Gao *et al.* 2009), leading to competition with DNRA organisms (usually strict anaerobes) (Brunel *et al.* 1992, Wittorf *et al.* 2016, Chen *et al.* 2017a). According to the coefficients of the general model (10) of the potential denitrification, this competition with DNRA seems secondary compared to landscape productivity. The latter depends on the altitude that marks the production conditions (e.g. nutrient availability, temperature, and growth period duration), and on the catchment size that determines the quality of the OM. The OM origin, autochthonous vs allochthonous, i.e. produced within or out of the lake, determines its quality.

Generally, autochthonous OM is more labile and has a higher quality (e.g. lower C/N). In lakes with smaller catchments, autochthonous OM represents a higher proportion of the total. Super-facultative catabolism bacteria can respire O_2 , NO_3^-/NO_2^- , or SO_x , using the latter when the other electron acceptors, with a higher energy benefit, are depleted (Marietou 2016). Mountain lake sediments are environments with a contrasted seasonality resulting in high fluctuations of different electron acceptors, which favour these super-facultative bacteria and could explain the positive influence of sulphates in potential denitrification rates. An alternative explanation for this relationship is sulfur driven chemolithotrophic denitrification, a process where sulphur-reduced compounds act as electron donors producing sulphate (Sweerts *et al.* 1990, Kamp *et al.* 2006, Burgin and Hamilton 2007). However, sulphide can inhibit the last steps of denitrification (Brunet and Garcia-Gil 1996) reducing the energy profit of the pathway and diminishing the presence of denitrifiers, which would point to an opposite (negative) relation between the sulphate produced and denitrification. It might also happen that the relationship was purely spurious because sulphates came from the watershed and could not be involved in the sediment denitrification.

Control on current denitrification rates

There is a biogeochemical control rather than a microbiological on current rates. The molecular model (1) explains low rate variation and gene pools are not included in the general model (5) of current denitrification rates. This latter model shows the substrate availability effect by the significance of the water-column nitrate and the recycling coupling denitrification to AOA nitrification. Nitrate concentration shows higher positive relations with r_c than temperature (Table 6.3, models 3 and 5); other studies show the same hierarchy (Cavaliere and Baulch 2018, **article III**). Higher current activities in littoral habitats respect to the deep part of the lake seems due to favouring denitrification conditions, such as warmer temperature and, especially, higher nitrate availability due to higher diffusion through wave action, higher nitrate inputs via runoff, surface and groundwater flows, and higher coupling to nitrification, because of the more permanent aerobic conditions resulting in higher AOA and lower *nrfA* (DNRA) abundances. The same pattern of higher littoral activities was found in an oligo/mesotrophic lake in summer (Gull Lake, Michigan, USA) (Bruesewitz *et al.* 2012), while activities were related with nitrate and oxygen availability, changing the importance of the zone depending on the season in an eutrophic boreal lake (Rissanen *et al.* 2011).

Denitrification rates estimated in this study show values within the range of other mountain lakes (McCrackin and Elser 2010, 2012); although a bit lower if we compare similar nitrate concentration and temperature. However, it should be taken into account that previous rates were estimated from sediment slurry incubations, while we used cores. All the studies (including our) used the acetylene inhibition technique to estimate the rates, which partially blocks nitrification. In locations where nitrification is high and coupled to denitrification as, for instance, rocky littoral areas of alpine lakes and in isoetid beds where archaeal *amoA* and *nirS* abundances are highly correlated (**article I**), the measured current rates could be underestimates of actual *in situ* activities, which could be more similar to the measured potential (nitrate added) rates (Seitzinger 1994).

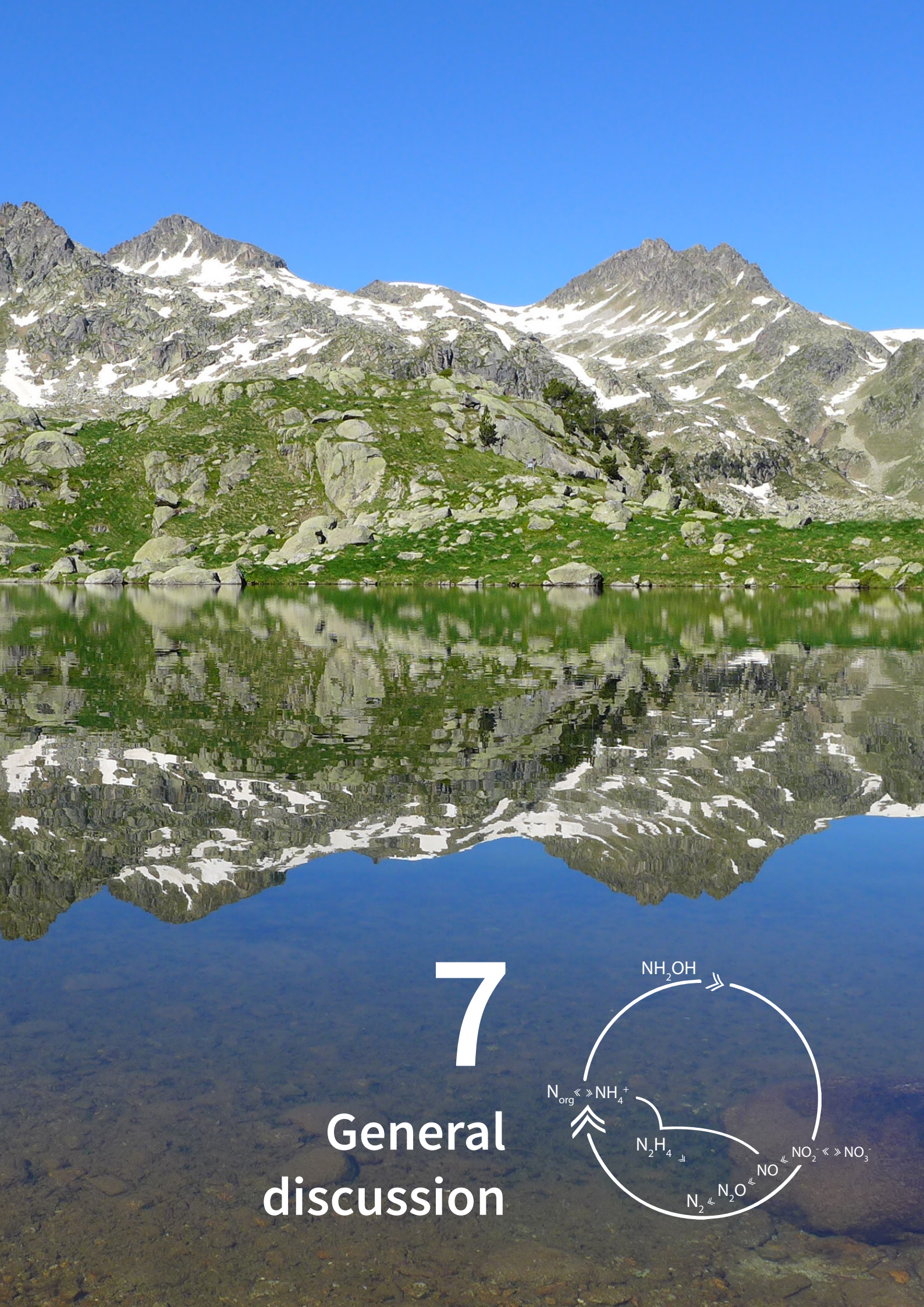
Consequences of increased N_r deposition on denitrification

The N_r removal from lakes by denitrification, according to the rates measured, would require absurd times. About 1,060 and 139 days average removal time calculated using the current and the potential (28 μM nitrate added) denitrification rates, respectively, and assuming that nitrate use did not slow down during nitrate depletion, which if considered will result in even longer times. This simple calculation explains why nitrate accumulates in some lakes, but why is depleted in others? As N_r is depleted in more productive lakes, the assimilation by primary producers is the main candidate process. Even so, provided the general nitrate limitation observed, we can conclude that the increase in N_r deposition should have increased the denitrification rates in the lakes; however, not at a sufficient rate to compensate the nitrate accumulation in the most oligotrophic sites.

Does this mean that denitrifier's density has also increased with N_r high deposition? As we have seen above, denitrifier's density is controlled by other factors, so it should not necessarily be the case. However, N_r deposition does not come alone. Especially in dusty regions, it is associated with an increase in P (Mahowald *et al.* 2008, Vicars *et al.* 2010, Jiménez *et al.* 2018) also with an anthropogenic origin and probably favouring a higher N_r removal (Bernhardt 2013, Finlay *et al.* 2013). Warming could also increase denitrifier's density through enhancing mountain lake productivity (Sommaruga-Wograth *et al.* 1997, Vicars *et al.* 2010, Preston *et al.* 2016, Belle *et al.* 2018), and also expanding the oxygen fluctuations (Veraart *et al.* 2011b), and extending the anoxic periods (North *et al.* 2014, España *et al.* 2017); although this latter aspect could be more favourable to DNRA bacteria (Pajares *et al.* 2017). Changes in the land use (e.g. agriculture, livestock (Catalan *et al.* 1993, Belle *et al.* 2017, España *et al.* 2017) or fish invasions (Gacia *et al.* 2018)), acting at a more local level, could also favour denitrifiers through enhancing the productivity and the N_r availability. Overall, the main effect of Global Change is an increase in mountain lake productivity, which enhances denitrifier's density, although not necessarily denitrification.

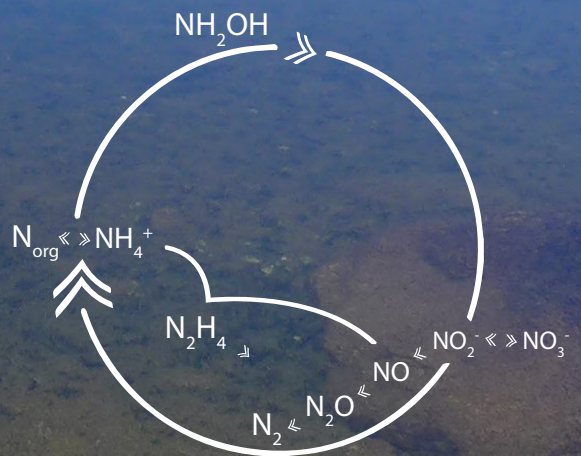
Acknowledgments

Thanks to Berta Fueyo, Marc Sala-Faig, Rober Sánchez and Pau Giménez-Grau for help in the laboratory and field sampling. We thank the authorities of the Aiguestortes and Estany de Sant Maurici National Park for sampling facilities in protected areas and support. The Spanish Government provided funds through the research grants of the Ministerio de Economía y Competitividad: NitroPir (CGL2010-19737), Lacus (CGL2013-45348-P) and Transfer (CGL2016-80124-C2-1-P) and a predoctoral fellowship to CPL (FPU12-00644).



7

General discussion



7. General discussion

The overall goal of this thesis was to improve the current knowledge of denitrification in mountain lakes. Denitrification is part of the N cycle, and other processes may facilitate (e.g. nitrification) or compete (e.g. DNRA) with it. Using molecular tools, we have quantified guilds in the main N-transformation pathways in benthic habitats (**article I**) and related to the denitrification rates (**article IV**). We have also developed a method appropriate for estimating denitrification rates in any aquatic system with retrievable sediment cores (**article II**). Furthermore, we have shown the interest of quantifying the temperature dependence of a process at a different substrate limitation within the range — or a bit above — the *in situ* substrate levels (**article III**). This thesis contributes to increase knowledge — beyond denitrification — of other processes of the N cycle, and probably the findings are not restricted only to mountain lakes but also might be relevant for other oligotrophic, remote, and/or aquatic ecosystems.

7.1. NITROGEN CYCLE IN MOUNTAIN LAKES: Nitrogen-transforming guilds

In **Article I**, we found four main N-transforming communities based on the N functional dominant genes, depending on the habitat and productivity of the lake. Each of the four consists of a highly diverse and distinct consortium of co-occurring bacterial taxa, with many OTUs detected. The high degree of similarity observed between unconstrained and functional gene-constrained OTU-based ordinations indicates that shifts in the genetic potential of different N-transformation processes are tightly linked to changes in the overall prokaryotic community structure, which itself is shaped by differences in environmental conditions across habitats. The high similarity between the constrained and unconstrained ordinations indicates that N cycling is fundamental in the benthic habitats of mountain lakes. The ability to metabolize the N-compounds is widely distributed across the phylogeny, as occur with the two more abundant N-functional genes in the studied habitats, i.e. *nrfA* (DNRA) and *nirS* (partial denitrification). It may happen that the same drivers govern the N functional guilds and the entire prokaryotic community. Temperature, abundance and quality of OM and spatiotemporal redox conditions are the best candidates to be these drivers (Small *et al.* 2016, Liao *et al.* 2019).

DNRA-Denitrification competition

The abundance of OM in the sediments is a surrogate of the system carbon flow. All the accounted N-functional genes correlated with OM, generally increasing (**article I**). Nevertheless, the dominant pathways changed depending on habitat and lake productivity. The fate of nitrite is the main diverging point according to the *nrfA-nirS* gradient (**article I**). The environmental controls that govern the end product of bacterial nitrate respiration (DNRA or denitrification) have long been studied in other systems. In our case, we found higher partial denitrification (*nirS*) in the more productive habitats, with warmer temperatures, more labile OM (lower C/N), and probably more fluctuating oxygen levels. DNRA (*nrfA*) dominates in sediments of the deepest and coldest lakes and at deeper sediment layers, overall in less productive habitats and less fluctuating reducing conditions. Similar features influencing the DNRA-denitrification dichotomy have been described in previous studies, e.g. lower C/N ratios (Tiedje 1988) and shorter generation times (Kraft *et al.* 2014) favours denitrification, the latter being a plausible adaptation to more productive places. The same DNRA-denitrification competition influences the denitrification rates, as *nirS* and *nrfA* abundances were selected as the best molecular descriptors in the global model of potential (nitrate added) denitrification rates (**article IV**).

A more precise determination of the OM quality will improve the interpretation of its influence on the denitrification of mountain lakes. Higher denitrification rates in streams were related to richer protein-like OM (Barnes *et al.* 2012). Similarly, we found higher potential denitrification rates in sediments with higher N content (**article IV**). Autochthonous OM is more labile than the one originated in the catchment, e.g. OM resulting from algal blooms is used as electron donors by denitrifiers in eutrophic lakes (Chen *et al.* 2012, Gardner *et al.* 2017). Agreeing with that, we found higher denitrification potential rates in lakes with smaller catchments where the autochthonous OM proportion is higher (**article IV**). The ability and yield using alternative C sources explain niche differentiation between a set of denitrifying bacterial strains commonly occurring in the soil or plant rhizosphere (Salles *et al.* 2012)). The availability of fermentable C compounds is another control influencing the prevalence of either DNRA or denitrification (Akunna *et al.* 1993, Tugtas and Pavlostathis 2007). OM stoichiometry, flux and oxygen controlling N loss has been suggested governing the ratios between denitrification and anammox in the ocean (Babbin *et al.* 2014). Although we found the anammox gene (*hdh*) in the studied mountain lakes (**article I**), it is not significantly influencing the denitrification rates according to the statistical modelling (**article IV**).

The redox conditions has long considered a key driver of the N cycle (e.g. (Thamdrup and Dalsgaard 2008, Small *et al.* 2014)) determining the abundances of the N intermediates (Table 1.1) and which N processes are happening (Fig. 1.1). However, the redox influence in the N cycle is more grayscale than a black or white mechanism, i.e. the intensity and frequency of the reducing conditions matters (Wittorf *et al.* 2016, Chen *et al.* 2017a). Denitrifiers have an advantage over other (strict) aerobic respirators in an oxygen fluctuating environment, such as mountain lake sediments. Particularly, in the more productive shallow lakes, where fluctuations can be stronger and *nirS*-harbouring bacteria prevails (**article I**). The denitrifier's advantage comes from its ability to use $\text{NO}_3^-/\text{NO}_2^-$ if oxygen is scarce (Trevors and Starodub 1987, Gao *et al.* 2009). DNRA organisms usually are strict anaerobes (Wittorf *et al.* 2016). We found DNRA prevalence in habitats with lower oxygen diffusion (lower sediment size) and lower redox potential (**article I**). Similarly, Pajares *et al.* (2017) explored the vertical and seasonal variation of DNRA potential (*nrfA*) in the water column of a tropical mountain lake finding the highest DNRA abundance in the deepest part of the hypolimnion with anoxic

conditions during late stratification. DNRA seems to be also important in other aquatic reducing environments, such as deep sediments layers of rivers (Huang *et al.* 2011), in estuaries (Kessler *et al.* 2018), and fjords (De Brabandere *et al.* 2015). The oxygen inhibitions of some processes are not complete or do not affect all “actors”, e.g. aerobic denitrification exists if $\text{NO}_3^-/\text{NO}_2^-$ are available (Trevors and Starodub 1987, Gao *et al.* 2009), and AOB perform nitrifier denitrification at hypoxia emitting N_2O (Kozłowski *et al.* 2016, Stein 2019). Moreover, there are super-facultative bacteria able to respire O_2 , $\text{NO}_3^-/\text{NO}_2^-$, or SO_x , using the latter when the other electron acceptors, with a higher energy benefit, are depleted (Marietou 2016). These bacteria could be important in the studied mountain lakes explaining the positive influence of sulphates in potential denitrification (**article IV**). In summary, lake productivity influences the amount and quality of OM but also the fluctuations of electron acceptors availability largely governing the DNRA-denitrification competition in mountain lakes.

NO-forming denitrifying bacteria

The abundance of *nirS* was ~50-fold greater than *nirK* across all the mountain lakes studied (**article I**). The abundance of *nirK* exhibited an overall trend of increasing abundance with lake DIN levels, as opposed to the observed for *nirS*. Primary producers consume DIN and thus generate an opposed trend between water DIN levels and lake productivity within the oligotrophy range of mountain lakes. Therefore, the two NO-forming guilds showed different habitat preferences, mainly according to lake productivity. Several studies in other environments have shown distinct habitats for these two guilds (e.g. (Desnues *et al.* 2007, Enwall *et al.* 2010)), and responses to environmental gradients (Jones and Hallin 2010). However, there are few studies about the two guilds in lakes either analysing the community (Junier *et al.* 2008, Kim *et al.* 2011), quantifying the genes (Martins *et al.* 2011, Saarenheimo *et al.* 2015a, Vila-Costa *et al.* 2016, Yao *et al.* 2018), or both (Hou *et al.* 2013, Vila-Costa *et al.* 2014, Saarenheimo *et al.* 2015b). Previous studies in some of the same mountain lakes here studied found higher *nirK* than *nirS* abundances in epilithic biofilms and sediments (Vila-Costa *et al.* 2014, Vila-Costa *et al.* 2016), while we found a *nirS* dominance. This discrepancy may be due to sampling similar but not the exactly the same habitats. We sampled upper sediment layers (0-0.5, 0.5-2, and 2-4cm) while they sampled deeper ones (2-4, 6-10, and 11-18 cm) (Vila-Costa *et al.* 2016), and we sampled lithic biofilms from the entire cobble surface while they just sample the upper-side of the cobbles (Vila-Costa *et al.* 2014). It may also be due to different qPCR protocols. The same primers were used in both studies, but we used a step-down protocol (**article I**). In any case, similar relations with environmental variables were found in Vila-Costa *et al.* (2016) and in this thesis: *nirS* abundance correlates positively with productivity (**article I**) and with the denitrification potential (**article IV**), while *nirK* was related with more oxidizing conditions. Oxygen levels, OM supply, and the thickness of biofilms also split these two guilds in rivers (Knapp *et al.* 2009, Tatariw *et al.* 2013). Interestingly, in the littoral cobbles, we found the highest *nirS* and *nirK* abundances in the thicker biofilms from the more productive Plan lake, and in the thinner from the more oligotrophic Redon lake, respectively (**article I**). Similarly, *nirK*-harbouring bacteria seems to be more diverse and abundant than *nirS* in the water column of lakes and rivers, while the opposite happens in sediments, according to the few available pieces of evidence (Graham

et al. 2010, Kim *et al.* 2011). In conclusion, although both guilds seem to be favoured in an oxygen fluctuating environment, *nirS* dominates when reducing conditions are more persistent (Yuan *et al.* 2012) (Fig.7.1).

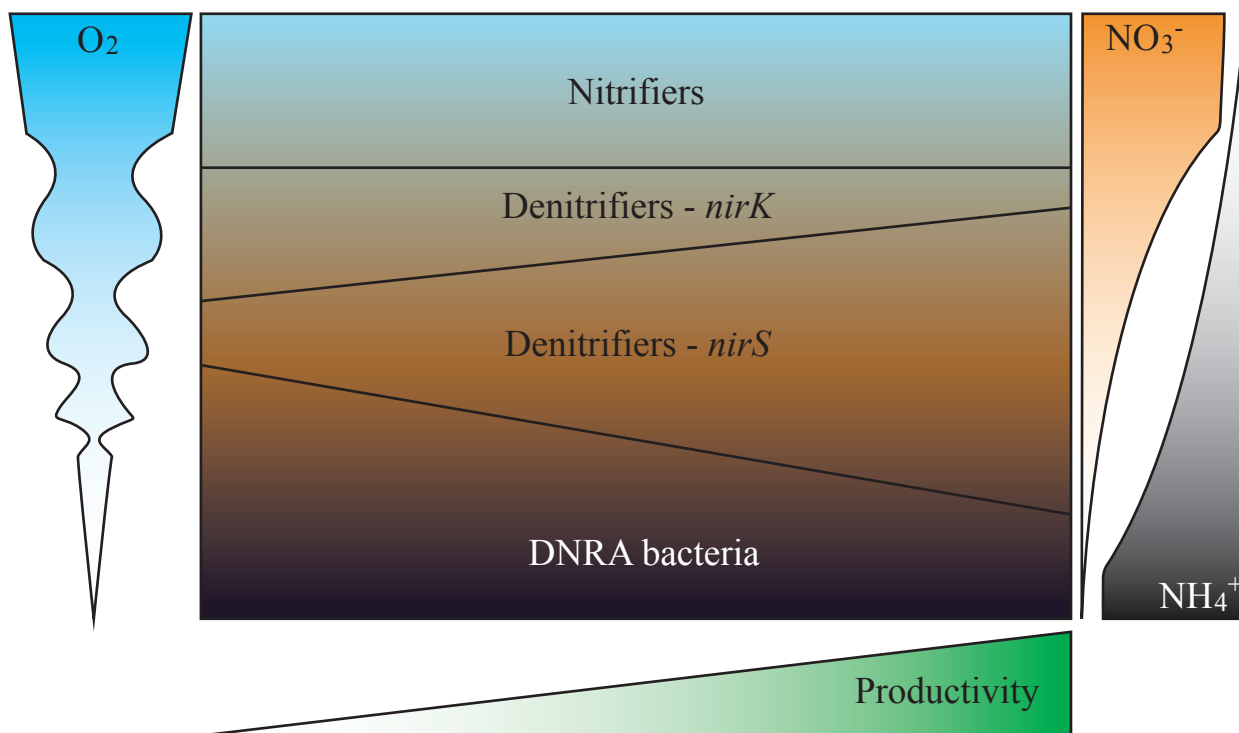


Figure 7.1. Ecological niche of the N-transforming guilds modulated by the oxygen, nitrate, ammonium, and productivity gradients.

The overall measured *nirS* relative abundance standardized to the 16S rRNA abundance — $7 \pm 6\%$ (mean \pm SD) with maximum values up to $\sim 30\%$ (**article I**) — are near or above the highest abundances reported in the literature for lakes (0.5-8%) (Martins *et al.* 2011, Saarenheimo *et al.* 2015a, Saarenheimo *et al.* 2015b). *NirS*, *nirK* and *nosZ*, like 16S rRNA gene, can have more than one gene copy by genome. However, 16S rRNA gene presents more copies (4.2 on average) per genome (Větrovský and Baldrian 2013) than the denitrification genes (2, seldom 3) (Graf *et al.* 2014). Therefore, the high *nirS* relative abundance, even standardized by the 16S, suggests that nitrate reduction capacity by the *nirS* guild is a central process within the entire prokaryotic community of benthic habitats of mountain lakes.

Partial denitrification

From a modular perspective of denitrification is even more exceptional the overall high *nirS* abundance respect to the other denitrification genes quantified (*nirK* and *nosZ*), suggesting that most of the denitrifiers in the studied mountain lakes harbour only *nirS*. This finding contrasts the previously assumed balanced denitrification gene co-occurrence in freshwaters (Graf *et al.* 2014). The overall high proportion of denitrifying nitrite versus nitrous oxide reductase genes (~30 *nir:nosZ* ratio on average) suggests a dominance of partial denitrification especially in productive habitats dominated by *nirS* denitrifier communities, with increased risk of N₂O emissions (**article I**). This observation agrees with Castellano-Hinojosa *et al.* (2017) who found high N₂O/N₂ emissions in a productive, shallow warm Mediterranean mountain lake, as well as Myrstener *et al.* (2016) who demonstrated that addition of nitrate, phosphorus and labile C to sediments from a boreal lake resulted in higher relative N₂O production compared to addition of nitrate alone. Other studies have shown that higher *nir:nosZ* ratios in the sediments of boreal lakes are associated with hypolimnion N₂O excess, as well as increased phosphate and nitrate concentrations (Saarenheimo *et al.* 2015a). Before arriving at the atmosphere, N₂O might be consumed in the hypolimnion of deep lakes. *NosZ*-harbouring bacteria have been found in the hypolimnion of boreal lakes (Peura *et al.* 2018). However, in the sediments studied, the higher *nir:nosZ* ratios were found in shallow lakes in which N₂O may easily reach the atmosphere (Dore *et al.* 1998). *NirS* abundance correlates positively to potential denitrification rates but negatively to current rates, which make sense from a dynamic view, genes are in excess to usual resource levels, so they are not a limiting factor. Consequently, the current rates depend on biogeochemical (substrate and temperature limitation) rather than genetic controls (**article IV**).

Metal influence in the Nitrogen cycle

The extreme *nirS* abundance and dominance respect the other denitrification genes (*nirK* and *nosZ*) in the benthic habitats of mountain lakes could be related to copper (Cu) and iron (Fe) levels. Bioavailability of Cu can control the expression and activity of nitrite and nitrous oxide reductases (Sullivan *et al.* 2013, Black *et al.* 2016). While *nirK* and *nosZ* are copper-containing reductases, *nirS* is a Fe-containing cd1-type reductase (Tavares *et al.* 2006, Glass and Orphan 2012). Cu limitation may lead to *nirS* dominance and to increased N₂O accumulation (Granger and Ward 2003). The measured high *nrfA* abundance also agrees with a situation of Cu limitation; this gene encodes a formate-dependent nitrite reductase involved in DNRA being also a Fe-containing cytochrome type protein (like *nirS*; Tavares *et al.* (2006)). Higher Cu levels can also inhibit denitrification due to its toxicity (Magalhaes *et al.* 2011, Liu *et al.* 2016). ~20-50 μM Cu is the optimal level for complete denitrification without N₂O accumulation in *Pseudomonas stutzeri* (Black *et al.* 2016). Not all Cu is available for denitrifying metalloenzymes, >99% is bound to OM (e.g. in lake sediments; Twining *et al.* (2007)) or to S-reduced compounds (e.g. in the ocean; Moffett *et al.* (2012)). Cu limitation seems more important in the oceans than in inland waters, but even in the oceans, denitrifiers seems to have strategies to make available the main Cu-bound fraction (Glass and Orphan 2012). However, biological competition with methanotrophs (Chang *et al.* 2018) or higher nitrate levels (Felgate *et al.* 2012) can influence Cu limitation of denitrification, accumulating N₂O. In the studied

Pyrenean mountains lakes, Fe is much more abundant than Cu, three orders of magnitude (~4% vs ~20 ppm) in sediments (Lluís Camarero pers. comm.), and ~30 folds (38.5 vs 1.3 mg m⁻² yr⁻¹) in deposition (Camarero *et al.* 2017), with lithology and deposition as the main sources of Fe and Cu, respectively. However, Cu levels are around the optimal for denitrification (Black *et al.* 2016). Therefore, there is probably neither Cu toxicity nor limitation in the studied mountain lakes. Unless it is unavailable due to being strongly linked to other compounds. The high levels of Fe suggest that Fe-driven nitrate reduction — i.e. the Fe(II) oxidation coupled to NO₃⁻/NO₂⁻ reduction (chemodenitrification (Davidson *et al.* 2003, Zhu-Barker *et al.* 2015) or DNRA (Robertson *et al.* 2016, Robertson and Thamdrup 2017, Kessler *et al.* 2018)) — could be important in the studied mountain lakes. Prokaryotes with Fe-driven DNRA capability are abundant in the benthic habitats of the Pyrenean mountain lakes, *Anaeromyxobacter* is the 4th most abundant genus, and others are present (e.g. *Geobacter*) (**article I**) (Weber *et al.* 2006, Onley *et al.* 2018)). The dominance of DNRA in the less productive mountain lakes and habitats suggest the importance of Fe-driven DNRA with Fe(II) being an alternative electron donor to OM in places with scarce OM. Further studies exploring the metal influence in the N cycle processes in mountain lakes may address these hypotheses.

Nitrifying hotspots

Ammonia-oxidising archaea (AOA) prevailed over the bacterial (AOB) counterpart in benthic habitats of mountain lakes, with nitrifying hotspots in the isoetid rhizosphere and rocky littoral sediments (**article I**). The former habitat was already known to have a tightly coupled nitrification-denitrification (Vila-Costa *et al.* 2016), but the latter was unknown. There was only indirect evidence as similar, and adjacent habitats in alpine watersheds (scree and talus with snow accumulation) were identified as important nitrification landscapes (Campbell *et al.* 2000, Campbell *et al.* 2002). AOA abundance showed a positive influence in current denitrification rates of mountain lake sediments, probably being an important NO₃⁻/NO₂⁻ source for denitrifiers (**article IV**). Furthermore, we identify two nitrifying-denitrifying coupled community types (**article I**). The first type includes AOB coupled to *nirK*-type denitrifiers reducing nitrite and *nosZI*-N₂O reduction in the lithic biofilms from littoral cobbles. The second is based on nitrification by AOA coupled to Nitrospirae (NOB) and denitrification by *nirS*-denitrifiers, being the most abundant, especially in the mentioned hotspots. The coupling between AOA and Nitrospira (NOB) have been found in agricultural soils (Jones and Hallin 2019) and grasslands (Simonin *et al.* 2015), and was also suggested by Parro *et al.* (2019) in deep sediments of an Andean mountain lake because they found high abundance of both nitrifiers guilds. Therefore, this coupling is probably occurring in more ecosystems on a global scale. Nitrospira is an abundant class within the studied Pyrenean lakes (**article I**) and also in sediments from Hengduan Mountain Lakes (China). We sampled lakes with a circumneutral pH at the water-column (~7 pH; (Bartrons *et al.* 2010, Vila-Costa *et al.* 2014)), although we did not measure the pH of the sediments. Nitrospira abundance was negatively related to pH in sediments from Hengduan lakes, which cover a wide pH (6.0 - 9.6; Liao *et al.* (2019)). Interestingly, in Pyrenean lakes, pH values established an upper limit for nitrite water levels (Catalan *et al.* 1994), opposed to the one found for Nitrospira in Hengduan lakes, suggesting that more basic lakes showed higher nitrite water levels due to some nitrification (nitrite oxidation) limitation.

Unknown anammox guilds?

We found the first evidence of anammox functional gene (*hdh*) presence in mountain lakes (**article I**). The process seems more important in the lithic biofilms from the littoral cobbles, at least this habitat show the higher *hdh* abundances, although we found the gene in all benthic habitats. This process is better known in the ocean or in wastewater treatment systems than in inland waters (Kuypers *et al.* 2018), where most of the evidence is from eutrophic ecosystems (Zhu *et al.* 2011, Zhu *et al.* 2013). Martins *et al.* (2011) studied sediments of four lakes in the Azores; Anammox bacteria were more abundant than the NO-forming denitrifiers in the three eutrophic, while denitrifiers dominated the meso-oligotrophic. Anammox capacity is restricted to the phylum Planctomycetes, and usually, only five candidate genera (*Kuenenia*, *Brocardia*, *Anammoxoglobus*, *Jettenia*, and *Scalindua*) are mentioned in the literature (e.g. ((Oshiki *et al.* 2016))). The taxonomy of anammox bacteria in oligotrophic freshwaters is largely unknown. Another genus “*Candidatus Anammoximicrobium*” (Khramenkov *et al.* 2013) was the only taxa with demonstrated anammox capacity present in the mountain lakes studied, although more bacteria within the numerous uncultured Planctomycetes detected in our samples could perform anammox (**article I**).

7.2. DENITRIFICATION: SPATIAL VARIATION AND DRIVERS IN MOUNTAIN LAKE SEDIMENTS

We found a biogeochemical rather than microbiological control on denitrification rates in mountain lake sediments (**article IV**). There is mainly a nitrate limitation and, secondarily, a temperature limitation (**article III and IV**). Nitrate consumption by primary producers seems a more important N_r depleting process than denitrification in mountain lakes (**article IV**), agreeing with the previous thought that the opposite trend between water DIN levels and lake productivity is due to N_r consumption by primary producers (Camarero and Catalan 2012). This opposite gradient and the facultative ability of denitrifiers explains the decoupling and coupling of *nirS* abundance with current (no nitrate added) and potential (nitrate added) denitrification rates, respectively (**article IV**). Littoral habitats showed higher current rates than sediments of the deep zone of the lakes because in the littoral concur more factors favouring higher activities, e.g. higher nitrate availability and temperature (**article IV**). The denitrification potential correlates with landscape productivity (**article IV**). Despite the high N_r deposition, the denitrification capacity of the studied mountain lake sediments is not saturated. Therefore, it is able to respond to future scenarios of higher N_r availability or warming (**article III and IV**).

Denitrification rates in mountain lake sediments

Current denitrification rates ranged from 0 to 9 $\mu\text{mol N}_2\text{O m}^{-2} \text{ h}^{-1}$ with a mean of $1.5 \pm 1.6 \mu\text{mol N}_2\text{O m}^{-2} \text{ h}^{-1}$ (mean \pm SD) (**article IV**). The estimated rates in this study show values within the range (0 to 114 $\mu\text{mol N}_2\text{O m}^{-2} \text{ h}^{-1}$) of other mountain lakes (McCrackin and Elser 2010, 2012), with lower values respect lakes also receiving high N deposition $42 \pm 7 \mu\text{mol N}_2\text{O m}^{-2} \text{ h}^{-1}$ (mean \pm SE; (McCrackin and Elser 2010)) and $8 \pm 6 \mu\text{mol N}_2\text{O m}^{-2} \text{ h}^{-1}$ (mean \pm SD; (McCrackin and Elser 2012)), on average those lakes have higher nitrate available in the overlying water ($\sim 23 \mu\text{M}$) than the ones studied in this thesis ($5 \mu\text{M}$). Sediments from those lakes were incubated at 15°C and 5°C , respectively, within the temperature range that we used. In our study, higher rates $15 \pm 10 \mu\text{mol N}_2\text{O m}^{-2} \text{ h}^{-1}$ (mean \pm SD) were obtained by adding $28 \mu\text{M}$ of nitrate in more similar conditions to the lakes studied by McCrackin & Elser, highlighting the importance of substrate availability in denitrification of mountain lakes (**article IV**). Differences between the procedures can also explain part of the differences between the estimated rates. We made longer incubations ($\sim 12\text{h}$) while the cited values are for shorter incubations ($\sim 4\text{h}$); although we do not see a clear saturation of the N_2O accumulated during the incubation, shorter incubations results in higher denitrification rates on average (42 vs $12 \mu\text{mol N}_2\text{O m}^{-2} \text{ h}^{-1}$, for incubations periods of 0-4h and 4-12h, respectively; McCrackin and Elser (2010)). We use sediment cores while they use slurries, the latter result in denitrification rates overestimated if there is substrate limitation due to diffusion (Ambus 1993), which is probably the case in sediments of mountain lakes. The methodology that we used to estimate denitrification rates is the acetylene inhibition technique (the same as McCrackin and Elser studies), which partially blocks nitrification (Groffman *et al.* 2006); so in locations where nitrification is important and is coupled to denitrification, e.g. archaeal *amoA* and *nirS* abundances are highly correlated in rocky littoral areas of alpine lakes and in isoetid beds (**article I**), the measured current rates could be underestimates of *in situ* activities, being more similar to potential (nitrate added) rates (Seitzinger 1994).

Spatial variation

The denitrification variation in different sediment types is still poorly understood (Piña-Ochoa and Alvarez-Cobelas 2006). We found higher current denitrification rates in littoral habitats than in sediments of the deep zone of the lakes (**article IV**), because in the littoral more factors favouring higher activities occur: warmer temperatures and especially higher $\text{NO}_3^-/\text{NO}_2^-$ availability due to higher diffusion through wave action; higher nitrate inputs via runoff, surface and groundwater flows; and higher coupling with nitrification due to more permanent aerobic conditions resulting in higher AOA and lower *nrfA* (DNRA) abundances (**article I**). The same pattern of higher littoral activities was found in an oligo/mesotrophic lake in summer (Bruesewitz *et al.* 2012), while activities were related with nitrate and oxygen availability changing the importance of the zone depending on the season in a eutrophic lake (Rissanen *et al.* 2011). Similarly, littoral zones of boreal lakes release N_2O , while pelagic zones show negligible fluxes (Huttunen *et al.* 2003). Sediments with isoetid macrophytes are one of the littoral habitats studied and are known to be a hotspot for denitrification due to a tight coupling with nitrification (Vila-Costa *et al.* 2016). We found a clear relation between denitrification rates and macrophyte density in this habitat (**article IV**).

Drivers of denitrification activity

The absence of correlation between current and potential denitrification rates, i.e. without and with nitrate added respectively, suggests that different factors govern them. In fact, it was, the models of the two types of denitrification activity include different descriptors (**article IV**). Potential denitrification rates were better explained (67%) than current rates (34%) by the multiple regression models using sediment, water and lake descriptors (**article IV**). As already mentioned, there is a biogeochemical control rather than a microbiological for current denitrification rates in the lake sediments studied. In **article IV**, the molecular model (1) explains low variation and gene pools are not included in the general model (5) of current denitrification rates. This model shows the substrate availability effect with the external water-column nitrate and the internal sediment recycling coupling denitrification to AOA nitrification, with temperature secondarily controlling the process. Nitrate concentration shows higher positive relations with current denitrification rates than temperature (models 3 and 5, **article IV**). In the denitrification temperature dependence study, we found the same hierarchy with nitrate limitation controlling the apparent energy activation (**article III**). In other cold waterbodies, this hierarchy is also found (Cavaliere and Baulch 2018).

The denitrification capacity in the sediments studied is not saturated, since potential (nitrate added) denitrification rates were always higher than current rates (**article IV**). Potential denitrification rates were related to landscape productivity (model 10, **article IV**), which depends on the altitude that marks the production conditions (e.g. nutrient availability, temperature, and growth period duration), and on the catchment size that determines the quality of the OM. The OM origin, autochthonous vs allochthonous, i.e. produced within or out of the lake, determines its quality. Generally, autochthonous OM is fresher and has a higher quality (e.g. lower C/N). In lakes with a smaller catchment autochthonous OM represents a higher proportion. Besides the primary influence of productivity in denitrification potential, water sulphate concentration and *nirS* abundance also have a positive influence while *nrfA* abundance has a negative (**article IV**). Bacteria with super-facultative catabolism are able to respire O_2 , NO_3^-/NO_2^- , or SO_x , using the latter when the other electron acceptors, with a higher energy benefit, are depleted (Marietou 2016). We found some of these bacteria in the sediments of the lakes studied, e.g. members of the genus *Desulfobacterium*, *Desulfobulbus*, *Desulforhopalus*, *Desulfovibrio*, and of the family Thermodesulfovibrionaceae. Mountain lake sediments are environments with a contrasted seasonality resulting in high fluctuations of electron acceptors availability, which favour these super-facultative bacteria and can explain the positive influence of sulphates in potential denitrification. An alternative explanation is sulfur driven chemolithotrophic denitrification, a process where sulphur-reduced compounds act as electron donors producing sulphate (Sweerts *et al.* 1990, Kamp *et al.* 2006, Burgin and Hamilton 2007). However, sulphide can inhibit the last steps of denitrification (Brunet and Garcia-Gil 1996) reducing the energy benefit of the pathway and diminishing the presence of denitrifiers, which would point to an opposite (negative) relation between the sulphate produced and denitrification. Furthermore, bacteria with the known capacity to perform sulfur driven chemolithotrophic denitrification (e.g. genus *Thiobacillus* or *Beggiatoa*) show low abundances in the sediments studied. The relationship could be spurious because sulphates come from the watershed and are not involved in denitrification in lake sediments. The negative influence of *nrfA* abundance in the denitrification potential suggests that DNRA is the most important competing process of denitrification. The potential capacity of denitrification differs between habitats, littoral sediments in rocky areas show the lower increase between potential and current rates, maybe because they are the habitats with a more important C limitation, having the lower OM content (**article IV**). Other studies showed the same higher

denitrification potential in more productive locations, e.g. denitrification potential was related to the P/C ratio in sediments from the Rocky Mountains (McCrackin and Elser 2012), and sediments of the Laurentian great lakes where operating at or near their maximum denitrification rates in the more oligotrophic Lakes Superior and Ontario while in the eutrophic Lake Erie showed increased capacity (2-3 orders) in response to additional nitrate and carbon (Small *et al.* 2016).

7.3. UNSOLVED QUESTIONS OF THE NITROGEN CYCLE IN MOUNTAIN LAKES

In this thesis, we focused on spatial variation (**article IV**) instead of in temporal variation of denitrification in mountain lake sediments. Lakes have been identified as the aquatic ecosystems with the highest seasonal variation in denitrification rates (Piña-Ochoa and Alvarez-Cobelas 2006). To my knowledge, there is not any study focusing in the temporal variation of denitrification in mountain lakes, although I expect important variations in denitrification activity at short (e.g. daily) and long (e.g. annually) timescales. I expect higher temporal variation in denitrification in the lake littoral than in profundal zones due to the fluctuating physicochemical conditions. Daily higher variations are expected in spring/summer due to wider temperature range and differences in irradiation; the latter affecting benthic primary producers, modifying the redox conditions and generating labile OM ready to be used in denitrification (Fork and Heffernan 2014). Summer storms could be a hot moment for denitrification with peaks of DIN due to the run-off in the warmest moment. This is supposed to be more important in shallow, warmer, and productive lakes, with nitrate depleted in summer but with labile OM and genetic potential (*nirS*); and since in smaller lakes this DIN input will suppose higher increments. It will be interesting to study the catchment influence on denitrification as DIN assimilation in the catchment (especially in the more vegetated) can reduce the run-off input of DIN (Bernal *et al.* 2019). Freeze and thaw cycles, and dry, and flood episodes are two moments with an expected high denitrification activity in mountain lake sediments (Sharma *et al.* 2006, Groffman *et al.* 2009, Tenuta and Sparling 2011). Freeze and thaw cycles affect more littoral sediments as the profundal part of the lake have a more constant water temperature. Although freezing temperatures in the mountains are reached in all months, I expect higher activities in the first cycles after summer due to the availability of more labile OM. Dry and flood episodes due to water flow fluctuations will also enhance denitrifying activity (Baldwin and Mitchell 2000). This can be of particular importance in anthropogenic dammed lakes which suffer a higher and frequent littoral water level fluctuations due to hydropower generation activities. Annual denitrification variation is also expected to be high due to the fluctuating redox conditions in dimictic mountain lakes. During winter stratification low irradiance (due to ice-cover) and temperature limit the growth of primary producers being a season of nitrate accumulation available for denitrifiers. In spring, snowmelt is an additional DIN source being a period of intense nitrification, and when the water-column mix, is the time of the year with the highest $\text{NO}_3^-/\text{NO}_2^-$ availability in sediments for denitrifiers, and the temperature is rising, then I will expect the higher maintained denitrification rates. During late summer/fall allochthonous organic matter could be an important source for denitrifiers, especially in lakes with important decidual vegetation in the catchments.

We studied the N-transforming guilds of nitrification, denitrification, anammox and DNRA (Fig. 1.1) in the main benthic habitats of mountain lakes (**article I**) pending the study of diazotrophs (N-fixing bacteria). We have estimated the activity just for denitrification. Despite that, we analyzed the influence of facilitating (nitrification) and competing (DNRA and anammox) denitrification processes, by targeting N-functional genes abundance in the modelled rates (**article IV**), the use of ^{15}N tracers will enable to measure the rates of all these N processes simultaneously. However, it is important to say that ^{15}N tracers have the main disadvantage of modifying the N_i availability (Robertson and Thamdrup 2017), which is a crucial aspect in the biogeochemistry of oligotrophic ecosystems, as we have seen $\text{NO}_3^-/\text{NO}_2^-$ availability is the main control of denitrification rates in mountain lakes (**article III** and **IV**). The use of deuterium and ^{18}O tracers can overcome this problem. Anyway using ^{15}N tracers methods could resolve questions about the competing processes influencing the denitrification temperature dependence (**article III**). In particular, corroborating the suggested more psychrophilic activity of anammox respect denitrification bacteria (Rysgaard *et al.* 2004, Canion *et al.* 2014b), and the higher influence of DNRA in denitrification temperature dependence at nitrate limiting conditions and high temperature (**article III**). There is evidence of higher temperature dependence of DNRA than of denitrification, but only at higher nitrate levels [1mM] (Kraft *et al.* 2014, Yoon *et al.* 2015).

The proportion of N_2O in the entire denitrification N gases emissions ($\text{N}_2\text{O}+\text{N}_2$) in mountain lakes is still unclear, with results of high N_2O proportions in one mountain lake (Castellano-Hinojosa *et al.* 2017) and the historical idea of lower proportions (supported by some results, e.g. (McCrackin and Elser 2010)) in aquatic ecosystems (Seitzinger 1988, Mengis *et al.* 1997a). We suggest a risk of higher N_2O emissions in more productive mountain lakes, due to the partial denitrification potential (**article I**). We estimated the denitrification rates with acetylene (**article III** and **IV**), so not discerning between the production of N_2 and N_2O . Even so the estimated current denitrification rates, without nitrate added, were some times around the limit of detection ($0.4\text{-}1 \mu\text{mol N}_2\text{O m}^{-2} \text{h}^{-1}$, **article II**). Due to these methodological limitations, researchers can estimate the proportion of N_2O adding nitrate estimating potential denitrification rates, unless using other methods with lower N_2O detections limits (e.g. GC-MS). Higher abundances of *nosZ* and *hdh* genes in the lithic biofilms from littoral cobbles suggest a low proportion of N_2O produced respect the entire N gases in this benthic habitat (**article I**); measurements of N-gases from littoral cobbles are needed to corroborate this suggestion. Even trickier is to know the sources of N_2O within the multiple N-processes generating it (Butterbach-Bahl *et al.* 2013), using ^{15}N or analysing the isotopic signatures of N_2O seems the best methodology to resolve this question (Santoro *et al.* 2011, Thuan *et al.* 2017).

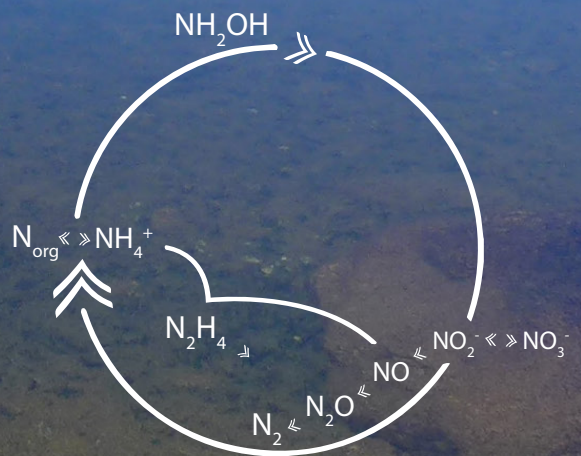
In this thesis we determine the OM quality only with the C/N content, studies determining more precisely the OM quality are required to definitely understand its influence in the denitrification and in other related processes in mountain lakes. Similarly, further studies exploring the metal influence in N processes in mountain lakes are needed to corroborate: I) possible Cu limitation or toxicity influence in denitrification, and II) the suggested Fe-driven DNRA and/or chemodenitrification importance in the less productive mountain lakes and habitats where Fe (II) bounds and OM is scarce.

The proportion of the comammox bacteria within abundant *Nitrospira* in mountain lakes is unknown. Their oligotrophic lifestyle (Kits *et al.* 2017) and high abundances in other surface-attached habitats (Pjevac *et al.* 2017, Fowler *et al.* 2018) support the idea that comammox bacteria are abundant in benthic habitats of mountain lakes. The relationship between comammox bacteria with AOA is not known, they are supposed to compete with each other when they use the same substrate (ammonium), but comammox bacteria can use the nitrite produced by AOA in a similar way to the NOB (non-comammox) *Nitrospira*.



8

Conclusions



8. Conclusions

The N-transforming guild composition in benthic habitats of mountain lakes is complex and deeply embedded in the overall prokaryotic community.

The dominant N pathways change depending on the habitat and productivity of the lake. The fate of nitrite is the main diverging point. The genetic potential for DNRA dominates in the deep part of the lakes and the lower sediment layers, which indicates the recycling of the N_r . By contrast, the denitrifying *nirS* nitrite reduction potential prevails in the upper layer of the sediments in the shallow, warmer and more productive lakes.

Emissions of N_2O and N_2 are likely spatially segregated within lakes, with lithic biofilms being candidates for preferential N loss as N_2 since they show a more balanced gene abundance of nitrous oxide reductases (*nosZI+II*) and anammox (*hdh*) in relation to NO-forming nitrite reductases (*nirS+nirK*). The more productive and *nirS*-dominated habitats may be a main source of N_2O because of the striking excess of this gene over the ones of the final steps of complete denitrification.

There are two types of nitrifying-denitrifying coupled community types: I) based on nitrification by AOA coupled to Nitrospirae (NOB) and denitrification by *nirS*-denitrifiers, with hotspots in sediments near the isoetid rhizosphere and in rocky littoral sediments of alpine lakes; II) includes AOB coupled to *nirK*-type denitrifiers reducing nitrite and *nosZI*- N_2O reduction in the lithic biofilms.

We estimate an average current denitrification rate of $1.5 \mu\text{mol } N_2O \text{ m}^{-2} \text{ h}^{-1}$ in sediments of the Pyrenean lakes with higher (~2.8 fold) activity in the littoral than in the profundal zone.

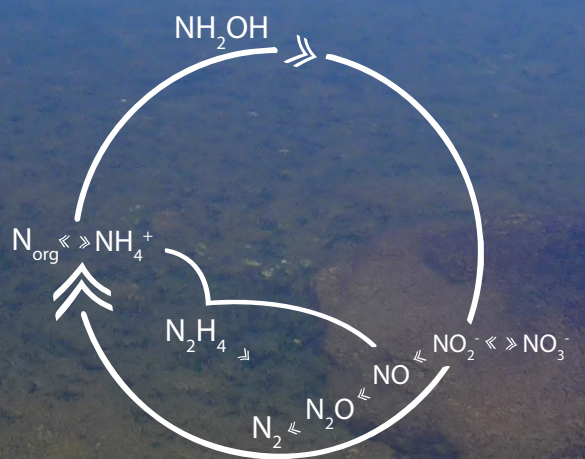
Potential denitrification rates were always higher than current, although there were not correlated. Higher current rates occurred in warmer sediments with substrate availability, via coupling with archaeal nitrification or using the nitrate in the water overlying the sediment. By contrast, higher denitrification potentials occur in *nirS*-rich and *nrfA*-poor sediments from a lower altitude, smaller catchment, and more productive lakes with sulphate rich and nitrate poor overlying water.

Denitrification rates are not nitrate saturated, and mountain lakes can respond to warming and increased N_r loadings. The increase in N deposition has increased the current activities by raising the substrate availability but not at a sufficient rate to compensate for the nitrate accumulation in the most oligotrophic sites.

Depending on nitrate availability three situations of denitrification temperature dependence occur I) under nitrate saturation conditions (e.g., $>100 \mu\text{M}$) a denitrification energy activation significantly different from 46 kJ mol^{-1} would suggest that there is another factor interfering. II) Below saturation and not at extremely low nitrate levels ($>3 \mu\text{M}$), denitrification temperature dependence increases with nitrate limitation. III) In natural environments of remote areas, *in situ* nitrate values are still far from denitrification saturation, leading to very high apparent denitrification energy activation values but this does not mean that with warming higher denitrification rates could be sustained. In case of temperature increase, a short transitory period of high denitrification would lead to a rapid depletion of nitrate unless nitrate supply rates would proportionally increase. Therefore, in a warmer scenario, variation in denitrification rates will continue mostly depending on nitrate supply processes.



References



References

- Ahlgren, I. 1994. Nitrogen budgets in relation to microbial transformations in lakes. *Ambio* 23:367-377.
- Akunna, J. C., C. Bizeau, and R. Moletta. 1993. Nitrate and nitrite reductions with anaerobic sludge using various carbon sources: Glucose, glycerol, acetic acid, lactic acid and methanol. *Water Research* 27:1303-1312.
- Ambus, P. 1993. Control of denitrification enzyme-activity in a streamside soil. *FEMS Microbiology Ecology* 102:225-234.
- Andersen, J. M. 1974. Nitrogen and phosphorus budgets and the role of sediments in six shallow Danish lakes. *Archiv Fur Hydrobiologie* 74:528-550.
- Andersen, K., T. Kjaer, and N. P. Revsbech. 2001. An oxygen insensitive microsensor for nitrous oxide. *Sensors and Actuators B-Chemical* 81:42-48.
- Arranz, E. 1997. Petrología del mazizo granítico de La Maladeta (Huesca - Lérida): estructura, mineralogía, geoquímica y petrogénesis. University of Zaragoza.
- Arrhenius, S. 1915. The influence of temperature on the velocity of reactions - Reactions of cells. Pages 1-164 in G. B. a. Sons, editor. *Quantitative Laws in Biological Chemistry*. Ltd., London.
- Axler, R., C. Rose, and C. A. Tikkanen. 1994. Phytoplankton nutrient deficiency as related to atmospheric nitrogen deposition in northern Minnesota acid-sensitive lakes. *Canadian Journal of Fisheries and Aquatic Sciences* 51:1281-1296.
- Babbin, A. R., R. G. Keil, A. H. Devol, and B. B. Ward. 2014. Organic matter stoichiometry, flux, and oxygen control nitrogen loss in the ocean. *Science* 344:406-408.
- Bachand, P. A. M., and A. J. Horne. 2000. Denitrification in constructed free-water surface wetlands: II. Effects of vegetation and temperature. *Ecological Engineering* 14:17-32.
- Balderston, W. L., B. Sherr, and W. Payne. 1976. Blockage by acetylene of nitrous oxide reduction in *Pseudomonas perfectomarinus*. *Applied and Environmental Microbiology* 31:504-508.
- Baldwin, D. S., and A. M. Mitchell. 2000. The effects of drying and re-flooding on the sediment and soil nutrient dynamics of lowland river-floodplain systems: a synthesis. *Regulated Rivers: Research & Management* 16:457-467.
- Barnes, R. T., R. L. Smith, and G. R. Aiken. 2012. Linkages between denitrification and dissolved organic matter quality, Boulder Creek watershed, Colorado. *Journal of Geophysical Research* 117:G01014.
- Baron, J. S., C. T. Driscoll, J. L. Stoddard, and E. E. Richer. 2011. Empirical critical loads of atmospheric nitrogen deposition for nutrient enrichment and acidification of sensitive US lakes. *Bioscience* 61:602-613.
- Baron, J. S., E. K. Hall, B. T. Nolan, J. C. Finlay, E. S. Bernhardt, J. A. Harrison, F. Chan, and E. W. Boyer. 2013. The interactive effects of excess reactive nitrogen and climate change on aquatic ecosystems and water resources of the United States. *Biogeochemistry* 114:71-92.
- Bartoń, K. 2016. MuMIn: multi-model inference. R package version 1.15.6. <https://CRAN.R-project.org/package=MuMIn>.

- Bartrons, M., L. Camarero, and J. Catalan. 2010. Isotopic composition of dissolved inorganic nitrogen in high mountain lakes: variation with altitude in the Pyrenees. *Biogeosciences* 7:1469-1479.
- Bates, D., M. Mächler, B. Bolker, and S. Walker. 2015. Fitting linear mixed-effects models using lme4. *Journal of Statistical Software* 67:1-48.
- Battin, T. J., K. Besemer, M. M. Bengtsson, A. M. Romani, and A. I. Packmann. 2016. The ecology and biogeochemistry of stream biofilms. *Nature Reviews Microbiology* 14:251-263.
- Behrendt, A., D. de Beer, and P. Stief. 2013. Vertical activity distribution of dissimilatory nitrate reduction in coastal marine sediments. *Biogeosciences* 10:7509-7523.
- Belle, S., S. Musazzi, I. Tönno, A. Poska, B. Leys, and A. Lami. 2018. Long-term effects of climate change on carbon flows through benthic secondary production in small lakes. *Freshwater Biology* 63:530-538.
- Belle, S., D. Rius, V. Bichet, C. Massa, C. Mavon, and L. Millet. 2017. Combining limnology and paleolimnology to assess the influence of climate change on two lakes in Southern Greenland. *Polar Biology* 40:1707-1719.
- Bennett, A. F., and R. E. Lenski. 2007. An experimental test of evolutionary trade-offs during temperature adaptation. *Proceedings of the National Academy of Sciences* 104:8649-8654.
- Bergstrom, A. K., and M. Jansson. 2006. Atmospheric nitrogen deposition has caused nitrogen enrichment and eutrophication of lakes in the northern hemisphere. *Global change biology* 12:635-643.
- Bernal, S., A. Lupon, W. M. Wollheim, F. Sabater, S. Poblador, and E. Martí. 2019. Supply, Demand, and In-Stream Retention of Dissolved Organic Carbon and Nitrate During Storms in Mediterranean Forested Headwater Streams. *Frontiers in Environmental Science* 7:60.
- Bernhard, J. M., V. P. Edgcomb, K. L. Casciotti, M. R. McIlvin, and D. J. Beaudoin. 2012. Denitrification likely catalyzed by endobionts in an allogromiid foraminifer. *The ISME Journal* 6:951-960.
- Bernhardt, E. S. 2013. Ecology. Cleaner lakes are dirtier lakes. *Science* 342:205-206.
- Berry, D., K. Ben Mahfoudh, M. Wagner, and A. Loy. 2011. Barcoded primers used in multiplex amplicon pyrosequencing bias amplification. *Applied and Environmental Microbiology* 77:7846-7849.
- Black, A., P. C. L. Hsu, K. E. Hamonts, T. J. Clough, and L. M. Condon. 2016. Influence of copper on expression of *nirS*, *norB* and *nosZ* and the transcription and activity of NIR, NOR and N2OR in the denitrifying soil bacteria *Pseudomonas stutzeri*. *Microbial biotechnology* 9:381-388.
- Blanchet, F. G., P. Legendre, and D. Borcard. 2008. Forward selection of explanatory variables. *Ecology* 89:2623-2632.
- Bonilla-Rosso, G., L. Wittorf, C. M. Jones, and S. Hallin. 2016. Design and evaluation of primers targeting genes encoding NO-forming nitrite reductases: implications for ecological inference of denitrifying communities. *Scientific Reports* 6:39208.
- Borcard, D., F. Gillet, and P. Legendre. 2011. *Numerical ecology with R*. Springer, New York.
- Boulêtreau, S., E. Salvo, E. Lyautey, S. Mastrorillo, and F. Garabetian. 2012. Temperature dependence of denitrification in phototrophic river biofilms. *Science of The Total Environment* 416:323-328.
- Bowen, J. L., A. R. Babbin, P. J. Kearns, and B. B. Ward. 2014. Connecting the dots: linking

- nitrogen cycle gene expression to nitrogen fluxes in marine sediment mesocosms. *Frontiers in microbiology* 5:429.
- Brezonik, P. L. 1994. Chemical kinetics and process dynamics in aquatic systems. Lewis Publishers, Boca Raton, Florida.
- Brin, L. D., A. E. Giblin, and J. J. Rich. 2017. Similar temperature responses suggest future climate warming will not alter partitioning between denitrification and anammox in temperate marine sediments. *Global change biology* 23:331-340.
- Bruesewitz, D. A., J. L. Tank, and S. K. Hamilton. 2012. Incorporating spatial variation of nitrification and denitrification rates into whole-lake nitrogen dynamics. *Journal of Geophysical Research-Biogeosciences* 117:G00N07.
- Brunel, B., J. Janse, H. Laanbroek, and J. Woldendorp. 1992. Effect of transient oxic conditions on the composition of the nitrate-reducing community from the rhizosphere of *Typha angustifolia*. *Microbial ecology* 24:51-61.
- Brunet, R. C., and L. J. Garcia-Gil. 1996. Sulfide-induced dissimilatory nitrate reduction to ammonia in anaerobic freshwater sediments. *FEMS Microbiology Ecology* 21:131-138.
- Burgin, A. J., and S. K. Hamilton. 2007. Have we overemphasized the role of denitrification in aquatic ecosystems? a review of nitrate removal pathways. *Frontiers in Ecology and the Environment* 5:89-96.
- Butterbach-Bahl, K., E. M. Baggs, M. Dannenmann, R. Kiese, and S. Zechmeister-Boltenstern. 2013. Nitrous oxide emissions from soils: how well do we understand the processes and their controls? *Philosophical Transactions of the Royal Society of London Series B-Biological Sciences* 368:20130122.
- Cáceres, M. D., and P. Legendre. 2009. Associations between species and groups of sites: indices and statistical inference. *Ecology* 90:3566-3574.
- Camarero, L. 2017. Atmospheric chemical loadings in the high mountain: current forcing and legacy pollution. Pages 325-341 in J. Catalan, J. Ninot, and M. M. Aniz, editors. *High Mountain Conservation in a Changing World*. Springer.
- Camarero, L., M. Bacardit, A. de Diego, and G. Arana. 2017. Decadal trends in atmospheric deposition in a high elevation station: Effects of climate and pollution on the long-range flux of metals and trace elements over SW Europe. *Atmospheric Environment* 167:542-552.
- Camarero, L., and J. Catalan. 1993. Chemistry of bulk precipitation in the central and eastern Pyrenees, northeast Spain. *Atmospheric Environment. Part A. General Topics* 27:83-94.
- Camarero, L., and J. Catalan. 1996. Variability in the chemistry of precipitation in the Pyrenees (northeastern Spain): Dominance of storm origin and lack of altitude influence. *Journal of Geophysical Research: Atmospheres* 101:29491-29498.
- Camarero, L., and J. Catalan. 1998. A simple model of regional acidification for high mountain lakes: application to the Pyrenean lakes (north-east Spain). *Water Research* 32:1126-1136.
- Camarero, L., and J. Catalan. 2012. Atmospheric phosphorus deposition may cause lakes to revert from phosphorus limitation back to nitrogen limitation. *Nature Communications* 3:1118.
- Camarero, L., M. Felip, M. Ventura, F. Bartumeus, and J. Catalan. 1999. The relative importance of the planktonic food web in the carbon cycle of an oligotrophic mountain lake in a poorly vegetated catchment (Redó, Pyrenees). *Journal of*

- Limnology 58:203-212.
- Cameron, S. G., and L. A. Schipper. 2010. Nitrate removal and hydraulic performance of organic carbon for use in denitrification beds. *Ecological Engineering* 36:1588-1595.
- Campbell, D. H., J. S. Baron, K. A. Tonnessen, P. D. Brooks, and P. F. Schuster. 2000. Controls on nitrogen flux in alpine/subalpine watersheds of Colorado. *Water Resources Research* 36:37-47.
- Campbell, D. H., C. Kendall, C. C. Y. Chang, S. R. Silva, and K. A. Tonnessen. 2002. Pathways for nitrate release from an alpine watershed: Determination using delta N-15 and delta O-18. *Water Resources Research* 38:1052.
- Canfield, D. E., A. N. Glazer, and P. G. Falkowski. 2010. The evolution and future of Earth's nitrogen cycle. *Science* 330:192-196.
- Canion, A., J. Kostka, T. Gihring, M. Huettel, J. Van Beusekom, H. Gao, G. Lavik, and M. Kuypers. 2014a. Temperature response of denitrification and anammox reveals the adaptation of microbial communities to *in situ* temperatures in permeable marine sediments that span 50° in latitude. *Biogeosciences* 11:309-320.
- Canion, A., W. A. Overholt, J. E. Kostka, M. Huettel, G. Lavik, and M. M. M. Kuypers. 2014b. Temperature response of denitrification and anaerobic ammonium oxidation rates and microbial community structure in Arctic fjord sediments. *Environmental Microbiology* 16:3331-3344.
- Canion, A., O. Prakash, S. J. Green, L. Jahnke, M. M. M. Kuypers, and J. E. Kostka. 2013. Isolation and physiological characterization of psychrophilic denitrifying bacteria from permanently cold Arctic fjord sediments (Svalbard, Norway). *Environmental Microbiology* 15:1606-1618.
- Castellano-Hinojosa, A., D. Correa-Galeote, P. Carrillo, E. J. Bedmar, and J. M. Medina-Sánchez. 2017. Denitrification and biodiversity of denitrifiers in a high-mountain Mediterranean lake. *Frontiers in microbiology* 8:1911.
- Catalan, J., E. Ballesteros, E. Gacia, A. Palau, and L. Camarero. 1993b. Chemical-composition of disturbed and undisturbed high-mountain lakes in the Pyrenees: a reference for acidified sites. *Water Research* 27:133-141.
- Catalan, J., M. G. Barbieri, F. Bartumeus, P. Bitušik, I. Botev, A. Brancelj, D. A. N. Cogălniceanu, M. Manca, A. Marchetto, N. Ognjanova-Rumenova, S. Pla, M. Rieradevall, S. Sorvari, E. Štefková, E. Stuchlík, and M. Ventura. 2009. Ecological thresholds in European alpine lakes. *Freshwater Biology* 54:2494-2517.
- Catalan, J., L. Camarero, D. D. de Quijano, M. Felip, S. Pla, M. Ventura, T. Buchaca, F. Bartumeus, G. de Mendoza, A. Miró, and E. O. Casamayor. 2006. High mountain lakes: extreme habitats and witnesses of environmental changes. *Limnetica* 25:551-584.
- Catalan, J., L. Camarero, E. Gacia, E. Ballesteros, and M. Felip. 1994. Nitrogen in the Pyrenean lakes (Spain). *Hydrobiologia* 274:17-27.
- Catalan, J., and E. Fee. 1994. Interannual variability in limnic ecosystems: origin, patterns, and predictability. Pages 81-97 *in* R. Margalef, editor. *Limnology now: A paradigm of planetary problems*. Elsevier Science, Amsterdam.
- Catalan, J., S. Pla, M. Rieradevall, M. Felip, M. Ventura, T. Buchaca, L. Camarero, A. Brancelj, P. G. Appleby, A. Lami, A. Grytnes, A. Agusti-Panareda, and R. Thompson. 2002a. Lake Redo ecosystem response to an increasing warming in the Pyrenees during the twentieth century. *Journal of Paleolimnology* 28:129-145.
- Catalan, J., S. Pla-Rabés, J. García, and L. Camarero. 2014. Air temperature-driven CO₂ consumption by rock weathering at short timescales: Evidence from a Holocene lake

- sediment record. *Geochimica et Cosmochimica Acta* 136:67-79.
- Catalan, J., S. Pla-Rabes, A. P. Wolfe, J. P. Smol, K. M. Ruhland, N. J. Anderson, J. Kopacek, E. Stuchlik, R. Schmidt, K. A. Koinig, L. Camarero, R. J. Flower, O. Heiri, C. Kamenik, A. Korhola, P. R. Leavitt, R. Psenner, and I. Renberg. 2013. Global change revealed by palaeolimnological records from remote lakes: a review. *Journal of Paleolimnology* 49:513-535.
- Catalan, J., M. Ventura, A. Brancelj, I. Granados, H. Thies, U. Nickus, A. Korhola, A. F. Lotter, A. Barbieri, E. Stuchlík, L. Lien, P. Bitušík, T. Buchaca, L. Camarero, G. H. Goudsmit, J. Kopáček, G. Lemcke, D. M. Livingstone, B. Müller, M. Rautio, M. Šiško, S. Sorvari, F. Šporka, O. Strunec, and M. Toro. 2002b. Seasonal ecosystem variability in remote mountain lakes: implications for detecting climatic signals in sediment records. *Journal of Paleolimnology* 28:25-46.
- Cavaliere, E., and H. M. Baulch. 2018. Denitrification under lake ice. *Biogeochemistry* 137:285-295.
- Cavari, B. Z., and G. Phelps. 1977. Denitrification in lake Kinneret in presence of oxygen. *Freshwater Biology* 7:385-391.
- Chambers, J. M. 1992. Linear models. Wadsworth & Brooks/Cole, Pacific Grove, California.
- Chang, J., W. Gu, D. Park, J. D. Semrau, A. A. DiSpirito, and S. Yoon. 2018. Methanobactin from *Methylosinus trichosporium* OB3b inhibits N₂O reduction in denitrifiers. *The ISME Journal* 12:2086-2089.
- Chen, J., A. Hanke, H. E. Tegetmeyer, I. Kattelman, R. Sharma, E. Hamann, T. Hargesheimer, B. Kraft, S. Lenk, and J. S. Geelhoed. 2017a. Impacts of chemical gradients on microbial community structure. *The ISME Journal* 11:920-931.
- Chen, R., M. Deng, X. He, and J. Hou. 2017b. Enhancing Nitrate Removal from Freshwater Pond by Regulating Carbon/Nitrogen Ratio. *Frontiers in microbiology* 8:1712.
- Chen, X., L. Yang, L. Xiao, A. Miao, and B. Xi. 2012. Nitrogen removal by denitrification during cyanobacterial bloom in Lake Taihu. *Journal of Freshwater Ecology* 27:243-258.
- Christensen, P. B., L. P. Nielsen, N. P. Revsbech, and J. Sorensen. 1989. Microzonation of denitrification activity in stream sediments as studied with a combined oxygen and nitrous-oxide microsensor. *Applied and Environmental Microbiology* 55:1234-1241.
- Christensen, P. B., S. Rysgaard, N. P. Sloth, T. Dalsgaard, and S. Schwærter. 2000. Sediment mineralization, nutrient fluxes, denitrification and dissimilatory nitrate reduction to ammonium in an estuarine fjord with sea cage trout farms. *Aquatic Microbial Ecology* 21:73-84.
- Crowther, T. W., and M. A. Bradford. 2013. Thermal acclimation in widespread heterotrophic soil microbes. *Ecology Letters* 16:469-477.
- Daims, H., E. V. Lebedeva, P. Pjevac, P. Han, C. Herbold, M. Albertsen, N. Jehmlich, M. Palatinszky, J. Vierheilig, A. Bulaev, R. H. Kirkegaard, M. v. Bergen, T. Rattei, B. Bendinger, P. H. Nielsen, and M. Wagner. 2015. Complete nitrification by Nitrospira bacteria. *Nature* 528:504-509.
- Davidson, E. A., J. Chorover, and D. B. Dail. 2003. A mechanism of abiotic immobilization of nitrate in forest ecosystems: the ferrous wheel hypothesis. *Global change biology* 9:228-236.
- De Brabandere, L., S. Bonaglia, M. Y. Kononets, L. Viktorsson, A. Stigebrandt, B. Thamdrup, and P. O. J. Hall. 2015. Oxygenation of an anoxic fjord basin strongly stimulates benthic denitrification and DNRA. *Biogeochemistry* 126:131-152.
- Dendooven, L., E. Pemberton, and J. M. Anderson. 1996. Denitrification potential and

- reduction enzymes dynamics in a Norway spruce plantation. *Soil Biology and Biochemistry* 28:151-157.
- Desnues, C., V. D. Michotey, A. Wieland, C. Zhizang, A. Fourcans, R. Duran, and P. C. Bonin. 2007. Seasonal and diel distributions of denitrifying and bacterial communities in a hypersaline microbial mat (Camargue, France). *Water Research* 41:3407-3419.
- Deutzmann, J. S., P. Stief, J. Brandes, and B. Schink. 2014. Anaerobic methane oxidation coupled to denitrification is the dominant methane sink in a deep lake. *Proceedings of the National Academy of Sciences of the United States of America* 111:18273-18278.
- Dodla, S. K., J. J. Wang, R. D. DeLaune, and R. L. Cook. 2008. Denitrification potential and its relation to organic carbon quality in three coastal wetland soils. *Science of The Total Environment* 407:471-480.
- Dong, L. F., C. J. Smith, S. Papaspyrou, A. Stott, A. M. Osborn, and D. B. Nedwell. 2009. Changes in benthic denitrification, nitrate ammonification, and anammox process rates and nitrate and nitrite reductase gene abundances along an estuarine nutrient gradient (the Colne estuary, United Kingdom). *Applied and Environmental Microbiology* 75:3171-3179.
- Dong, L. F., M. N. Sobey, C. J. Smith, I. Rusmana, W. Phillips, A. Stott, A. M. Osborn, and D. B. Nedwell. 2011. Dissimilatory reduction of nitrate to ammonium, not denitrification or anammox, dominates benthic nitrate reduction in tropical estuaries. *Limnology and Oceanography* 56:279-291.
- Dore, J. E., B. N. Popp, D. M. Karl, and F. J. Sansone. 1998. A large source of atmospheric nitrous oxide from subtropical North Pacific surface waters. *Nature* 396:63-66.
- Edgar, R. C. 2013. UPARSE highly accurate OTU sequences from microbial amplicon reads. *Nature Methods* 10:996-998.
- Enwall, K., L. Philippot, and S. Hallin. 2005. Activity and composition of the denitrifying bacterial community respond differently to long-term fertilization. *Applied and Environmental Microbiology* 71:8335-8343.
- Enwall, K., I. N. Throback, M. Stenberg, M. Soderstrom, and S. Hallin. 2010. Soil resources influence spatial patterns of denitrifying communities at scales compatible with land management. *Applied and Environmental Microbiology* 76:2243-2250.
- Eriksson, P. G., and S. E. Weisner. 1999. An experimental study on effects of submersed macrophytes on nitrification and denitrification in ammonium - rich aquatic systems. *Limnology and Oceanography* 44:1993-1999.
- Erismann, J. W., J. Galloway, S. Seitzinger, A. Bleeker, and K. Butterbach-Bahl. 2011. Reactive nitrogen in the environment and its effect on climate change. *Current Opinion in Environmental Sustainability* 3:281-290.
- Erismann, J. W., M. A. Sutton, J. Galloway, Z. Klimont, and W. Winiwarter. 2008. How a century of ammonia synthesis changed the world. *Nature Geoscience* 1:636.
- España, J., M. d. P. Mata, J. Vegas, M. Morellón, J. Rodriguez, Á. Salazar, I. Yusta, A. Chaos, C. Pérez-Martínez, and A. Navas. 2017. Anthropogenic and climatic factors enhancing hypolimnetic anoxia in a temperate mountain lake. *Journal of Hydrology* 555:832-850.
- Ettwig, K. F., M. K. Butler, D. Le Paslier, E. Pelletier, S. Mangenot, M. M. Kuypers, F. Schreiber, B. E. Dutilh, J. Zedelius, D. de Beer, J. Gloerich, H. J. Wessels, T. van Alen, F. Luesken, M. L. Wu, K. T. van de Pas-Schoonen, H. J. Op den Camp, E. M. Janssen-Megens, K. J. Francoijs, H. Stunnenberg, J. Weissenbach, M. S. Jetten, and M. Strous. 2010. Nitrite-driven anaerobic methane oxidation by oxygenic bacteria. *Nature* 464:543-548.

- Felgate, H., G. Giannopoulos, M. J. Sullivan, A. J. Gates, T. A. Clarke, E. Baggs, G. Rowley, and D. J. Richardson. 2012. The impact of copper, nitrate and carbon status on the emission of nitrous oxide by two species of bacteria with biochemically distinct denitrification pathways. *Environmental Microbiology* 14:1788-1800.
- Fields, S. 2004. Global nitrogen: cycling out of control. *Environmental health perspectives* 112:A556-A563.
- Finlay, J. C., G. E. Small, and R. W. Sterner. 2013. Human influences on nitrogen removal in lakes. *Science* 342:247-250.
- Firestone, M. K., R. B. Firestone, and J. M. Tiedje. 1980. Nitrous oxide from soil denitrification: factors controlling its biological production. *Science* 208:749-751.
- Foley, J., D. de Haas, Z. Yuan, and P. Lant. 2010. Nitrous oxide generation in full-scale biological nutrient removal wastewater treatment plants. *Water Research* 44:831-844.
- Fork, M., and J. Heffernan. 2014. Direct and Indirect Effects of Dissolved Organic Matter Source and Concentration on Denitrification in Northern Florida Rivers. *Ecosystems* 17:14-28.
- Fowler, S. J., A. Palomo, A. Dechesne, P. D. Mines, and B. F. Smets. 2018. Comammox Nitrospira are abundant ammonia oxidizers in diverse groundwater - fed rapid sand filter communities. *Environmental Microbiology* 20:1002-1015.
- Freedman, Z., S. D. Eisenlord, D. R. Zak, K. Xue, Z. L. He, and J. Z. Zhou. 2013. Towards a molecular understanding of N cycling in northern hardwood forests under future rates of N deposition. *Soil Biology & Biochemistry* 66:130-138.
- Gacia, E., E. Ballesteros, L. Camarero, O. Delgado, A. Palau, J. L. Riera, and J. Catalan. 1994. Macrophytes from lakes in the eastern Pyrenees: community composition and ordination in relation to environmental factors. *Freshwater Biology* 32:73-81.
- Gacia, E., T. Buchaca, N. Bernal-Mendoza, I. Sabás, E. Ballesteros, and M. Ventura. 2018. Non-native Minnows Threaten Quillwort Populations in High Mountain Shallow Lakes. *Frontiers in Plant Science* 9:329.
- Gacia, E., E. Chappuis, A. Lumbreras, J. L. Riera, and E. Ballesteros. 2009. Functional diversity of macrophyte communities within and between Pyrenean lakes. *Journal of Limnology* 68:25-36.
- Gal, G., J. Imberger, T. Zohary, J. Antenucci, A. Anis, and T. Rosenberg. 2003. Simulating the thermal dynamics of Lake Kinneret. *Ecological Modelling* 162:69-86.
- Galloway, J. N. 2004. Nitrogen cycles: past, present, and future. *Biogeochemistry* 70:153-226.
- Galloway, J. N., J. D. Aber, J. W. Erisman, S. P. Seitzinger, R. W. Howarth, E. B. Cowling, and B. J. Cosby. 2003. The nitrogen cascade. *Bioscience* 53:341-356.
- Galloway, J. N., A. R. Townsend, J. W. Erisman, M. Bekunda, Z. Cai, J. R. Freney, L. A. Martinelli, S. P. Seitzinger, and M. A. Sutton. 2008. Transformation of the nitrogen cycle: Recent trends, questions, and potential solutions. *Science* 320:889-892.
- Gao, H., F. Schreiber, G. Collins, M. M. Jensen, J. E. Kostka, G. Lavik, D. de Beer, H.-y. Zhou, and M. M. M. Kuypers. 2009. Aerobic denitrification in permeable Wadden Sea sediments. *The ISME Journal* 4:417.
- Gardner, W. S., and M. J. McCarthy. 2009. Nitrogen dynamics at the sediment-water interface in shallow, sub-tropical Florida Bay: why denitrification efficiency may decrease with increased eutrophication. *Biogeochemistry* 95:185-198.
- Gardner, W. S., M. J. McCarthy, S. An, D. Sobolev, K. S. Sell, and D. Brock. 2006. Nitrogen fixation and dissimilatory nitrate reduction to ammonium (DNRA) support nitrogen dynamics in Texas estuaries. *Limnology and Oceanography* 51:558-568.

- Gardner, W. S., S. E. Newell, M. J. McCarthy, D. K. Hoffman, K. Lu, P. J. Lavrentyev, F. L. Hellweger, S. W. Wilhelm, Z. Liu, D. A. Bruesewitz, and H. W. Paerl. 2017. Community biological ammonium demand: a conceptual model for Cyanobacteria blooms in eutrophic lakes. *Environmental science & technology* 51:7785-7793.
- Glass, J. B., and V. J. Orphan. 2012. Trace metal requirements for microbial enzymes involved in the production and consumption of methane and nitrous oxide. *Frontiers in microbiology* 3:61.
- Glew, J. 1991. Miniature gravity corer for recovering short sediment cores. *Journal of Paleolimnology* 5:285-287.
- Glew, J. R., J. P. Smol, and W. M. Last. 2001. Sediment Core Collection and Extrusion. Pages 73-105 in W. M. Last and J. P. Smol, editors. *Tracking Environmental Change Using Lake Sediments: Basin Analysis, Coring, and Chronological Techniques*. Springer Netherlands, Dordrecht.
- Graf, D. R. H., C. M. Jones, and S. Hallin. 2014. Intergenomic comparisons highlight modularity of the denitrification pathway and underpin the importance of community structure for N₂O emissions. *PLoS One* 9:e114118.
- Graham, D. W., C. Trippett, W. K. Dodds, J. M. O'Brien, E. B. K. Banner, I. M. Head, M. S. Smith, R. K. Yang, and C. W. Knapp. 2010. Correlations between *in situ* denitrification activity and nir-gene abundances in pristine and impacted prairie streams. *Environmental pollution* 158:3225-3229.
- Graham, E. B., J. E. Knelman, A. Schindlbacher, S. Siciliano, M. Breulmann, A. Yannarell, J. M. Beman, G. Abell, L. Philippot, and J. Prosser. 2016. Microbes as engines of ecosystem function: When does community structure enhance predictions of ecosystem processes? *Frontiers in microbiology* 7:214.
- Graham, P. H., and C. P. Vance. 2003. Legumes: Importance and Constraints to Greater Use. *Plant Physiology* 131:872-877.
- Granger, J., and B. B. Ward. 2003. Accumulation of nitrogen oxides in copper-limited cultures of denitrifying bacteria. *Limnology and Oceanography* 48:313-318.
- Greaver, T., C. Clark, J. Compton, D. Vallano, A. Talhelm, C. Weaver, L. Band, J. Baron, E. Davidson, and C. Tague. 2016. Key ecological responses to nitrogen are altered by climate change. *Nature Climate Change* 6:836-843.
- Groffman, P. M., M. A. Altabet, J. K. Bohlke, K. Butterbach-Bahl, M. B. David, M. K. Firestone, A. E. Giblin, T. M. Kana, L. P. Nielsen, and M. A. Voytek. 2006. Methods for measuring denitrification: Diverse approaches to a difficult problem. *Ecological Applications* 16:2091-2122.
- Groffman, P. M., K. Butterbach-Bahl, R. W. Fulweiler, A. J. Gold, J. L. Morse, E. K. Stander, C. Tague, C. Tonitto, and P. Vidon. 2009. Challenges to incorporating spatially and temporally explicit phenomena (hotspots and hot moments) in denitrification models. *Biogeochemistry* 93:49-77.
- Gross-Wittke, A., G. Gunkel, and A. Hoffmann. 2010. Temperature effects on bank filtration: redox conditions and physical-chemical parameters of pore water at Lake Tegel, Berlin, Germany. *Journal of Water and Climate Change* 1:55-66.
- Gruber, N., and J. N. Galloway. 2008. An Earth-system perspective of the global nitrogen cycle. *Nature* 451:293-296.
- Hall, E. K., C. Neuhauser, and J. B. Cotner. 2008. Toward a mechanistic understanding of how natural bacterial communities respond to changes in temperature in aquatic ecosystems. *The ISME Journal* 2:471-481.

- Hall, E. K., G. A. Singer, M. J. Kainz, and J. T. Lennon. 2010. Evidence for a temperature acclimation mechanism in bacteria: an empirical test of a membrane - mediated trade - off. *Functional Ecology* 24:898-908.
- Hallin, S., and P. E. Lindgren. 1999. PCR detection of genes encoding nitrile reductase in denitrifying bacteria. *Applied and Environmental Microbiology* 65:1652-1657.
- Hallin, S., L. Philippot, F. E. Löffler, R. A. Sanford, and C. M. Jones. 2018. Genomics and ecology of novel N₂O-reducing microorganisms. *Trends in microbiology* 26:43-55.
- Heiri, O., A. F. Lotter, and G. Lemcke. 2001. Loss on ignition as a method for estimating organic and carbonate content in sediments: reproducibility and comparability of results. *Journal of Paleolimnology* 25:101-110.
- Hendriks, J., A. Oubrie, J. Castresana, A. Urbani, S. Gemeinhardt, and M. Saraste. 2000. Nitric oxide reductases in bacteria. *Biochimica et Biophysica Acta* 1459:266-273.
- Henry, S., D. Bru, B. Stres, S. Hallet, and L. Philippot. 2006. Quantitative detection of the *nosZ* gene, encoding nitrous oxide reductase, and comparison of the abundances of 16S rRNA, *narG*, *nirK*, and *nosZ* genes in soils. *Applied and Environmental Microbiology* 72:5181-5189.
- Herbert, R. A., and D. B. Nedwell. 1990. Role of environmental factors in regulating nitrate respiration in intertidal sediments. Pages 77-90 in N. P. Revsbech and J. Sørensen, editors. *Denitrification in soil and sediment*. Springer US, New York.
- Higgins, S. A., A. Welsh, L. H. Orellana, K. T. Konstantinidis, J. C. Chee-Sanford, R. A. Sanford, C. W. Schadt, and F. E. Löffler. 2016. Detection and Diversity of Fungal Nitric Oxide Reductase Genes (*p450nor*) in Agricultural Soils. *Applied and Environmental Microbiology* 82:2919-2928.
- Holmes, R. M., J. B. Jones, S. G. Fisher, and N. B. Grimm. 1996. Denitrification in a nitrogen-limited stream ecosystem. *Biogeochemistry* 33:125-146.
- Holtgrieve, G. W., D. E. Schindler, W. O. Hobbs, P. R. Leavitt, E. J. Ward, L. Bunting, G. Chen, B. P. Finney, I. Gregory-Eaves, S. Holmgren, M. J. Lisac, P. J. Lisi, K. Nydick, L. A. Rogers, J. E. Saros, D. T. Selbie, M. D. Shapley, P. B. Walsh, and A. P. Wolfe. 2011. A coherent signature of anthropogenic nitrogen deposition to remote watersheds of the northern hemisphere. *Science* 334:1545-1548.
- Hou, J., X. Cao, C. Song, and Y. Zhou. 2013. Predominance of ammonia-oxidizing archaea and *nirK*-gene-bearing denitrifiers among ammonia-oxidizing and denitrifying populations in sediments of a large urban eutrophic lake (Lake Donghu). *Canadian journal of microbiology* 59:456-464.
- Huang, S., C. Chen, X. Yang, Q. Wu, and R. Zhang. 2011. Distribution of typical denitrifying functional genes and diversity of the *nirS*-encoding bacterial community related to environmental characteristics of river sediments. *Biogeosciences* 8:3041-3051.
- Huttunen, J. T., J. Alm, A. Liikanen, S. Juutinen, T. Larmola, T. Hammar, J. Silvola, and P. J. Martikainen. 2003. Fluxes of methane, carbon dioxide and nitrous oxide in boreal lakes and potential anthropogenic effects on the aquatic greenhouse gas emissions. *Chemosphere* 52:609-621.
- Hvorslev, M. J. 1949. *Subsurface Exploration and Sampling of Soils for Civil Engineering Purposes*. American Society of Civil Engineers, Waterways Experiment Station, Corps of Engineers, U.S. Army, Vicksburg, Mississippi.
- Hynes, R. K., and R. Knowles. 1978. Inhibition by acetylene of ammonia oxidation in *Nitrosomonas europaea*. *FEMS Microbiology Letters* 4:319-321.
- Inwood, S. E., J. L. Tank, and M. J. Bernot. 2007. Factors controlling sediment denitrification in

- midwestern streams of varying land use. *Microbial ecology* 53:247-258.
- IPCC. 2013. *Climate Change 2013: The Physical Science Basis. Contribution of Working Group I to the fifth assessment report of the intergovernmental panel on climate change.* Cambridge University Press.
- Jiménez, L., K. M. Rühland, A. Jeziorski, J. P. Smol, and C. Pérez-Martínez. 2018. Climate change and Saharan dust drive recent cladoceran and primary production changes in remote alpine lakes of Sierra Nevada, Spain. *Global change biology* 24:e139-e158.
- Jones, C. M., D. R. Graf, D. Bru, L. Philippot, and S. Hallin. 2013. The unaccounted yet abundant nitrous oxide-reducing microbial community: a potential nitrous oxide sink. *The ISME Journal* 7:417-426.
- Jones, C. M., and S. Hallin. 2010. Ecological and evolutionary factors underlying global and local assembly of denitrifier communities. *The ISME Journal* 4:633-641.
- Jones, C. M., and S. Hallin. 2019. Geospatial variation in co-occurrence networks of nitrifying microbial guilds. *Molecular Ecology* 00:0-14.
- Jones, C. M., A. Spor, F. P. Brennan, M.-C. Breuil, D. Bru, P. Lemanceau, B. Griffiths, S. Hallin, and L. Philippot. 2014. Recently identified microbial guild mediates soil N₂O sink capacity. *Nature Climate Change* 4:801-805.
- Jørgensen, C. J., O. S. Jacobsen, B. Elberling, and J. Aamand. 2009. Microbial Oxidation of Pyrite Coupled to Nitrate Reduction in Anoxic Groundwater Sediment. *Environmental science & technology* 43:4851-4857.
- Jørgensen, K. S. 1989. Annual pattern of denitrification and nitrate ammonification in estuarine sediment. *Applied and Environmental Microbiology* 55:1841-1847.
- Junier, P., O.-S. Kim, K.-P. Witzel, J. F. Imhoff, and O. Hadas. 2008. Habitat partitioning of denitrifying bacterial communities carrying nirS or nirK genes in the stratified water column of Lake Kinneret, Israel. *Aquatic Microbial Ecology* 51:129-140.
- Kamp, A., P. Stief, and H. N. Schulz-Vogt. 2006. Anaerobic sulfide oxidation with nitrate by a freshwater *Beggiatoa* enrichment culture. *Applied and Environmental Microbiology* 72:4755-4760.
- Kessler, A. J., K. L. Roberts, A. Bissett, and P. L. Cook. 2018. Biogeochemical controls on the relative importance of denitrification and dissimilatory nitrate reduction to ammonium in estuaries. *Global Biogeochemical Cycles* 32:1045-1057.
- Khramenkov, S. V., M. N. Kozlov, M. V. Kevbrina, A. G. Dorofeev, E. A. Kazakova, V. A. Grachev, B. B. Kuznetsov, D. Y. Polyakov, and Y. A. Nikolaev. 2013. A novel bacterium carrying out anaerobic ammonium oxidation in a reactor for biological treatment of the filtrate of wastewater fermented sludge. *Microbiology* 82:628-636.
- Kim, O.-S., J. F. Imhoff, K.-P. Witzel, and P. Junier. 2011. Distribution of denitrifying bacterial communities in the stratified water column and sediment-water interface in two freshwater lakes and the Baltic Sea. *Aquatic ecology* 45:99-112.
- King, D., and D. B. Nedwell. 1984. Changes in the nitrate-reducing community of an anaerobic saltmarsh sediment in response to seasonal selection by temperature. *Microbiology* 130:2935-2941.
- King, D., and D. B. Nedwell. 1985. The influence of nitrate concentration upon the end-products of nitrate dissimilation by bacteria in anaerobic salt marsh sediment. *FEMS Microbiology Letters* 31:23-28.
- King, D., and D. B. Nedwell. 1987. The adaptation of nitrate-reducing bacterial communities in estuarine sediments in response to overlying nitrate load. *FEMS Microbiology Ecology* 3:15-20.

- Kits, K. D., D. J. Campbell, A. R. Rosana, and L. Y. Stein. 2015a. Diverse electron sources support denitrification under hypoxia in the obligate methanotroph *Methylomicrobium album* strain BG8. *Frontiers in microbiology* 6:1072.
- Kits, K. D., M. G. Klotz, and L. Y. Stein. 2015b. Methane oxidation coupled to nitrate reduction under hypoxia by the Gammaproteobacterium *Methylomonas denitrificans*, sp. nov. type strain FJG1. *Environmental Microbiology* 17:3219-3232.
- Kits, K. D., C. J. Sedlacek, E. V. Lebedeva, P. Han, A. Bulaev, P. Pjevac, A. Daebeler, S. Romano, M. Albertsen, L. Y. Stein, H. Daims, and M. Wagner. 2017. Kinetic analysis of a complete nitrifier reveals an oligotrophic lifestyle. *Nature* 549:269-272.
- Knapp, C. W., W. K. Dodds, K. C. Wilson, J. M. O'Brien, and D. W. Graham. 2009. Spatial Heterogeneity of Denitrification Genes in a Highly Homogenous Urban Stream. *Environmental science & technology* 43:4273-4279.
- Kobayashi, M., and H. Shoun. 1995. The copper-containing dissimilatory nitrite reductase involved in the denitrifying system of the fungus *Fusarium oxysporum*. *Journal of Biological Chemistry* 270:4146-4151.
- Koike, I. 1990. Measurement of sediment denitrification using 15-N tracer method. Pages 291-300 in N. P. Revsbech, Sørensen, J, editor. *Denitrification in Soil and Sediment*. Springer US.
- Kopàček, J., J. Hejzlar, J. Vrba, and E. Stuchlík. 2011. Phosphorus loading of mountain lakes: Terrestrial export and atmospheric deposition. *Limnology and Oceanography* 56:1343-1354.
- Kozłowski, J. A., K. D. Kits, and L. Y. Stein. 2016. Comparison of Nitrogen Oxide Metabolism among Diverse Ammonia-Oxidizing Bacteria. *Frontiers in microbiology* 7:1090.
- Kraft, B., H. E. Tegetmeyer, R. Sharma, M. G. Klotz, T. G. Ferdelman, R. L. Hettich, J. S. Geelhoed, and M. Strous. 2014. The environmental controls that govern the end product of bacterial nitrate respiration. *Science* 345:676-679.
- Kumon, Y., Y. Sasaki, I. Kato, N. Takaya, H. Shoun, and T. Beppu. 2002. Codenitrification and denitrification are dual metabolic pathways through which dinitrogen evolves from nitrate in *Streptomyces antibioticus*. *Journal of bacteriology* 184:2963-2968.
- Kuypers, M. M. M., H. K. Marchant, and B. Kartal. 2018. The microbial nitrogen-cycling network. *Nature Reviews Microbiology* 16:263-276.
- Lashof, D. A., and D. R. Ahuja. 1990. Relative contributions of greenhouse gas emissions to global warming. *Nature* 344:529-531.
- Laughlin, R. J., and R. J. Stevens. 2002. Evidence for Fungal Dominance of Denitrification and Codenitrification in a Grassland Soil. *Soil Science Society of America Journal* 66:1540-1548.
- Laverman, A. M., C. Meile, P. Van Cappellen, and E. B. A. Wieringa. 2007. Vertical distribution of denitrification in an estuarine sediment: Integrating sediment flowthrough reactor experiments and microprofiling via reactive transport modeling. *Applied and Environmental Microbiology* 73:40-47.
- Laverman, A. M., P. Van Cappellen, D. van Rotterdam-Los, C. Pallud, and J. Abell. 2006. Potential rates and pathways of microbial nitrate reduction in coastal sediments. *FEMS Microbiology Ecology* 58:179-192.
- Liao, B., X. Yan, J. Zhang, M. Chen, Y. Li, J. Huang, M. Lei, H. He, and J. Wang. 2019. Microbial community composition in alpine lake sediments from the Hengduan Mountains. *Microbiologyopen*:e832.
- Liu, Y., Y. Liu, H. Zhou, L. Li, J. Zheng, X. Zhang, J. Zheng, and G. Pan. 2016. Abundance,

- composition and activity of denitrifier communities in metal polluted paddy soils. *Scientific Reports* 6:19086.
- Long, A., J. Heitman, C. Tobias, R. Philips, and B. Song. 2013. Co-occurring anammox, denitrification, and codenitrification in agricultural soils. *Applied and Environmental Microbiology* 79:168-176.
- Lopez-Gutierrez, J. C., S. Henry, S. Hallet, F. Martin-Laurent, G. Catroux, and L. Philippot. 2004. Quantification of a novel group of nitrate-reducing bacteria in the environment by real-time PCR. *Journal of microbiological methods* 57:399-407.
- Lorenzen, J., L. H. Larsen, T. Kjaer, and N. P. Revsbech. 1998. Biosensor determination of the microscale distribution of nitrate, nitrate assimilation, nitrification, and denitrification in a diatom-inhabited freshwater sediment. *Applied and Environmental Microbiology* 64:3264-3269.
- Luque-Almagro, V. M., A. J. Gates, C. Moreno-Vivian, S. J. Ferguson, D. J. Richardson, and M. Dolores Roldan. 2011. Bacterial nitrate assimilation: gene distribution and regulation. *Biochemical Society transactions* 39:1838-1843.
- MacFarlane, G., and R. Herbert. 1982. Nitrate dissimilation by *Vibrio* spp. isolated from estuarine sediments. *Microbiology* 128:2463-2468.
- Maeda, K., A. Spor, V. Edel-Hermann, C. Heraud, M.-C. Breuil, F. Bizouard, S. Toyoda, N. Yoshida, C. Steinberg, and L. Philippot. 2015. N₂O production, a widespread trait in fungi. *Scientific Reports* 5:9697.
- Magalhaes, C. M., A. Machado, P. Matos, and A. A. Bordalo. 2011. Impact of copper on the diversity, abundance and transcription of nitrite and nitrous oxide reductase genes in an urban European estuary. *FEMS Microbiology Ecology* 77:274-284.
- Mahowald, N., T. D. Jickells, A. R. Baker, P. Artaxo, C. R. Benitez-Nelson, G. Bergametti, T. C. Bond, Y. Chen, D. D. Cohen, B. Herut, N. Kubilay, R. Losno, C. Luo, W. Maenhaut, K. A. McGee, G. S. Okin, R. L. Siefert, and S. Tsukuda. 2008. Global distribution of atmospheric phosphorus sources, concentrations and deposition rates, and anthropogenic impacts. *Global Biogeochemical Cycles* 22:GB4026.
- Mania, D., K. Heylen, R. J. M. van Spanning, and A. Frostegard. 2014. The nitrate-ammonifying and nosZ-carrying bacterium *Bacillus vireti* is a potent source and sink for nitric and nitrous oxide under high nitrate conditions. *Environmental Microbiology* 16:3196-3210.
- Marietou, A. 2016. Nitrate reduction in sulfate-reducing bacteria. *FEMS Microbiology Letters* 363:fnw155.
- Mariotti, A., J. Germon, P. Hubert, P. Kaiser, R. Letolle, A. Tardieux, and P. Tardieux. 1981. Experimental determination of nitrogen kinetic isotope fractionation: some principles; illustration for the denitrification and nitrification processes. *Plant and Soil* 62:413-430.
- Martins, G., A. Terada, D. C. Ribeiro, A. M. Corral, A. G. Brito, B. F. Smets, and R. Nogueira. 2011. Structure and activity of lacustrine sediment bacteria involved in nutrient and iron cycles. *FEMS Microbiology Ecology* 77:666-679.
- Martiny, J. B., S. E. Jones, J. T. Lennon, and A. C. Martiny. 2015. Microbiomes in light of traits: a phylogenetic perspective. *Science* 350:aac9323.
- Mazerolle, M. J. 2016. AICcmodavg: model selection and multimodel inference based on (Q) AIC (c). R package version 2.0-4 <http://CRAN.R-project.org/package=AICcmodavg>.
- McClain, M. E., E. W. Boyer, C. L. Dent, S. E. Gergel, N. B. Grimm, P. M. Groffman, S. C. Hart, J. W. Harvey, C. A. Johnston, and E. Mayorga. 2003. Biogeochemical hot spots and hot

- moments at the interface of terrestrial and aquatic ecosystems. *Ecosystems* 6:301-312.
- McCrackin, M. L., and J. J. Elser. 2010. Atmospheric nitrogen deposition influences denitrification and nitrous oxide production in lakes. *Ecology* 91:528-539.
- McCrackin, M. L., and J. J. Elser. 2011. Greenhouse gas dynamics in lakes receiving atmospheric nitrogen deposition. *Global Biogeochemical Cycles* 25:GB4005.
- McCrackin, M. L., and J. J. Elser. 2012. Denitrification kinetics and denitrifier abundances in sediments of lakes receiving atmospheric nitrogen deposition (Colorado, USA). *Biogeochemistry* 108:39-54.
- Melton, E. D., P. Stief, S. Behrens, A. Kappler, and C. Schmidt. 2014. High spatial resolution of distribution and interconnections between Fe- and N-redox processes in profundal lake sediments. *Environmental Microbiology* 16:3287-3303.
- Mengis, M., R. Gächter, and B. Wehrli. 1997a. Sources and sinks of nitrous oxide (N₂O) in deep lakes. *Biogeochemistry* 38:281-301.
- Mengis, M., R. Gächter, B. Wehrli, and S. Bernasconi. 1997b. Nitrogen elimination in two deep eutrophic lakes. *Limnology and Oceanography* 42:1530-1543.
- Merbt, S. N., S. Bernal, L. Proia, E. Martí, and E. O. Casamayor. 2017. Photoinhibition on natural ammonia oxidizers biofilm populations and implications for nitrogen uptake in stream biofilms. *Limnology and Oceanography* 62:364-375.
- Messer, J. J., and P. L. Brezonik. 1984. Laboratory evaluation of kinetic-parameters for lake sediment denitrification models. *Ecological Modelling* 21:277-286.
- Mezzari, M. P., M. L. B. da Silva, R. S. Nicoloso, A. M. G. Ibelli, M. Bortoli, A. Viancelli, and H. M. Soares. 2013. Assessment of N₂O emission from a photobioreactor treating ammonia-rich swine wastewater digestate. *Bioresource Technology* 149:327-332.
- Moffett, J. W., C. B. Tuit, and B. B. Ward. 2012. Chelator-induced inhibition of copper metalloenzymes in denitrifying bacteria. *Limnology and Oceanography* 57:272-280.
- Mohan, S. B., M. Schmid, M. Jetten, and J. Cole. 2004. Detection and widespread distribution of the *nrfA* gene encoding nitrite reduction to ammonia, a short circuit in the biological nitrogen cycle that competes with denitrification. *FEMS Microbiology Ecology* 49:433-443.
- Mrkonjic Fuka, M., M. Engel, J.-C. Munch, and M. Schloter. 2007. Chapter 19 - Characterization of proteolytic microbes and their activities in soils. Pages 303-309 in S. J. Ferguson and W. E. Newton, editors. *Biology of the nitrogen cycle*. Elsevier, Amsterdam.
- Mulder, A., A. A. Vandegraaf, L. A. Robertson, and J. G. Kuenen. 1995. Anaerobic ammonium oxidation discovered in a denitrifying fluidized-bed reactor. *FEMS Microbiology Ecology* 16:177-183.
- Myrstener, M., A. Jonsson, and A. K. Bergstrom. 2016. The effects of temperature and resource availability on denitrification and relative N₂O production in boreal lake sediments. *Journal of Environmental Sciences* 47:82-90.
- Naqvi, S. W. A., P. Lam, G. Narvenkar, A. Sarkar, H. Naik, A. Pratihary, D. M. Shenoy, M. Gauns, S. Kurian, S. Damare, M. Duret, G. Lavik, and M. M. M. Kuypers. 2018. Methane stimulates massive nitrogen loss from freshwater reservoirs in India. *Nature Communications* 9:1265.
- Nizzoli, D., M. Bartoli, R. Azzoni, D. Longhi, G. Castaldelli, and P. Viaroli. 2018. Denitrification in a meromictic lake and its relevance to nitrogen flows within a moderately impacted forested catchment. *Biogeochemistry* 137:143-161.
- Nizzoli, D., E. Carraro, V. Nigro, and P. Viaroli. 2010. Effect of organic enrichment and thermal

- regime on denitrification and dissimilatory nitrate reduction to ammonium (DNRA) in hypolimnetic sediments of two lowland lakes. *Water Research* 44:2715-2724.
- Nizzoli, D., D. T. Welsh, D. Longhi, and P. Viaroli. 2014. Influence of *Potamogeton pectinatus* and microphytobenthos on benthic metabolism, nutrient fluxes and denitrification in a freshwater littoral sediment in an agricultural landscape: N assimilation versus N removal. *Hydrobiologia* 737:183-200.
- Nogaro, G., and A. J. Burgin. 2014. Influence of bioturbation on denitrification and dissimilatory nitrate reduction to ammonium (DNRA) in freshwater sediments. *Biogeochemistry* 120:279-294.
- North, R. P., R. L. North, D. M. Livingstone, O. Koster, and R. Kipfer. 2014. Long-term changes in hypoxia and soluble reactive phosphorus in the hypolimnion of a large temperate lake: consequences of a climate regime shift. *Global change biology* 20:811-823.
- Ogilvie, B., M. Rutter, and D. Nedwell. 1997. Selection by temperature of nitrate-reducing bacteria from estuarine sediments: species composition and competition for nitrate. *FEMS Microbiology Ecology* 23:11-22.
- Onley, J. R., S. Ahsan, R. A. Sanford, and F. E. Löffler. 2018. Denitrification by *Anaeromyxobacter dehalogenans*, a common soil bacterium lacking the nitrite reductase genes *nirS* and *nirK*. *Applied and Environmental Microbiology* 84:e1985-1917.
- Oshiki, M., H. Satoh, and S. Okabe. 2016. Ecology and physiology of anaerobic ammonium oxidizing bacteria. *Environmental Microbiology* 18:2784-2796.
- Pajares, S., M. Merino-Ibarra, M. Macek, and J. Alcocer. 2017. Vertical and seasonal distribution of picoplankton and functional nitrogen genes in a high-altitude warm-monomictic tropical lake. *Freshwater Biology* 62:1180-1193.
- Parkin, T. B. 1987. Soil microsites as a source of denitrification variability. *Soil Science Society of America Journal* 51:1194-1199.
- Parro, V., F. Puente-Sánchez, N. A. Cabrol, I. Gallardo-Carreño, M. Moreno-Paz, Y. Blanco, M. García-Villadangos, C. Tambley, V. C. Tilot, C. Thompson, E. Smith, P. Sobrón, C. S. Demergasso, A. Echeverría-Vega, M. Á. Fernández-Martínez, L. G. Whyte, and A. G. Fairén. 2019. Microbiology and Nitrogen Cycle in the Benthic Sediments of a Glacial Oligotrophic Deep Andean Lake as Analog of Ancient Martian Lake-Beds. *Frontiers in microbiology* 10:929.
- Pattinson, S. N., R. Garcia-Ruiz, and B. A. Whitton. 1998. Spatial and seasonal variation in denitrification in the Swale-Ouse system, a river continuum. *Science of The Total Environment* 210:289-305.
- Peter, N. L. 1992. Denitrification in sediment determined from nitrogen isotope pairing. *FEMS Microbiology Ecology* 9:357-361.
- Peterson, C., A. D Daley, S. M Pechauer, K. N Kalscheur, M. J Sullivan, S. L Kufta, M. Rojas, K. Gray, and J. Kelly. 2011. Development of associations between microalgae and denitrifying bacteria in streams of contrasting anthropogenic influence. *FEMS Microbiology Ecology* 77:477-492.
- Peura, S., M. Buck, S. L. Aalto, S. E. Morales, H. Nykanen, and A. Eiler. 2018. Novel Autotrophic Organisms Contribute Significantly to the Internal Carbon Cycling Potential of a Boreal Lake. *MBio* 9:e916-918.
- Peura, S., L. Sinclair, S. Bertilsson, and A. Eiler. 2015. Metagenomic insights into strategies of aerobic and anaerobic carbon and nitrogen transformation in boreal lakes. *Scientific Reports* 5:12102.
- Pfenning, K., and P. McMahon. 1997. Effect of nitrate, organic carbon, and temperature on

- potential denitrification rates in nitrate-rich riverbed sediments. *Journal of Hydrology* 187:283-295.
- Philippot, L. 2002. Denitrifying genes in bacterial and Archaeal genomes. *Biochimica Et Biophysica Acta-Gene Structure and Expression* 1577:355-376.
- Philippot, L., and S. Hallin. 2005. Finding the missing link between diversity and activity using denitrifying bacteria as a model functional community. *Current Opinion in Microbiology* 8:234-239.
- Piña-Ochoa, E., and M. Alvarez-Cobelas. 2006. Denitrification in aquatic environments: A cross-system analysis. *Biogeochemistry* 81:111-130.
- Pinheiro, J., D. Bates, S. DebRoy, and D. Sarkar. 2007. Linear and nonlinear mixed effects models. Page 57 R package version.
- Pinheiro, J. C., and D. M. Bates. 1978. *Mixed-Effects Models in S and S-plus*. Springer, New York, NY.
- Pjevac, P., C. Schauburger, L. Poghosyan, C. W. Herbold, M. van Kessel, A. Daebeler, M. Steinberger, M. S. M. Jetten, S. Lucker, M. Wagner, and H. Daims. 2017. AmoA-targeted polymerase chain reaction primers for the specific detection and quantification of comammox *Nitrospira* in the environment. *Frontiers in microbiology* 8:1508.
- Preston, D. L., N. Caine, D. M. McKnight, M. W. Williams, K. Hell, M. P. Miller, S. J. Hart, and P. T. J. Johnson. 2016. Climate regulates alpine lake ice cover phenology and aquatic ecosystem structure. *Geophysical Research Letters* 43:5353-5360.
- Quast, C., E. Pruesse, P. Yilmaz, J. Gerken, T. Schweer, P. Yarza, J. Peplies, and F. O. Glockner. 2013. The SILVA ribosomal RNA gene database project: improved data processing and web-based tools. *Nucleic Acids Research* 41:D590-596.
- R Core Team. 2019. *R: A Language and Environment for Statistical Computing*. R Foundation for Statistical Computing, Vienna, Austria. Available at: <http://www.r-project.org>.
- Ravishankara, A. R., J. S. Daniel, and R. W. Portmann. 2009. Nitrous Oxide (N₂O): The Dominant Ozone-Depleting Substance Emitted in the 21st Century. *Science* 326:123-125.
- Revsbech, N. P., L. P. Nielsen, P. B. Christensen, and J. Sorensen. 1988. Combined oxygen and nitrous-oxide microsensor for denitrification studies. *Applied and Environmental Microbiology* 54:2245-2249.
- Risgaard-Petersen, N., A. M. Langezaal, S. Ingvarsdén, M. C. Schmid, M. S. Jetten, H. J. Op den Camp, J. W. Derksen, E. Pina-Ochoa, S. P. Eriksson, L. P. Nielsen, N. P. Revsbech, T. Cedhagen, and G. J. van der Zwaan. 2006. Evidence for complete denitrification in a benthic foraminifer. *Nature* 443:93-96.
- Risgaard-Petersen, N., L. P. Nielsen, S. Rysgaard, T. Dalsgaard, and R. L. Meyer. 2003. Application of the isotope pairing technique in sediments where anammox and denitrification coexist. *Limnology and Oceanography-Methods* 1:63-73.
- Rissanen, A., M. Tiirola, and A. Ojala. 2011. Spatial and temporal variation in denitrification and in the denitrifier community in a boreal lake. *Aquatic Microbial Ecology* 64:27-40.
- Robertson, E. K., K. L. Roberts, L. D. W. Burdorf, P. Cook, and B. Thamdrup. 2016. Dissimilatory nitrate reduction to ammonium coupled to Fe(II) oxidation in sediments of a periodically hypoxic estuary. *Limnology and Oceanography* 61:365-381.
- Robertson, E. K., and B. Thamdrup. 2017. The fate of nitrogen is linked to iron (II) availability in a freshwater lake sediment. *Geochimica et Cosmochimica Acta* 205:84-99.

- Rocca, J. D., E. K. Hall, J. T. Lennon, S. E. Evans, M. P. Waldrop, J. B. Cotner, D. R. Nemergut, E. B. Graham, and M. D. Wallenstein. 2015. Relationships between protein-encoding gene abundance and corresponding process are commonly assumed yet rarely observed. *The ISME Journal* 9:1693-1699.
- Rockstrom, J., W. Steffen, K. Noone, A. Persson, F. S. Chapin, 3rd, E. F. Lambin, T. M. Lenton, M. Scheffer, C. Folke, H. J. Schellnhuber, B. Nykvist, C. A. de Wit, T. Hughes, S. van der Leeuw, H. Rodhe, S. Sorlin, P. K. Snyder, R. Costanza, U. Svedin, M. Falkenmark, L. Karlberg, R. W. Corell, V. J. Fabry, J. Hansen, B. Walker, D. Liverman, K. Richardson, P. Crutzen, and J. A. Foley. 2009. A safe operating space for humanity. *Nature* 461:472-475.
- Rotthauwe, J. H., K. P. Witzel, and W. Liesack. 1997. The ammonia monooxygenase structural gene *amoA* as a functional marker: molecular fine-scale analysis of natural ammonia-oxidizing populations. *Applied and Environmental Microbiology* 63:4704-4712.
- Rysgaard, S., R. N. Glud, N. Risgaard-Petersen, and T. Dalsgaard. 2004. Denitrification and anammox activity in Arctic marine sediments. *Limnology and Oceanography* 49:1493-1502.
- Saarenheimo, J., A. J. Rissanen, L. Arvola, H. Nykanen, M. F. Lehmann, and M. Tirola. 2015a. Genetic and environmental controls on nitrous oxide accumulation in lakes. *PLoS One* 10:e0121201.
- Saarenheimo, J., M. Tirola, and A. J. Rissanen. 2015b. Functional gene pyrosequencing reveals core proteobacterial denitrifiers in boreal lakes. *Frontiers in microbiology* 6:674.
- Salles, J. F., X. Le Roux, and F. Poly. 2012. Relating Phylogenetic and Functional Diversity among Denitrifiers and Quantifying their Capacity to Predict Community Functioning. *Frontiers in microbiology* 3:209.
- Sand-Jensen, K., C. Prahl, and H. Stokholm. 1982. Oxygen release from roots of submerged aquatic macrophytes. *Oikos* 38:349-354.
- Sanford, R. A., D. D. Wagner, Q. Wu, J. C. Chee-Sanford, S. H. Thomas, C. Cruz-Garcia, G. Rodriguez, A. Massol-Deya, K. K. Krishnani, K. M. Ritalahti, S. Nissen, K. T. Konstantinidis, and F. E. Loeffler. 2012. Unexpected nondenitrifier nitrous oxide reductase gene diversity and abundance in soils. *Proceedings of the National Academy of Sciences of the United States of America* 109:19709-19714.
- Santoro, A. E., C. Buchwald, M. R. McIlvin, and K. L. Casciotti. 2011. Isotopic Signature of N₂O Produced by Marine Ammonia-Oxidizing Archaea. *Science* 333:1282-1285.
- Saunders, D., and J. Kalff. 2001. Denitrification rates in the sediments of Lake Memphremagog, Canada-USA. *Water Research* 35:1897-1904.
- Schlesinger, W. H. 2013. *Biogeochemistry : an analysis of global change*. Third edition. San Diego, Calif. : Academic Press, [1997] ©1997.
- Schmid, M. C., A. B. Hooper, M. G. Klotz, D. Woebken, P. Lam, M. M. M. Kuypers, A. Pommerening-Roeser, H. J. M. op den Camp, and M. S. M. Jetten. 2008. Environmental detection of octahaem cytochrome c hydroxylamine/hydrazine oxidoreductase genes of aerobic and anaerobic ammonium-oxidizing bacteria. *Environmental Microbiology* 10:3140-3149.
- Schreiber, F., P. Wunderlin, K. M. Udert, and G. F. Wells. 2012. Nitric oxide and nitrous oxide turnover in natural and engineered microbial communities: biological pathways, chemical reactions, and novel technologies. *Frontiers in microbiology* 3:372.
- Schwing, P. T., I. C. Romero, R. A. Larson, B. J. O'Malley, E. E. Fridrik, E. A. Goddard, G. R.

- Brooks, D. W. Hastings, B. E. Rosenheim, D. J. Hollander, G. Grant, and J. Mulhollan. 2016. Sediment Core Extrusion Method at Millimeter Resolution Using a Calibrated, Threaded-rod. *Journal of visualized experiments : JoVE*:54363.
- Sebilo, M., G. Billen, M. Grably, and A. Mariotti. 2003. Isotopic composition of nitrate-nitrogen as a marker of riparian and benthic denitrification at the scale of the whole Seine river system. *Biogeochemistry* 63:35-51.
- Seitzinger, S. 1994. Linkages between organic matter mineralization and denitrification in eight riparian wetlands. *Biogeochemistry* 25:19-39.
- Seitzinger, S. P. 1988. Denitrification in fresh-water and coastal marine ecosystems- ecological and geochemical significance. *Limnology and Oceanography* 33:702-724.
- Seitzinger, S. P. 2008. Nitrogen cycle: out of reach. *Nature* 452:162-163.
- Seitzinger, S. P., J. A. Harrison, J. K. Bohlke, A. F. Bouwman, R. Lowrance, B. Peterson, C. Tobias, and G. Van Drecht. 2006. Denitrification across landscapes and waterscapes: A synthesis. *Ecological Applications* 16:2064-2090.
- Seitzinger, S. P., L. P. Nielsen, J. Caffrey, and P. B. Christensen. 1993. Denitrification measurements in aquatic sediments - a comparison of 3 methods. *Biogeochemistry* 23:147-167.
- Sharma, S., Z. Szele, R. Schilling, J. C. Munch, and M. Schloter. 2006. Influence of freeze-thaw stress on the structure and function of microbial communities and denitrifying populations in soil. *Applied and Environmental Microbiology* 72:2148-2154.
- Sheibley, R. W., A. P. Jackman, J. H. Duff, and F. J. Triska. 2003. Numerical modeling of coupled nitrification-denitrification in sediment perfusion cores from the hyporheic zone of the Shingobee River USA. *Advances in Water Resources* 26:977-987.
- Shen, L.-d., L. Ouyang, Y. Zhu, and M. Trimmer. 2018. Active pathways of anaerobic methane oxidation across contrasting riverbeds. *The ISME Journal* 13:752-766.
- Silvennoinen, H., A. Liikanen, J. Torssonen, C. F. Stange, and P. J. Martikainen. 2008. Denitrification and N₂O effluxes in the Bothnian Bay (northern Baltic Sea) river sediments as affected by temperature under different oxygen concentrations. *Biogeochemistry* 88:63-72.
- Simon, J., and M. G. Klotz. 2013. Diversity and evolution of bioenergetic systems involved in microbial nitrogen compound transformations. *Biochimica et Biophysica Acta (BBA)- Bioenergetics* 1827:114-135.
- Simonin, M., X. Le Roux, F. Poly, C. Lerondelle, B. A. Hungate, N. Nunan, and A. Niboyet. 2015. Coupling between and among ammonia oxidizers and nitrite oxidizers in grassland mesocosms submitted to elevated CO₂ and nitrogen supply. *Microbial ecology* 70:809-818.
- Small, G., J. Cotner, J. Finlay, R. A. Stark, and R. Sterner. 2014. Nitrogen transformations at the sediment-water interface across redox gradients in the Laurentian Great Lakes. *Hydrobiologia* 731:95-108.
- Small, G. E., J. C. Finlay, R. M. L. McKay, M. J. Rozmarynowycz, S. Brovold, G. S. Bullerjahn, K. Spokas, and R. W. Sterner. 2016. Large differences in potential denitrification and sediment microbial communities across the Laurentian great lakes. *Biogeochemistry* 128:353-368.
- Smil, V. 2001. *Enriching the earth: Fritz Haber, Carl Bosch, and the transformation of world food production*. MIT Press, Cambridge, Mass.
- Smith, C., R. DeLaune, and W. Patrick. 1982. Nitrate reduction in *Spartina alterniflora* marsh soil. *Soil Science Society of America Journal* 46:748-750.

- Smol, J. P. 2012. A planet in flux: how is life on Earth reacting to climate change? *Nature* 483:S12-S15.
- Sommaruga-Wogath, S., K. A. Koinig, R. Schmidt, and R. Sommaruga. 1997. Temperature effects on the acidity of remote alpine lakes. *Nature* 387:64-67.
- Sørensen, J. 1978. Denitrification rates in a marine sediment as measured by the acetylene inhibition technique. *Applied and Environmental Microbiology* 36:139-143.
- Spott, O., and C. Florian Stange. 2011. Formation of hybrid N₂O in a suspended soil due to co-denitrification of NH₂OH. *Journal of Plant Nutrition and Soil Science* 174:554-567.
- Staley, T. E., and J. B. Griffin. 1981. Simultaneous enumeration of denitrifying and nitrate reducing bacteria in soil by a microtiter most-probable-number (MPN) procedure. *Soil Biology and Biochemistry* 13:385-388.
- Steffen, W., K. Richardson, J. Rockström, S. E. Cornell, I. Fetzer, E. M. Bennett, R. Biggs, S. R. Carpenter, W. de Vries, C. A. de Wit, C. Folke, D. Gerten, J. Heinke, G. M. Mace, L. M. Persson, V. Ramanathan, B. Reyers, and S. Sörlin. 2015. Planetary boundaries: Guiding human development on a changing planet. *Science* 347:1259855.
- Stein, L. Y. 2019. Insights into the physiology of ammonia-oxidizing microorganisms. *Current Opinion in Chemical Biology* 49:9-15.
- Stein, L. Y., and M. G. Klotz. 2016. The nitrogen cycle. *Current biology* 26:R94-98.
- Stelzer, R., J. T. Scott, L. A. Bartsch, and T. Parr. 2014. Particulate organic matter quality influences nitrate retention and denitrification in stream sediments: Evidence from a carbon burial experiment. *Biogeochemistry* 119:387-402.
- Stoddard, J. L. 1994. Long-term changes in watershed retention of nitrogen. Its causes and aquatic consequences. Pages 223-284 in L. A. Baker, editor. *Environmental Chemistry of Lakes and Reservoirs*. Am. Chem. Soc., Washington, DC.
- Storey, J. D., J. E. Taylor, and D. Siegmund. 2004. Strong control, conservative point estimation and simultaneous conservative consistency of false discovery rates: a unified approach. *Journal of the Royal Statistical Society: Series B (Statistical Methodology)* 66:187-205.
- Strohm, T. O., B. Griffin, W. G. Zumft, and B. Schink. 2007. Growth yields in bacterial denitrification and nitrate ammonification. *Applied and Environmental Microbiology* 73:1420-1424.
- Strous, M., J. A. Fuerst, E. H. Kramer, S. Logemann, G. Muyzer, K. T. van de Pas-Schoonen, R. Webb, J. G. Kuenen, and M. S. Jetten. 1999. Missing lithotroph identified as new planctomycete. *Nature* 400:446-449.
- Sullivan, M. J., A. J. Gates, C. Appia-Ayme, G. Rowley, and D. J. Richardson. 2013. Copper control of bacterial nitrous oxide emission and its impact on vitamin B12-dependent metabolism. *Proceedings of the National Academy of Sciences* 110:19926-19931.
- Sweerts, J.-P. R. A., D. D. Beer, L. P. Nielsen, H. Verdouw, J. C. V. den Heuvel, Y. Cohen, and T. E. Cappenberg. 1990. Denitrification by sulphur oxidizing *Beggiatoa* spp. mats on freshwater sediments. *Nature* 344:762-763.
- Takahashi, S., J. Tomita, K. Nishioka, T. Hisada, and M. Nishijima. 2014. Development of a prokaryotic universal primer for simultaneous analysis of Bacteria and Archaea using next-generation sequencing. *PLoS One* 9:e105592.
- Tanimoto, T., K.-i. Hatano, D.-h. Kim, H. Uchiyama, and H. Shoun. 1992. Co-denitrification by the denitrifying system of the fungus *Fusarium oxysporum*. *FEMS Microbiology Letters* 93:177-180.
- Tatariw, C., E. L. Chapman, R. A. Sponseller, B. Mortazavi, and J. W. Edmonds. 2013.

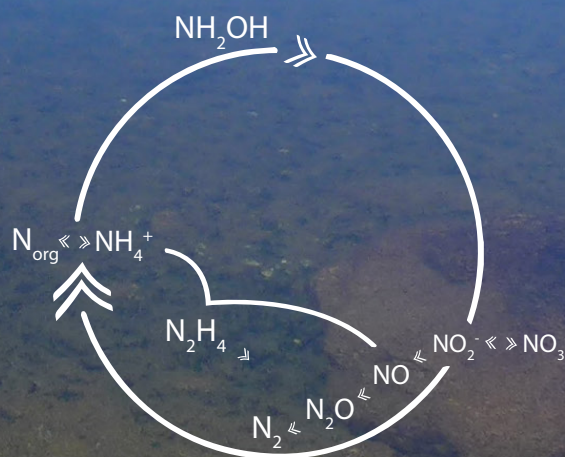
- Denitrification in a large river: consideration of geomorphic controls on microbial activity and community structure. *Ecology* 94:2249-2262.
- Tavares, P., A. S. Pereira, J. J. G. Moura, and I. Moura. 2006. Metalloenzymes of the denitrification pathway. *Journal of Inorganic Biochemistry* 100:2087-2100.
- Tenuta, M., and B. Sparling. 2011. A laboratory study of soil conditions affecting emissions of nitrous oxide from packed cores subjected to freezing and thawing. *Canadian Journal of Soil Science* 91:223-233.
- Thamdrup, B., and T. Dalsgaard. 2008. Chapter 14: Nitrogen cycling in sediments. Pages 527-569 in D. L. Kirchman, editor. *Microbial ecology of the oceans*. Wiley & Sons, New York.
- Throbäck, I. N., K. Enwall, Å. Jarvis, and S. Hallin. 2004. Reassessing PCR primers targeting nirS, nirK and nosZ genes for community surveys of denitrifying bacteria with DGGE. *FEMS Microbiology Ecology* 49:401-417.
- Thuan, n. c., K. Keisuke, Y. Midori, M. Akiko, T. K. Co, T. Akihiko, T. Sakae, Y. Naohiro, T. Yotaro, K. Masanori, and Y. Muneoki. 2017. N₂O production by denitrification in an urban river: evidence from isotopes, functional genes, and dissolved organic matter. *Limnology* 19:115-126.
- Tiedje, J. M. 1988. Ecology of denitrification and dissimilatory nitrate reduction to ammonium. Pages 179-244 in A. J. B. Zehnder, editor. *Environmental Microbiology of Anaerobes*. John Wiley and Sons, New York.
- Tiedje, J. M., A. J. Sexstone, D. D. Myrold, and J. A. Robinson. 1982. Denitrification: ecological niches, competition and survival. *Antonie van Leeuwenhoek* 48:569-583.
- Tourna, M., T. E. Freitag, G. W. Nicol, and J. I. Prosser. 2008. Growth, activity and temperature responses of ammonia-oxidizing archaea and bacteria in soil microcosms. *Environmental Microbiology* 10:1357-1364.
- Trevors, J. T., and M. E. Starodub. 1987. Effect of oxygen concentration on denitrification in freshwater sediment. *Journal of Basic Microbiology* 27:387-391.
- Tugtas, A. E., and S. G. Pavlostathis. 2007. Electron donor effect on nitrate reduction pathway and kinetics in a mixed methanogenic culture. *Biotechnology and Bioengineering* 98:756-763.
- Twining, B. S., S. E. Mylon, and G. Benoit. 2007. Potential role of copper availability in nitrous oxide accumulation in a temperate lake. *Limnology and Oceanography* 52:1354-1366.
- Unisense S/A. 2010. SensorTrace BASIC 3.0 user manual.
- Unisense S/A. 2011. Nitrous Oxide sensor user manual.
- Unisense S/A. 2018. Nitrous Oxide Microsensors Specifications.
- Van Kessel, M. A. H. J., D. R. Speth, M. Albertsen, P. H. Nielsen, H. J. M. Op den Camp, B. Kartal, M. S. M. Jetten, and S. Lücker. 2015. Complete nitrification by a single microorganism. *Nature* 528:555-559.
- Van Mooy, B., R. Keil, and A. Devol. 2002. Impact of suboxia on sinking particulate organic carbon: Enhanced carbon flux and preferential degradation of amino acids via denitrification. *Geochimica et Cosmochimica Acta* 66:457-465.
- Veraart, A. J., W. J. de Bruijne, J. J. de Klein, E. T. Peeters, and M. Scheffer. 2011a. Effects of aquatic vegetation type on denitrification. *Biogeochemistry* 104:267-274.
- Veraart, A. J., J. J. M. de Klein, and M. Scheffer. 2011b. Warming can boost denitrification disproportionately due to altered oxygen dynamics. *PLoS One* 6:e18508.
- Větrovský, T., and P. Baldrian. 2013. The variability of the 16S rRNA gene in bacterial genomes and its consequences for bacterial community analyses. *PLoS One* 8:e57923.

- Vicars, W. C., J. O. Sickman, and P. J. Ziemann. 2010. Atmospheric phosphorus deposition at a montane site: Size distribution, effects of wildfire, and ecological implications. *Atmospheric Environment* 44:2813-2821.
- Vila-Costa, M., M. Bartrons, J. Catalan, and E. O. Casamayor. 2014. Nitrogen-cycling genes in epilithic biofilms of oligotrophic high-altitude lakes (Central Pyrenees, Spain). *Microbial ecology* 68:60-69.
- Vila-Costa, M., C. Pulido, E. Chappuis, A. Calviño, E. O. Casamayor, and E. Gacia. 2016. Macrophyte landscape modulates lake ecosystem-level nitrogen losses through tightly coupled plant-microbe interactions. *Limnology and Oceanography* 61:78-88.
- Wallenstein, M. D., D. D. Myrold, M. Firestone, and M. Voytek. 2006. Environmental controls on denitrifying communities and denitrification rates: insights from molecular methods. *Ecological Applications* 16:2143-2152.
- Wang, Q., G. M. Garrity, J. M. Tiedje, and J. R. Cole. 2007. Naive Bayesian classifier for rapid assignment of rRNA sequences into the new bacterial taxonomy. *Applied and Environmental Microbiology* 73:5261-5267.
- Warneke, S., L. A. Schipper, D. A. Bruesewitz, I. McDonald, and S. Cameron. 2011. Rates, controls and potential adverse effects of nitrate removal in a denitrification bed. *Ecological Engineering* 37:511-522.
- Weber, K. A., M. M. Urrutia, P. F. Churchill, R. K. Kukkadapu, and E. E. Roden. 2006. Anaerobic redox cycling of iron by freshwater sediment microorganisms. *Environmental Microbiology* 8:100-113.
- Weiss, R. F., and B. A. Price. 1980. Nitrous oxide solubility in water and seawater. *Marine Chemistry* 8:347-359.
- Welsh, A., J. C. Chee-Sanford, L. M. Connor, F. E. Löffler, and R. A. Sanford. 2014. Refined *NrfA* phylogeny improves PCR-based *nrfA* gene detection. *Applied and Environmental Microbiology* 80:2110-2119.
- Westermann, P., and B. K. Ahring. 1987. Dynamics of methane production, sulfate reduction, and denitrification in a permanently waterlogged alder swamp. *Applied and Environmental Microbiology* 53:2554-2559.
- Wittorf, L., G. Bonilla-Rosso, C. M. Jones, O. Backman, S. Hulth, and S. Hallin. 2016. Habitat partitioning of marine benthic denitrifier communities in response to oxygen availability. *Environmental microbiology reports* 8:486-492.
- Wittorf, L., C. M. Jones, G. Bonilla-Rosso, and S. Hallin. 2018. Expression of *nirK* and *nirS* genes in two strains of *Pseudomonas stutzeri* harbouring both types of NO-forming nitrite reductases. *Research in microbiology* 169:343-347.
- Wrage, N., G. L. Velthof, H. J. Laanbroek, and O. Oenema. 2004. Nitrous oxide production in grassland soils: assessing the contribution of nitrifier denitrification. *Soil Biology and Biochemistry* 36:229-236.
- Wrage-Mönnig, N., M. A. Horn, R. Well, C. Müller, G. Velthof, and O. Oenema. 2018. The role of nitrifier denitrification in the production of nitrous oxide revisited. *Soil Biology and Biochemistry* 123:A3-A16.
- Xu, K., C. Wang, and X. Yang. 2017. Five-year study of the effects of simulated nitrogen deposition levels and forms on soil nitrous oxide emissions from a temperate forest in northern China. *PLoS One* 12:e0189831.
- Yao, L., C. Chen, G. Liu, and W. Liu. 2018. Sediment nitrogen cycling rates and microbial abundance along a submerged vegetation gradient in a eutrophic lake. *Science of The Total Environment* 616:899-907.

- Yoon, S., C. Cruz-Garcia, R. Sanford, K. M. Ritalahti, and F. E. Löffler. 2015. Denitrification versus respiratory ammonification: environmental controls of two competing dissimilatory NO₃⁻/NO₂⁻ reduction pathways in *Shewanella loihica* strain PV-4. *The ISME Journal* 9:1093-1104.
- Yoshinari, T., and R. Knowles. 1976. Acetylene inhibition of nitrous-oxide reduction by denitrifying bacteria. *Biochemical and Biophysical Research Communications* 69:705-710.
- Yuan, Q., P. Liu, and Y. Lu. 2012. Differential responses of nirK- and nirS-carrying bacteria to denitrifying conditions in the anoxic rice field soil. *Environmental microbiology reports* 4:113-122.
- Zhang, J., K. Kobert, T. Flouri, and A. Stamatakis. 2013. PEAR: a fast and accurate Illumina paired-end read merger. *Bioinformatics* 30:614-620.
- Zhao, S., Q. Wang, J. Zhou, D. Yuan, and G. Zhu. 2018. Linking abundance and community of microbial N₂O-producers and N₂O-reducers with enzymatic N₂O production potential in a riparian zone. *Science of The Total Environment* 642:1090-1099.
- Zhu, G., S. Wang, W. Wang, Y. Wang, L. Zhou, B. Jiang, H. J. M. Op den Camp, N. Risgaard-Petersen, L. Schwark, Y. Peng, M. M. Hefting, M. S. M. Jetten, and C. Yin. 2013. Hotspots of anaerobic ammonium oxidation at land-freshwater interfaces. *Nature Geoscience* 6:103-107.
- Zhu, G., S. Wang, Y. Wang, C. Wang, N. Risgaard-Petersen, M. S. Jetten, and C. Yin. 2011. Anaerobic ammonia oxidation in a fertilized paddy soil. *The ISME Journal* 5:1905-1912.
- Zhu-Barker, X., A. Cavazos, N. Ostrom, W. Horwath, and J. Glass. 2015. The importance of abiotic reactions for nitrous oxide production. *Biogeochemistry* 126:251-267.
- Zopfi, J., T. Kjær, L. P. Nielsen, and B. B. Jørgensen. 2001. Ecology of *Thioploca* spp.: Nitrate and Sulfur Storage in Relation to Chemical Microgradients and Influence of *Thioploca* spp. on the Sedimentary Nitrogen Cycle. *Applied and Environmental Microbiology* 67:5530-5537.
- Zumft, W. G. 1997. Cell biology and molecular basis of denitrification. *Microbiology and Molecular Biology Reviews* 61:533-616.
- Zumft, W. G. 2005. Nitric oxide reductases of prokaryotes with emphasis on the respiratory, heme-copper oxidase type. *Journal of Inorganic Biochemistry* 99:194-215.
- Zuur, A., E. Ieno, N. Walker, A. Saveliev, and G. Smith. 2009. *Mixed effects models and extensions in ecology with R*. Springer-Verlag New York, New York, NY.
- Zwart, H. J. 1979. The Geology of the Central Pyrenees. *Leidse Geologische Mededelingen*. 50:1-74.



Supplementary material



Supplementary material

This section comprises supplementary material for Chapter 3, Chapter 4, Chapter 5 and Chapter 6.

Appendix A provides de supplementary Table S1 with the sediment and water descriptors by sediment habitat of Chapter 6 (article IV).

Appendix B provides the original publications and the supplementary material of Chapter 3, Chapter 4, and Chapter 5.

**APPENDIX A. TABLE S.1. SEDIMENTS AND WATER DESCRIPTORS BY
SEDIMENT HABITAT**

			Sediment habitat ^a					
			All	R	C	I	D	E
Temperature ^b	° C	mean	9.1	8.4	9.8	16.5	7.4	16.4
		SD	5.3	4.3	6.5	0.8	4.5	0.4
		min	0.8	0.8	0.8	15.0	3.6	16.2
		max	17.5	12.9	16.2	17.5	16.1	16.9
[NO ₃ ⁻] ^b	μM	mean	5	9	6	0	5	0
		SD	6	7	6	0	6	0
		min	0	2	0	0	0	0
		max	17	16	13	0	17	0
[NO ₂ ⁻] ^b	μM	mean	0.10	0.15	0.09	0.06	0.10	0.04
		SD	0.06	0.07	0.04	0.04	0.06	0.02
		min	0.02	0.07	0.04	0.03	0.03	0.02
		max	0.27	0.21	0.15	0.14	0.27	0.06
[NH ₄ ⁺] ^b	μM	mean	5.6	5.6	8.8	1.0	6.3	1.0
		SD	9.4	9.5	9.9	0.1	10.2	0.2
		min	0.8	1.0	1.2	0.8	1.0	0.8
		max	51.3	25.0	25.0	1.2	51.3	1.2
[SO ₄ ²⁻] ^b	μM	mean	14	18	24	10	14	11
		SD	7	10	15	1	5	0
		min	6	6	7	9	6	10
		max	40	32	40	13	27	11
DOC ^b	mg * L ⁻¹	mean	66	52	119	94	58	57
		SD	53	32	108	33	48	5
		min	2	8	2	60	6	52
		max	301	86	233	155	301	62
z (water column depth) ^{b, c}	m	mean	17.4	0.5	0.5	0.5	25.3	0.5
		SD	22.8	0.0	0.0	0.0	23.9	0.0
		min	0.5	0.5	0.5	0.5	4.0	0.5
		max	72.0	0.5	0.5	0.5	72.0	0.5
Organic matter ^d	%	mean	32	6	29	50	32	49
		SD	14	5	18	12	9	6
		min	1	1	6	30	17	42
		max	66	14	48	66	48	54
Nitrogen (N) ^d	%	mean	1.39	0.20	1.10	1.82	1.46	1.99
		SD	0.59	0.21	0.81	0.41	0.42	0.30
		min	0.02	0.02	0.08	1.21	0.76	1.75
		max	2.44	0.57	1.93	2.44	2.34	2.32
δ ¹⁵ N ^d	‰	mean	-0.92	1.37	-0.32	0.02	-1.46	-0.68
		SD	1.73	1.75	0.71	0.89	1.65	0.81
		min	-4.36	-1.10	-1.09	-1.14	-4.36	-1.52
		max	3.52	3.52	0.45	1.42	1.93	0.09
Carbon (C) ^d	%	mean	14.24	2.73	13.54	21.83	14.09	20.51
		SD	6.48	2.54	8.99	5.45	4.42	2.26
		min	0.20	0.20	2.01	14.05	7.47	18.43
		max	29.35	6.02	22.96	29.35	24.18	22.91
δ ¹³ C ^d	‰	mean	-24.45	-23.52	-23.44	-20.49	-25.70	-19.02
		SD	3.53	2.59	3.82	2.68	2.96	1.07
		min	-31.73	-27.54	-26.61	-24.36	-31.73	-20.10
		max	-17.47	-20.11	-18.62	-17.47	-21.26	-17.96
C/N ^d	a/a	mean	12.49	16.06	17.53	14.08	11.25	12.09
		SD	3.10	4.32	6.75	2.30	0.99	0.50
		min	9.38	12.35	13.52	11.64	9.38	11.52
		max	29.52	22.82	29.52	18.17	15.21	12.45
Dry weight / wet weight ^d		mean	0.13	0.56	0.23	0.08	0.08	0.08
		SD	0.17	0.29	0.24	0.04	0.03	0.01
		min	0.02	0.25	0.09	0.05	0.02	0.08
		max	0.88	0.88	0.65	0.18	0.14	0.09
Sediment density ^d	g * cm ⁻³	mean	1.55	2.21	1.72	0.83	1.60	0.99
		SD	0.47	0.45	0.48	0.37	0.29	0.24
		min	0.45	1.59	1.29	0.45	1.10	0.84
		max	2.64	2.64	2.48	1.41	2.49	1.27
Sediment grain size ^d	μm	mean	328	438	282	361	308	394
		SD	90	130	135	107	63	58
		min	130	288	130	182	197	328
		max	627	627	433	511	440	435

		Sediment habitat ^a						
			All	R	C	I	D	E
[DNA] ^e	ng * g DW ^{-1 f}	mean	2.3E+05	2.6E+04	1.3E+05	2.9E+05	2.6E+05	3.0E+05
		SD	1.3E+05	3.0E+04	1.2E+05	6.8E+04	1.2E+05	2.1E+04
		min	4.0E+03	4.0E+03	5.5E+03	1.4E+05	7.1E+04	2.8E+05
		max	7.1E+05	8.1E+04	2.6E+05	3.7E+05	7.1E+05	3.3E+05
[DNA] ^e	ng * m ⁻²	mean	1.6E+08	2.5E+08	1.3E+08	9.5E+07	1.6E+08	1.2E+08
		SD	9.8E+07	2.3E+08	5.3E+07	5.2E+07	7.6E+07	1.8E+07
		min	9.9E+05	4.3E+07	6.8E+07	5.1E+07	9.9E+05	1.0E+08
		max	7.0E+08	7.0E+08	2.0E+08	1.8E+08	3.3E+08	1.4E+08
[16S] ^e	copies * g DW ⁻¹	mean	6.7E+10	7.9E+09	3.7E+10	6.9E+10	7.7E+10	7.7E+10
		SD	4.7E+10	9.0E+09	3.1E+10	2.9E+10	4.9E+10	1.1E+10
		min	9.1E+08	9.1E+08	2.1E+09	3.1E+10	8.3E+09	6.5E+10
		max	2.4E+11	2.3E+10	7.2E+10	1.2E+11	2.4E+11	8.4E+10
<i>nirS</i> /16S ^e	%	mean	7.97	2.41	3.70	12.19	7.95	15.27
		SD	6.59	2.43	3.06	7.25	6.48	2.28
		min	0.34	0.63	1.18	6.18	0.34	12.64
		max	29.34	7.11	8.84	29.34	23.88	16.68
<i>nirK</i> /16S ^e	%	mean	0.30	0.58	0.36	0.30	0.25	0.31
		SD	0.21	0.36	0.20	0.09	0.18	0.02
		min	0.01	0.23	0.11	0.19	0.01	0.29
		max	1.18	1.18	0.59	0.42	0.97	0.33
<i>nosZ1</i> /16S ^e	%	mean	0.23	0.60	0.17	0.25	0.19	0.17
		SD	0.21	0.50	0.09	0.15	0.13	0.04
		min	0.00	0.08	0.07	0.07	0.00	0.14
		max	1.47	1.47	0.25	0.48	0.50	0.22
<i>nosZ2</i> /16S ^e	%	mean	0.10	0.19	0.04	0.13	0.08	0.10
		SD	0.08	0.18	0.03	0.09	0.06	0.04
		min	0.00	0.01	0.02	0.03	0.00	0.06
		max	0.47	0.47	0.09	0.25	0.23	0.14
Archaeal <i>amoA</i> /16S ^e	%	mean	0.51	2.12	0.05	1.56	0.21	0.04
		SD	1.09	1.75	0.05	2.13	0.28	0.03
		min	0.00	0.02	0.00	0.09	0.00	0.02
		max	6.11	4.17	0.10	6.11	1.12	0.07
Bacterial <i>amoA</i> /16S ^e	%	mean	0.07	0.11	0.01	0.01	0.08	0.01
		SD	0.18	0.13	0.01	0.00	0.21	0.00
		min	0.00	0.00	0.00	0.00	0.00	0.01
		max	1.22	0.35	0.02	0.01	1.22	0.01
<i>nrfA</i> /16S ^e	%	mean	7.19	3.45	6.37	4.35	8.42	4.18
		SD	4.50	1.59	2.77	2.18	4.77	1.75
		min	1.55	1.78	3.41	1.55	3.18	2.67
		max	30.69	5.68	10.40	8.54	30.69	6.10
<i>hdh</i> /16S ^e	%	mean	0.17	0.08	0.08	0.18	0.18	0.19
		SD	0.16	0.08	0.05	0.15	0.18	0.11
		min	0.00	0.02	0.04	0.04	0.00	0.07
		max	0.70	0.21	0.16	0.49	0.70	0.28

^a Studied sediment habitat: littoral sediments from rocky areas (R), helophyte (*Carex rostrata*) belts (C), beds of isoetids (I) and elodeid (E) macrophytes, and non-vegetated deep (D) sediments.

^b Water (overlying the sediment core) and sediment (^d no molecular or ^e molecular) descriptors used for modeling denitrification rates.

^c Water column depth coded as 0.5 m for littoral sediments.

^f Dry weight (DW).

APPENDIX B. PUBLICATIONS OF THE PRESENT DISSERTATION

This Appendix provides the original publications of:

Chapter 3: Palacin-Lizarbe C, Camarero L, Hallin S, Jones CM, Cáliz J, Casamayor EO, and Catalan J (2019). The DNRA-denitrification dichotomy differentiates nitrogen transformation pathways in mountain lake benthic habitats. *Frontiers in Microbiology*. <https://doi.org/10.3389/fmicb.2019.01229>. It is also included the supplementary material of this publication but Tables S1, S2, S4 and S6. Please download this tables online at:

<http://journal.frontiersin.org/article/10.3389/fmicb.2019.01229/full#supplementary-material>

Chapter 4: Palacin-Lizarbe, C., Camarero L., and Catalan J (2018). Estimating sediment denitrification rates using cores and N₂O microsensors. *Journal of Visualized Experiments* (142), e58553. <https://doi.org/10.3791/58553>. It is included the Materials list.

Chapter 5: Palacin-Lizarbe C., Camarero L., and Catalan J. (2018). Denitrification temperature dependence in remote, cold, and N-poor lake sediments. *Water Resources Research* 54, 1161-1173. <https://doi.org/10.1002/2017WR021680>. It is included the supplementary material.



The DNRA-Denitrification Dichotomy Differentiates Nitrogen Transformation Pathways in Mountain Lake Benthic Habitats

Carlos Palacin-Lizarbe^{1*}, Lluís Camarero^{2†}, Sara Hallin^{3‡}, Christopher M. Jones^{3§}, Joan Cáliz^{2||}, Emilio O. Casamayor^{2¶} and Jordi Catalan^{1,4#}

¹ Centro de Investigación Ecológica y Aplicaciones Forestales, Cerdanyola del Vallès, Spain, ² Center for Advanced Studies of Blanes, (CEAB-CSIC), Girona, Spain, ³ Department of Forest Mycology and Plant Pathology, Swedish University of Agricultural Sciences, Uppsala, Sweden, ⁴ Consejo Superior de Investigaciones Científicas, Cerdanyola del Vallès, Spain

OPEN ACCESS

Edited by:

Haihan Zhang,
Xi'an University of Architecture
and Technology, China

Reviewed by:

Marja Tirola,
University of Jyväskylä, Finland
Katharina Kujala,
University of Oulu, Finland

*Correspondence:

Carlos Palacin-Lizarbe
cpalaci17@gmail.com
orcid.org/0000-0002-1572-6053

† orcid.org/0000-0003-4271-8988

‡ orcid.org/0000-0002-9069-9024

§ orcid.org/0000-0002-2723-6019

|| orcid.org/0000-0001-5714-7431

¶ orcid.org/0000-0001-7074-3318

orcid.org/0000-0002-2934-4013

Specialty section:

This article was submitted to
Aquatic Microbiology,
a section of the journal
Frontiers in Microbiology

Received: 15 January 2019

Accepted: 16 May 2019

Published: 04 June 2019

Citation:

Palacin-Lizarbe C, Camarero L,
Hallin S, Jones CM, Cáliz J,
Casamayor EO and Catalan J (2019)
The DNRA-Denitrification Dichotomy
Differentiates Nitrogen Transformation
Pathways in Mountain Lake Benthic
Habitats. *Front. Microbiol.* 10:1229.
doi: 10.3389/fmicb.2019.01229

Effects of nitrogen (N) deposition on microbially-driven processes in oligotrophic freshwater ecosystems are poorly understood. We quantified guilds in the main N-transformation pathways in benthic habitats of 11 mountain lakes along a dissolved inorganic nitrogen gradient. The genes involved in denitrification (*nirS*, *nirK*, *nosZ*), nitrification (archaeal and bacterial *amoA*), dissimilatory nitrate reduction to ammonium (DNRA, *nrfA*) and anaerobic ammonium oxidation (anammox, *hdh*) were quantified, and the bacterial 16S rRNA gene was sequenced. The dominant pathways and associated bacterial communities defined four main N-transforming clusters that differed across habitat types. DNRA dominated in the sediments, except in the upper layers of more productive lakes where *nirS* denitrifiers prevailed with potential N₂O release. Loss as N₂ was more likely in lithic biofilms, as indicated by the higher *hdh* and *nosZ* abundances. Archaeal ammonia oxidisers predominated in the isoetid rhizosphere and rocky littoral sediments, suggesting nitrifying hotspots. Overall, we observed a change in potential for reactive N recycling via DNRA to N losses via denitrification as lake productivity increases in oligotrophic mountain lakes. Thus, N deposition results in a shift in genetic potential from an internal N accumulation to an atmospheric release in the respective lake systems, with increased risk for N₂O emissions from productive lakes.

Keywords: denitrification, DNRA, lithic biofilms, mountain lake, nitrogen deposition, remote ecosystems, sediment, 16S

INTRODUCTION

According to the planetary boundaries framework (Rockström et al., 2009), anthropogenic alteration of the nitrogen (N) cycle is one of the major challenges facing the Earth system. Human activities have at least doubled the levels of reactive N (N_r) available in the biosphere (Erisman et al., 2011), resulting in deposition of N_r in or near heavily populated areas as well as remote ecosystems (Catalan et al., 2013). In the context of global change, remote ecosystems — defined here as being affected by atmospheric processes rather than direct human action in catchment areas — can be particularly informative about potential large-scale changes in the Earth system

(Catalan et al., 2013). Alpine lakes of the Northern hemisphere and subarctic regions are examples of remote ecosystems that have been exposed to increased N_r deposition during the last decades (Holtgrieve et al., 2011; Camarero, 2017), triggering a nutrient imbalance in these freshwater systems which are otherwise known to have low nutrient availability (Catalan et al., 2006). While alpine and subarctic lakes are often considered important sensors of global change (Smol, 2012), there is minimal understanding of how increased N_r availability affects microbially-driven N-cycle pathways in these ecosystems (McCrackin and Elser, 2010; Palacin-Lizarbe et al., 2018).

The N cycle is best described as a modular and complex network of biological N-transformation reactions carried out by metabolically versatile communities of microorganisms (Graf et al., 2014; Kuypers et al., 2018), whose overall composition largely determines whether N_r is lost, via denitrification or anammox, or retained in the system via dissimilatory nitrate reduction to ammonium (DNRA). Within lakes, benthic habitats are known as hotspots of N cycling due to steep redox gradients in the sediments and biofilms (Melton et al., 2014). Furthermore, the presence and composition of macrophytes also influence the biogeochemistry of the sediment (Gacia et al., 2009). In particular, isoetid species oxygenate the sediment and may promote coupled nitrification-denitrification (Vila-Costa et al., 2016). However, the effect of increased N deposition on the N-cycling microbial communities, and the factors controlling their distribution are poorly understood in mountain lakes.

Our study aims to investigate how the distribution of microbial communities in general and those that drive different N-transformation pathways changes across a range of different benthic habitats in mountain lakes that have been affected by enhanced N deposition in the absence of significant acidification (Camarero and Catalan, 1998). We hypothesise that benthic habitat type and lake productivity together determines the fate of deposited N and that increased productivity will promote pathways resulting in N_r loss. Lakes at lower altitudes tend to be more productive, particularly if they are small since the productive period is longer (Catalan et al., 2009) and phosphorus loading to the lake increases as the catchment is more vegetated (Kopáček et al., 2011). In the Pyrenees, more than 70% of the lakes are considered ultraoligotrophic based on total phosphorus (TP; <150 nM), whereas 22 and 6% are oligotrophic and mesotrophic, respectively (Catalan et al., 2006). In general, more productive oligotrophic mountain lakes exhibit low dissolved inorganic nitrogen (DIN) concentrations due to higher consumption of excess N from atmospheric loading by primary producers (Camarero and Catalan, 2012). We therefore selected lakes to establish a DIN gradient and sampled lithic biofilms, sediments with elodeid, isoetid and helophyte macrophytes, and littoral and deep non-vegetated sediments (Figure 1). We then characterised the N-functional pathways by quantifying the abundances of key N-functional genes involved in denitrification, nitrification, DNRA and anammox pathways (Table 1). We also determined the bacterial community composition in the benthic habitats and linked these to the functional guilds using a multivariate approach combined with indicator species analyses. The environment was characterised by

including proximal (benthic) and more distal (lake) descriptors to capture potential drivers acting at different spatial scales (Wallenstein et al., 2006; Battin et al., 2016).

MATERIALS AND METHODS

Sampling Location and Habitat Description

The lakes are located in the central region of the Pyrenees mountain range within the Aigüestortes i Estany de Sant Maurici National Park (Table 2 and Figure 1). All lakes are dimictic and ultra-oligotrophic (TP < 150 nM) except for Bassa de les Granotes, which is classified as oligotrophic (150 < TP < 300 nM; Catalan et al., 1993) with a circumneutral pH (~7; Vila-Costa et al., 2014). All main benthic habitats in the lakes were considered (Figure 1), although certain habitats were present in only a few lakes (Table 2 and Supplementary Table S1). Plan Lake is particularly rich in macrophytes, including isoetids (*Isoetes setacea*, *I. palustris*, and *Subularia aquatica*), elodeids (*Myriophyllum alterniflorum*, *Potamogeton alpinus*, and *P. berchtoldii*) and the helophyte *Carex rostrata* (Gacia et al., 1994). Sampling was carried out during the ice-free period (June–November) of 2013 and 2014, with a total of 30 sites and 226 samples analysed.

Water, Lithic Biofilm, and Sediment Characterisation

The overlying water, sediments and lithic biofilms were characterised using physical, chemical and biological variables (Supplementary Table S1). The temperature of the overlying water was measured at the time of sampling. For chemical analyses, water samples were filtered through a pre-combusted (4 h at 450°C) GF/F glass fibre filter. Nitrate and sulphate were determined by capillary electrophoresis using a Quanta 4000 (Waters) instrument. Ammonium and nitrite were determined by colourimetric methods in a segmented-flow autoanalyser (AA3HR, Seal), using the Berthelot reaction for ammonium (Bran+Luebbe method G-171-96) and the Griess reaction for nitrite (Bran+Luebbe method G-173-96). Dissolved organic carbon (DOC) was measured by catalytic combustion to CO₂ and detection by IR spectroscopy in a TOC5000 (Shimadzu) analyser.

Lithic biofilms were sampled collecting several cobbles (ø ~10 cm) from different sites of the lake. Cobbles were scraped entirely (upper and lower sides) with clean metal brushes and washed with deionized water and pooling together the collected material. Biofilm subsamples were collected on 0.2-μm pore polycarbonate membranes for DNA analysis, and triplicate volumes were filtered through a pre-combusted and pre-weighted GF/F glass fibre filter for chemical and physical analyses. Sediment cores (ø 6.35 cm) were collected with a gravity corer (Glew, 1991) around the deepest point of each lake or manually by scuba diving for the littoral sediments. The cores were sliced in three sections (0–0.5, 0.5–2, and 2–4 cm) to capture the oxic and the nitrate reduction zones (Melton et al., 2014).

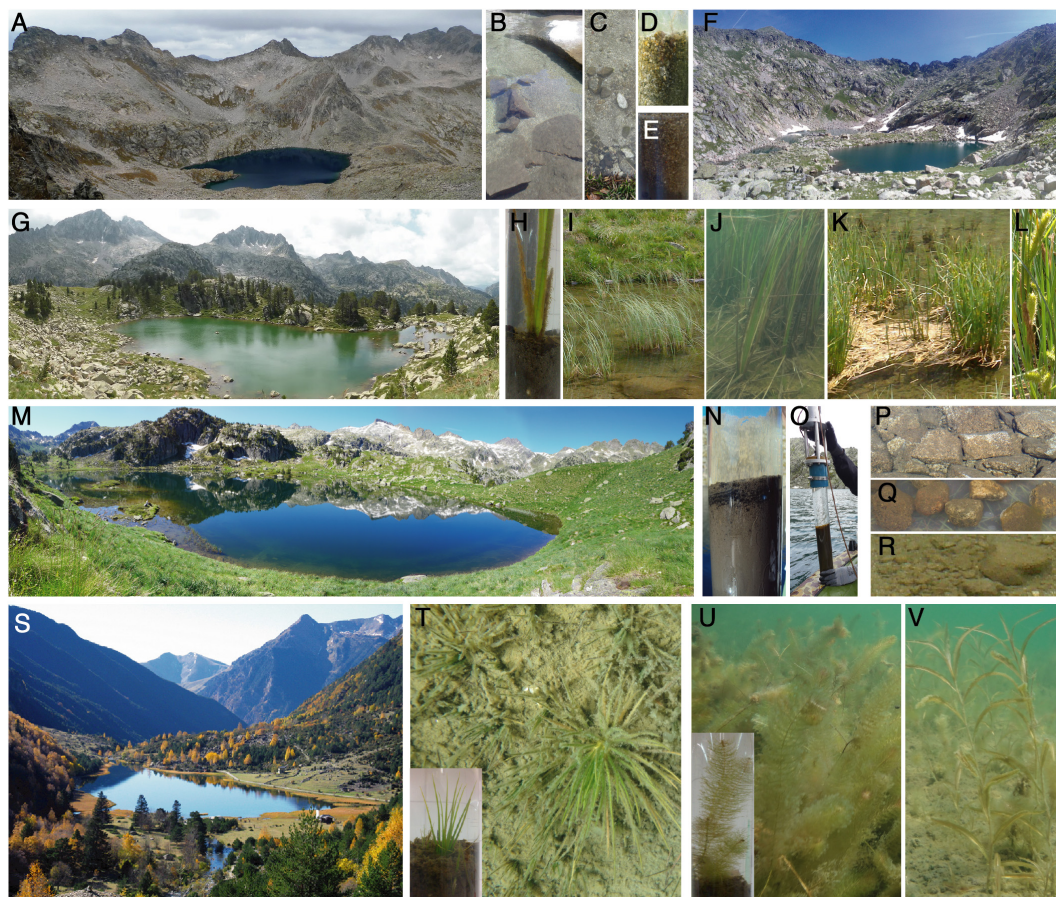


FIGURE 1 | Examples of the lakes and habitats studied. Lakes: Contraix (A), Gelats de Bergús (F), Bassa de les Granotes (G), Plan (M), and Llebretra (S). Benthic habitats: sediments near the deepest point of the lake (non-vegetated) (N,O); littoral sediments from beds of isoetids [*Isoetes lacustris* (T)] and elodeids [*Myriophyllum alterniflorum* (U), *Potamogeton alpinus* (V)] macrophytes, helophyte (*Carex rostrata*) belts (H–L) and rocky areas (B–E); and lithic biofilms from littoral cobbles (P–R).

For total carbon (C) and N and isotopic composition, ca. 5 mg of the freeze-dried sample was placed with a catalyst (Va_2O_5) in tin capsules, and the analyses were performed by the

University of California Davis Stable Isotope Facility. Organic matter (OM) content was determined using the loss on ignition (LOI) procedure (Heiri et al., 2001). The median grain size of the sediment was determined by laser diffraction (Mastersizer, 2000, Malvern Instruments Ltd, United Kingdom), using freeze-dried sediment rehydrated in distilled water and introduced into the sample dispersion unit (Hydro 2000 G, Malvern Instruments Ltd, United Kingdom) after adding hexametaphosphate and sonicating to avoid aggregates. Laser obscuration was between 10–20% and the measuring range between 0.02 and 2000 μm .

TABLE 1 | N-functional genes accounted for in this study.

Gene	Enzyme	Pathway	Reaction	Process type
<i>amoA</i>	Ammonium monooxygenase	Nitrification	Ammonium oxidation to hydroxylamine	Aerobic
<i>nirS</i>	Nitrite reductase (cytochrome-cd1)	Denitrification	Nitrite reduction to nitric oxide	Anaerobic
<i>nirK</i>	Nitrite reductase (copper-based)	Denitrification	Nitrite reduction to nitric oxide	Anaerobic
<i>nosZ</i>	Nitrous oxide reductase	Denitrification	Nitrous oxide reduction to dinitrogen	Anaerobic
<i>nrfA</i>	Nitrite reductase (formate-dependent)	DNRA	Nitrite reduction to ammonium	Anaerobic
<i>hdh</i>	Hydrazine dehydrogenase	Anammox	Hydrazine oxidation to dinitrogen	Anaerobic

DNA Extraction and Quantitative PCR of 16S rRNA and N Cycle Genes

DNA was extracted from 0.33 ± 0.06 g of sediment or lithic biofilm using the FastDNA® Spin Kit for Soil (MP Biomedical) following the manufacturer's instructions. The extracted DNA was quantified using the Qubit® fluorometer (Thermo Fisher Scientific Inc.).

Quantitative real-time PCR (qPCR) was used to quantify functional genes encoding enzyme involved in N-cycle pathways

TABLE 2 | Site location, habitats studied and characteristics sorted by the dissolved inorganic nitrogen (DIN) concentration.

Lake (Abbreviation)	Vegetation belt	Habitats Studied ^a	Latitude (N)	Longitude (E)	Altitude (m a.s.l.)	Area (ha)	Catchment (ha)	Depth ^b (m)	Renewal time (months)	TP ^c (mM)	DIN ^d (μM)
Redon de Vilamòs (R)	Alpine	I	42.76078	0.76233	2209	0.6	12	5	1.7	NA	1.2
Plan (P)	Subalpine	D, I, E, C, L	42.62248	0.9307	2188	5	23	9	15.1	102	1.7 ± 0.9
Bassa de les Granotes (G)	Alpine	D, L	42.5733	0.97124	2330	0.7	3	5	9.9	292	2.4 ± 0.7
Redó Aigüestortes (RA)	Subalpine	D, L	42.58216	0.95949	2117	6.3	325	11	1.6	76	8.5 ± 0.9
Gelat de Bergús (GB)	Alpine	D, R, L	42.59106	0.96331	2493	1.4	24	8	2.3	42	8.8 ± 3.3
Llong (Lo)	Montane	D, R, L	42.57431	0.95063	2000	7.1	1111	13	0.6	89	10.3 ± 11.6
Bergús (B)	Alpine	D, L	42.58947	0.95717	2449	6.2	126	50	3.9	44	17.1 ± 11.3
Llebreia (Le)	Montane	D, C, R, L	42.55083	0.89031	1620	8	5438	12	0.1	89	17.9 ± 2.7
Contraix (C)	Alpine	D, R, L	42.58874	0.91861	2572	9.3	100	59	9.9	49	18.0 ± 1.3
Redon (RO)	Alpine	D, R, L	42.64208	0.77951	2235	24.1	153	73	36	58	23.5 ± 19.6
Podo (Po)	Alpine	D, L	42.60307	0.93906	2450	4.6	33	25	9.4	75	25.2 ± 14.7

^aD, sediments in the deepest point of the lake; I, isoeitid littoral sediments; E, eboidid littoral sediments; C, Carex rostrata belts littoral sediments; R, rocky areas littoral sediments; L, lithic biofilms from littoral cobbles.

^bMaximum water column depth. ^cTotal phosphorus (Camarero and Catalan, 2012). ^dDIN concentration (sum of nitrate, nitrite and ammonium) in the overlying water.

(Table 1 and Supplementary Table S2), as well as the bacterial 16S rRNA gene. All qPCR reactions were performed in duplicate in a total reaction volume of 20 μL using DyNAmo Flash SYBR Green qPCR kit (Thermo Fisher Scientific Inc.), 0.1% Bovine Serum Albumin, 0.5–1.0 μM of each primer and 15 ng DNA on the Biorad CFX Connect Real-Time System. Primers (Rotthauwe et al., 1997; Hallin and Lindgren, 1999; Lopez-Gutierrez et al., 2004; Mohan et al., 2004; Throbäck et al., 2004; Henry et al., 2006; Schmid et al., 2008; Tourna et al., 2008; Jones et al., 2013; Welsh et al., 2014), amplification protocols and resulting efficiencies for each assay are listed in Supplementary Table S3. Potential inhibition of the PCR reactions was checked by amplifying a known amount of the pGEM-T plasmid (Promega) with the plasmid-specific T7 and SP6 primers added to the DNA extracts and non-template controls. No inhibition of the amplification reactions was detected with the amount of template DNA used. Standard curves for each assay were generated by serial dilutions of linearized plasmids with cloned fragments of the respective gene. Standard curves were linear ($R^2 = 0.997 \pm 0.003$) in the range used, and amplification efficiency was 90% for the 16S rRNA gene and 65–88% for the functional genes (Supplementary Table S3). Melting curve profiles were inspected, and final products were run on an agarose gel to confirm amplicon size. Non-template controls resulted in negligible values.

Sequencing of the 16S rRNA Gene, Sequence Processing and OTU Clustering

The diversity and structure of total bacterial and archaeal communities were determined by targeting the V3-V4 region of the 16S rRNA gene (Takahashi et al., 2014). Amplicon libraries for each sample were generated using a two-step protocol (Berry et al., 2011). First, PCR products were generated in duplicate 20 μL reactions per sample using 16S rRNA primer constructs that included Nextera adapter sequences, with reactions consisting of Phusion PCR mastermix (Thermo Fisher Scientific), 0.5 μg μL⁻¹ BSA, 0.25 μM of each primer and 10 ng extracted DNA. Thermal cycling was performed for 25 cycles, and cycling conditions and primer sequences are listed in Supplementary Table S3. The resulting PCR products were pooled and purified using the AMPure bead purification kit, and 3 μL of the purified product was used as template in the second PCR using barcodes. Duplicate 30 μL reactions were performed for each sample, with similar reagent concentrations as in the first step except for the use of 0.2 μM final primer concentrations. PCR was performed according to Supplementary Table S3. Products were pooled, bead purified, followed by equimolar pooling and sequencing performed by Microsynth AG (Balgach, Sweden) using the Illumina MiSeq platform with v3 chemistry (2 × 300 bp paired-end reads).

Paired-end reads were merged using PEAR (Zhang et al., 2013) and dereplicated and clustered into operational taxonomic units (OTUs) at a cut-off of 3% identity using UPARSE (Edgar, 2013). The final dataset comprised 13069 OTUs after removal of chimaeras and singletons, with 83% of the quality filtered sequence pool mapped back to OTUs. Taxonomic assignment

was carried out with the RDP classifier (Wang et al., 2007) against the SILVA reference database (release 119) (Quast et al., 2013). Sequences classified as mitochondria or chloroplasts were excluded. The original OTU table was rarefied (100 random subsampling) to 10660 sequences per sample. The sequences are available in the NCBI Sequence Read Archive (PRJNA494630).

Statistical Methods

All multivariate, clustering and correlation analyses were performed using R (R Core Team, 2017). Comparisons of gene abundances between habitat types were performed using Kruskal–Wallis (KW) and Wilcoxon–Mann–Whitney (WMW) tests. Principal component analysis (PCA) and Redundancy analysis (RDA) using Hellinger distances (Borcard et al., 2011) were used to investigate the unconstrained ordination of the relative abundances of the N-functional genes studied (PCA) and of the bacterial community composition (PCA), and the relationship between the relative abundance of the N-functional genes and the environmental conditions (RDA), as well as between the overall bacterial community composition and the relative abundance of the N-functional genes (RDA). Hereafter, we refer to the PCAs as gene-PCA (gen-PCA) and community-PCA (com-PCA), and to the RDAs as gene-environment-RDA (gen-env-RDA) and community-gene-RDA (com-gen-RDA), respectively. In the analyses, functional gene abundances were standardised to total 16S rRNA gene copy numbers. Taxa < 5% occurrence (3453 of the total 13069 OTUs) were excluded from the bacterial community composition analysis (com-PCA and com-gen-RDA), and values for nitrate, nitrite, ammonium and sulphate were log-transformed in the gen-env-RDA. In the RDAs, forward selection was used to identify a minimum set of significant explanatory variables ($p < 0.05$; Blanchet et al., 2008), which exhibited low collinearity (variance inflation factors well below 10). Permutation tests of the resulting ordinations showed significant pseudo- F values ($p < 0.05$, $n = 1000$) for the main explanatory axes in each ordination — first to third axes in the gen-env-RDA, and first to fifth axes in the com-gen-RDA.

A structure of four sample clusters was present in both RDAs. Consequently, we used the samples scores of the three main axes of the com-gen-RDA as coordinates in four-group k -means clustering. We looked for indicative OTUs of each cluster performing a multi-level pattern analysis using the *multipatt* function from the *indicspecies* R package (Cáceres and Legendre, 2009), considering site group combinations, and the entire OTU set (13069) as the community data table. For each OTU, the method provides an indicator value (IndVal) of each cluster or a joint set of them. We accepted as significant indicator taxa those with adjusted p -value < 0.001, using the false discovery rate method to calculate the adjusted p -value (Storey et al., 2004).

RESULTS

Genetic Potentials

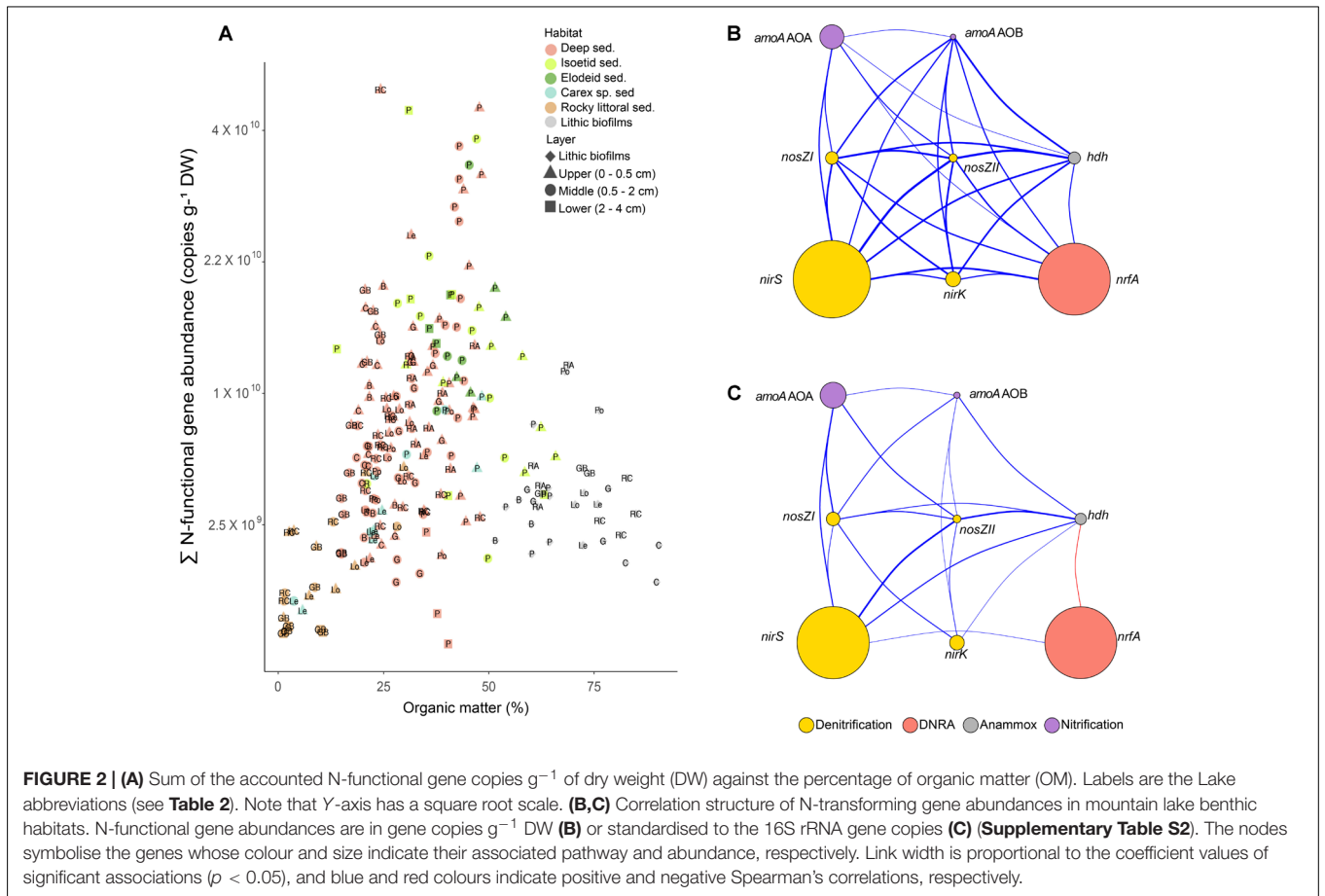
The sum of the N-functional gene copies per dry weight of sediment increased with OM ($r = 0.42$, $p < 0.001$, **Figure 2A**) but with a large scattering. Individual gene abundances were highly

positively correlated among them (**Figure 2B**). However, the correlation structure markedly simplified when standardising by the 16S rRNA copy number in each sample (**Figure 2C**), showing that the *nrfA* pool was weakly related to the rest of N-functional gene pools. The sum of the N-functional gene copies accounted for an average of $15 \pm 8\%$ (mean \pm SD) of bacterial 16S rRNA gene copies across all samples (**Supplementary Figure S1**). Maximum values of 52% were found in the lower sediment layer (2–4 cm) near the isoetid rhizosphere, while minimum values of 2% were observed in lithic biofilms. Hereafter, unless otherwise indicated, we report the N-functional gene abundance standardised to total bacterial 16S rRNA gene copies.

The *nirS* and *nrfA* genes showed the highest relative abundances, up to 33 and 18% of total 16S gene copies, respectively. The abundance of *nirS* was approximately 50-fold greater than *nirK* across all lakes, with the highest numbers detected in the more productive lakes (R, P and G, **Table 2** and **Figures 3A,B**). The abundance of *nirK* genes exhibited an overall trend of increasing abundance with lake DIN levels (**Figure 3B**), opposed to that observed for *nirS*. Higher *nrfA* abundance was observed in the sediments of the deepest part of the lakes (**Figure 3E**), while abundances in the elodeid sediments were significantly higher than those of the isoetids (KW test, $p = 0.028$). Closer inspection of the macrophyte sediment profiles showed a significant *nrfA* increase deeper in the elodeid sediments ($r = 0.85$, $p < 0.001$; **Supplementary Figure S2A**), while no trend was observed in the isoetid sediments.

The *amoA* gene of ammonia-oxidising archaea (AOA) was more abundant than the bacterial (AOB) counterpart. No obvious trend was observed for either AOA or AOB abundance across the lake DIN gradient. Although the average total abundance of ammonia oxidisers across all lakes was low relative to those of 16S rRNA genes ($0.87 \pm 2.66\%$ and $0.05 \pm 0.14\%$ for AOA and AOB, respectively), several lakes showed AOA and AOB proportions of 57 and 23% of the total N-functional gene abundance. The highest AOA abundance was observed in the lower sediment layers of the isoetid rhizosphere and rocky littoral sediments of high-altitude lakes in the alpine belt, that is, those located above treeline (**Figure 3G**). Abundances of AOA were significantly higher in isoetid than elodeid sediments (KW test, $p < 0.001$), and increased with depth in the former ($r = 0.64$, $p = 0.001$; **Supplementary Figure S2B**). All habitats of the highest altitude lakes (GB and C lakes, **Table 2** and **Figure 3H**) showed a relatively high abundance of AOB copies compared to the same habitats in lakes at lower elevations.

The gene variants of the nitrous oxide reductase, *nosZ* clade I and II, as well as the *hdh* gene associated with the anammox pathway, exhibited low relative abundances (**Figures 3C,D,F**). The abundance of clade I *nosZ* genes was typically higher (~7-fold on average) than that of clade II *nosZ* across all lakes and habitats. The lithic biofilm habitats of Contraix, the most elevated lake, showed the highest abundance of *nosZ* clade I genes (**Figure 3C**), while *nosZ* clade II abundances were higher in the rocky littoral sediments of alpine lakes (**Figure 3D**). Relative abundances of *hdh* were higher in the lithic biofilms (**Figure 3F**), with no obvious relationship with DIN levels across the lakes.



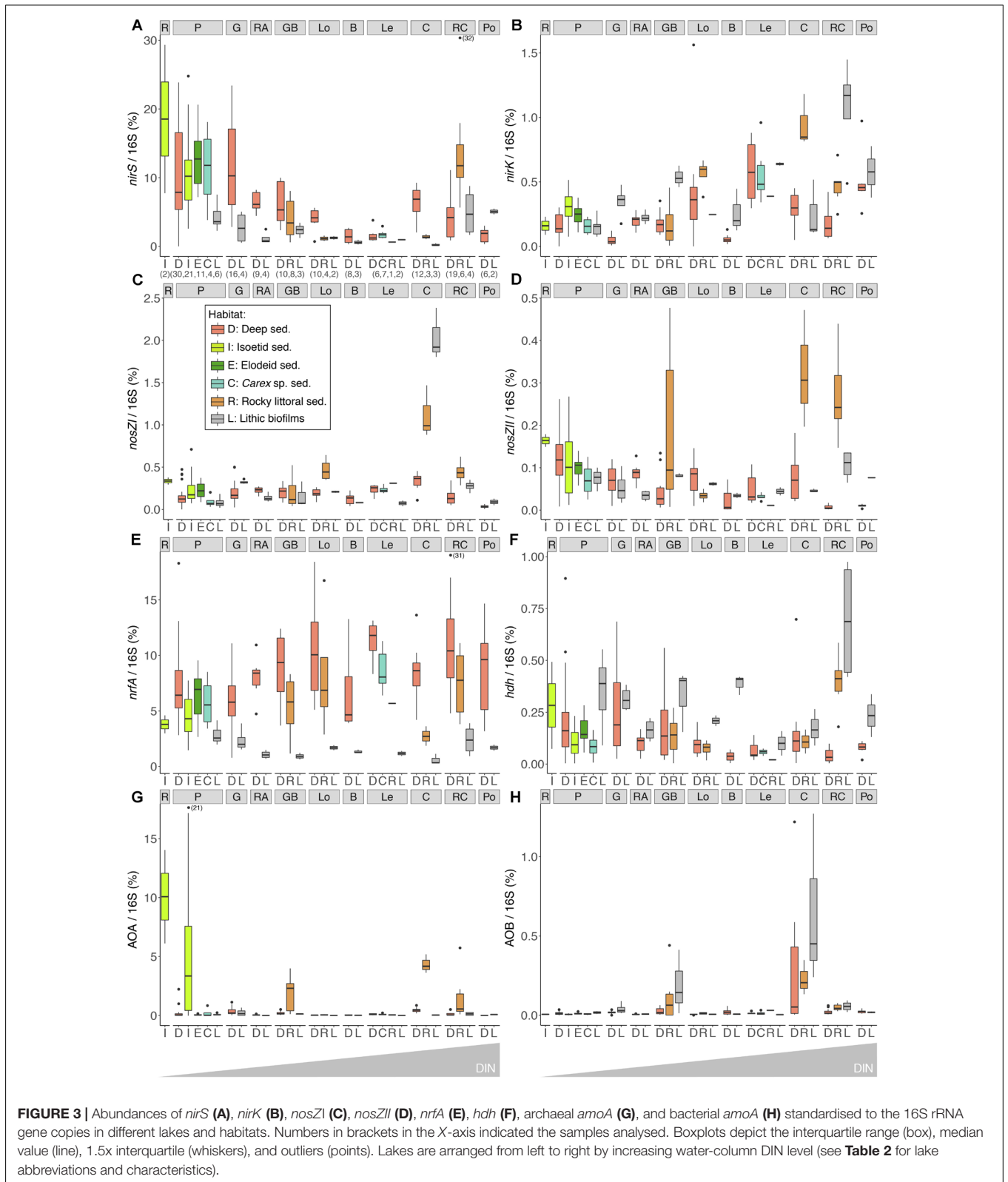
N-Functional Genes and the Environment

The constrained ordination of N-functional gene abundances identified three distinct gradients explaining 54% of the total variation across habitats and lakes (**Figure 4**). A similar result was obtained in a non-constrained analysis (**Supplementary Figure S3**), indicating that the main environmental drivers were captured by the constrained analysis. The main variation of benthic N-cycling genetic potentials was across a *nirS* vs *nrfA* abundance gradient (**Figure 4**). The *nirS*-rich samples corresponded to those from shallow and productive lakes (R, P, and G, **Table 2** and **Supplementary Figures S4A,B**), specifically the upper sediments in all habitats and sediments near the roots of isoetids. These sites were associated with higher temperature, DNA content, isotopic signatures, DOC content, and C and N content, as well as coarser granulometry (**Supplementary Figure S5**) and lower C/N and nitrate/nitrite ratios (**Figure 4**). In contrast, *nrfA* rich environments occurred in the deep parts of the deep lakes, the lower layers of all sediments (except the isoetid rhizosphere) and the littoral sediments of the montane belt lakes (**Table 2** and **Supplementary Figures S4A,B**). Sulphate, ammonium, nitrate and nitrite concentrations were higher in these sites compared to those associated with *nirS*. The same *nirS*-*nrfA* main axis was also found if only samples from the deep habitat were included in the analysis.

The gen-env-RDA second axis of variation discriminated between sediments and lithic biofilms. The latter characterised by higher abundances of *nirK*, *nosZI*, *nosZII*, *hdh* and AOB (**Figure 4A**). The rocky littoral sediments of Lake Contraix separated from the other sediment samples (**Supplementary Figure S4A**). These sites shared relatively high concentrations of nitrate, nitrite and sulphate in the overlying water, high OM content, and particular isotopic signatures (high $\delta^{13}C$ and low $\delta^{15}N$). Finally, the third axis of variation was associated with the AOA abundance (**Figure 4B**) and resulted in the segregation of the majority of the isoetid sediments from the other habitats. The sites with the highest abundance of AOA were located close to the isoetid rhizosphere and in the rocky littoral sediments of the alpine lakes (**Supplementary Figure S4B** and **Table 2**). These samples showed high $\delta^{15}N$ values and likely corresponded to more oxygenated sediments (**Figure 4B**).

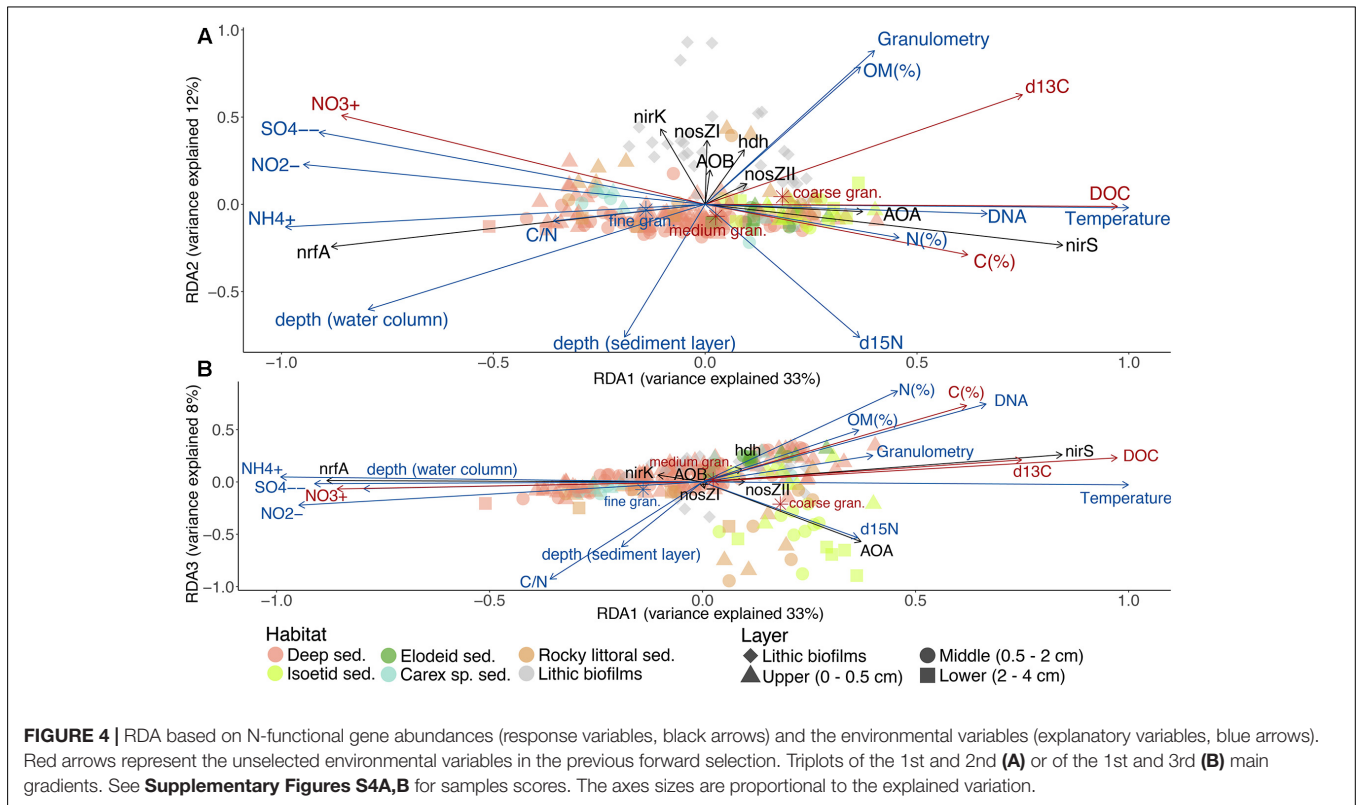
N-Functional Genes and the Associated Microbial Community

The ordination of the OTU composition constrained by the N-functional gene abundances resulted in a pattern of four distinct sample clusters (**Figure 5**), similar to that obtained in an unconstrained ordination (**Supplementary Figure S6**). The four clusters consisted of samples associated with a high relative abundance of *nrfA*, *nirS*, AOA, or a combination of the rest of



the targeted genes. Classification of samples into the four clusters using *k*-means followed by indicator species analysis resulted in approximately 29% of OTUs being identified as exclusively

associated with samples from a single cluster (**Figure 6** and **Supplementary Tables S4, S5**). Approximately 12% of OTUs were significant indicators of the AOA sample cluster and found



across a wide range of different bacterial taxa. By contrast, 6% of OTUs were significant indicators of the mixed N-transformation cluster, with large numbers of indicators concentrated within the phyla Cyanobacteria, Bacteroidetes, and Planctomycetes, as well as Alpha- and Betaproteobacteria classes. Similarly, 6% of OTUs were associated with samples in the *nrfA* cluster and were classified into Firmicutes, Bacteroidetes, Actinobacteria, and Chloroflexi phyla, and Epsilon- and Deltaproteobacterial classes. Finally, 4% of OTUs were exclusive indicators of samples in the *nirS* cluster and were found across a large number of bacterial taxa, similar to the AOA sample cluster.

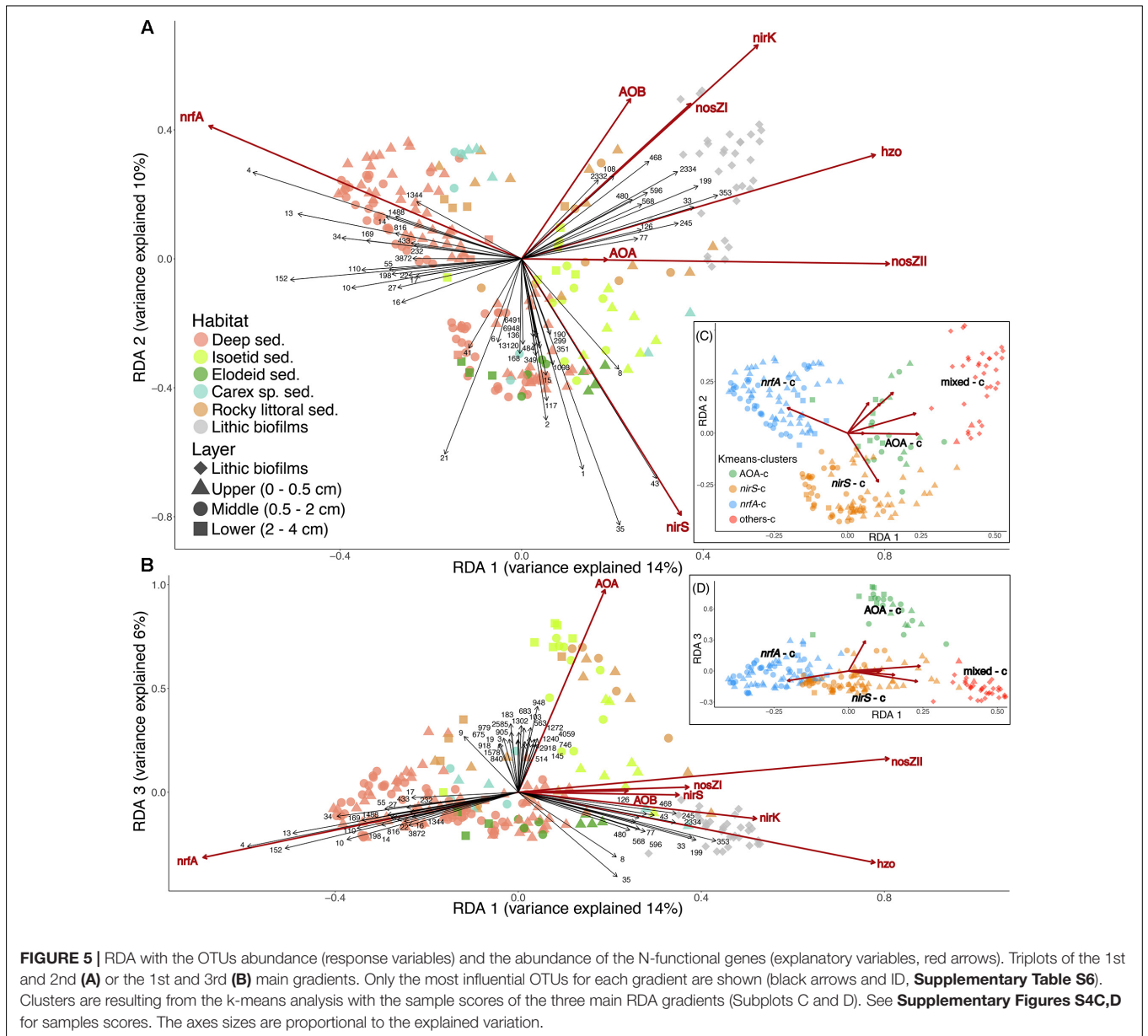
DISCUSSION

The DNRA-Denitrification Gradient

The gradient of *nrfA* to *nirS* dominance was the main pattern of variation in the N-transforming microbial communities of the benthic habitats. From an ecosystem perspective, this gradient indicates a shift from habitats with a higher potential for internal N_r cycling via DNRA, and thus retention of N_r in the system, to those in which loss of N_r from the lake is more likely through denitrification. The environments with the lowest ratios of denitrifying to DNRA nitrite reductase genes were characterised by variables indicating refractory OM with high C/N, lower oxygen diffusion and lower redox potentials. This was particularly the case in the deepest part of the deep lakes (maximum depth ≥ 25 m) and in the deeper regions of the reduced elodeid sediments. In agreement with our result,

previous work in a tropical high-altitude oligotrophic lake has shown *nrfA* abundance to be highest in the deepest part of the hypolimnion with anoxic conditions during late stratification (Pajares et al., 2017), and more reduced conditions favoured DNRA over denitrification in Australian estuaries (Kessler et al., 2018). Increased C/N ratio may favour DNRA over denitrification (Kraft et al., 2014).

The highest genetic potential for denitrification, based on *nirS* abundance, was detected in shallower and less oligotrophic lakes, where DIN levels were lower in the water column due to higher primary productivity. These lakes also have lower C/N ratios (**Supplementary Table S1**). Generally, lake autochthonous OM is fresher and of higher quality (e.g., lower C/N), and is a substantial proportion of total OM in lakes with a lower ratio of the catchment to the lake area. This fresh OM can be used as electron donors for denitrifiers, as demonstrated in several aquatic ecosystems [eutrophic lakes (Chen et al., 2012; Gardner et al., 2017), streams (Barnes et al., 2012; Stelzer et al., 2014), wetlands (Dodla et al., 2008), and oceans (Van Mooy et al., 2002)]. Oxygen levels in upper sediments of shallow and productive lakes likely fluctuate to a greater degree than those observed in habitats dominated by DNRA, thereby favouring organisms with facultative anaerobic respiration pathways such as denitrification (Wittorf et al., 2016; Chen J. et al., 2017). The *nirS* denitrifiers along the DNRA-denitrification gradient were associated with *nosZ* clade II N_2O reduction and AOA communities involved in ammonia oxidation, whereas denitrifier communities present in lithic biofilms dominated by *nirK*-types were associated with *nosZ* clade I N_2O reduction and AOB. These patterns indicate

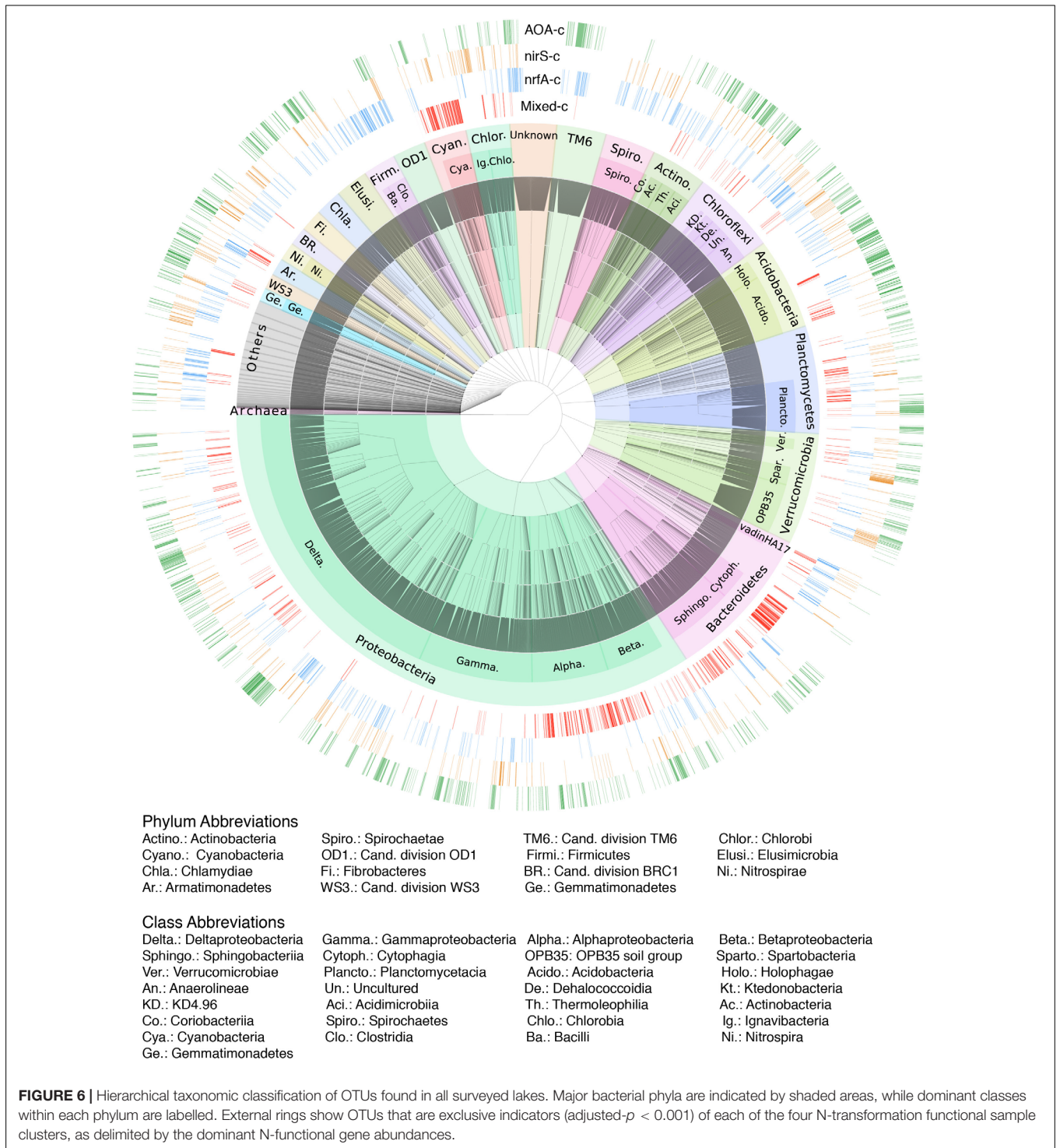


that different N transformation networks developed in these habitats even when in both cases exhibited potential for linked nitrification and denitrification.

The overall high proportion of denitrifying nitrite versus nitrous oxide reductase genes (~30 *nir:nosZ* ratio on average) suggests a dominance of partial denitrification, especially in productive habitats dominated by *nirS* denitrifier communities (i.e., *nirS*-cluster showed *nir:nosZ* higher ratios compared to the other clusters, WMW test, $p < 0.01$). This observation agrees with Castellano-Hinojosa et al. (2017) who found high N_2O/N_2 emissions in a productive, shallow warm Mediterranean mountain lake, as well as Myrstener et al. (2016) who demonstrated that addition of nitrate, phosphorus and labile C to sediments from a boreal lake resulted in higher relative N_2O production compared to addition of nitrate alone. Other

studies have shown that higher *nir:nosZ1* ratios in the sediments of boreal lakes were associated with hypolimnion N_2O excess, as well as increased phosphate and nitrate concentrations (Saarenheimo et al., 2015a). Thus, productive sites could favour partial denitrifiers that survive anoxic periods. Before arriving to the atmosphere, N_2O might be consumed in the hypolimnion of deep lakes. *NosZ*-harbouring bacteria have been found in the hypolimnion of boreal lakes (Peura et al., 2018). However, in the sediments studied, the higher *nir:nosZ* ratios were found in shallower lakes, in which N_2O may easily reach the atmosphere (Dore et al., 1998). Further studies accounting for real N_2O emissions could corroborate our conjecture.

Nitrite-dependent anaerobic methane oxidation (N-DAMO, Simon and Klotz, 2013) is a potential alternative to DNRA, denitrification and anammox nitrite consumption. N-DAMO



has been found as a key driver of methane oxidation in nitrate-rich lakes (Deutzmann et al., 2014) and reduced sandy riverbeds (Shen et al., 2019). In these habitats, bacteria related to *Candidatus Methyloirabilis oxyfera*, known to perform this pathway, were abundant. In our study, we detected only two OTUs of low relative abundance (0.02%) classified as *Candidatus Methyloirabilis*. Nonetheless,

OTUs belonging to the genus *Methylocaldum* were more abundant (~0.3%), and were significant indicators of the 'nirS' cluster. These findings are similar to those of a survey of methane oxidation in Indian reservoirs (Naqvi et al., 2018), where low relative abundance of NC10 bacteria capable of N-DAMO (0.003–0.022%) was found; whereas Type I aerobic methanotrophs, which include *Methylocaldum* and other

members of the Methylococcaceae family, were predominant and co-occurred with a diverse community of potential *nirS* type denitrifiers. Other Methylococcaceae are partial denitrifying aerobic methanotrophs with N_2O as the end product (Kits et al., 2015a,b). Overall, these results, added to the high ratio of *nir* to *nosZ* gene abundance, suggest that N_2O emissions are the most likely endpoint of nitrite reduction in *nirS*-cluster sediments, independent of the pathway. Further studies are required to elucidate the importance and distribution of methane dependent processes in mountain lakes and to evaluate their role as a bypass of partial denitrification.

The Idiosyncratic Lithic Biofilms

Microbial N-transforming guilds in the lithic biofilms differentiate from those in the sediments. Gene abundance results indicate a complex N-transformation structure in this habitat, consisting of processes demanding both oxic and anoxic conditions, which suggest highly structured microbial communities in relatively short spatial distances. The idiosyncratic nature of the guild composition (e.g., *nosZI*, *hdh*, *nirK*) declines as the productivity of the lake increases; *nirS* becomes more prominent compared to *nirK*, and the N-transforming communities are more similar to the upper sediments. The high abundance of *nirS* differs from the dominance of *nirK* previously found in another study of epilithic biofilms from a subset of the same lakes. A main difference between the two studies is that in Vila-Costa et al. (2014) only sampled the upper side of the cobbles, whereas we sampled both sides. Differences in ammonia oxidisers between the upper (light-side) and lower (dark-side) sides of cobbles have been previously reported (Merbt et al., 2017). The higher relative abundance of *hdh* and *nosZ* genes indicates that N loss in the form of N_2 could be higher in the lithic biofilms compared to the other benthic habitats in the studied lakes.

Archaeal Nitrification Hotspots

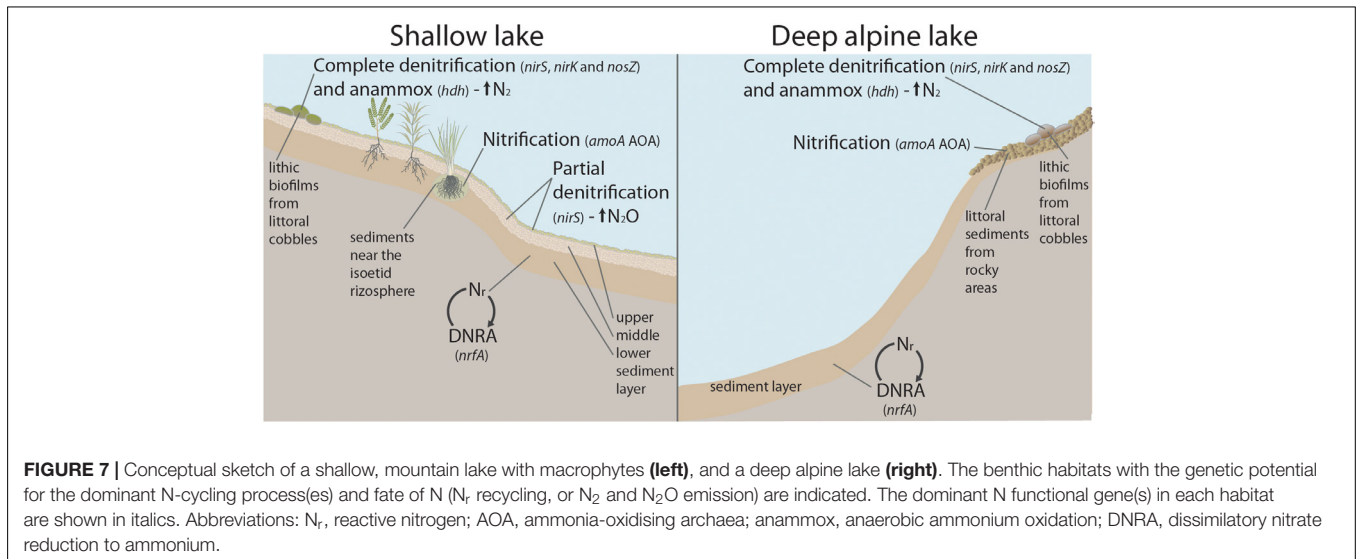
The positive $\delta^{15}N$ signals observed in samples from the lower sediment layers of the isoetid rhizosphere and the rocky littoral sediments of the alpine lakes support the view of them as nitrification hotspots (Mariotti et al., 1981), likely performed by AOA as suggested by the *amoA* gene abundance. Nitrification in rocky littoral sediments could be quantitatively more relevant than the isoetid rhizosphere given that rocky littorals occupy large areas in alpine lakes. Nevertheless, the archaeal *amoA* densities observed in the lower isoetid sediment layer were nearly 100-fold higher than in the rocky sediment samples with the highest AOA abundance. Sediments close to the roots of isoetids are episodically well-oxygenated due to the release of oxygen through roots during photosynthetic periods (Sand-Jensen et al., 1982), which increases the interface between oxidised and reduced sediments where the NH_4^+ oxidation occurs. Intensive nitrification would result in high NO_3^- accumulation in the sediment porewater (maximun 2 mM; Catalan et al., 1994). However, this is likely transient as the NO_3^- concentration in the overlying water column was negligible, suggesting a close coupling of nitrification and denitrification in this habitat (Vila-Costa et al., 2016). Indeed, there was a positive correlation

($r = 0.68$, $p < 0.001$) between nitrification and denitrification gene abundances in the isoetid sediments of Plan lake. Lakes at a higher altitude, Contraix and Gelats de Bergús, also showed significant correlations between nitrification and denitrification gene abundances for deep and littoral habitats ($r = 0.48$, $p = 0.02$ and $r = 0.44$, $p = 0.08$, respectively), suggesting that nitrification and denitrification are also linked in the nitrification hotspots.

Linking the Taxonomic Distribution and Functional Potential

Each of the four main N-transforming communities consists of a highly diverse and distinct consortium of co-occurring bacterial taxa, based on the large number of indicator OTUs detected. However, taxonomic classification does not necessarily predict functioning, as different prokaryotic traits may be conserved at different phylogenetic depths (Martiny et al., 2015). While ammonia oxidation and anammox capacities are restricted to only a few lineages, denitrification and DNRA are widely distributed across the phylogeny (Graf et al., 2014; Welsh et al., 2014). Thus, many of the indicator OTUs identified are likely not directly involved in each N-transformation pathway. However, the high degree of similarity observed between unconstrained and functional gene-constrained OTU-based ordinations indicates that shifts in the genetic potential of different N-transformation processes are tightly linked to changes in the overall prokaryotic community structure, which itself is shaped by differences in environmental conditions across habitats.

Links between taxonomic composition and functional potential has been observed in previous works in lakes based on metagenomes or sequencing of functional genes. The occurrence of several proteobacterial families, in particular, Rhodobacteraceae (Alphaproteobacteria), Methylococcaceae (Gammaproteobacteria), and Burkholderiales, Comamonadaceae and Rhodocyclaceae (Betaproteobacteria) has been shown to be strongly associated with denitrification gene presence or abundance (Vila-Costa et al., 2014; Peura et al., 2015; Saarenheimo et al., 2015b; Castellano-Hinojosa et al., 2017; Chen R. et al., 2017). These taxa were also highly abundant in samples within the *nirS*-denitrifier and mixed functional gene communities, which included *nirK*-type denitrifiers. Moreover, metagenomic studies of boreal lakes water columns have identified *nosZ* sequences originating from Myxococcales (Deltaproteobacteria) and Sphingobacteriaceae (Bacteroidetes) in the hypolimnion near the oxycline (Peura et al., 2015, 2018). Many organisms within these families are known to possess the clade II variant of the *nosZ* gene (Hallin et al., 2018). Accordingly, a large proportion of indicator OTUs for the mixed N-cycling communities, which includes the clade II *nosZ* variant, were also classified as belonging to these families. The 4th most abundant genus in the studied lakes is *Anaeromyxobacter*, one member of this Deltaproteobacteria genus is *A. dehalogenans* a chemodenitrifier, an organism that combines chemical chemodenitrification reactions and enzymatic reaction(s) to reduce NO_3^- to N_2O or N_2 , without



having denitrifying nitrite reductases codified by *nirS* or *nirK*, also performs DNRA and Fe-reduction (Onley et al., 2018). *Rhodoferrax* (Beta-) and *Desulfomonile* (Delta-) possible chemodenitrifiers (Onley et al., 2018) were also common genus present. There are other eubacteria non-proteobacteria taxa also carrying denitrifying genes (Graf et al., 2014) present in our samples (e.g., Actinobacteria).

Operational taxonomic units associated with samples in the *nrfA* cluster were classified as Firmicutes, Epsilon- and Deltaproteobacteria (Campylobacterales and *Anaeromyxobacter*, *Desulfovibrio*, and *Geobacter*, respectively), Bacteroidetes (Bacteroidia), Actinobacteria (Coriobacterales and Corynebacterales) and Chloroflexi (Anaerolineaceae), all these taxa include microbes that are known to carry *nrfA* (Welsh et al., 2014).

Regarding the ammonia oxidisers, the primers used in the 16S rRNA sequencing mainly target bacteria, but also pick up Euryarchaeota (Takahashi et al., 2014). Therefore, OTUs assigned to Thaumarchaeota were not detected, although AOA hotspots could be identified based on qPCR data. Nitrosomonadaceae was the most common AOB, with 89 OTUs classified as being similar to uncultured members of this family. *Nitrospira* was the only identified nitrite oxidising bacteria (NOB) in our samples. There was a likely coupling between AOA and NOB, as suggested by the correlation between archaeal *amoA* genes and the relative abundance of Nitrospirae members in general, and *Nitrospira* in particular, in the AOA-cluster samples ($r = 0.65$, $p = 0.0005$; $r = 0.47$, $p = 0.02$, respectively). This coupling has previously also been found in grasslands (Simonin et al., 2015), agricultural soils (Jones and Hallin, 2019), and sediments of an Andean mountain lake (Parro et al., 2019). Comammox *Nitrospira* could be important in the nitrifying hotspots found in the present study, as suggested by previous studies in other surface-attached oligotrophic habitats (Kits et al., 2017; Pjevac et al., 2017; Fowler et al., 2018). For anaerobic ammonia oxidation, OTUs belonging to the “*Candidatus Anammoximicrobium*” (Khramenkov et al., 2013)

was the only taxa present with demonstrated anammox capacity. However, more bacteria within the numerous uncultured Planctomycetes detected in our samples could potentially perform anammox.

CONCLUSION

The N-transforming guild composition in benthic habitats of mountain lakes is complex and deeply embedded in the overall prokaryotic community. There is a high positive correlation among all the genes, and they all generally increase with OM. The dominant pathways change depending on the habitat and productivity of the lake (Figure 7). The fate of nitrite is the main diverging point differentiating the N-transforming guilds. The genetic potential for DNRA dominate in the deep part of the lakes and the lower sediment layers, which indicates recycling of the N_r . By contrast, the denitrifying *nirS* nitrite reduction potential prevails in the upper layer of the sediments in the shallow, warmer and more productive lakes, which indicates a loss of N_r . Emissions of N_2O and N_2 are likely spatially segregated within lakes, with lithic biofilms being candidates for preferential N loss as N_2 as they show a more balanced gene abundance of nitrous oxide reductases (*nosZI+II*) and anammox (*hdh*) in relation to NO-forming nitrite reductases (*nirS+nirK*). The more productive and *nirS*-dominated habitats may be a main source of N_2O because of the striking excess of this gene over the ones of the final steps of complete denitrification unless another bypass process is relevant (e.g., N-DAMO). There may be two types of nitrifying-denitrifying coupled community types in the benthic habitats of mountain lakes. The first is based on nitrification by AOA coupled to Nitrospirae (NOB) and denitrification by *nirS*-denitrifiers, with hotspots in the rocky littoral sediments of the lakes above treeline and the sediments near the isoetid rhizosphere. The second includes AOB coupled to *nirK*-type denitrifiers reducing nitrite and *nosZI*- N_2O reduction in the lithic biofilms. Overall, our results point out two types of potential

response to high atmospheric N deposition in these lakes. In highly oligotrophic lakes, there will be an accumulation of N_r because of the predominance of internal N_r recycling via DNRA. In less oligotrophic lakes, generally with macrophyte growth, the N_r deposition loads may be more effectively directed toward N gas release to the atmosphere via denitrification.

ETHICS STATEMENT

The authors declare that the present study does not involve human or animals, that they have all the licenses, and that they follow all the rules for sampling in the Aigüestortes National Park.

AUTHOR CONTRIBUTIONS

CP-L and JCat contributed to the study design. LC and CP-L carried out sampling. CP-L, CJ, and JCal carried out the lab work and data analysis. JCat, SH, LC, and EC contributed to reagents, materials, and analysis tools. CP-L and JCat wrote the manuscript. All authors substantially contributed to commenting and revising it.

REFERENCES

- Barnes, R. T., Smith, R. L., and Aiken, G. R. (2012). Linkages between denitrification and dissolved organic matter quality, Boulder Creek watershed, Colorado. *J. Geophys. Res.* 117:G01014.
- Battin, T. J., Besemer, K., Bengtsson, M. M., Romani, A. M., and Packmann, A. I. (2016). The ecology and biogeochemistry of stream biofilms. *Nat. Rev. Microbiol.* 14, 251–263. doi: 10.1038/nrmicro.2016.15
- Berry, D., Ben Mahfoudh, K., Wagner, M., and Loy, A. (2011). Barcoded primers used in multiplex amplicon pyrosequencing bias amplification. *Appl. Environ. Microbiol.* 77, 7846–7849. doi: 10.1128/AEM.05220-11
- Blanchet, F. G., Legendre, P., and Borcard, D. (2008). Forward selection of explanatory variables. *Ecology* 89, 2623–2632. doi: 10.1890/07-0986.1
- Borcard, D., Gillet, F., and Legendre, P. (2011). *Numerical Ecology with R*. New York, NY: Springer.
- Cáceres, M. D., and Legendre, P. (2009). Associations between species and groups of sites: indices and statistical inference. *Ecology* 90, 3566–3574. doi: 10.1890/08-1823.1
- Camarero, L. (2017). “Atmospheric chemical loadings in the high mountain: current forcing and legacy pollution,” in *High Mountain Conservation in a Changing World*, eds J. Catalan, J. Ninot, and M. M. Aniz (New York, NY: Springer), 325–341. doi: 10.1007/978-3-319-55982-7_14
- Camarero, L., and Catalan, J. (1998). A simple model of regional acidification for high mountain lakes: application to the Pyrenean lakes (north-east Spain). *Water Res.* 32, 1126–1136. doi: 10.1016/s0043-1354(97)00291-1
- Camarero, L., and Catalan, J. (2012). Atmospheric phosphorus deposition may cause lakes to revert from phosphorus limitation back to nitrogen limitation. *Nat. Commun.* 3:1118. doi: 10.1038/ncomms2125
- Castellano-Hinojosa, A., Correa-Galeote, D., Carrillo, P., Bedmar, E. J., and Medina-Sánchez, J. M. (2017). Denitrification and biodiversity of denitrifiers in a high-mountain Mediterranean lake. *Front. Microbiol.* 8:1911. doi: 10.3389/fmicb.2017.01911
- Catalan, J., Ballesteros, E., Gacia, E., Palau, A., and Camarero, L. (1993). Chemical-composition of disturbed and undisturbed high-mountain lakes in the Pyrenees: a reference for acidified sites. *Water Res.* 27, 133–141. doi: 10.1016/0043-1354(93)90203-t

FUNDING

The Spanish Government provided funds through the Ministerio de Educación as a predoctoral fellowship to CP-L (FPU12-00644) and research grants of the Ministerio de Economía y Competitividad: NitroPir (CGL2010-19737), DARKNESS (CGL2012-32747), LACUS (CGL2013-45348-P), TRANSFER (CGL2016-80124-C2-1-P). The REPLIM grant (INRE - INTERREG Programme. EUUN – European Union. EFA056/15) and the ALTER-NET Mobility Scheme supported the final writing.

ACKNOWLEDGMENTS

We thank the authorities of the Aigüestortes and Estany de Sant Maurici National Park for sampling facilities in protected areas and support.

SUPPLEMENTARY MATERIAL

The Supplementary Material for this article can be found online at: <https://www.frontiersin.org/articles/10.3389/fmicb.2019.01229/full#supplementary-material>

- Catalan, J., Barbieri, M. G., Bartumeus, F., Bitušik, P., Botev, I., Brancelj, A., et al. (2009). Ecological thresholds in European alpine lakes. *Freshw. Biol.* 54, 2494–2517. doi: 10.1111/j.1365-2427.2009.02286.x
- Catalan, J., Camarero, L., De Quijano, D. D., Felip, M., Pla, S., Ventura, M., et al. (2006). High mountain lakes: extreme habitats and witnesses of environmental changes. *Limnetica* 25, 551–584.
- Catalan, J., Camarero, L., Gacia, E., Ballesteros, E., and Felip, M. (1994). Nitrogen in the Pyrenean lakes (Spain). *Hydrobiologia* 274, 17–27. doi: 10.1007/978-94-017-2095-3_3
- Catalan, J., Pla-Rabes, S., Wolfe, A. P., Smol, J. P., Ruhland, K. M., Anderson, N. J., et al. (2013). Global change revealed by palaeolimnological records from remote lakes: a review. *J. Paleolimnol.* 49, 513–535. doi: 10.1007/s10933-013-9681-2
- Chen, J., Hanke, A., Tegetmeyer, H. E., Kattelmann, I., Sharma, R., Hamann, E., et al. (2017). Impacts of chemical gradients on microbial community structure. *ISME J.* 11, 920–931. doi: 10.1038/ismej.2016.175
- Chen, R., Deng, M., He, X., and Hou, J. (2017). Enhancing nitrate removal from freshwater pond by regulating carbon/nitrogen ratio. *Front. Microbiol.* 8:1712. doi: 10.3389/fmicb.2017.01712
- Chen, X., Yang, L., Xiao, L., Miao, A., and Xi, B. (2012). Nitrogen removal by denitrification during cyanobacterial bloom in Lake Taihu. *J. Freshw. Ecol.* 27, 243–258. doi: 10.1080/02705060.2011.644405
- Deutzmann, J. S., Stief, P., Brandes, J., and Schink, B. (2014). Anaerobic methane oxidation coupled to denitrification is the dominant methane sink in a deep lake. *Proc. Natl. Acad. Sci. U.S.A.* 111, 18273–18278. doi: 10.1073/pnas.1411617111
- Dodla, S. K., Wang, J. J., Delaune, R. D., and Cook, R. L. (2008). Denitrification potential and its relation to organic carbon quality in three coastal wetland soils. *Sci. Total Environ.* 407, 471–480. doi: 10.1016/j.scitotenv.2008.08.022
- Dore, J. E., Popp, B. N., Karl, D. M., and Sansone, F. J. (1998). A large source of atmospheric nitrous oxide from subtropical North Pacific surface waters. *Nature* 396, 63–66. doi: 10.1038/23921
- Edgar, R. C. (2013). UPARSE highly accurate OTU sequences from microbial amplicon reads. *Nat. Methods* 10, 996–998. doi: 10.1038/nmeth.2604
- Erismann, J. W., Galloway, J., Seitzinger, S., Bleeker, A., and Butterbach-Bahl, K. (2011). Reactive nitrogen in the environment and its effect on climate change. *Curr. Opin. Environ. Sustain.* 3, 281–290. doi: 10.1016/j.cosust.2011.08.012

- Fowler, S. J., Palomo, A., Dechesne, A., Mines, P. D., and Smets, B. F. (2018). Comammox nitrospira are abundant ammonia oxidizers in diverse groundwater-fed rapid sand filter communities. *Environ. Microbiol.* 20, 1002–1015. doi: 10.1111/1462-2920.14033
- Gacia, E., Ballesteros, E., Camarero, L., Delgado, O., Palau, A., Riera, J. L., et al. (1994). Macrophytes from lakes in the eastern pyrenees: community composition and ordination in relation to environmental factors. *Freshw. Biol.* 32, 73–81. doi: 10.1111/j.1365-2427.1994.tb00867.x
- Gacia, E., Chappuis, E., Lumbreras, A., Riera, J. L., and Ballesteros, E. (2009). Functional diversity of macrophyte communities within and between Pyrenean lakes. *J. Limnol.* 68, 25–36.
- Gardner, W. S., Newell, S. E., Mccarthy, M. J., Hoffman, D. K., Lu, K., Lavrentyev, P. J., et al. (2017). Community biological ammonium demand: a conceptual model for Cyanobacteria blooms in eutrophic lakes. *Environ. Sci. Technol.* 51, 7785–7793. doi: 10.1021/acs.est.6b06296
- Glew, J. (1991). Miniature gravity corer for recovering short sediment cores. *J. Paleolimnol.* 5, 285–287. doi: 10.1007/BF00200351
- Graf, D. R. H., Jones, C. M., and Hallin, S. (2014). Intergenomic comparisons highlight modularity of the denitrification pathway and underpin the importance of community structure for N₂O emissions. *PLoS One* 9:e114118. doi: 10.1371/journal.pone.0114118
- Hallin, S., and Lindgren, P. E. (1999). PCR detection of genes encoding nitrite reductase in denitrifying bacteria. *Appl. Environ. Microbiol.* 65, 1652–1657.
- Hallin, S., Philippot, L., Löffler, F. E., Sanford, R. A., and Jones, C. M. (2018). Genomics and ecology of novel N₂O-reducing microorganisms. *Trends Microbiol.* 26, 43–55. doi: 10.1016/j.tim.2017.07.003
- Heiri, O., Lotter, A. F., and Lemcke, G. (2001). Loss on ignition as a method for estimating organic and carbonate content in sediments: reproducibility and comparability of results. *J. Paleolimnol.* 25, 101–110.
- Henry, S., Bru, D., Stres, B., Hallet, S., and Philippot, L. (2006). Quantitative detection of the nosZ gene, encoding nitrous oxide reductase, and comparison of the abundances of 16S rRNA, narG, nirK, and nosZ genes in soils. *Appl. Environ. Microbiol.* 72, 5181–5189. doi: 10.1128/aem.00231-06
- Holtgrieve, G. W., Schindler, D. E., Hobbs, W. O., Leavitt, P. R., Ward, E. J., Bunting, L., et al. (2011). A coherent signature of anthropogenic nitrogen deposition to remote watersheds of the northern hemisphere. *Science* 334, 1545–1548. doi: 10.1126/science.1212267
- Jones, C. M., Graf, D. R., Bru, D., Philippot, L., and Hallin, S. (2013). The unaccounted yet abundant nitrous oxide-reducing microbial community: a potential nitrous oxide sink. *ISME J.* 7, 417–426. doi: 10.1038/ismej.2012.125
- Jones, C. M., and Hallin, S. (2019). Geospatial variation in co-occurrence networks of nitrifying microbial guilds. *Mol. Ecol.* 28, 293–306. doi: 10.1111/mec.14893
- Kessler, A. J., Roberts, K. L., Bissett, A., and Cook, P. L. (2018). Biogeochemical controls on the relative importance of denitrification and dissimilatory nitrate reduction to ammonium in estuaries. *Glob. Biogeochem. Cycles* 32, 1045–1057. doi: 10.1029/2018gb005908
- Khramenkov, S. V., Kozlov, M. N., Kevbrina, M. V., Dorofeev, A. G., Kazakova, E. A., Grachev, V. A., et al. (2013). A novel bacterium carrying out anaerobic ammonium oxidation in a reactor for biological treatment of the filtrate of wastewater fermented sludge. *Microbiology* 82, 628–636. doi: 10.1134/s002626171305007x
- Kits, K. D., Campbell, D. J., Rosana, A. R., and Stein, L. Y. (2015a). Diverse electron sources support denitrification under hypoxia in the obligate methanotroph Methylobacterium album strain BG8. *Front. Microbiol.* 6:1072. doi: 10.3389/fmicb.2015.01072
- Kits, K. D., Klotz, M. G., and Stein, L. Y. (2015b). Methane oxidation coupled to nitrate reduction under hypoxia by the Gammaproteobacterium Methylomonas denitrificans, sp. nov. type strain FJG1. *Environ. Microbiol.* 17, 3219–3232. doi: 10.1111/1462-2920.12772
- Kits, K. D., Sedlacek, C. J., Lebedeva, E. V., Han, P., Bulaev, A., Pjevac, P., et al. (2017). Kinetic analysis of a complete nitrifier reveals an oligotrophic lifestyle. *Nature* 549, 269–272. doi: 10.1038/nature23679
- Kopaček, J., Hejzlar, J., Vrba, J., and Stuchlík, E. (2011). Phosphorus loading of mountain lakes: terrestrial export and atmospheric deposition. *Limnol. Oceanogr.* 56, 1343–1354. doi: 10.4319/lo.2011.56.4.1343
- Kraft, B., Tegetmeyer, H. E., Sharma, R., Klotz, M. G., Ferdelman, T. G., Hettich, R. L., et al. (2014). The environmental controls that govern the end product of bacterial nitrate respiration. *Science* 345, 676–679. doi: 10.1126/science.1254070
- Kuypers, M. M. M., Marchant, H. K., and Kartal, B. (2018). The microbial nitrogen-cycling network. *Nat. Rev. Microbiol.* 16, 263–276. doi: 10.1038/nrmicro.2018.9
- Lopez-Gutierrez, J. C., Henry, S., Hallet, S., Martin-Laurent, F., Catroux, G., and Philippot, L. (2004). Quantification of a novel group of nitrate-reducing bacteria in the environment by real-time PCR. *J. Microbiol. Methods* 57, 399–407. doi: 10.1016/j.mimet.2004.02.009
- Mariotti, A., Germon, J., Hubert, P., Kaiser, P., Letolle, R., Tardieux, A., et al. (1981). Experimental determination of nitrogen kinetic isotope fractionation: some principles; illustration for the denitrification and nitrification processes. *Plant Soil* 62, 413–430. doi: 10.1007/bf02374138
- Martiny, J. B., Jones, S. E., Lennon, J. T., and Martiny, A. C. (2015). Microbiomes in light of traits: a phylogenetic perspective. *Science* 350:aac9323. doi: 10.1126/science.aac9323
- McCrackin, M. L., and Elser, J. J. (2010). Atmospheric nitrogen deposition influences denitrification and nitrous oxide production in lakes. *Ecology* 91, 528–539. doi: 10.1890/08-2210.1
- Melton, E. D., Stief, P., Behrens, S., Kappler, A., and Schmidt, C. (2014). High spatial resolution of distribution and interconnections between Fe- and N-redox processes in profundal lake sediments. *Environ. Microbiol.* 16, 3287–3303. doi: 10.1111/1462-2920.12566
- Merbt, S. N., Bernal, S., Proia, L., Martí, E., and Casamayor, E. O. (2017). Photoinhibition on natural ammonia oxidizers biofilm populations and implications for nitrogen uptake in stream biofilms. *Limnol. Oceanogr.* 62, 364–375. doi: 10.1002/lno.10436
- Mohan, S. B., Schmid, M., Jetten, M., and Cole, J. (2004). Detection and widespread distribution of the nrfA gene encoding nitrite reduction to ammonia, a short circuit in the biological nitrogen cycle that competes with denitrification. *FEMS Microbiol. Ecol.* 49, 433–443. doi: 10.1016/j.femsec.2004.04.012
- Myrstener, M., Jonsson, A., and Bergstrom, A. K. (2016). The effects of temperature and resource availability on denitrification and relative N₂O production in boreal lake sediments. *J. Environ. Sci.* 47, 82–90. doi: 10.1016/j.jes.2016.03.003
- Naqvi, S. W. A., Lam, P., Narvenkar, G., Sarkar, A., Naik, H., Pratihary, A., et al. (2018). Methane stimulates massive nitrogen loss from freshwater reservoirs in India. *Nat. Commun.* 9:1265. doi: 10.1038/s41467-018-03607-z
- Onley, J. R., Ahsan, S., Sanford, R. A., and Löffler, F. E. (2018). Denitrification by Anaeromyxobacter dehalogenans, a common soil bacterium lacking the nitrite reductase genes nirS and nirK. *Appl. Environ. Microbiol.* 84:e1985-17. doi: 10.1128/AEM.01985-17
- Pajares, S., Merino-Ibarra, M., Macek, M., and Alcocer, J. (2017). Vertical and seasonal distribution of picoplankton and functional nitrogen genes in a high-altitude warm-monomictic tropical lake. *Freshw. Biol.* 62, 1180–1193. doi: 10.1111/fwb.12935
- Palacin-Lizarbe, C., Camarero, L., and Catalan, J. (2018). Denitrification temperature dependence in remote, cold, and N-poor lake sediments. *Water Resour. Res.* 54, 1161–1173. doi: 10.1002/2017wr021680
- Parro, V., Puente-Sánchez, F., Cabrol, N. A., Gallardo-Carreño, I., Moreno-Paz, M., Blanco, Y., et al. (2019). Microbiology and nitrogen cycle in the benthic sediments of a glacial oligotrophic deep andean lake as analog of ancient martian lake-beds. *Front. Microbiol.* 10:929. doi: 10.3389/fmicb.2019.00929
- Peura, S., Buck, M., Aalto, S. L., Morales, S. E., Nykanen, H., and Eiler, A. (2018). Novel autotrophic organisms contribute significantly to the internal carbon cycling potential of a boreal lake. *mBio* 9, e916–e918. doi: 10.1128/mBio.00916-18
- Peura, S., Sinclair, L., Bertilsson, S., and Eiler, A. (2015). Metagenomic insights into strategies of aerobic and anaerobic carbon and nitrogen transformation in boreal lakes. *Sci. Rep.* 5:12102. doi: 10.1038/srep12102
- Pjevac, P., Schaubberger, C., Poghosyan, L., Herbold, C. W., Van Kessel, M., Daebeler, A., et al. (2017). AmoA-targeted polymerase chain reaction primers for the specific detection and quantification of comammox Nitrospira in the environment. *Front. Microbiol.* 8:1508. doi: 10.3389/fmicb.2017.01508
- Quast, C., Pruesse, E., Yilmaz, P., Gerken, J., Schweer, T., Yarza, P., et al. (2013). The SILVA ribosomal RNA gene database project: improved data processing and web-based tools. *Nucleic Acids Res.* 41, D590–D596. doi: 10.1093/nar/gks1219

- Rockström, J., Steffen, W., Noone, K., Persson, A., Chapin, F. S. III, Lambin, E. F., et al. (2009). A safe operating space for humanity. *Nature* 461, 472–475.
- Rotthauwe, J. H., Witzel, K. P., and Liesack, W. (1997). The ammonia monooxygenase structural gene *amoA* as a functional marker: molecular fine-scale analysis of natural ammonia-oxidizing populations. *Appl. Environ. Microbiol.* 63, 4704–4712.
- R Core Team (2017). *R: A Language and Environment for Statistical Computing*. Available at: <http://www.r-project.org> (accessed May 22, 2019).
- Saarenheimo, J., Rissanen, A. J., Arvola, L., Nykanen, H., Lehmann, M. F., and Tirola, M. (2015a). Genetic and environmental controls on nitrous oxide accumulation in lakes. *PLoS One* 10:e0121201. doi: 10.1371/journal.pone.0121201
- Saarenheimo, J., Tirola, M., and Rissanen, A. J. (2015b). Functional gene pyrosequencing reveals core proteobacterial denitrifiers in boreal lakes. *Front. Microbiol.* 6:674. doi: 10.3389/fmicb.2015.00674
- Sand-Jensen, K., Prah, C., and Stokholm, H. (1982). Oxygen release from roots of submerged aquatic macrophytes. *Oikos* 38, 349–354.
- Schmid, M. C., Hooper, A. B., Klotz, M. G., Woebken, D., Lam, P., Kuypers, M. M. M., et al. (2008). Environmental detection of octahemal cytochrome *c* hydroxylamine/hydrazine oxidoreductase genes of aerobic and anaerobic ammonium-oxidizing bacteria. *Environ. Microbiol.* 10, 3140–3149. doi: 10.1111/j.1462-2920.2008.01732.x
- Shen, L.-D., Ouyang, L., Zhu, Y., and Trimmer, M. (2019). Active pathways of anaerobic methane oxidation across contrasting riverbeds. *ISME J.* 13, 752–766.
- Simon, J., and Klotz, M. G. (2013). Diversity and evolution of bioenergetic systems involved in microbial nitrogen compound transformations. *Biochim. Biophys. Acta* 1827, 114–135. doi: 10.1016/j.bbabi.2012.07.005
- Simonin, M., Le Roux, X., Poly, F., Lerondelle, C., Hungate, B. A., Nunan, N., et al. (2015). Coupling between and among ammonia oxidizers and nitrite oxidizers in grassland mesocosms submitted to elevated CO₂ and nitrogen supply. *Microb. Ecol.* 70, 809–818. doi: 10.1007/s00248-015-0604-9
- Smol, J. P. (2012). A planet in flux: how is life on Earth reacting to climate change? *Nature* 483, S12–S15.
- Stelzer, R., Scott, J. T., Bartsch, L. A., and Parr, T. (2014). Particulate organic matter quality influences nitrate retention and denitrification in stream sediments: evidence from a carbon burial experiment. *Biogeochemistry* 119, 387–402. doi: 10.1007/s10533-014-9975-0
- Storey, J. D., Taylor, J. E., and Siegmund, D. (2004). Strong control, conservative point estimation and simultaneous conservative consistency of false discovery rates: a unified approach. *J. R. Stat. Soc. B Met.* 66, 187–205. doi: 10.1111/j.1467-9868.2004.00439.x
- Takahashi, S., Tomita, J., Nishioka, K., Hisada, T., and Nishijima, M. (2014). Development of a prokaryotic universal primer for simultaneous analysis of Bacteria and Archaea using next-generation sequencing. *PLoS One* 9:e105592. doi: 10.1371/journal.pone.0105592
- Throback, I. N., Enwall, K., Jarvis, Å., and Hallin, S. (2004). Reassessing PCR primers targeting *nirS*, *nirK* and *nosZ* genes for community surveys of denitrifying bacteria with DGGE. *FEMS Microbiol. Ecol.* 49, 401–417. doi: 10.1016/j.femsec.2004.04.011
- Tourna, M., Freitag, T. E., Nicol, G. W., and Prosser, J. I. (2008). Growth, activity and temperature responses of ammonia-oxidizing archaea and bacteria in soil microcosms. *Environ. Microbiol.* 10, 1357–1364. doi: 10.1111/j.1462-2920.2007.01563.x
- Van Mooy, B., Keil, R., and Devol, A. (2002). Impact of suboxia on sinking particulate organic carbon: enhanced carbon flux and preferential degradation of amino acids via denitrification. *Geochim. Cosmochim. Acta* 66, 457–465. doi: 10.1016/s0016-7037(01)00787-6
- Vila-Costa, M., Bartrons, M., Catalan, J., and Casamayor, E. O. (2014). Nitrogen-cycling genes in epilithic biofilms of oligotrophic high-altitude lakes (Central Pyrenees, Spain). *Microb. Ecol.* 68, 60–69. doi: 10.1007/s00248-014-0417-2
- Vila-Costa, M., Pulido, C., Chappuis, E., Calviño, A., Casamayor, E. O., and Gacia, E. (2016). Macrophyte landscape modulates lake ecosystem-level nitrogen losses through tightly coupled plant-microbe interactions. *Limnol. Oceanogr.* 61, 78–88. doi: 10.1002/lno.10209
- Wallenstein, M. D., Myrold, D. D., Firestone, M., and Voytek, M. (2006). Environmental controls on denitrifying communities and denitrification rates: insights from molecular methods. *Ecol. Appl.* 16, 2143–2152. doi: 10.1890/1051-0761(2006)016%5B2143:ecodca%5D2.0.co;2
- Wang, Q., Garrity, G. M., Tiedje, J. M., and Cole, J. R. (2007). naive bayesian classifier for rapid assignment of rRNA sequences into the new bacterial taxonomy. *Appl. Environ. Microbiol.* 73, 5261–5267. doi: 10.1128/aem.00062-07
- Welsh, A., Chee-Sanford, J. C., Connor, L. M., Löffler, F. E., and Sanford, R. A. (2014). Refined *NrfA* phylogeny improves PCR-based *nrfA* gene detection. *Appl. Environ. Microbiol.* 80, 2110–2119. doi: 10.1128/AEM.03443-13
- Wittorf, L., Bonilla-Rosso, G., Jones, C. M., Backman, O., Hulth, S., and Hallin, S. (2016). Habitat partitioning of marine benthic denitrifier communities in response to oxygen availability. *Environ. Microbiol. Rep.* 8, 486–492. doi: 10.1111/1758-2229.12393
- Zhang, J., Kobert, K., Flouri, T., and Stamatakis, A. (2013). PEAR: a fast and accurate Illumina paired-end read merger. *Bioinformatics* 30, 614–620. doi: 10.1093/bioinformatics/btt593

Conflict of Interest Statement: The authors declare that the research was conducted in the absence of any commercial or financial relationships that could be construed as a potential conflict of interest.

Copyright © 2019 Palacin-Lizarbe, Camarero, Hallin, Jones, Cáliz, Casamayor and Catalan. This is an open-access article distributed under the terms of the Creative Commons Attribution License (CC BY). The use, distribution or reproduction in other forums is permitted, provided the original author(s) and the copyright owner(s) are credited and that the original publication in this journal is cited, in accordance with accepted academic practice. No use, distribution or reproduction is permitted which does not comply with these terms.

SUPPLEMENTARY MATERIAL for

The DNRA-denitrification dichotomy differentiates nitrogen transformation pathways in mountain lake benthic habitats

Carlos Palacin-Lizarbe¹, Lluís Camarero², Sara Hallin³, Christopher M Jones³, Joan Caliz², Emilio O Casamayor², and Jordi Catalan^{1,4}

¹CREAF, Campus UAB, Cerdanyola del Vallès, Spain, ²Center for Advanced Studies of Blanes, (CEAB-CSIC), Girona, Spain, ³Swedish University of Agricultural Sciences, Department of Forest Mycology and Plant Pathology, Uppsala, Sweden, ⁴CSIC, Cerdanyola del Vallès, Spain

Supplementary tables: Environmental (Table S1) and gene abundance (Table S2) data by lake and habitat, OTUs exclusive indicators of one cluster (Table S4), and most influential OTUs of the prokaryotic community ordinations (com-gen-RDA and com-PCA, Table S6) are in separate excel files.

Current file content:

- **Table S3.** Primers and thermal cycling conditions for quantification of 16S rRNA and N-functional genes, and Illumina pyrosequencing of *16S* rRNA.
- **Table S5.** Primary indicator taxa of the microbial community associated with each N-transforming functional cluster, indicated by the dominant gene and process and the characteristics of the habitat where they were detected.
- **Figures S1-6.**
 - S1. Abundance of the accounted N-functional per sediment DW.
 - S2. Sediment profiles of *nrfA* and archaeal *amoA* abundance.
 - S3. Unconstrained principal component analysis ordination of the N-functional gene abundance (gen-PCA).
 - S4. Site scores of the gen-env-RDA and com-gen-RDA.
 - S5. Mean size of the sediment particles by habitat and lake and gene-ordination clusters.
 - S6. Principal component analysis using the Hellinger distance of the prokaryotic community (com-PCA).

Table S3. Primers and thermal cycling conditions for quantification of 16S rRNA and N-functional genes, and Illumina pyrosequencing of 16S rRNA.

Process/Taxa	Genes Primer names	Sequences (5'-3')	References	Thermal cycling	Efficiency (%)
Bacteria	16S rRNA				
	Sequencing			(98 C, 3 min) x 1	
	Pro341F	CCTACGGNBBGCASCAG	Takahashi et al. (2014)	(98 C, 30 s; 55 C, 30 s; 72 C, 30 s) x 25	
	Pro805R	GACTACVNYGGTATCTAAATCC		(72 C, 10 min) x 1	
Bacteria	16S rRNA				
	341F	CCT ACG GGA GGC AGC AG	Lopez-Gutierrez et al. (2004)	(95 C, 15 s; 60 C, 30 s; 72 C, 30 s; 80 C, 30 s) x 40	90
	534R	ATT ACC GCG GCT GCT GGC A		(95°C, 15 s;(60 to 95°C, 10 s, increment 0.5°), x 1	
Denitrification	nirK				
	nirK F1aCu	ATCATGTSCTGCCCGC	Hallin and Lindgren (1999)	(95 C, 7 min) x 1	
	nirK R3Cu	GCCTCGATCAGRTTGTGGTT		(95 C, 15 s; (63 C – 58 C, -1 /cycle), 30 s; 72 C, 30 s) x 6	83
				(95 C, 15 s; 58 C, 30 s; 72 C, 30 s; 80 C, 30 s) x 35	
				(95°C, 15 s;(60 to 95°C, 10 s, increment 0.5°), x 1	
Denitrification	nirS				
	nirS cd3aFm	AACGYSAAAGGARACSCGG	Throbäck et al. (2004)	(95 C, 7 min) x 1	
	nirS R3cdm	GASTTCGGRTGSGTCTTSAYGAA		(95 C, 15 s; (65 C – 60 C, -1 /cycle), 30 s; 72 C, 30 s) x 6	76
				(95 C, 15 s; 60 C, 30 s; 72 C, 30 s; 80 C, 30 s) x 35	
				(95°C, 15 s;(60 to 95°C, 10 s, increment 0.5°), x 1	
Denitrification	nosZI				
	1840F	CGC RAC GGC AAS AAG GTS MSS GT	Henry et al. (2006)	(95 C, 7 min) x 1	
	2090R	CAK RTG CAK SGC RTG GCA GAA		(95 C, 15 s; (65 C – 60 C, -1 /cycle), 30 s; 72 C, 30 s) x 6	79
				(95 C, 15 s; 60 C, 30 s; 72 C, 30 s; 80 C, 30 s) x 35	
				(95°C, 15 s;(60 to 95°C, 10 s, increment 0.5°), x 1	
Denitrification	nosZII				
	nosZII-F	CTI GGI CCI YTK CAY AC	Jones et al. (2013)	(95 C, 7 min) x 1	
	nosZII-R	GCI GAR CAR AAI TCB GTR C		(95 C, 15 s; 54 C, 30 s; 72 C, 30 s; 80 C, 30 s) x 40	65
Anammox*	hdh				
	hzoc11F1	TGY AAG ACY TGY CAY TGG	Schmid et al. (2008)	(95 C, 7 min) x 1	
	hzoc11R2	ACT CCA GAT RTG CTG ACC		(95 C, 15 s; 52.5 C, 30 s; 72 C, 30 s; 77 C, 30 s) x 35	88
DNRA**	nrfA				
	nrfAF2aw	CAR TGY CAY GTB GAR TA	Welsh et al. (2014)	(95 C, 5 min) x 1	
	nrfAR1	TWN GCC ATR TGR CAR TC	Mohan et al. (2004)	(95 C, 15 s; 57 C, 30 s; 72 C, 30 s) x 7	70
				(95 C, 15 s; 52 C, 35 s; 72 C, 35 s; 80 C, 15 s) x 35	
				(95°C, 15 s;(60 to 95°C, 10 s, increment 0.5°), x 1	
Nitrification	amoA				
	crenamoA23F	ATG GTC TGG CTW AGA CG	Tourna et al. (2008)	(95 C, 5 min) x 1	
	crenamoA616R	GCC ATC CAT CTG TAT GTC CA		(95 C, 15 s; 55 C, 30 s; 72 C, 40 s; 80 C, 10 s) x 35	84
				(95°C, 15 s;(60 to 95°C, 10 s, increment 0.5°), x 1	
Nitrification	amoA				
	AmoA1F	GGG GTT TCT ACT GGT GGT	Rothauwe et al. (1997)	(95 C, 5 min) x 1	
	AmoA2R	CCC CTC KGS AAA GCC TTC TTC		(95 C, 15 s; 55 C, 30 s; 72 C, 40 s; 80 C, 10 s) x 35	85
				(95°C, 15 s;(60 to 95°C, 10 s, increment 0.5°), x 1	

*Anammox: Anaerobic ammonium oxidation. **DNRA: Dissimilatory nitrate reduction to ammonium

Table S5. Primary indicator taxa of the microbial community associated with each N-transforming functional cluster, indicated by the dominant gene and process and the characteristics of the habitat where they were detected.

Characteristic N-functional gene(s) and process(es) of the N-transforming cluster	Habitat	Main indicator taxa of the associated microbial community
<i>nirS</i> , denitrification (nitrite reduction)	All sediment habitats of the less oligotrophic, shallower and warmer lakes. Sediments with high organic matter content and low C/N ratio.	Candidate divisions TA06 and GOUTA4 Chlorobi (Ignavibacteriales & SJA-28) Elusimicrobia (Endomicrobia) Fibrobacteres (TG3-1) Spirochaetae (genus <i>Spirochaeta</i>) Nitrospirae (Thermodesulfobivibrionaceae & 4-29) Planctomycetes (Candidatus genus <i>Anammoxomicrobium</i>) Proteobacteria: Gamma- (genus <i>Methylocaldum</i> and species <i>Achromatium oxaliferum</i>) Verrucomicrobia (S-BQ2-57 soil group)
<i>nrfA</i> , DNRA (nitrite reduction)	Deep part of all lakes, littoral of low-altitude (montane) lakes and the deepest sediment layers. Anoxic and fine grain sediment with low $\delta^{13}C$ and high C/N ratio.	Actinobacteria (OPB41, PeM15, and Coriobacteriaceae) Armatimonadetes (SJA-176) Bacteroidetes (Bacteroidia) Candidate divisions OP3, OP8, SR1 and WCHB1-60 Chloroflexi (Dehalococcidia & Anaerolinaceae) Cyanobacteria, non-photosynthetic (Melainabacteria order Gastranaerophilales) Firmicutes Fusobacteria (uncultured Leptotrichiaceae genus) Proteobacteria: Delta- (<i>Syntrophorhabdus</i> and Syntrophaceae) and Epsilon- (Campylobacteriales) Spirochaetae (PL-11B10)
Mixed (<i>nirK</i> , <i>nosZI</i> , <i>nosZII</i> , denitrification (nitrate reduction, nitrous oxide reduction); <i>hdh</i> , anammox (hydrazine oxidation), and <i>amoA</i> AOB, nitrification (ammonium oxidation))	Lithic biofilms. Highly organic thin aggregates with low $\delta^{15}N$ and high $\delta^{13}C$.	Cyanobacteria: photosynthetic class Cyanobacteria (especially subsection III family I (genus <i>Leptolyngbya</i> , <i>Phormidium</i> and <i>Chamaesiphon</i>) and subsection IV) Acidobacteria (genus <i>Blastocatella</i>) Armatimonadetes (Armatimonadales) Bacteroidetes (mainly Cytophagales, but also Sphingobacteriia (Chitinophagaceae, Saprospiraceae, NS11-12 marine group, and class SM1A07) Chlorobi (Chlorobiaceae) Deinococcus-Thermus (Deinococcaceae) Planctomycetes (genus <i>Gemmata</i> , <i>Pirellula</i> and SM1A02) Proteobacteria: mainly Alpha- (especially Caulobacteriales, Rhizobiales, Rhodospirillales (Acetobacteraceae), Rickettsiales and Sphingomonadales); but also Beta- (Burkholderiales) and Gamma- (Pseudomonadales)

amoA nitrification (ammonium oxidation)	(AOA) , Deep sediments near the rhizosphere of isoetid macrophytes. Rocky littoral sediments of lakes in the alpine belt. Sediments with high $\delta^{15}\text{N}$.	Acidobacteria (subgroups 1, 2, 5, 6, 7, 10, 12, 13, 15 and 17) Actinobacteria (orders Acidimicrobiales, Gaiellales and class MB-A2-108) Bacteroidetes (Sphingobacteriales (families AKYH767, CWT CU03-E12, PHOs-HE51 and S15-21)) Candidate divisions TM6 and WD272 Chlamydiae (Chlamydiales, mainly families Parachlamydiaceae, Simkaniaceae and cvE6) Chloroflexi (classes Ktedonobacteria, JG30-KF-CM66, JG37-AG-4, P2-11E, S085 and TK10) Cyanobacteria (non-photosynthetic, Melainabacteria (order Obscuribacterales)) Elusimicrobia (lineages (IIa, IIb, IIc, IV), FCPU453 and MVP-88) Fibrobacteres (order 258ds10) Gemmatimonadetes (Gemmatimonadaceae) Nitrospirae (family 0319-6A21 and uncultured members of the genus <i>Nitrospira</i>) Planctomycetes (OM190, Pla4 lineage, and an uncultured Genus of Planctomycetaceae) Proteobacteria: Alpha- (Rhodospirillales (DA111, I-10 and KCM-B-15)); Beta- (uncultured Nitrosomonadaceae genus), Gamma- (genus <i>Beggiatoa</i> and orders Legionellales (especially genus <i>Aquicella</i> , <i>Coxiella</i> and <i>Legionella</i>), Xanthomonadales, and NKB5); and Delta- (GR-WP33-30 and myxococcales (especially genus <i>Haliangium</i> , and families Cystobacteraceae, Polyangiaceae, Sandaracinaceae and mle1-27) Verrucomicrobia (order Chthoniobacterales mainly from family DA101 soil group)
--	--	---

Figure S1. Sum of the accounted N-functional gene copies standardised to 16S rRNA gene copy abundance. Lakes are arranged from left to right by increasing water-column DIN level (see Table 2 for lake abbreviations and features) Hereafter, boxplots depict the interquartile range (box), median value (line), 1.5 x interquartile range (whiskers), and outliers (points).

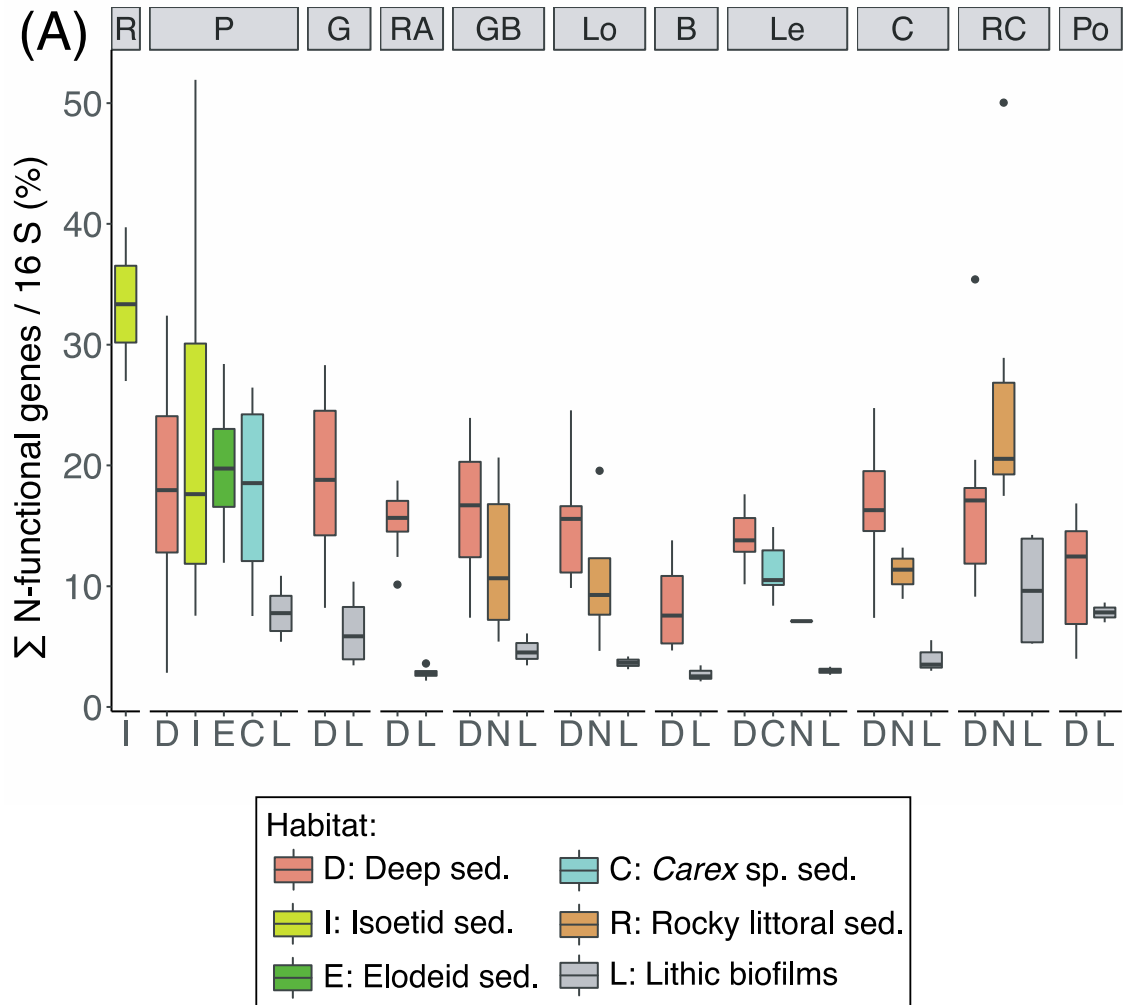


Figure S2. A) *NrfA* abundance sediment profiles. B) Archaeal (AOA) *amoA* abundance sediment profiles. Note that *amoA* abundance (X-axis) is square root transformed. Dashed lines connect sediment samples from the same core but different layer. All samples are from Plan Lake except two from Redon de Vilamòs Lake (star symbol).

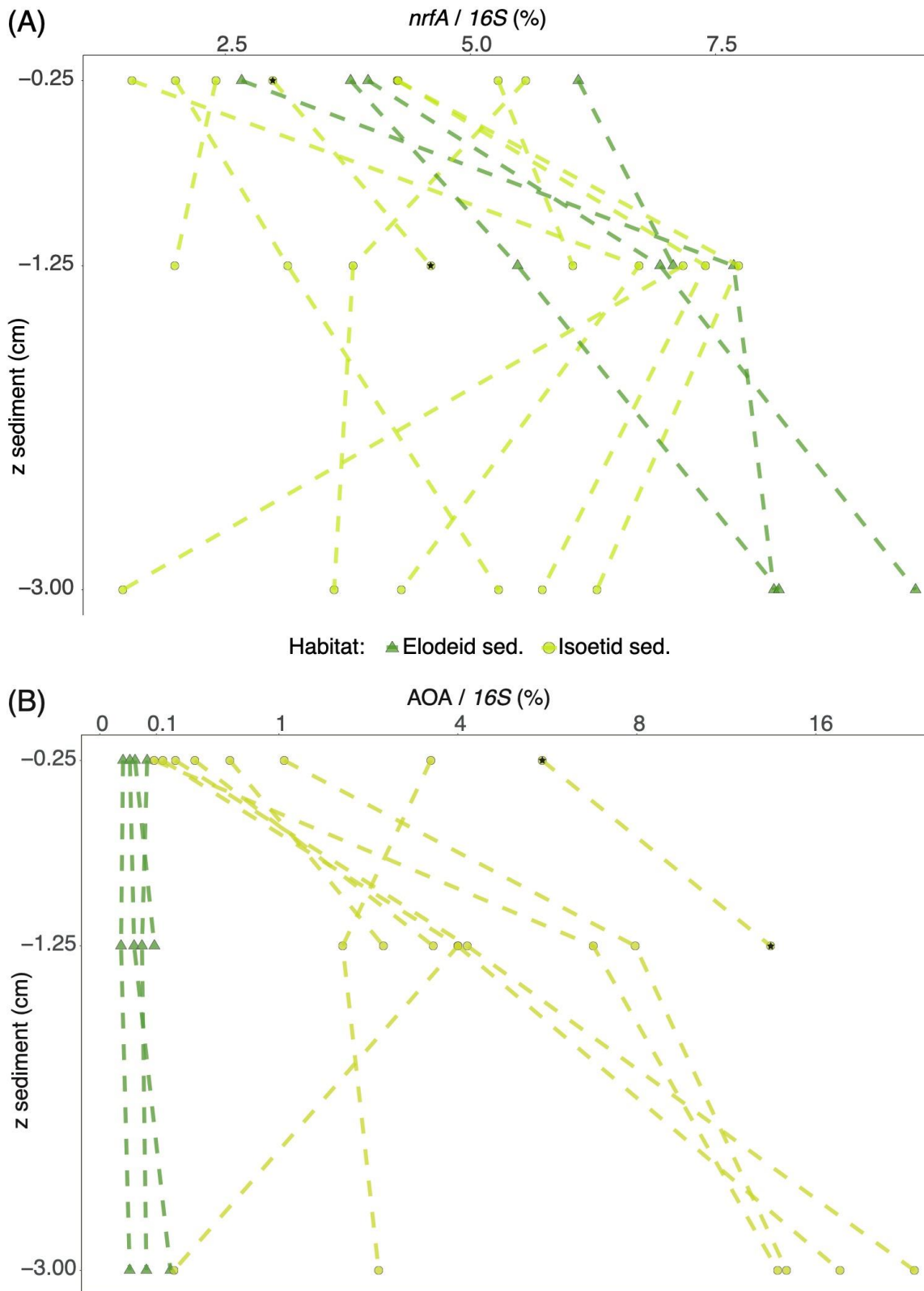
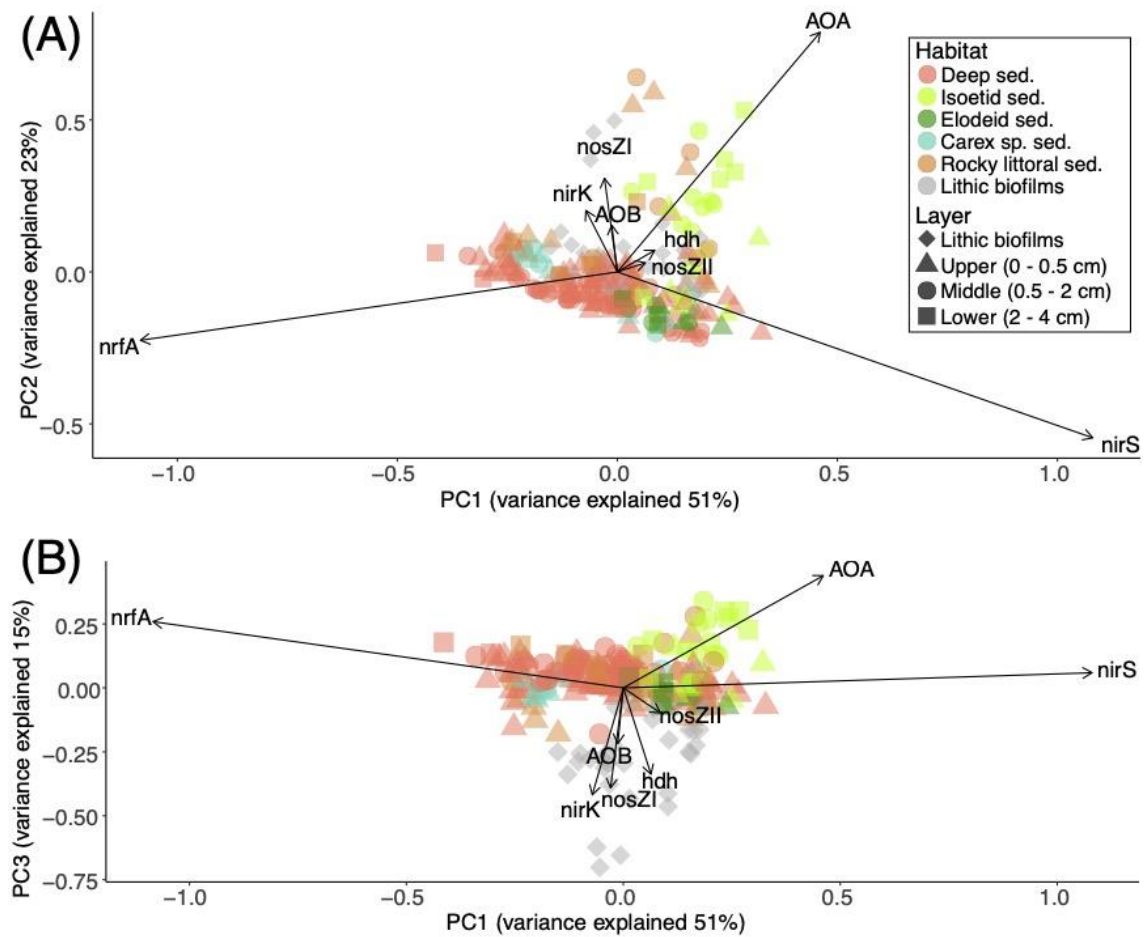


Figure S3. Unconstrained ordination of the N-functional gene abundances resulted from a principal component analysis using Hellinger distance (gen-PCA). A) Biplot of the 1st and 2nd and (B)) 1st and 3rd main gradients. The PCA axes' length is scaled to the variation explained.



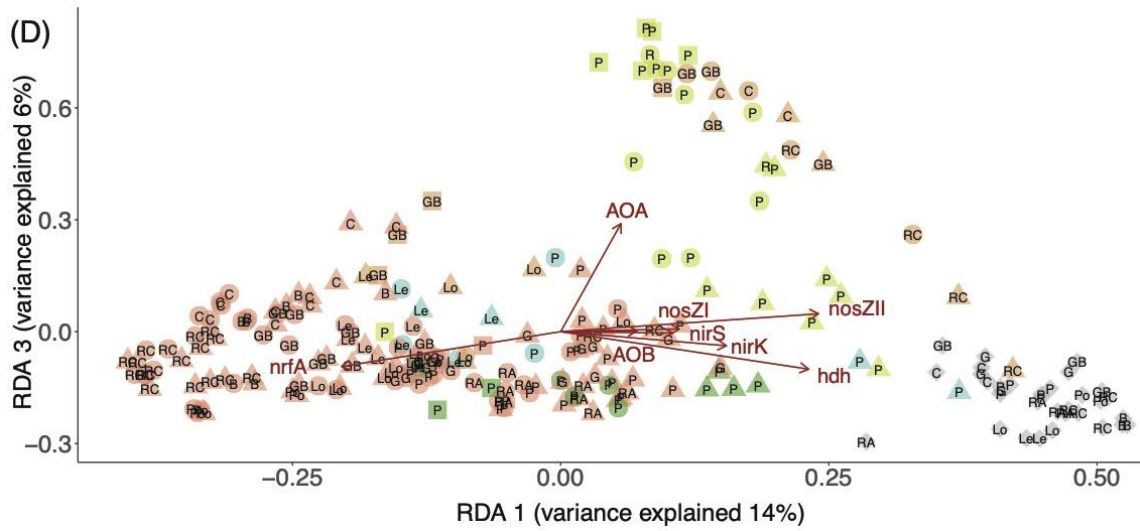
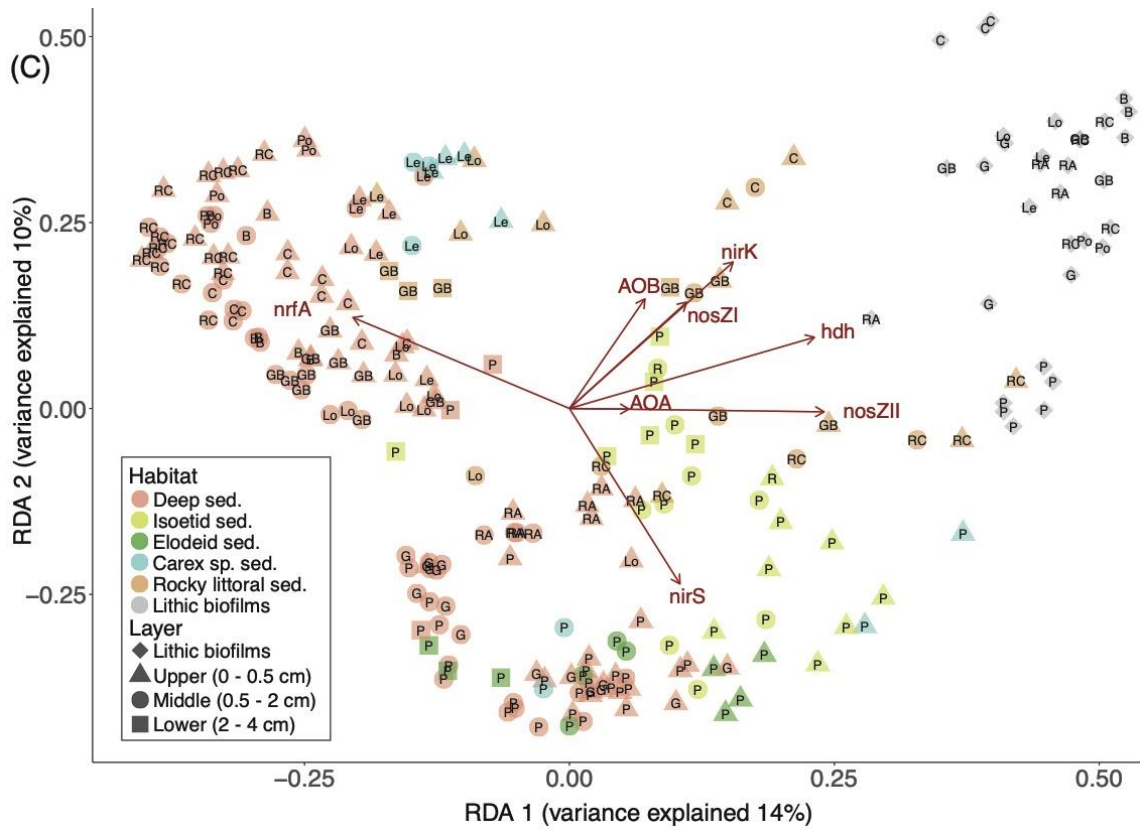


Figure S5. Mean size of sediment particles by habitat and lake (A) or gene-rich cluster (B). Note: Granulometry of lithic biofilms was not analysed. Size of sediment particles differed between the gene-rich clusters (Kruskal-Wallis test $\chi^2 = 52$, $p < 0.001$, followed by a Wilcoxon-Mann Whitney test $p < 0.05$, differences are indicated in the cluster labels by “(letter)”).

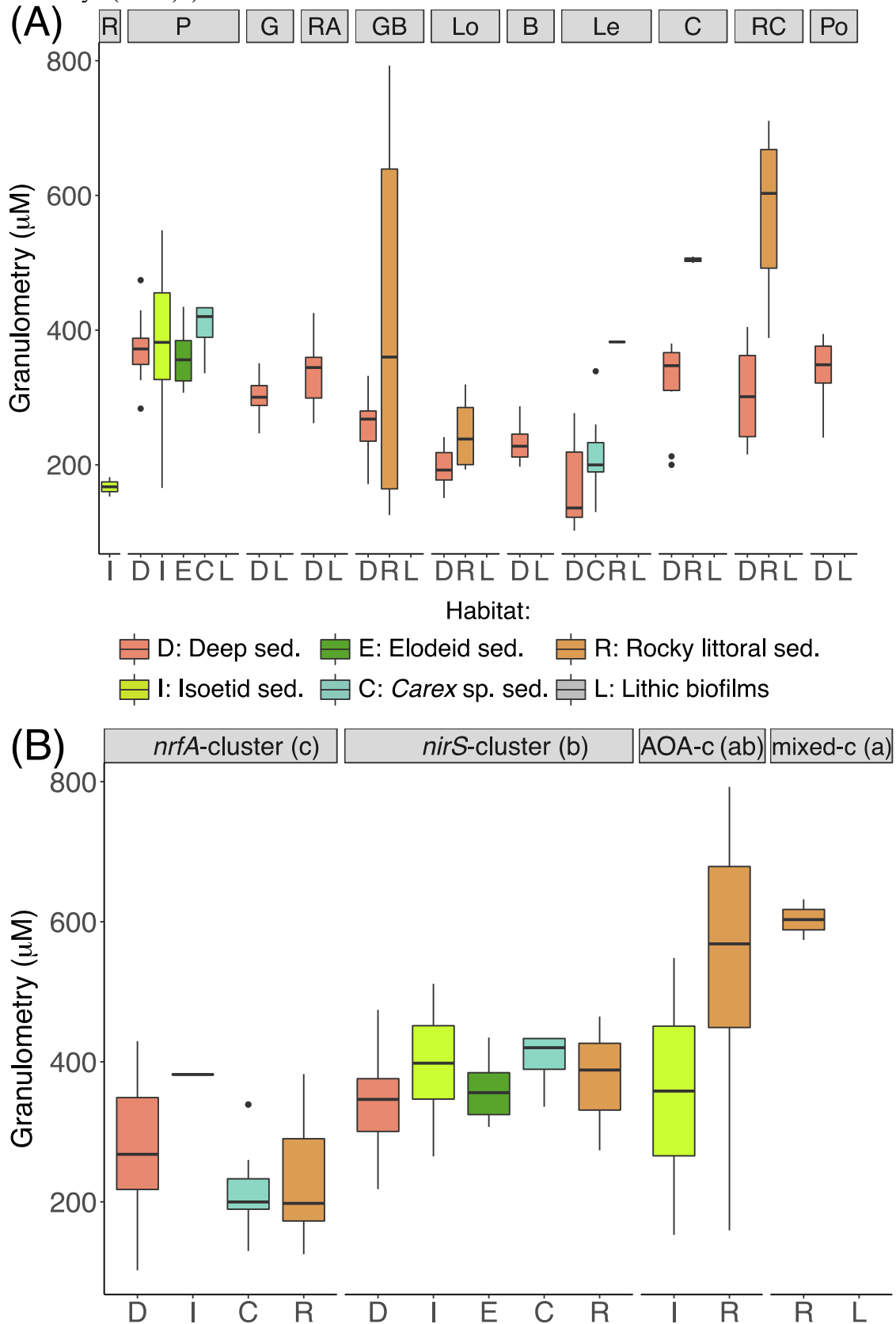
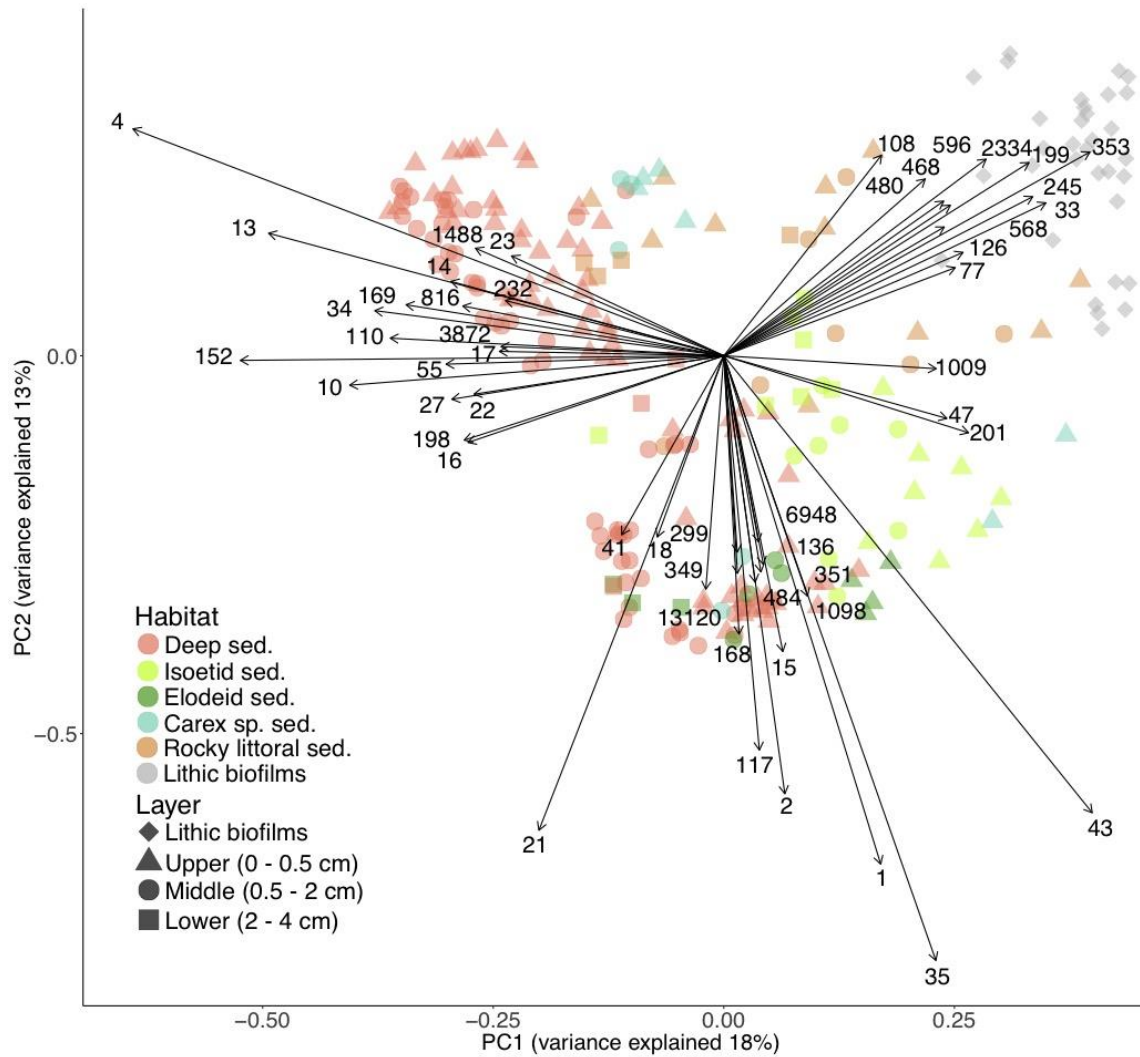


Figure S6. Unconstrained ordination of the prokaryotic community resulted from a principal component analysis based on the OTUs abundance using Hellinger distance (com-PCA). Biplot of the 1st and 2nd main gradients. Note that PCA axes sizes are proportional to the explained variation. Only the most influential OTUs for each gradient are shown (black arrows and ID, Table S6)



Video Article

Estimating Sediment Denitrification Rates Using Cores and N₂O Microsensors

Carlos Palacin-Lizarbe¹, Lluís Camarero², Jordi Catalan^{1,3}¹Campus UAB, CREAM²Center for Advanced Studies of Blanes, (CEAB, CSIC)³CSICCorrespondence to: Carlos Palacin-Lizarbe at cpalacli7@gmail.comURL: <https://www.jove.com/video/58553>DOI: [doi:10.3791/58553](https://doi.org/10.3791/58553)

Keywords: Environmental Sciences, Issue 142, Biogeochemistry, limnology, marine chemistry, water chemistry, nitrogen, nitrous oxide, voltammetry, acetylene inhibition, temperature

Date Published: 12/6/2018

Citation: Palacin-Lizarbe, C., Camarero, L., Catalan, J. Estimating Sediment Denitrification Rates Using Cores and N₂O Microsensors. *J. Vis. Exp.* (142), e58553, doi:10.3791/58553 (2018).

Abstract

Denitrification is the primary biogeochemical process removing reactive nitrogen from the biosphere. The quantitative evaluation of this process has become particularly relevant for assessing the anthropogenic-altered global nitrogen cycle and the emission of greenhouse gases (*i.e.*, N₂O). Several methods are available for measuring denitrification, but none of them are completely satisfactory. Problems with existing methods include their insufficient sensitivity, and the need to modify the substrate levels or alter the physical configuration of the process using disturbed samples. This work describes a method for estimating sediment denitrification rates that combines coring, acetylene inhibition, and microsensor measurements of the accumulated N₂O. The main advantages of this method are a low disturbance of the sediment structure and the collection of a continuous record of N₂O accumulation; these enable estimates of reliable denitrification rates with minimum values up to 0.4-1 μmol N₂O m⁻² h⁻¹. The ability to manipulate key factors is an additional advantage for obtaining experimental insights. The protocol describes procedures for collecting the cores, calibrating the sensors, performing the acetylene inhibition, measuring the N₂O accumulation, and calculating the denitrification rate. The method is appropriate for estimating denitrification rates in any aquatic system with retrievable sediment cores. If the N₂O concentration is above the detection limit of the sensor, the acetylene inhibition step can be omitted to estimate the N₂O emission instead of denitrification. We show how to estimate both actual and potential denitrification rates by increasing nitrate availability as well as the temperature dependence of the process. We illustrate the procedure using mountain lake sediments and discuss the advantages and weaknesses of the technique compared to other methods. This method can be modified for particular purposes; for instance, it can be combined with ¹⁵N tracers to assess nitrification and denitrification or field *in situ* measurements of denitrification rates.

Video Link

The video component of this article can be found at <https://www.jove.com/video/58553/>

Introduction

Anthropogenic alteration of the nitrogen cycle is one of the most challenging problems for the Earth system¹. Human activity has at least doubled the levels of reactive nitrogen available to the biosphere². However, there remain large uncertainties regarding how the global N cycle is evaluated. A few flux estimates have been quantified with less than ±20% error, and many have uncertainties of ±50% and larger³. These uncertainties indicate the need for accurate estimations of denitrification rates across ecosystems and an understanding of the underlying mechanisms of variation. Denitrification is a microbial activity through which nitrogenous oxides, mainly nitrate and nitrite, are reduced to dinitrogen gasses, N₂O and N₂⁴. The pathway is highly relevant to the biosphere availability of reactive nitrogen because it is the primary process of removal⁵. N₂O is a greenhouse gas with a warming potential nearly 300 times that of CO₂ over 100 years, and it is the current major cause of stratospheric ozone depletion due to the large quantities being emitted^{6,7}.

In the following, we present a protocol for estimating sediment denitrification rates using cores and N₂O microsensors experimentally (**Figure 1**). Denitrification rates are estimated using the acetylene inhibition method^{8,9} and measurements of the accumulation of N₂O during a defined period (**Figure 2** and **Figure 3**). We demonstrate the method by applying it to mountain lake sediments. This case study highlights the performance of the method for detecting relatively low rates with minimal disturbance to the physical structure of the sediments.

Denitrification is particularly difficult to measure¹⁰. There are several alternative approaches and methods, each with advantages and disadvantages. Drawbacks to available methods include their use of expensive resources, insufficient sensitivity, and the need to modify the substrate levels or alter the physical configuration of the process using disturbed samples¹⁰. An even more fundamental challenge to measuring N₂ is its elevated background levels in the environment¹⁰. The reduction of N₂O to N₂ is inhibited by acetylene (C₂H₂)^{8,9}. Thus, denitrification can be quantified by measuring the accumulated N₂O in the presence of C₂H₂, which is feasible due to low environmental N₂O levels.

The use of C₂H₂ to measure denitrification rates in sediments was developed about 40 years ago¹¹, and the incorporation of N₂O sensors occurred about 10 years later¹². The most widely applied acetylene-based approach is the "static core". The accumulated N₂O is measured

during an incubation period of up to 24 h after the C_2H_2 is added to the headspace of the sealed sediment core¹⁰. The method described here follows this procedure with some innovations. We add the C_2H_2 by bubbling the gas in the water phase of the core for some minutes, and we fill all the headspace with sample water before measuring the accumulation of N_2O with a microsensor. We also include a stirring system that prevents the stratification of the water without resuspending the sediment. The procedure quantifies the denitrification rate per sediment surface area (e.g., $\mu\text{mol } N_2O \text{ m}^{-2} \text{ h}^{-1}$).

The high spatial and temporal variation of denitrification presents another difficulty in its accurate quantification¹⁰. Usually, N_2O accumulation is measured sequentially by gas chromatography of headspace samples that are collected during the incubation. The method described provides improved monitoring of the temporal variation of the N_2O accumulation, because the microsensor provides a continuous signal. The microsensor multimeter is a digital microsensor amplifier (picoammeter) that interfaces with the sensor(s) and the computer (**Figure 1a**). The multimeter allows several N_2O microsensors to be used at the same time. For instance, up to four sediment cores from the same study site can be measured simultaneously to account for the spatial variability.

The core approach barely disturbs the sediment structure compared to some other methods (e.g., slurries). If the integrity of the sediments is altered, this leads to unrealistic denitrification rates¹³ that are only adequate for relative comparisons. Higher rates are always obtained with slurry methods compared to core methods¹⁴, because the latter preserves the limitation of denitrification by substrate diffusion¹⁵. Slurry measures cannot be considered representative of *in situ* rates¹⁶; they provide relative measures for comparisons made with the exact same procedure.

The method described is appropriate for estimating denitrification rates in any sediment type that can be cored. We particularly recommend the method for performing experimental manipulations of some of the driving factors. Examples are experiments that modify nitrate availability and temperature as needed for estimating the energy activation (E_a) of denitrification¹⁷ (**Figure 2**).



Figure 1: Experimental setup. (a) General experimental setup to estimate sediment denitrification rates using cores and N_2O microsensors. The incubation chamber ensures darkness and controlled-temperature (± 0.3 °C) conditions. Five intact sediment cores can be processed simultaneously using their respective N_2O sensors. (b) N_2O sensor calibration chamber. We adapted it with rubber stoppers and syringes to mix the N_2O water (see protocol step 3.4.3). There is a thermometer to control the water temperature. (c) Close-up of a sediment core sample with the sensor inserted into the central hole of the PVC cover and the joints sealed with adhesive tape. The stirrer is hanging in the water, and the electromagnet is close to it and fixed to the external part of the acrylic tube. (d) Close-up of the N_2O microsensor tip protected by a metal piece. (e) A sediment core that has just been recovered. It was sampled from a boat in a deep lake; the acrylic tube with the core is still fixed to the messenger-adapted gravity corer¹⁹. See the **Table of Materials** for all the items needed to perform this method. [Please click here to view a larger version of this figure.](#)

Protocol

1. Preparation

NOTE: Begin this on the day before the measurements are taken.

1. Assemble the measurement setup (**Figure 1a**, see the **Table of Materials**).
NOTE: To ensure a constant and high-quality power supply, the measurement device is connected to the grip via an uninterruptible power supply (UPS) that can also act as a backup. In the case of a long-duration power failure, a car battery serve as an extra power source.
2. Start the sensor's software and apply a -0.8 V voltage to **polarize the N_2O microsensors**. The signal shows a rapid descent and a subsequent rise, then it finally decreases until it is low and stable.
NOTE: The microsensor manufacturer recommends polarization at least overnight (or longer) to ensure the stability of the sensor's signal. Another recommendation is to keep the sensor polarized if measurements are planned for multiple or consecutive days¹⁸.
3. Switch on the incubation chamber and **adjust the experimental conditions** (e.g., selected light off and temperature set to be similar to that expected in the field). Place a container with deionized water inside the chamber so that water is available later at the measurement temperature for calibration of the sensors.
NOTE: This step can be done the same day of the planned measurements, before the departure to collect the cores. For standard measurements, it is advisable to use dark conditions.
4. Pack the field core collection materials: corer device, sampling tubes, rubber stoppers, polyvinyl chloride (PVC) taps, screwdriver, global positioning system (GPS) unit, thermometer, handheld sounder, wader, and inflatable boat (see the **Table of Materials**). Use a checklist to ensure that all materials are included.

2. Sediment Core Collection

1. Depending on the water depth, follow 2.1.1 or 2.1.2.
 1. **For deep water bodies**
 1. Use a **messenger-adapted gravity corer**¹⁹ from a boat or a platform (**Figure 1e**).
 2. Fix the sampling tube (acrylic, \varnothing 6.35 cm, length \geq 50 cm) to the corer with a screwdriver.
 3. Select the sampling point according to the investigation aims. Take note of the position (e.g., using GPS coordinates) and measurement depth (e.g., using a handheld sounder). If sampling from a boat, use an anchor (e.g., a bag with stones) to avoid drifting during core collection.
 4. Deploy the coring system until the sampling tube is \sim 1 m from the sediment. Use a rope with regular marks (e.g., intervals of 1 m) to control the depth position of the sampling equipment.
 5. Stabilize the sampling equipment for 60 s (e.g., to minimize the movement of the boat). This will ensure the correct sediment penetration and recovery of a scarcely disturbed sediment core.
 6. Release \sim 1 m more rope so that the sampling tube penetrates the sediment. Be aware that if the sampling tube penetrates too much, it can disturb the water/sediment interface.
 7. Release the messenger while trying to keep tension in the rope so that the corer remains fixed and in a vertical position. When the messenger impacts the corer, a small difference can be felt in the tension of the rope. At that time, close the corer to generate the vacuum that allows for recovery of the sediment core.
 8. Recover the corer by pulling the rope constantly and gently.
 9. Once the core is close to the surface but still entirely submerged (including the rubber part of the corer that ensures the vacuum), place a rubber stopper at the bottom of the sampling tube. Inspect the water/sediment interface; it should be clear and not visibly disturbed (**Figure 1e**). If this is not the case, discard the core, clean the tube, and repeat steps 2.1.1.4-9.
 10. Uplift the entire coring system from the water. Release the sampling tube from the corer and place a PVC cover on the top. Seal it with adhesive tape. Avoid the formation of air space.
 2. **For littoral habitats and shallow water bodies**
 1. Dress in a **wader** for sampling in very shallow waters (<0.6 m).
 2. Use **snorkeling or scuba gear** for deeper sampling (up to 3 m).
 3. Select the sampling point according to the investigation aims. Take note of the position (e.g., GPS coordinates). Manually, insert the sampling tube (e.g., acrylic, \varnothing 6.35 cm) into the sediment.
 4. Place a rubber stopper in the top side of the sampling tube to obtain a vacuum.
 5. Remove the core from the sediment and quickly introduce another rubber stopper at the tube bottom.
NOTE: It is necessary to work with the tube underwater at all times; at very shallow sites, we recommend shortening the tube down to 20 cm. Sometimes the sediment has a high water content and drains when the tube is removed from the sediment bed. In this case, it is necessary to introduce the bottom stopper without uplifting the core outside the sediment. To do this, manually immerse the stopper in the sediment around the tube and place it carefully to close the bottom of the tube.
 6. Out of the water, substitute the topside rubber stopper with a PVC cover and seal the junction with adhesive tape.
2. Protect the core during its transfer to the laboratory by minimizing rotations and shaking.

3. Calibration of the Nitrous Oxide (N_2O) Microsensors

1. Using the computer (strip chart, sensor software), check that the sensor's signal is stable and low (<20 mV).
2. Create a new file (e.g., with the date and the sampling site (130903_Redon_Lake)) to record the calibration values and sensor signals.

NOTE: The sensor signals are sensitive to temperature (**Figure 4**). Use the **same temperature** for the measurements and the sensor calibration. The sensor responds linearly between 0%-2.5% N₂O²⁰. Therefore, a two-point calibration is sufficient¹⁸.

- For the calibration **value with zero nitrous oxide**, read the sensor signal keeping the sensor tip submerged in N₂O-free water (deionized).
- Calibrate with N₂O water at the desired concentration.

NOTE: Prepare water with a defined N₂O concentration, which will slightly exceed the maximum concentration expected during incubation. We use ~25 μM N₂O as the calibration value. Be aware of not exceeding the maximum sensor range concentration of 500 N₂O μM.

- Obtain N₂O-saturated water by bubbling N₂O in deionized water for a few minutes.
NOTE: The N₂O water solubility depends on temperature and salinity²¹; see the table in the appendix of the sensor manual¹⁸.
- Dilute the N₂O saturated water by adding a certain volume of saturated N₂O water to a volume of deionized water. For example, at 20 °C, add 0.3 mL of saturated N₂O water, which has a concentration of 28.7 mM N₂O, to a total of 375 mL of water to obtain a 22.9 μM N₂O concentration. Note that 375 mL is the total volume of the calibration chamber (**Figure 1b**).
- After gently mixing the N₂O saturated water with deionized water in the calibration vessel to dilute it to the desired concentration, read the sensor signal when it is constant. This reading is the **calibration value with X μM N₂O water**. When mixing the solution, be careful not to generate bubbles, as this would eliminate N₂O from the calibration solution.
NOTE: Be aware that the N₂O in the water will slowly escape into the air; thus, the prepared calibration solution can only be used for a few minutes.

4. Core Preparation and Acetylene Inhibition

- Change the PVC cover located at the top of each sediment core by another cover with a hole in the center and a hanging magnetic stirrer. Re-seal the junction with adhesive tape.
- Reduce the water phase of each sample to an approximate height of 12 cm (volume ≈ 380 mL). For this, first insert a silicone tube in the central hole. Then, put the sediment core in a cylinder and push the bottom stopper to create pressure. The stopper and sediment sample go up, and the excess water passes through the tube. Collect the water in a recipient vessel.
NOTE: Samples with coarse granularity can be problematic during this step. Sediment particles placed between the stopper and the tube can deform the stopper and open a hole through which air bubbles can pass and disturb the sample. To avoid this problem, put the cylinder in the center of the bottom stopper and try to push with a constant force. The joint between the silicone tube used to evacuate the excess water and the PVC cover consists of a solid part (e.g., a 5 mL pipette tip without its narrowest end) inserted in the silicone tube.
- Perform the acetylene inhibition by **bubbling with acetylene gas** in the water phase of the core for approximately 10 min. Avoid resuspending the sediment.
NOTE: As a possible modification of the method, add a substrate (nitrate) through a concentrated liquid medium before bubbling acetylene for potential denitrification measurements (e.g., as in **Figure 3b, c**).

5. Denitrification (N₂O accumulation measure)

- Fill all the air space in the sample with the previous leftover water. Place the sensor in the sediment core through the central hole of the topside PVC cover. The tip of the sensor should be located in the water phase above the stirrer (**Figure 1c**).
NOTE: All the joints of the acrylic sampling tube must be sealed to avoid gas and water leaks during the measurement (**Figure 1a, c**). In the bottom part of the tube, the rubber stopper is sufficient for this. Sealing the topside part is more difficult. The PVC cover must be tuned. It must be heated with a torch; then, when the material becomes flexible but is not scorched, the cover is placed in the tube so that its shape can be molded. After cooling, the cover needs more modifications (with the exception of the cover used to transport the samples to the laboratory in steps 2.1.1.10 or 2.1.2.6). The central hole where the sensor is inserted must be drilled. The stirrer can be held with a fishing line, which in turn is adhered with glue to the inside of the cover so that the stirrer hangs on the fishing line in the water (**Figure 1c**). Also, all the joints (PVC cover tube and PVC cover sensor) are sealed with adhesive tape. Place elastic adhesive tape to adjust the diameter of the sensor in order to seal the contact surface between the central hole of the PVC cover and the sensor (**Figure 1c**).
- Switch on the electromagnetic pulse circuit that is part of the stirring system.
NOTE: The stirring system prevents the stratification of the water phase without disturbing (resuspending) the sediment. The stirring system consists of a circuit that switches on/off the electromagnet that attracts/releases the magnetic stirrer (see the **Table of Materials** for a detailed description).
- Move the electromagnet around the external part of the acrylic tube until the stirrer moves continuously, and then fix it in place using adhesive tape (**Figure 1c**).
- Close the incubation chamber to ensure a constant temperature (e.g., variation of ±0.3 °C).
- Press the record button (sensor software) to **start recording the sensor signal**. Readings are typically recorded every 5 min.
- Press the stop button at the **end of the measurement period**.

6. Final Measurement Steps

- Wait at least ~10 min with the sensor's tip submerged in free-N₂O water (deionized) before reading the signal of the zero N₂O calibration measure.
- Perform a **final sensor calibration**. For this, repeat the sensor calibration, following Section 3 but starting with step 3.3.
- Save the file (sensor software).

7. Denitrification Rate Calculations

- Start with the tabulated output file generated by the sensor software that contains the record of the sensor's signal in mV and μM N₂O, and the calibration data.

- Plot the sensor signal against time to visualize the N_2O accumulation trend (e.g., **Figure 2a**).
- Use only the time range with a **linear accumulation**, excluding the initial acclimation period of the sample and a possible final saturation due to substrate limitation (e.g., **Figure 2b**). Create a linear model of the sensor signal (μM) over time (h).
 Note: The slope is the denitrification rate ($\mu M N_2O \text{ core}^{-1} h^{-1}$), which, if divided by the area of the core (πr^2), transforms into the rate in $\mu M N_2O m^{-2} h^{-1}$, and when multiplied by the water volume ($\pi r^2 h$, where h is the height of the water phase and r is the inner radius of the acrylic tube, in this case 0.12 m and 0.03175 m, respectively) transforms into the rate in $\mu mol N_2O m^{-2} h^{-1}$.

Representative Results

A total of 468 denitrification rates were estimated using the protocol above in sediments from Pyrenean mountain lakes over the period 2013-2014. We show some of these results to illustrate the procedure (**Figure 2** and **Figure 3**). In general, the linear model between the N_2O concentration and time has good correlation ($R^2 \geq 0.9$). The slope of the relationship provides an estimate of the denitrification rate (step 7.3; e.g., **Figure 2d**). If the denitrification activity is very low, the sensor's electronic noise becomes more important and the goodness of fit declines (e.g., sensors 4 and 5 in **Figure 2b** and **Figure 3a**). Although the baseline detection limit of N_2O is $\sim 0.1 \mu M$ in water²², which is an intermediate value concerning alternative methods²³, the possibility of accumulating thousands of continuous measurements to filter the noise permits estimates at relatively low denitrification rates, up to $\sim 1 \mu mol N_2O m^{-2} h^{-1}$ (**Figure 2** and **Figure 3**). Lower rates (i.e., $\sim 0.4 \mu mol N_2O m^{-2} h^{-1}$) can be estimated by narrowing the water phase of the core sample to a height of 8 cm (see protocol step 4.2).

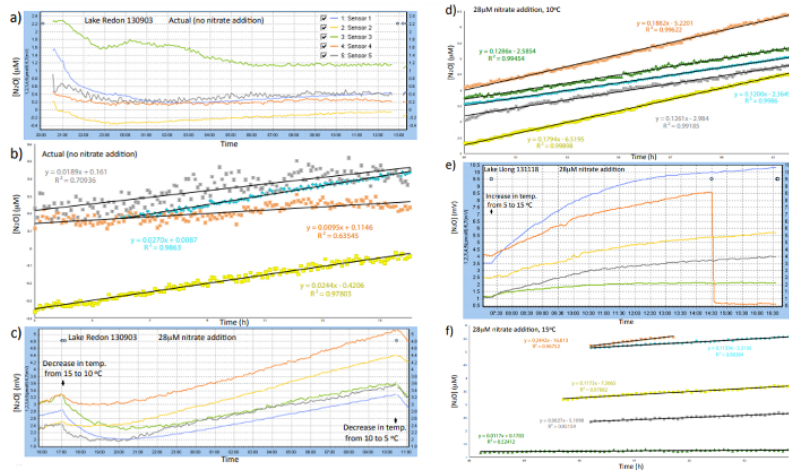


Figure 2: Denitrification rate calculations in a temperature dependence experiment. Actual (a and b) and potential denitrification measurements (c-f) are shown. When the temperature of the measurement is decreased (c), at first the sample cools and the sensor signal, which is temperature dependent, declines. (a) A similar event occurs at the start of the incubation in the actual denitrification measurement; the warmer laboratory environment with respect to the incubation conditions produces a cooling of the sample, again accompanied by a decline in the sensor signal. (e) When the temperature is increased, at first the samples warm and the sensor signal increases exponentially instead of linearly. When the samples reach a constant temperature, the sensor signal increases linearly as usual. In all cases, it is possible to calculate the denitrification rates just by using the period of linear N_2O accumulation (b, d, and f). (b) Inactive sample 3 is not shown. [Please click here to view a larger version of this figure.](#)

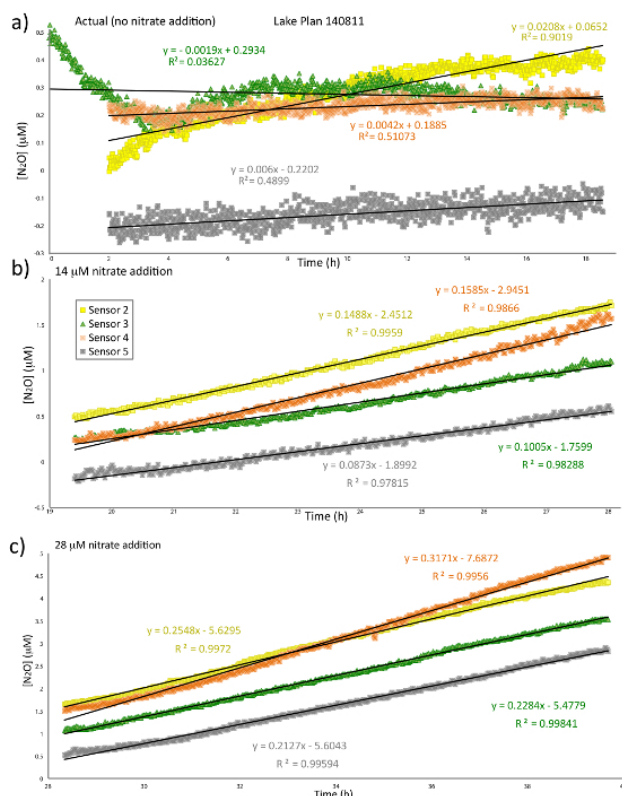


Figure 3: Examples of denitrification rate calculations. Actual (a) and potential (b and c) denitrification rates were estimated. We only used the time range with a linear N_2O accumulation to calculate the denitrification rate (slope of the linear model). However, in (a), for educational purposes, we show all the measurements (models) with more and less success; we would discard sample 3 due to the high instability of the sensor and sample 2 due to saturation in the N_2O accumulation. (a) Samples 4 and 5 with rates of 0.5 and 0.7 $\mu\text{mol } N_2O \text{ m}^{-2} \text{ h}^{-1}$, respectively, are cases of measurements near the detection limit of the method. [Please click here to view a larger version of this figure.](#)

Discussion

The main advantages of the described method are the use of minimally disturbed sediment core samples and the continuous recording of the N_2O accumulation. These allow estimation of relatively low denitrification rates that are likely similar to those occurring *in situ*. Nonetheless, some aspects concerning the coring, sensor performance, and potential improvements are discussed.

An apparently simple but critical step of the method is good core recovery. The sediment/water interface must satisfy three criteria: (i) no modification in its chemical or constituent composition, (ii) no alteration in the water content or void ratio, and (iii) no structure perturbation²⁴. The fewer disturbances suffered by the sample during the entire protocol, the more realistic and closer to *in situ* conditions will the measured denitrification rate be. There are several devices/techniques for the sediment core collection²⁵, and their selection depends on the water depth. We use a messenger-adapted gravity corer¹⁹ for deep samples (Figure 1e) because it is a reasonably light-weight device and can rapidly recover short cores²⁵ (a core sediment of ≥ 10 cm length is more than enough to encompass the oxic and denitrifying layers in the sediments^{26,27,28}). In coring jargon, "feel" is often referred to as the ability to know the location of the corer (whether it is still in the water column or already in the sediment) and whether it is open or closed²⁵. For intermediate water depths (5-50 m), usually there are no difficulties with feeling. A loss of feeling occurs in deeper water (>50 m) because the movements of the water column may mask the location of the corer²⁵. Feeling may also be lost in shallow water (<3 m) due to lateral drift and wave action²⁵; this is why we use a different method in shallow water, either direct manual coring by scuba diving or dressing in a wader. With this system, the person performing the sampling can see the sediment and choose the exact place before coring; this allows, e.g., the sampling of a sediment core that contains a macrophyte. After sampling, the researcher must continue to work carefully to minimally disturb the sediment core sample during the rest of the protocol, especially when performing acetylene inhibition by bubbling.

Some details must be considered when using N_2O microsensors. The sensor software provides a continuous visualization (strip chart) of the sensor signal (background frequency of 1000 Hz)²⁹. These raw data and the strip chart (e.g., Figure 2a) can be saved. It is necessary to check the correct behavior of the sensor after its polarization (e.g., when returning from field collection before step 4). In particular, a low (<20 mV) and constant base signal is expected when it is submerged in N_2O -free water. Recalibrate the sensor shortly (~2 h) after starting its use; if it has already been used for some days, the interval can be extended (~24 h)¹⁸. To minimize recalibrations, keep the sensor polarized unless it is not used for several days¹⁸. Over time, a change in the sensor signal may occur, up to 50% in months, which is due to a different permeability of its membrane¹⁸. The lower the electronic interference in the laboratory, the more constant and stable will be the sensor signal. In that sense,

using a UPS improves the quality of the electrical energy that reaches the measurement device by filtering the voltage fluctuations. The sampling interval, selected in the Logger tab, is different from the background frequency. Each registered point is generated from the average of many measurements. The sampling interval (up to 10 s) indicates the frequency with which a data point is recorded. The number of measurements per unit of time used in the average is defined by the background frequency²⁹. For instance, if we set a sampling frequency of 5 s and a background frequency of 500 measurements per second, then the data points are recorded every 5 s and the average of the 500 samples per second is measured during the previous 5 s. We record the sensor signal every 5 min (sampling interval) and set the background frequency to 1000 measurements per second. The study system must be known to select the correct sampling interval without "averaging" expected fluctuations. In highly active systems, short sampling intervals are recommended, while longer intervals allow optimizing the computer's memory²⁹. Some possible interfering substances (H_2S , NO , and CO_2) can affect the N_2O sensor's signal²². The sensor is calibrated with deionized water, but the samples can contain interfering substances and modify the sensor's reference signal. This situation could explain why negative values appear in samples 2 and 5 in **Figure 2b** and **Figure 3a**, respectively. However, when the objective is to estimate the denitrification rate, the exact level of N_2O is not the key parameter. What is key is the slope of the linear model (evidencing a linear accumulation of N_2O). Finally, it is necessary to work with a fixed temperature because the response of the N_2O sensor changes with temperature (**Figure 4**).

Simple modifications or additions to the protocol also enable (i) characterization of the environmental conditions controlling the measured denitrification rates, (ii) estimation of the potential denitrification rates by simulating the response to a driving gradient (e.g., nitrate), and (iii) estimation of the sediment N_2O emission rates by skipping the C_2H_2 inhibition. Depending on the study aims, several complementary measurements can be made: (i) just after recovering the core, *in situ* conditions, e.g., temperature; (ii) before the measurement, samples of the water phase, e.g., $[NO_3^-]$; and (iii) after the measurement, extrusions and slices of the core at different resolutions (mm-cm)^{25,30}, following the procedures explained by P. T. Schwing *et al.*³⁰.

To measure the potential denitrification rates, add nitrate to the water-phase of the core (e.g., **Figure 2** and **Figure 3**) as described in C. Palacin-Lizarbe, L. Camarero and J. Catalan¹⁷. If doing so, add the nitrate before the C_2H_2 inhibition (step 4.3). Also, if nitrate is added, it is advisable to also add carbon (C; e.g., acetate) and phosphorus (P) to maintain the *in situ* stoichiometric proportions of C, N, and P (e.g., in the surface sediment). This will prevent the limitation of denitrification by these elements^{31,32}, and will also keep the C/N ratio that can influence the dominance of the nitrate consumption process (i.e., denitrification versus dissimilatory nitrate reduction to ammonium (DNRA))⁴. Anoxia can be fixed by bubbling an N_2 - CO_2 mixture for a few minutes after the nitrate addition, to prevent oxygen interference with denitrification; however, note that this leads to a blockage of nitrification. To calculate sediment N_2O emission rates, omit the C_2H_2 inhibition (step 4.3). However, keep in mind that, as far as it is currently known in aquatic ecosystems, N_2O emissions are proportionally low compared to N_2 emissions (0%-4.3%)³³, so it is possible that the accumulated N_2O will be below the detection limit. If this is the case, an option is to add nitrate to increase the emitted N_2O , calculating potential N_2O emissions.

The main weakness of the method is the inhibition of nitrification by C_2H_2 ^{10,34}. During the incubation, this inhibition of nitrification and the incomplete inhibition of N_2O reduction may become apparent, as both are very time dependent. For instance, the starting N_2O accumulation rate must reveal the real denitrification rate and progressively decay as the nitrate availability drops and N_2O diffuses into the nitrate free zone, where it is reduced³⁵. Therefore, an estimated denitrification rate can be considered valid only if the readings show a linear accumulation of N_2O ¹⁰.

The method described estimates a denitrification rate per area that integrates the entire sediment activity. In this respect, there is some uncertainty about the radius of action of the acetylene inhibition when bubbling the gas in the aqueous phase of the sample. It is assumed that, at least, inhibition of the surficial layer of the sediment occurs, which is the one with the highest denitrification rates^{26,27}.

Possible improvements to this method are its combined use with ^{15}N tracers and modifications that could allow the measurement of denitrification *in situ*. ^{15}N tracer methods can be used to determine the proportion of nitrification-denitrification coupling occurring in the samples³⁶, and it can also account for other N flux processes besides denitrification (e.g., anammox and dissimilatory nitrate reduction to ammonium (DNRA))^{13,37}. However, these methods have the drawback of changing the substrate concentration¹⁰. A. Behrendt, D. de Beer and P. Stief²⁶ use a method combining N_2O microsensors, C_2H_2 inhibition, and ^{15}N tracers to analyze the vertical activity distribution of dissimilatory nitrate reduction processes (denitrification and DNRA) in sediments. They made vertical profiles in the sediment by penetrating the sediment with the sensors. The main difficulty in measuring denitrification *in situ* is the ability to handle a nonconstant temperature environment. It is necessary to record the N_2O accumulation and temperature simultaneously and then correct the N_2O sensor's signal by the temperature dependence during the denitrification rate calculations. This correction requires a previous analysis of the temperature dependence of the N_2O signal for each sensor. The sensors are handmade, and each one responds differently to temperature (e.g., sensor 1 shows a higher temperature dependence than the others in **Figure 2c, e**).

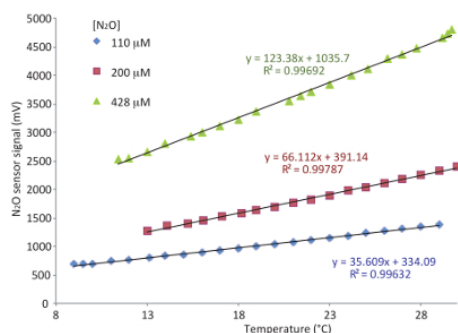


Figure 4: Temperature dependence of the N₂O microsensor response. The different slopes of the linear model of the sensor signal versus the temperature at each N₂O concentration shows the temperature effect on the sensor's signal. [Please click here to view a larger version of this figure.](#)

Disclosures

The authors have nothing to disclose.

Acknowledgements

The Spanish Government provided funds through the Ministerio de Educación as a predoctoral fellowship to C.P.-L. (FPU12-00644) and research grants of the Ministerio de Economía y Competitividad: NitroPir (CGL2010-19737), Lacus (CGL2013-45348-P), Transfer (CGL2016-80124-C2-1-P). The REPLIM project (INRE - INTERREG Programme. EUUN - European Union. EFA056/15) supported the final writing of the protocol.

References

1. Rockstrom, J. *et al.* A safe operating space for humanity. *Nature*. **461** (7263), 472-475, (2009).
2. Erisman, J. W., Galloway, J., Seitzinger, S., Bleeker, A., & Butterbach-Bahl, K. Reactive nitrogen in the environment and its effect on climate change. *Current Opinion in Environmental Sustainability*. **3** (5), 281-290, (2011).
3. Gruber, N., & Galloway, J. N. An Earth-system perspective of the global nitrogen cycle. *Nature*. **451** (7176), 293-296, (2008).
4. Tiedje, J. M. in *Environmental Microbiology of Anaerobes*. Vol. 717 (ed A J B Zehnder) Ch. 4. Ecology of denitrification and dissimilatory nitrate reduction to ammonium, 179-244, John Wiley and Sons, (1988).
5. Seitzinger, S. *et al.* Denitrification across landscapes and waterscapes: A synthesis. *Ecological Applications*. **16** (6), 2064-2090, (2006).
6. *Climate Change 2013: The Physical Science Basis*. Contribution of Working Group I to the fifth assessment report of the intergovernmental panel on climate change. Cambridge University Press, (2013).
7. Ravishankara, A. R., Daniel, J. S., & Portmann, R. W. Nitrous Oxide (N₂O): The Dominant Ozone-Depleting Substance Emitted in the 21st Century. *Science*. **326** (5949), 123-125, (2009).
8. Balderston, W. L., Sherr, B., & Payne, W. Blockage by acetylene of nitrous oxide reduction in *Pseudomonas perfectomarinus*. *Applied and Environmental Microbiology*. **31** (4), 504-508, (1976).
9. Yoshinari, T., & Knowles, R. Acetylene inhibition of nitrous-oxide reduction by denitrifying bacteria. *Biochemical and Biophysical Research Communications*. **69** (3), 705-710, (1976).
10. Groffman, P. M. *et al.* Methods for measuring denitrification: Diverse approaches to a difficult problem. *Ecological Applications*. **16** (6), 2091-2122, (2006).
11. Sorensen, J. Denitrification rates in a marine sediment as measured by the acetylene inhibition technique. *Applied and Environmental Microbiology*. **36** (1), 139-143, (1978).
12. Revsbech, N. P., Nielsen, L. P., Christensen, P. B., & Sorensen, J. Combined oxygen and nitrous-oxide microsensor for denitrification studies. *Applied and Environmental Microbiology*. **54** (9), 2245-2249, (1988).
13. Annual pattern of denitrification and nitrate ammonification in estuarine sediment. *Applied and Environmental Microbiology*. **55** (7), 1841-1847, (1989).
14. Laverman, A. M., Van Cappellen, P., van Rotterdam-Los, D., Pallud, C., & Abell, J. Potential rates and pathways of microbial nitrate reduction in coastal sediments. *FEMS Microbiology Ecology*. **58** (2), 179-192, (2006).
15. Ambus, P. Control of denitrification enzyme-activity in a streamside soil. *FEMS Microbiology Ecology*. **102** (3-4), 225-234, (1993).
16. Christensen, P. B., Rysgaard, S., Sloth, N. P., Dalsgaard, T., & Schwærter, S. Sediment mineralization, nutrient fluxes, denitrification and dissimilatory nitrate reduction to ammonium in an estuarine fjord with sea cage trout farms. *Aquatic Microbial Ecology*. **21** (1), 73-84, (2000).
17. Palacin-Lizarbe, C., Camarero, L., & Catalan, J. Denitrification Temperature Dependence in Remote, Cold, and N-Poor Lake Sediments. *Water Resources Research*. **54** (2), 1161-1173, (2018).
18. *Nitrous Oxide sensor user manual*. UNISENSE A/S, (2011).
19. Glew, J. Miniature gravity corer for recovering short sediment cores. *Journal of Paleolimnology*. **5** (3), 285-287, (1991).
20. Andersen, K., Kjaer, T., & Revsbech, N. P. An oxygen insensitive microsensor for nitrous oxide. *Sensors and Actuators B-Chemical*. **81** (1), 42-48, (2001).
21. Weiss, R. F., & Price, B. A. Nitrous oxide solubility in water and seawater. *Marine Chemistry*. **8** (4), 347-359, (1980).
22. *Nitrous Oxide Microsensors Specifications*. UNISENSE A/S, (2018).

23. Koike, I. in *Denitrification in Soil and Sediment*. 10.1007/978-1-4757-9969-9 *F.E.M.S. Symposium Series*. (ed N P Revsbech, Sørensen, J) Ch. 18. Measurement of sediment denitrification using 15-N tracer method, 291-300, Springer US, (1990).
24. Hvorslev, M. J. *Subsurface Exploration and Sampling of Soils for Civil Engineering Purposes*. 521 American Society of Civil Engineers, Waterways Experiment Station, Corps of Engineers, U.S. Army, (1949).
25. Glew, J. R., Smol, J. P., & Last, W. M. in *Tracking Environmental Change Using Lake Sediments: Basin Analysis, Coring, and Chronological Techniques*. Vol. 1 eds William M. Last & John P. Smol) Ch. 5. Sediment Core Collection and Extrusion, 73-105 Springer Netherlands, (2001).
26. Behrendt, A., de Beer, D., & Stief, P. Vertical activity distribution of dissimilatory nitrate reduction in coastal marine sediments. *Biogeosciences*. **10** (11), 7509-7523, (2013).
27. Laverman, A. M., Meile, C., Van Cappellen, P., & Wieringa, E. B. A. Vertical distribution of denitrification in an estuarine sediment: Integrating sediment flowthrough reactor experiments and microprofiling via reactive transport modeling. *Applied and Environmental Microbiology*. **73** (1), 40-47, (2007).
28. Melton, E. D., Stief, P., Behrens, S., Kappler, A., & Schmidt, C. High spatial resolution of distribution and interconnections between Fe- and N-redox processes in profundal lake sediments. *Environmental Microbiology*. **16** (10), 3287-3303, (2014).
29. *SensorTrace BASIC 3.0 user manual*. UNISENSE A/S, (2010).
30. Schwing, P. T. et al. Sediment Core Extrusion Method at Millimeter Resolution Using a Calibrated, Threaded-rod. *Journal of visualized experiments*. 10.3791/54363 (114), 54363, (2016).
31. Bernhardt, E. S. Ecology. Cleaner lakes are dirtier lakes. *Science*. **342** (6155), 205-206, (2013).
32. Finlay, J. C., Small, G. E., & Sterner, R. W. Human influences on nitrogen removal in lakes. *Science*. **342** (6155), 247-250, (2013).
33. Seitzinger, S. P. Denitrification in fresh-water and coastal marine ecosystems- ecological and geochemical significance. *Limnology and Oceanography*. **33** (4), 702-724, (1988).
34. Seitzinger, S. P., Nielsen, L. P., Caffrey, J., & Christensen, P. B. Denitrification measurements in aquatic sediments - a comparison of 3 methods. *Biogeochemistry*. **23** (3), 147-167, (1993).
35. Christensen, P. B., Nielsen, L. P., Revsbech, N. P., & Sorensen, J. Microzonation of denitrification activity in stream sediments as studied with a combined oxygen and nitrous-oxide microsensor. *Applied and Environmental Microbiology*. **55** (5), 1234-1241, (1989).
36. Peter, N. L. Denitrification in sediment determined from nitrogen isotope pairing. *FEMS Microbiology Ecology*. **9** (4), 357-361, (1992).
37. Risgaard-Petersen, N., Nielsen, L. P., Rysgaard, S., Dalsgaard, T., & Meyer, R. L. Application of the isotope pairing technique in sediments where anammox and denitrification coexist. *Limnology and Oceanography-Methods*. **1** 63-73, (2003).

Materials List for:

Estimating Sediment Denitrification Rates Using Cores and N₂O Microsensors

Carlos Palacin-Lizarbe¹, Lluís Camarero², Jordi Catalan^{1,3}

¹Campus UAB, CREAF

²Center for Advanced Studies of Blanes, (CEAB, CSIC)

³CSIC

Correspondence to: Carlos Palacin-Lizarbe at cpalaci7@gmail.com

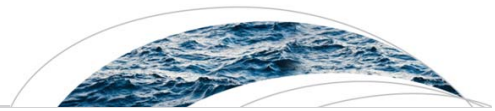
URL: <https://www.jove.com/video/58553>

DOI: [doi:10.3791/58553](https://doi.org/10.3791/58553)

Materials

Name	Company	Catalog Number	Comments
Messenger-adapted gravity corer	-	-	Reference in the manuscript. Made by Glew, J.
Sampling tube	-	-	Acrylic. Dimensions: 100 cm (h) × 6.35 cm (d) × 6.50 cm (D). Sharpen the edge of the sampling tube that penetrates into the sediment to minimize the disturbance in the recovered sediment core sample.
Handheld sounder	Plastimo	38074	Echotest II Depth Sounder.
Rubber stopper	VWR	DENE1012114	With two holes, used to mix the N ₂ O-water in the calibration chamber. Dimensions: 20 mm (h) × 14 mm (d) × 18 mm (D) (3 mm hole (D)).
Rubber stopper	VWR	217-0125	To seal the bottom part of the methacrylate tube and to sample in shallow water bodies. Dimensions: 45 mm (h) × 56 mm (d) × 65 mm (D).
Rubber stopper	VWR	217-0126	Place the rubber stopper in the top side of the sampling tube to obtain a vacuum for sampling in littoral zones and shallow water bodies. Dimensions: 50 mm (h) × 60 mm (d) × 70 mm (D).
PVC cover	-	-	To seal the top side part of the acrylic tube. Dimensions: 45 mm (h) × 56 mm (d) × 65 mm (D). Dimensions: 65 mm (D).
Adhesive tape	-	-	Waterproof. To ensure all joints (PVC cover sampling tube and PVC cover sensor) and to avoid water leaks.
Thermometer	-	-	Portable and waterproof, to measure the temperature in the water overlying the sediment just after sampling the cores.
GPS	-	-	To save the location of a new sampling site or to arrive at a previous site.
Wader	-	-	For littoral or shallow site samplings.

Boat	-	-	An inflatable boat is the best option for its lightness if the sampling site is not accessible by car.
Rope	-	-	Rope with marks showing its length (e.g., marked with a color code to distinguish each meter).
N ₂ O gas bottle and pressure reducer	Abelló Linde	32768-100	Gas bottle reference.
C ₂ H ₂ gas bottle and pressure reducer	Abelló Linde	32468-100	Gas bottle reference.
Tube used to evacuate the excess of water	-	-	Consists of a solid part (e.g., a 5 ml pipette tip without its narrowest end) inserted in a silicone tube.
Nitrous Oxide Minisensor w/ Cap	Unisense	N2O-R	We use 4 sensors at a time.
Microsensor multimeter 4 Ch. 4 pA channels	Unisense	Multimeter	Picoammeter logged to a laptop. The standard device allows for 2 sensor picoammeter connections (e.g., N ₂ O sensor), one pH/mV and a thermometer. We ordered a device with four picoammeter connections, allowing the use of 4 N ₂ O sensors simultaneously.
SensorTrace Basic 3.0 Windows software	Unisense		Sensor data acquisition software.
Calibration Chamber incl. pump	Unisense	CAL300	Calibration chamber. We tuned it with rubber stoppers and syringes to mix the N ₂ O-water without making bubbles.
Incubation chamber	Ibercex	E-600-BV	Indispensable equipment for working at a constant temperature (± 0.3 °C). It also allows control of the photoperiod.
Electric stirrer	-	-	Part of the stirring system. It hangs in the water, overlying the sediment subject, by a fishing line that is hooked to the PVC cover.
Electromagnet	-	-	Part of the stirring system. It is fixed to the outside of the acrylic tube, approximately at the same level as the stirrer. It is activated episodically (ca. 1 on-off per s) by a circuit, attracting the stirrer when it is on and releasing it when it is off, thereby generating the movement that agitates the water.
Electromagnetic pulse circuit	-	-	Part of the stirring system. It is connected by wires to the electromagnet and sends pulses of current that turn the electromagnet on and off.
Uninterruptible power supply (UPS)	-	-	It improves the quality of the electrical energy that reaches the measurement device, filtering the highs and low of the voltage, thereby ensuring a more constant and stable N ₂ O sensor signal.



RESEARCH ARTICLE

10.1002/2017WR021680

Key Points:

- Denitrification rates in mountain lakes are both nitrate and temperature limited
- The apparent activation energy (E_a , kJ mol^{-1}) for denitrification depends on nitrate (μM) as $E_a = 46 + 419 [\text{NO}_3^-]^{-1}$
- The impact of nitrogen emission reductions on the adjustment of the nitrogen cycle may be enhanced by climate warming

Supporting Information:

- Supporting Information S1

Correspondence to:

C. Palacin-Lizarbe,
cpalaci7@gmail.com

Citation:

Palacin-Lizarbe, C., Camarero, L., & Catalan, J. (2018). Denitrification temperature dependence in remote, cold, and N-poor lake sediments. *Water Resources Research*, 54, 1161–1173. <https://doi.org/10.1002/2017WR021680>

Received 9 AUG 2017

Accepted 3 FEB 2018

Accepted article online 8 FEB 2018

Published online 22 FEB 2018

Denitrification Temperature Dependence in Remote, Cold, and N-Poor Lake Sediments

Carlos Palacin-Lizarbe^{1,2} , Lluís Camarero² , and Jordi Catalan^{1,3} 

¹CREAF, Campus UAB, Edifici C, Cerdanyola del Vallès, Spain, ²Center for Advanced Studies of Blanes, (CEAB-CSIC), Blanes, Girona, Spain, ³CSIC, Cerdanyola del Vallès, Spain

Abstract The reservoir size and pathway rates of the nitrogen (N) cycle have been deeply modified by the human enhancement of N fixation, atmospheric emissions, and climate warming. Denitrification (DEN) transforms nitrate into nitrogenous gas and thus removes reactive nitrogen (N_r) back to the atmospheric reservoir. There is still a rather limited knowledge of the denitrification rates and their temperature dependence across ecosystems; particularly, for the abundant cold and N-poor freshwater systems (e.g., Arctic and mountain lakes). We experimentally investigated the denitrification rates of mountain lake sediments by manipulating nitrate concentration and temperature on field collected cores. DEN rates were nitrate limited in field conditions and showed a large potential for an immediate DEN increase with both warming and higher N_r load. The estimated activation energy (E_a) for denitrification at nitrate saturation was $46 \pm 7 \text{ kJ mol}^{-1}$ ($Q_{10} 1.7 \pm 0.4$). The apparent E_a increased with nitrate (μM) limitation as $E_a = 46 + 419 [\text{NO}_3^-]^{-1}$. Accordingly, we suggest that climate warming may have a synergistic effect with N emission reduction to readjusting the N cycle. Changes of nitrate availability might be more relevant than direct temperature effects on denitrification.

1. Introduction

The anthropogenic alteration of the nitrogen (N) cycle is one of the most challenging problems for the Earth system (Rockstrom et al., 2009). Human activity has at least doubled the levels of reactive nitrogen (N_r) available to the biosphere, largely as a result of the industrial N fixation for fertilizer productions and the burning of fossil fuels (Erismann et al., 2011). The global N cycle is still evaluated with high uncertainty. A few flux estimates are quantified with less than $\pm 20\%$ error and many have uncertainties of $\pm 50\%$ and larger (Gruber & Galloway, 2008). The transient situation of the planet with many factors that influence the N cycle changing simultaneously demands a deeper understanding of the factors controlling the rates of the N cycle pathways (Baron et al., 2013; Greaver et al., 2016). The temperature dependence of the rates of the distinct pathways is of particular interest for evaluating potential synergistic effects of climate warming and nitrogen emissions on N global cycle.

Denitrification (DEN) is the microbial activity by which nitrogenous oxides, mainly nitrate and nitrite, are reduced to dinitrogen gasses, N_2O and N_2 (Tiedje, 1988). DEN is the primary process removing N_r from the biosphere (Seitzinger et al., 2006). The DEN dynamics is typically episodic; driven by the fluctuating coexistence of primary resources, favorable conditions, and the microbial agents. Consequently, DEN rates are difficult to measure, model, and upscale. Existing methods are problematic for different reasons (Groffman et al., 2006). Much of the challenges arise from the fact that small areas (hot spots) and brief periods (hot moments) account for a high percentage of the denitrification activity both in terrestrial and aquatic ecosystems (Groffman et al., 2009; McClain et al., 2003; Parkin, 1987). A substantial proportion of denitrification occurs in the upper part of the sediments, where necessary resources (e.g., N-oxides, fresh organic matter) meet anaerobic conditions. Lakes have been identified as the aquatic ecosystems with the highest seasonal and site variation in DEN rates (Piña-Ochoa & Alvarez-Cobelas, 2006), although part of the observed variability could be due to the methods applied. Particularly, the alteration of the integrity of the samples markedly affects the DEN rate (r_d) measured. Higher values in slurries are obtained compared to undisturbed core sediments (Ambus, 1993). The former cannot be considered representing in situ rates. They only provide relative measures for comparisons, if applied in the same way. However, if the target is to integrate DEN rates in the evaluation of the nitrogen cycle, there is an urgent demand of measurements in conditions as close

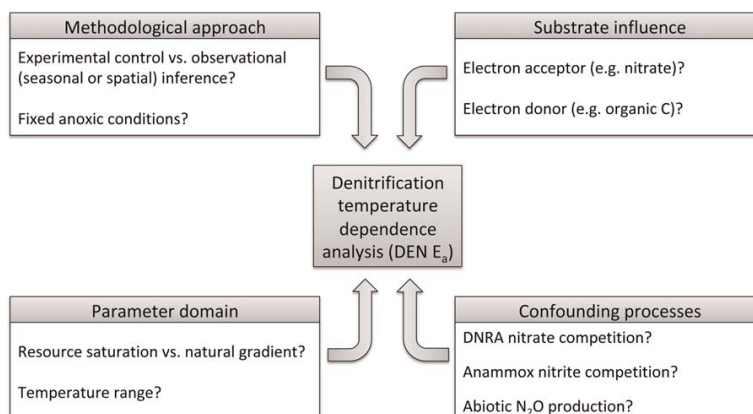


Figure 1. Main processes and aspects that affect the assessment of the denitrification temperature dependence.

as possible to the natural ones to reduce the uncertainty of the estimates and provide the elements for a reliable upscaling of the measurements (Galloway, 2004; Gruber & Galloway, 2008).

The temperature dependence of an enzymatic process can be described by its activation energy (E_a), which reflects the increase in the rate with temperature (Arrhenius, 1915) when there is no resource limitation. However, the biogeochemical E_a includes also temperature effects on molecular kinetics, physiological acclimation by microbial strains and microbial assemblage changes (Crowther & Bradford, 2013; Hall et al., 2010). In natural conditions, the E_a values reflect a multistep process and thus can vary with the substrate availability (Brezonik, 1994) and may depend on the particular assemblage of organisms performing the biogeochemical reaction (Hall et al., 2008). Each of these DEN control levels has a longer characteristic time, from instantaneous to a few days.

In lakes, sediment DEN rates at time scales below a few days are more likely to be constrained by the substrate supply than temperature fluctuations. Nitrate declines by the same DEN activity and their supply depend on other microbial activities (e.g., nitrification) and physical transport. When measuring DEN E_a , experimentally, some environmental conditions may depart easily from those in situ, either because of the use of an unrealistic temperature range (Boulétreau et al., 2012), very high nitrate addition (Holmes et al., 1996) or both. Alternatively, some observational approaches to estimate DEN E_a use activities (r_d) measured at periods of the year with contrasting temperature (Bachand & Horne, 2000; Sheibley et al., 2003). In this case, the substrate availability may change but also the assemblage of microorganisms present.

Consequently, there are a number of aspects to consider in an assessment of the biogeochemical DEN E_a for a certain type of ecosystems (Figure 1). They include (1) the general methodological approach; fundamentally, whether the approach is experimental, controlling the temperature change, or observational, using spatial or temporal natural temperature variation. (2) How the substrates (i.e., organic carbon, nitrogen) are considered; particularly, whether they are artificially saturated or maintained within natural conditions. And (3) which are the biogeochemical processes that could be a source of added uncertainty in the assessment provided their competition for nitrate or nitrite or their release of nitrous oxide.

There are few studies of the DEN E_a in oligotrophic systems (Holmes et al., 1996) and most are marine (Cannon et al., 2014a; Rysgaard et al., 2004). In the current situation of global change, the case of remote ecosystems, those that are mostly influenced by atmospheric processes rather than direct human action in the watershed, are of particular interest. Many of these sites (e.g., alpine and subarctic regions) have, are or would experience increased N_r deposition (Holtgrieve et al., 2011) and warming (Smol, 2012). Therefore, they are key sites for studying the interaction between temperature and the N cycle (Catalan et al., 2013).

The increase of N_r deposition is eventually reflected in the stream and lake loads depending on the degree of N saturation in the soil and vegetation (Stoddard, 1994). Long-term sustained high N_r deposition results in a watershed quasi steady state so that N_r deposition and streams show similar temporal trends and

fluctuations. One may expect that lakes would follow streams midterm temporal patterns. However, recently, Camarero and Catalan (2012) have found an opposite trend during the last decades in the Pyrenees between lakes and streams. The latter follows the still N_r increasing tendency in the deposition, but lakes show a decline. The authors have attributed the opposed trends to an increase in lake productivity related to a higher phosphorus deposition. However, they were not able to evaluate whether an enhancement of denitrification could be an alternative explanation due to the lack of empirical information. The difficulty of the measuring DEN rates at low N_r concentrations may justify why remote systems have been overlooked with a few exceptions (Castellano-Hinojosa et al., 2017; McCrackin & Elser, 2010, 2012; Vila-Costa et al., 2016). Indeed, it has been only one attempt to estimate DEN E_a in these systems (Myrstener et al., 2016). Consequently with this gap in knowledge, the aim of this study was to assess the DEN temperature dependence (E_a) in remote, cold and relatively N-poor lakes. From the several options above introduced (Figure 1), our approach was thought as one that could be useful for an evaluation of the actual in situ rates in the area studied, the potential upscaling of DEN estimations over large sets of oligotrophic lakes, and projections of future scenarios of air temperature and nitrate deposition. Therefore, DEN measurements were conducted using intact core sediments, the acetylene inhibition method combined with sensors for nitrous oxide and experimental control of temperature and nitrate availability within the natural range found in these lakes. For complementarity, we compiled the existing data on DEN temperature dependence in aquatic ecosystems across the literature and evaluated the results according to the framework introduced in Figure 1, emphasizing the likely reasons for the large variation in the estimations and, if so, the discrepancies with our results.

2. Materials and Methods

2.1. General Methodological Approach

Three lakes with contrasting morphology and carbon flow characteristics (Table 1) were sampled to consider potential different microbial communities. In each sampling date, we collected five core sediments in the field, which were immediately transported to the lab to control for temperature and nitrate availability within the ranges that can be found in these mountain lakes. We used sensors for nitrous oxide combined with the acetylene inhibition method and anoxic conditions to minimize the disturbance of the sediment structure. For each core, we performed sequential estimations of the DEN rates (r_d) at several temperature values and nitrate concentrations. This procedure reduces the noise that the sediment spatial heterogeneity can introduce in the estimations but may introduce autocorrelation effects. To overcome the latter constraint, we did not follow the same experimental sequence in each trial, so we could statistically evaluate the autocorrelation influence and distinguish it from other sources of variation (e.g., nitrate concentration, lake, and sensors). Although the experiment was planned for the same number of cores per lake (5), finally,

Table 1
Study Sites Location and Characteristics

Lake	Redon	Plan	Llong
Latitude (N)	42.64208	42.62248	42.57431
Longitude (E)	0.77951	0.9307	0.95063
Altitude (m asl)	2,235	2,188	2,000
Area (ha)	24	5	7
Maximum depth (m)	73	9	12
Temperature ^a (°C)	4	5	3
NO ₃ ^{-a} (μM)	5 (4–6)	1 (1–2)	8 (7–9)
NO ₂ ^{-a} (μM)	0.17 (0.13–0.21)	0.05 (0.05–0.05)	0.15 (0.13–0.18)
NH ₄ ⁺ ^a (μM)	9 (6–14)	3 (2–5)	25 (19–31)
DOC ^a (mg L ⁻¹)	52 (2–88)	74 (6–99)	15 (2–70)
LOI ^b (%)	25 (18–35)	44 (40–48)	27 (24–31)
Carbon ^b (% dry weight)	12 (10–18)	20 (17–24)	13 (11–14)
Nitrogen ^b (% dry weight)	1.2 (0.9–2.1)	1.9 (1.6–2.3)	1.2 (1.0–1.5)
Sediment grain size (median, μm) ^b	252 (166–351)	333 (205–465)	174 (130–223)

^aCharacteristics of the water overlying the sediment. Ice-free season average, minimum, and maximum values. ^bCharacteristics of the surface sediment (0–2 cm layer): loss on ignition (LOI), as a proxy of organic matter (carbonates < 2%, not shown).

we also included in the data set two preliminary tests—performed using only a part of the nitrate gradient in some Lake Redon cores—as they fitted in the general results obtained and thus increased the statistical robustness of the final model.

2.2. Sampling and Experimental Design

The selected three lakes are representative of the lake district of the Pyrenees (Table 1). They cover a broad range of maximum depth (9–73 m) and seasonal thermal variability (Catalan et al., 2002). The experimental temperature (5–15°C) and the nitrate added levels (7–14–28 μM) covered the natural variability in the region and possible future scenarios. A total of 25 sediment cores (methacrylate, \varnothing 6.35 cm) were assessed (15 from Redon, 5 from Plan, and 5 from Llong, supporting information Table S1). They were collected with a gravity corer (Glew, 1991) at midday around the deepest point of each lake (Table 1). Only undisturbed cores with clear overlying water and interface were used. The experimental setup included an incubation chamber that ensured dark conditions and controlled temperature ($\pm 1^\circ\text{C}$; Figure 2). Nitrate was measured at the beginning of the incubations (supporting information Table S1). As a precautionary action, glucose was added in excess (1.5 g L^{-1}) to avoid carbon limitation (Vila-Costa et al., 2016) despite that some previous tests did not show conclusive evidence of such limitation. DEN measurements at different nitrate concentrations and temperatures started the next morning and were conducted sequentially, commonly: step 1: first 7 μM nitrate addition at 5°C (0–12 h); 2: 15°C (12–24 h); 3: second 7 μM nitrate addition at 15°C (24–36 h); 4: 5°C (36–48 h); 5: 14 μM nitrate addition at 5°C (48–60 h); and 6: 15°C (60–72 h).

2.3. Denitrification Measurement

DEN measurements were performed using the acetylene inhibition method combined with sensors for nitrous oxide (N_2O). Anoxia, first, and acetylene inhibition, after, were achieved by bubbling N_2 and C_2H_2 sequentially, respectively, during 10 min in the water phase of the core before each DEN measurement. Acetylene inhibits the reduction of N_2O to N_2 (Balderston et al., 1976; Yoshinari & Knowles, 1976). The accumulated N_2O was measured using a modified Clark electrode probe (N_2O -R microsensors, Unisense A/S, Denmark; detection limit = 0.1 μM), in the water phase. A gentle magnet stirring was applied to avoid stratification but without resuspension of the sediment. Readings were taken every 5 min via a picoammeter logged to a laptop. The response of the electrochemical sensor is linear in the range of 0–1.2 mM (Andersen et al., 2001). The instrument was kept polarized during all the measurement period. It was calibrated at each temperature using a calibration chamber (CAL300, Unisense A/S, Denmark), zero gas water (Milli-Q) and a freshly prepared $\sim 50\text{ }\mu\text{M}$ N_2O solution. The latter was obtained adding a certain volume of N_2O saturated water (Weiss & Price, 1980) to the zero gas water following manufacturer's instructions as described in Foley et al. (2010).

2.4. Water and Sediment Characterization

Immediately after collection, we measured the temperature ($^\circ\text{C}$) of water overlying the sediment core (Table 1). For chemical analyses, water samples were filtered through a precombusted (4 h at 450°C) GF/F glass fiber filter. Nitrate was determined by capillary electrophoresis using a Quanta 4000 (Waters) instrument. Ammonium and nitrite were determined by colorimetric methods in a segmented-flow autoanalyzer (AA3HR, Seal), using the Berthelot reaction for ammonium (Bran + Luebbe method G-171-96) and the Griess reaction for nitrite (Bran + Luebbe method G-173-96). Dissolved organic carbon (DOC) was measured by catalytic combustion to CO_2 and detection by IR spectroscopy in a TOC5000 (Shimadzu) analyzer. The water column of the lakes sampled show a circumneutral pH (~ 7 ; Vila-Costa et al., 2014).

After DEN measurements, the surface sediment was sliced (2 cm) and freeze dried for 72 h. Around 5 mg of the dried sample was encapsulated together with a catalyst (V_2O_5) in tin capsules for the determination of C and N using a C–H–N–S (Carlo-Erba) analyzer. The dry weight percentage of organic matter content in the sediments was determined by loss on ignition (LOI) following Heiri et al. (2001). In all cases, the samples were equilibrated to room temperature in a desiccator before weighing them. The median grain size of the sediment was determined by laser diffraction (Mastersizer 2000, Malvern



Figure 2. Experimental setup. The incubation chamber ensured dark and controlled temperature ($\pm 1^\circ\text{C}$) conditions. Five intact lake sediment cores could be processed at once using their respective N_2O sensors.

Instruments Ltd, UK). Freeze-dried sediment was rehydrated in distilled water and introduced into the sample dispersion unit (Hydro 2000 G, Malvern Instruments Ltd, UK) adding hexametaphosphate and sonicating to avoid aggregates. Laser obscuration was between 10 and 20% and the measuring range between 0.02 and 2,000 μm .

2.5. Numerical Methods

Denitrification activity rates (r_d ; $N = 107$) were calculated by linear regression from the sequential readings of the N_2O sensors ($r = 0.89 \pm 0.02$ [mean \pm standard error], with an average of 66 point measurements). Raw r_d values in $\mu\text{M N}_2\text{O core}^{-1} \text{h}^{-1}$ were transformed to $\mu\text{mol N}_2\text{O m}^{-2} \text{h}^{-1}$ using the inner core section area. The apparent activation energy (E_a ; kJ mol^{-1}) of the denitrification process was estimated according to the Arrhenius equation: $\frac{r_{di}}{r_{dj}} = \exp\left[\frac{E_a}{R}\left(\frac{1}{T_i} - \frac{1}{T_j}\right)\right]$ where R is the gas constant ($8.314 \text{ J K}^{-1} \text{ mol}^{-1}$); T , the absolute temperature ($^\circ\text{K}$); and r_d , the denitrification activity rate. The subscripts (i, j) indicate two different thermal conditions. Statistics were conducted using R version 3.3.0 (R Development Core Team, 2016). Linear mixed-effects models were performed using the *lme* and *lmer* functions within the nlme and lme4 R packages, respectively (Bates et al., 2015; Pinheiro et al., 2007). Functions ANOVA of the R core package stats (R Development Core Team, 2016), AICc (Akaike Information Criterion for a small sample size) of the package AICcmodavg (Mazerolle, 2016) and fixed, global explained variance and *r.squaredGLMM* of MuMIn (Bartoń, 2016) were used to select the best fitting model.

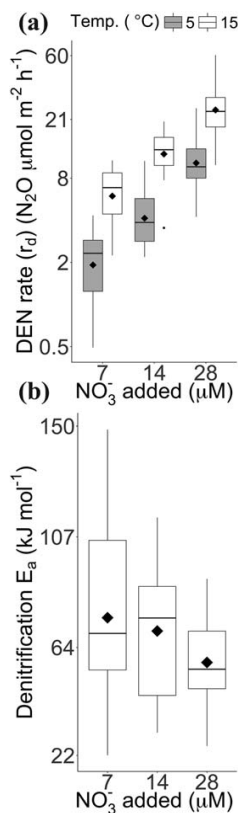


Figure 3. (a) Denitrification rates (r_d) at the two experimental temperatures and the three nitrate enrichments. Note the natural logarithm scale in y axis. (b) Apparent activation energy (E_a) at the three nitrate enrichments. The number of observations of DEN E_a was 12, 20, and 19, respectively for each level of nitrate added (7, 14, and 28 μM). Note that the actual experimental nitrate concentrations in each enrichment class varied according to the initial field concentration (supporting information Table S1).

2.6. Compiled Data of DEN E_a in Aquatic Ecosystems

For comparison, we compiled data about the denitrification temperature dependence in aquatic ecosystems across literature (supporting information Table S2). For each study, the apparent activation energy (E_a ; kJ mol^{-1}) of the denitrification process was estimated by the Arrhenius equation above or by the slope of an Arrhenius plot of $\ln(r_d)$ as a function of T^{-1} when more than two temperature data were available.

3. Results

3.1. Denitrification Temperature Dependence in Mountain Lakes Sediments

The denitrification activity rates (r_d) measured ranged from 0.5 to 60.5 $\mu\text{mol N}_2\text{O m}^{-2} \text{h}^{-1}$ (supporting information Table S1). The rates increased with the experimental temperature, and nitrate addition levels (Figure 3a). Rates (mean \pm standard error) for 7, 14, and 28 μM nitrate added were at 5°C 2.2 ± 0.3 , 4.6 ± 0.5 , $11.3 \pm 1.2 \mu\text{mol N}_2\text{O m}^{-2} \text{h}^{-1}$, respectively, and at 15°C 6.6 ± 0.8 , 12.7 ± 0.9 , $27.0 \pm 2.9 \mu\text{mol N}_2\text{O m}^{-2} \text{h}^{-1}$, respectively.

From the measured rates, the apparent activation energy was estimated for each nitrate level (supporting information Table S1, average $E_a = 67 \pm 4 \text{ kJ mol}^{-1}$). DEN r_d at 5°C had a larger influence on the E_a values than those at 15°C as shown by a significant negative correlation ($r = -0.51$, $p = 0.0001$) between E_a and $\ln(r_d)$ at 5°C and not significant at 15°C.

E_a values and their variation declined when the nitrate added increased (Figure 3b). E_a negatively correlated ($r = -0.33$, $p = 0.01$) with the initial experimental nitrate (water phase plus added) concentrations. E_a at nitrate saturation was estimated by fitting a linear relationship between the inverse of nitrate concentration and E_a (model 0 in Table 2). In this model, the intercept indicates the value of E_a when the influence of nitrate concentration tends to zero.

The variation of the rates measured under the same conditions of temperature and nitrate concentration was markedly high. Therefore,

Table 2

Alternative Regression Models Relating the DEN E_a (kJ mol^{-1}) to the Inverse of the Nitrate Concentration ($[\text{NO}_3^-]^{-1}$) (μM) in the Overlying Water of the Lake Sediments

Regression model	Random part	Formula	E_a at nitrate saturation			AICc	Fixed R^2	Global R^2	
			(intercept \pm se)	p -Value	Coefficient \pm se				p -Value
0	Lm model, no random part	mod0 = $\text{lm}(E_a \sim [\text{NO}_3^-]^{-1})$	50 ± 8	<0.00001	315 ± 141	0.0303	481	0.09	0.09
1	GLS model, no random part	mod1 = $\text{gls}(E_a \sim [\text{NO}_3^-]^{-1})$	50 ± 8	<0.00001	315 ± 141	0.0303	465	0.09	0.09
2	GLS model, no random part	mod2 = $\text{gls}(E_a \sim [\text{NO}_3^-]^{-1}, \text{correlation} = \text{corAR1}(\text{form} = \sim\text{Add phase} \text{Core}))$	50 ± 8	<0.00001	324 ± 139	0.0239	467	0.09	0.09
3	Sensor effect	mod3 = $\text{lme}(E_a \sim [\text{NO}_3^-]^{-1}, \text{random} = \sim 1 + [\text{NO}_3^-]^{-1} \text{Sensor})$	44 ± 8	<0.00001	451 ± 227	0.0529	464	0.15	0.47
4	Sensor effect (just slope)	mod4 = $\text{lme}(E_a \sim [\text{NO}_3^-]^{-1}, \text{random} = \sim 0 + [\text{NO}_3^-]^{-1} \text{Sensor})$	46 ± 7	<0.00001	419 ± 175	0.0207	460	0.13	0.42
5	Sensor (with nested core effect)	mod5 = $\text{lme}(E_a \sim [\text{NO}_3^-]^{-1}, \text{random} = \sim 1 + [\text{NO}_3^-]^{-1} \text{Sensor/Core})$	45 ± 8	<0.00001	438 ± 228	0.0666	473	0.14	0.49
6	Core effect	mod6 = $\text{lme}(E_a \sim [\text{NO}_3^-]^{-1}, \text{random} = \sim 1 + [\text{NO}_3^-]^{-1} \text{Core})$	48 ± 9	<0.00001	365 ± 177	0.0505	469	0.11	0.34
7	Core effect (just slope)	mod7 = $\text{lme}(E_a \sim [\text{NO}_3^-]^{-1}, \text{random} = \sim 0 + [\text{NO}_3^-]^{-1} \text{Core})$	49 ± 8	<0.00001	339 ± 153	0.0368	465	0.1	0.29
8	Nitrate added effect	mod8 = $\text{lme}(E_a \sim [\text{NO}_3^-]^{-1}, \text{random} = \sim 1 + [\text{NO}_3^-]^{-1} \text{Nitrate added})$	42 ± 15	0.0068	495 ± 298	0.1038	472	0.18	0.3
9	Nitrate addition phase effect	mod9 = $\text{lme}(E_a \sim [\text{NO}_3^-]^{-1}, \text{random} = \sim 1 + [\text{NO}_3^-]^{-1} \text{Add phase})$	48 ± 10	<0.00001	366 ± 200	0.0732	472	0.11	0.15
10	Lake effect	mod10 = $\text{lme}(E_a \sim [\text{NO}_3^-]^{-1}, \text{random} = \sim 1 + [\text{NO}_3^-]^{-1} \text{Lake})$	50 ± 8	<0.00001	315 ± 141	0.0307	472	0.09	0.09

Note. All the regression models have the same fixed part, that is the inverse of the nitrate concentration ($[\text{NO}_3^-]^{-1}$). Thus, the models differ in the random part. The coefficient is the slope of the model and shows the influence of the inverse of nitrate concentration in the E_a . AICc is the second-order Akaike's information criterion for a small sample size (Mazerolle, 2016). Fixed R^2 represents the variance explained by the fixed factor ($[\text{NO}_3^-]^{-1}$), and global R^2 represents the total variance explained by both fixed and random factors (i.e., the entire model; Bartoń, 2016). Model 2 takes into account the temporal autocorrelation. Models 3, 4, and 5 take into account the sensor (#1, #2, #3, #4, or #5) effect, thus correcting for differences in sensor performance. Models 5 (nested in the sensor), 6, and 7 consider the core (sample) effect. Model 8 takes into account the three nitrate enrichment levels, and model 9 the addition order (first, second, and third). Model 10 takes into account the lake effect. Models with more than one factor crossed in the random part (not shown) were also built with the *lmer* function within the *lme4* R package (Bates et al., 2015), these models did not improve model 1, 3, or 4 ($p > 0.05$) in ANOVAs and showed higher AICc values). Abbreviations: lm, linear model; gls, linear model fitted using generalized least squares; lme, linear mixed-effects model; se, standard error.

we investigated whether the estimation of the E_a dependency on nitrate concentration could be improved by taking into account other experimental issues and the lake idiosyncrasy (Table 2). We developed alternative mixed regression models including different factors in the random part and maintaining the inverse of nitrate concentration as the only factor in the fixed part (see supporting information for details (Chambers, 1992; Pinheiro & Bates, 1978; Zuur et al., 2009)). The alternative models took into account: the five sensor performance; the autocorrelation intrinsic to subsequent experimental additions; the nitrate addition level; the order of the addition level (not all the experiments followed the complete sequence from 7 to $28 \mu\text{M}$ NO_3^-) and the lake of the core. The only models that significantly improved the initial model 1 were those accounting for the sensor effects (models 3 and 4 in Table 2). They showed the lower AICc values and explained more variance (ANOVA p -values of 0.047 and 0.008 for models 3 and 4, respectively). When we considered core, lake, autocorrelation, or nitrate addition features did not improve the E_a estimation. We eventually selected model 4 as the best estimation because it is simpler than model 3. Consequently, the denitrification E_a at nitrate saturation is estimated to be $46 \pm 7 \text{ kJ mol}^{-1}$ (i.e., $Q_{10} = 1.7 \pm 0.4$) and the apparent E_a to vary according to nitrate concentration as

$$E_a = 46 + 419 [\text{NO}_3^-]^{-1} \quad (1)$$

3.2. Comparison With Other Aquatic Ecosystems

We identified a total of 21 previous studies (supporting information Table S2) to compare our results with estimations from other sites and methods. They included lakes (Cavari & Phelps, 1977; Messer & Brezonik, 1984; Myrstener et al., 2016), ponds (Veraart et al., 2011), streams (Boulêtreau et al., 2012; Holmes et al., 1996), rivers (Pattinson et al., 1998; Pfenning & McMahon, 1997; Silvennoinen et al., 2008), denitrification

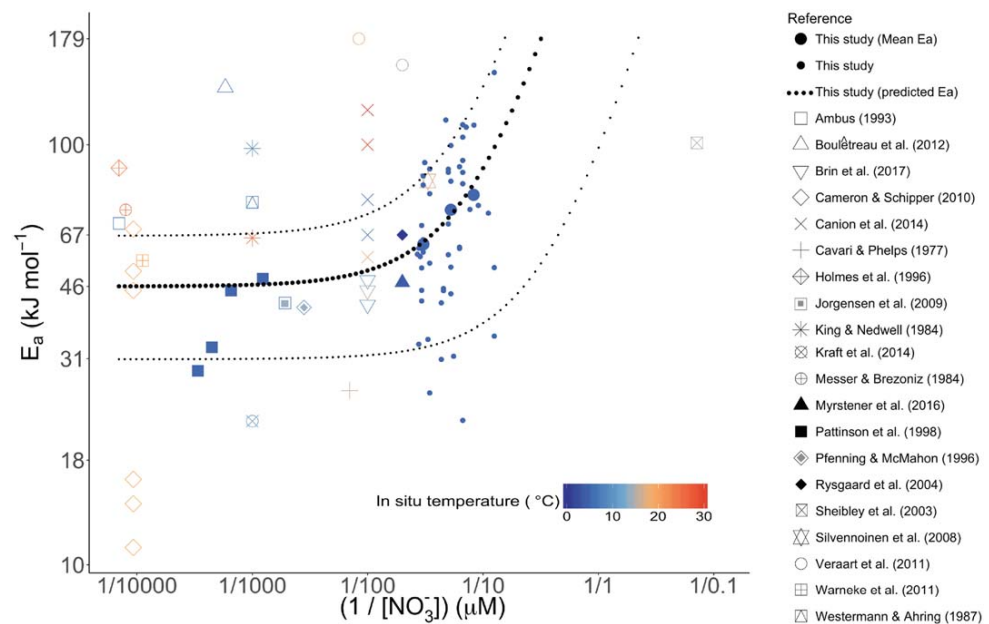


Figure 4. Denitrification temperature dependence (E_a) against the inverse of the nitrate concentration in compiled data from aquatic ecosystems. The solid circles are data from this study. The small circles are the E_a values resulting from each experiment ($N = 51$) and the large circles correspond to the average E_a values for each of the three nitrate enrichment levels. The black dotted line indicates the model $E_a = 46 + 419 [\text{NO}_3]^{-1}$. The thin dotted lines indicate the 95% confidence intervals (see model 4 in Table 2). Note that x and y axes are on a \log_{10} scale.

beds (i.e., carbon supply to promote denitrification in eutrophic rivers; Cameron & Schipper, 2010; Warneke et al., 2011), hyporheic (Sheibley et al., 2003) and riparian (Ambus, 1993) zones, groundwaters (Jørgensen et al., 2009), swamps (Westermann & Ahring, 1987), wetlands (King & Nedwell, 1984), estuaries (Brin et al., 2017), and marine environments (Brin et al., 2014, 2017; Canion et al., 2014a, 2014b; Kraft et al., 2014; Rysgaard et al., 2004). There is a large scattering in the E_a values estimated. However, the most similar sites to those in our study (Myrstener et al., 2016; Rysgaard et al., 2004) were also from remote, cold and N-poor areas, and showed similar E_a values plotted against the inverse of nitrate (Figure 4).

4. Discussion

4.1. Denitrification Rates, Nitrate, and Temperature

The denitrification rates (r_d) obtained were similar to the few other measurements in mountain lake sediments (McCrackin & Elser, 2012; Vila-Costa et al., 2016). The values are in the low range of freshwater sediments (Piña-Ochoa & Alvarez-Cobelas, 2006; Seitzinger, 1988) as expected from cold and oligotrophic environments. However, despite the apparent harsh conditions, the denitrification activity intensifies with increasing nitrate and temperature without becoming saturated (Figure 3a) within the range of values currently found in the Pyrenees (Camarero & Catalan, 2012). Therefore, the current denitrification potential of these systems can respond to warming or increased N₂ deposition (or watershed loading) without any time lag.

It could be argued that the experimental sequential procedure of 72 h incubations could facilitate an enrichment of denitrifiers in our experiment. We used the shortest time to obtain reliable measurements of the activity rate without disturbing the sediment interface. An alternative experimental design, based on pseudo-replicates of several cores from the same site incubated at the various levels of nitrate and temperature, would notably increase the sample-related heterogeneity due to the patchy nature of any sediment. We think that the cold and oligotrophic conditions of the studied system prevent any significant enrichment in denitrifiers during the experimental development.

In the compiled DEN E_a studies, there are variable values for similar NO_3^- enrichments (Figure 4), which may be attributed to changing assemblages of denitrifiers. A case of a latitudinal gradient in coastal marine

sediments, with higher values for subtropical locations (121 and 100 kJ mol^{-1} ; Canion et al., 2014b). A case of cultures with a different nitrate-reducing dominant species, *Pseudomonas* sp. or *Vibrio* sp., with 98 and 60 kJ mol^{-1} E_a values, respectively, isolated at 10 and 25°C from a salt-marsh sediment (King & Nedwell, 1984). And cases of seasonal variability, with E_a ranges of 70–76, 36–53, and 38–60 kJ mol^{-1} in swamp, estuary, and continental shelf sediments from temperate ecosystems, respectively (Brin et al., 2017; Westermann & Ahring, 1987). Beyond the sequential experimental issue, different denitrifier assemblages between lakes could also be a source of variation in our data. However, models including the lake site as a source of random variation did not improve the fitting (Table 2). Only the use of molecular techniques to characterize the microbial assemblages (i.e., 16S rRNA) will settle discussions about this issue and clarify the relative influence of physicochemical and biological constraints.

To our knowledge, only another study measured DEN activities experimentally controlling both temperature and nitrate gradients close to the in situ conditions (Pattinson et al., 1998). In this study, E_a values also declined with increasing nitrate. Provided the difference of about three orders of magnitude in nitrate concentrations between the two studies, one has to conclude that DEN saturation by nitrate is achieved at different concentrations in eutrophic and oligotrophic ecosystems. Even so, the range of E_a estimated in the eutrophic experiment fell within the 95% confidence limit of our model (Figure 4).

The higher E_a values (155–179 kJ mol^{-1}) have been found in eutrophic ponds (Veraart et al., 2011). In this case, there was not an experimental forcing of the anoxia, so the authors attribute the high effect of warming on denitrification rates to a decline in the oxygen interference due to a synergic effect of lowering both the oxygen solubility and the production/respiration ratio when the temperature increases. Boulétreau et al. (2012) also found a high E_a (137 kJ mol^{-1}): they were using a wide, and high experimental temperature range (1–40°C) compared to the in situ temperature ($7.2 \pm 1.7^\circ\text{C}$) of their sites. The same experimental set, indicate a lower E_a (43 kJ mol^{-1}) when calculated only for a narrower temperature range (1–12°C) closer to that in situ (supporting information Table S2). The lowest E_a values (<20 kJ mol^{-1}) were found by Cameron and Schipper (2010).

Coupled nitrification could also interfere the DEN experiments if ammonium levels are high. Sheibley et al. (2003) performed the only study of DEN E_a at markedly low nitrate concentrations without any addition. Their E_a estimates depart from our model (Figure 4). In that case, there was an intense nitrification, also highly dependent on temperature and ammonium concentrations (22 μM), and DEN E_a was estimated using activity rates at different seasons as a surrogate for temperature control.

In our compiled data, including our study, we did not find any significant correlation between DEN E_a values and any statistical temperature descriptor (T max, T min, T mean, T in situ, or annual T mean, supporting information Table S2). Canion et al. (2014b) found a higher DEN E_a value for warmer (subtropical) than colder (temperate or polar) environments. They suggested an adaptation of denitrifiers to in situ temperature, supported by a previous study in the polar region (Canion et al., 2013). Although not universally, there are trade-offs between genetic adaptation to low and high temperature (Bennett & Lenski, 2007). In a salt-marsh study, culture isolates at 10, and 25°C from the same sediment sample resulted in different nitrate-reducing dominant species, *Pseudomonas* sp. and *Vibrio* sp., and showed different E_a (98 and 60 kJ mol^{-1} , respectively). The highest E_a was in the culture isolated at the closer temperature to in situ (15°C; King & Nedwell, 1984). Recurrently, DEN E_a values are higher when obtained from temperatures around in situ. In the literature data, a mean increase of $42 \pm 11\%$ (\pm se) is achieved when E_a is calculated with a narrow temperature range close to the in situ one compared with the result using the complete temperature range of the experiment (supporting information Table S2). We found a similar increase (51%) when the temperature range was reduced to values close to the in situ temperature in the samples of Lake Redon (supporting information Table S2). Consequently, we highlight the convenience of measuring DEN temperature dependence as close as possible to in situ conditions of temperature.

In the current context of results (Figure 4), it seems necessary to recommend experiments following a common procedure including an experimental nitrate gradient and temperatures no more than 15°C beyond the in situ values. The spatial or temporal distribution of the samples should not be a surrogate for these gradients.

4.2. Carbon Limitation, Nitrate Supply, and Competing Process

There were two aspects with potential influence on DEN temperature dependence (Figure 1) that we did not explicitly consider, carbon limitation and competing processes. We did not expect a denitrification

limitation by carbon in the Pyrenean mountain lakes. There is a higher ratio of primary production to respiration in both the water column and the surface sediments, resulting in an elevated fresh carbon stock for bacterial activity (Camarero et al., 1999). All in all, our experimental measurements were made with the addition of glucose. In fact, one can expect a C availability influence on the denitrification temperature dependence mostly in warm and eutrophic (nitrate-rich) aquatic ecosystems. The lowest DEN E_a values ($<20 \text{ kJ mol}^{-1}$) in the compiled data were found by Cameron and Schipper (2010) in an extended 10 months incubation experiment. The low E_a values could be due to a C-limitation in the warmer treatments using labile C sources (green waste, maize cobs, and wheat straw). C deficiency could also cause the low E_a (26 kJ mol^{-1}) assessed in a *Pseudomonas aeruginosa* culture isolated from Lake Kinneret as there was no addition of any C source (Cavari & Phelps, 1977; Gal et al., 2003).

In the method that we applied, the experimental assumption is that nitrification is not acting because of the induced anoxic conditions and the inhibition of the ammonium monooxygenase by acetylene (Hynes & Knowles, 1978). Consequently, sources of NO_3^- supply variation restrict to diffusive transport and uptake by alternative biogeochemical pathways. Nitrate diffusion aspects appear to have had no significant influence in our experiment as core and lake factors, which implicitly account for differences in sediment particle size, did not improve the models (Table 2).

Nitrate uptake, anammox, and dissimilatory nitrate reduction to ammonium (DNRA) are the biogeochemical processes that can compete with DEN for nitrate. We may assume that nitrate assimilation should not be relevant because of the high abundance of ammonium—the preferred N source (Luque-Almagro et al., 2011)—and the common low rates of nitrogen uptake in dark conditions (Lorenzen et al., 1998).

Anammox competes with DEN for nitrite. To our knowledge, there is no evidence of the dominance of anammox or DEN depending on the nitrate concentration. Anammox seems more sensitive to nitrate fluctuations than DEN (Rysgaard et al., 2004). The highest anammox activity respect to DEN has been found at 5°C in Arctic marine sediments (Rysgaard et al., 2004). Canion et al. (2014a) found similar results in Arctic fjord sediments with anammox bacteria being more specialized for psychrophilic activity than denitrification. Recently, Brin et al. (2017) in a warmer habitat, temperate marine sediments did not find differences in temperature responses for the two processes.

The ratio of electron acceptor (i.e., NO_3^-) to electron donor (i.e., organic C) is the most frequently mentioned partitioning factor between DEN and DNRA (Tiedje et al., 1982). DNRA is the dominant pathway under nitrate-limited conditions, while DEN is the favored pathway under nitrate-replete conditions (Dong et al., 2009; Herbert & Nedwell, 1990; King & Nedwell, 1985, 1987; Laverman et al., 2006; Mania et al., 2014; Nogaro & Burgin, 2014; Smith et al., 1982). Slightly more energy is obtained per mol of NO_3^- by DNRA than by DEN (Strohm et al., 2007) and, additionally, DNRA consumes more electrons (8 versus 5) during the reduction of NO_3^- to NH_4^+ (Burgin & Hamilton, 2007). Low NO_3^- and high organic C availability can thus create more favorable conditions for DNRA than DEN (MacFarlane & Herbert, 1982; Tiedje et al., 1982). The in situ C/N ratios of the sediment (Table 1) were always higher than 10 in our samples, in the range of values more favorable to DNRA. A C/N ratio for an equal contribution of the two processes of nitrate reduction is ~ 7.5 (Yoon et al., 2015). In all our experimental treatments, the DOC/nitrate ratio was above 100 (a/a), thus with similar conditions favoring DNRA as in field conditions.

Some studies have also shown a dominance of DNRA over DEN at higher temperatures (Ogilvie et al., 1997; Yoon et al., 2015). This dominance could be temporal during summer periods (Jørgensen, 1989; King & Nedwell, 1984) or spatial as occurs in some warm tropical ecosystems (Dong et al., 2011). Nonetheless, this apparent temperature effect may mask the true influence of the cooccurring higher reducing conditions and lower nitrate concentrations at higher temperatures that eventually determine a low ratio of electron acceptor to electron donor (Gardner et al., 2006; Gardner & McCarthy, 2009; Gross-Wittke et al., 2010; Jørgensen, 1989; Nizzoli et al., 2010; Zhu-Barker et al., 2015). The only two studies with data of temperature dependence for the two nitrate reduction processes are at a high nitrate concentration (1 mM). Kraft et al. (2014) shows E_a values of 22 and 40 kJ mol^{-1} , for DEN and DNRA respectively, in the complete experimental range of temperatures ($10\text{--}30^\circ\text{C}$), and 26 and 79 kJ mol^{-1} , respectively, in a narrow segment of temperature ($10\text{--}15^\circ\text{C}$)—based on E_a values calculated from supporting information Figure S8A. Yoon et al. (2015) investigated the switch between the two processes in a single microbial model, *Shewanella loihica*, a species capable of performing the two pathways. They found a dominance of DNRA at warmer temperatures, with

DEN showing a decline from 21 to 30°C and a null activity at 37°C. Temperature does not appear to be an issue in our experiment concerning DNRA and DEN partition. Using slurry incubations overestimate DNRA by enhancing nitrate availability to deeper layers of the sediments, where ammonifiers dominate over denitrifiers (Behrendt et al., 2013). This procedure could have affected other DEN estimates in mountain lakes (Vila-Costa et al., 2016) but their results do not differ markedly from our ones.

The generation of N₂O due to abiotic processes could let to an overestimation of the denitrification activity. At the current stage of knowledge, it is hard to infer any contribution of chemical processes to the overall NO and N₂O production (Schreiber et al., 2012). There are two major abiotic N₂O production pathways. The NH₂OH decomposition to N₂O at circumneutral pH is favored by high Mn (IV), temperature and salinity, and low organic carbon. The chemodenitrification of NO and NO₂⁻ to N₂O is favored by high pH, low O₂ and solid Fe (III) or Cu (II) catalysts (Zhu-Barker et al., 2015). Few of these favorable conditions are present in the studied lakes (e.g., the granitic nature of the bedrock in the studied lakes confers low levels of iron to the sediments; Catalan et al., 2014). However, these processes may be relevant in watersheds of metamorphic rocks rich in metals, which are common in some parts of the Pyrenees and other mountain ranges (Catalan et al., 1993).

We can conclude that DNRA, at nitrate limiting conditions and high temperature, and anammox, at low temperature and C/N, are the most like processes influencing DEN yield in mountain lakes. Future experiments on the temperature dependence of DEN, Anammox, and DNRA across gradients of nitrate, C/N and temperature are necessary to clarify these interactions.

5. Conclusions

There is still a limited knowledge about denitrification rates and their temperature dependence in general and, particularly, for cold and N-poor systems, despite that the latter cover a high percentage of the continental aquatic ecosystems. Our study shows that the low rates of denitrification observed are not nitrate saturated and the system can respond to warming and increased N_i loadings, either from deposition or the watershed. The case-by-case estimation of DEN E_a present much variability, but there is a robust statistical behavior that can be applied to modeling, upscaling and as a benchmark for actual measurements. Three main conclusions derive from our results:

1. Under nitrate saturation conditions (e.g., >100 μM) a DEN E_a significantly different from 46 kJ mol⁻¹ (e.g., >67 or <31) would suggest that there is another factor interfering (e.g., C quality or quantity limitation; or very distinct microbial assemblage related to other features of the system).
2. Below saturation and not at extremely low nitrate levels (>3 μM), equation (1) can be applied for modeling the temperature influence on DEN rates, accounting for nitrate levels.
3. In the natural environments of remote areas, in situ nitrate values are still far from DEN saturation. Currently, this feature leads to very high apparent DEN E_a values but this does not mean that with warming higher DEN rates could be sustained. In case of temperature increase, a short transitory period of high DEN would lead to a rapid depletion of nitrate unless nitrate supply rates would proportionally increase. Therefore, in a warmer scenario, variation in denitrification rates will continue mostly depending on nitrate supply processes that include proximal (e.g., sediment-related nitrification), local (e.g., Nr leaching from soils), and regional (e.g., atmospheric Nr deposition) components (Wallenstein et al., 2006).

Acknowledgments

Thanks to Berta Fueyo, Marc Sala-Faig, Rober Sánchez, and Pau Giménez-Grau for help in the laboratory and field sampling. The Spanish Government provided funds through the research grants of the Ministerio de Economía y Competitividad: NitroPir (CGL2010–19737), Lacus (CGL2013–45348-P), and Transfer (CGL2016–80124-C2-1-P) and a predoctoral fellowship to C.P.-L. (FPU12–00644). All the experimental and compiled data are available in the supporting information.

References

- Ambus, P. (1993). Control of denitrification enzyme-activity in a streamside soil. *FEMS Microbiology Ecology*, 102(3–4), 225–234.
- Andersen, K., Kjaer, T., & Revsbech, N. P. (2001). An oxygen insensitive microsensor for nitrous oxide. *Sensors and Actuators B: Chemical*, 81(1), 42–48.
- Arrhenius, S. (1915). The influence of temperature on the velocity of reactions—Reactions of cells. In *Quantitative laws in biological chemistry* (pp. 1–164). London, UK: G. Bell and Sons, Limited.
- Bachand, P. A. M., & Horne, A. J. (2000). Denitrification in constructed free-water surface wetlands: II. Effects of vegetation and temperature. *Ecological Engineering*, 14(1–2), 17–32.
- Balderston, W. L., Sherr, B., & Payne, W. (1976). Blockage by acetylene of nitrous oxide reduction in *Pseudomonas perfectomarinus*. *Applied and Environmental Microbiology*, 31(4), 504–508.
- Baron, J. S., Hall, E. K., Nolan, B. T., Finlay, J. C., Bernhardt, E. S., Harrison, J. A., et al. (2013). The interactive effects of excess reactive nitrogen and climate change on aquatic ecosystems and water resources of the United States. *Biogeochemistry*, 114(1), 71–92.
- Bartoń, K. (2016). *MuMIn: Multi-model inference. R package version 1.15.6*. Retrieved from <https://CRAN.R-project.org/package=MumIn>

- Bates, D., Mächler, M., Bolker, B., & Walker, S. (2015). Fitting linear mixed-effects models using lme4. *Journal of Statistical Software*, *67*(1), 1–48.
- Behrendt, A., de Beer, D., & Stief, P. (2013). Vertical activity distribution of dissimilatory nitrate reduction in coastal marine sediments. *Biogeosciences*, *10*(11), 7509–7523.
- Bennett, A. F., & Lenski, R. E. (2007). An experimental test of evolutionary trade-offs during temperature adaptation. *Proceedings of the National Academy of Sciences of the United States of America*, *104*(Suppl. 1), 8649–8654.
- Boulétreau, S., Salvo, E., Lyautey, E., Mastroiello, S., & Garabetian, F. (2012). Temperature dependence of denitrification in phototrophic river biofilms. *Science of the Total Environment*, *416*, 323–328.
- Brezonik, P. L. (1994). *Chemical kinetics and process dynamics in aquatic systems* (754 pp.). Boca Raton, FL: Lewis.
- Brin, L. D., Giblin, A. E., & Rich, J. J. (2014). Environmental controls of anammox and denitrification in southern New England estuarine and shelf sediments. *Limnology and Oceanography*, *59*(3), 851–860.
- Brin, L. D., Giblin, A. E., & Rich, J. J. (2017). Similar temperature responses suggest future climate warming will not alter partitioning between denitrification and anammox in temperate marine sediments. *Global Change Biology*, *23*, 331–340.
- Burgin, A. J., & Hamilton, S. K. (2007). Have we overemphasized the role of denitrification in aquatic ecosystems? A review of nitrate removal pathways. *Frontiers in Ecology and the Environment*, *5*(2), 89–96.
- Camarero, L., & Catalan, J. (2012). Atmospheric phosphorus deposition may cause lakes to revert from phosphorus limitation back to nitrogen limitation. *Nature Communications*, *3*, 1118.
- Camarero, L., Felip, M., Ventura, M., Bartumeus, F., & Catalan, J. (1999). The relative importance of the planktonic food web in the carbon cycle of an oligotrophic mountain lake in a poorly vegetated catchment (Redó, Pyrenees). *Journal of Limnology*, *58*(2), 203–212.
- Cameron, S. G., & Schipper, L. A. (2010). Nitrate removal and hydraulic performance of organic carbon for use in denitrification beds. *Ecological Engineering*, *36*(11), 1588–1595.
- Canion, A., Kostka, J., Gihring, T., Huettel, M., Van Beusekom, J., Gao, H., et al. (2014b). Temperature response of denitrification and anammox reveals the adaptation of microbial communities to in situ temperatures in permeable marine sediments that span 50° in latitude. *Biogeosciences*, *11*(2), 309–320.
- Canion, A., Overholt, W. A., Kostka, J. E., Huettel, M., Lavik, G., & Kuypers, M. M. M. (2014a). Temperature response of denitrification and anaerobic ammonium oxidation rates and microbial community structure in Arctic fjord sediments. *Environmental Microbiology*, *16*(10), 3331–3344.
- Canion, A., Prakash, O., Green, S. J., Jahnke, L., Kuypers, M. M. M., & Kostka, J. E. (2013). Isolation and physiological characterization of psychrophilic denitrifying bacteria from permanently cold Arctic fjord sediments (Svalbard, Norway). *Environmental Microbiology*, *15*(5), 1606–1618.
- Castellano-Hinojosa, A., Correa-Galeote, D., Carrillo, P., Bedmar, E. J., & Medina-Sánchez, J. M. (2017). Denitrification and biodiversity of denitrifiers in a high-mountain Mediterranean Lake. *Frontiers in Microbiology*, *8*, 1911.
- Catalan, J., Ballesteros, E., Gacia, E., Palau, A., & Camarero, L. (1993). Chemical composition of disturbed and undisturbed high-mountain lakes in the Pyrenees: A reference for acidified sites. *Water Research*, *27*(1), 133–141.
- Catalan, J., Pla-Rabés, S., García, J., & Camarero, L. (2014). Air temperature-driven CO₂ consumption by rock weathering at short timescales: Evidence from a Holocene lake sediment record. *Geochimica et Cosmochimica Acta*, *136*, 67–79.
- Catalan, J., Pla-Rabés, S., Wolfe, A. P., Smol, J. P., Ruhland, K. M., Anderson, N. J., et al. (2013). Global change revealed by palaeolimnological records from remote lakes: A review. *Journal of Paleolimnology*, *49*(3), 513–535.
- Catalan, J., Ventura, M., Brancelj, A., Granados, I., Thies, H., Nickus, U., et al. (2002). Seasonal ecosystem variability in remote mountain lakes: Implications for detecting climatic signals in sediment records. *Journal of Paleolimnology*, *28*(1), 25–46.
- Cavari, B. Z., & Phelps, G. (1977). Denitrification in lake Kinneret in presence of oxygen. *Freshwater Biology*, *7*(4), 385–391.
- Chambers, J. M. (1992). *Linear models*. Pacific Grove, CA: Wadsworth & Brooks/Cole.
- Crowther, T. W., & Bradford, M. A. (2013). Thermal acclimation in widespread heterotrophic soil microbes. *Ecology Letters*, *16*(4), 469–477.
- Dong, L. F., Smith, C. J., Pappaspyrou, S., Stott, A., Osborn, A. M., & Nedwell, D. B. (2009). Changes in benthic denitrification, nitrate ammonification, and anammox process rates and nitrate and nitrite reductase gene abundances along an estuarine nutrient gradient (the Colne estuary, United Kingdom). *Applied and Environmental Microbiology*, *75*(10), 3171–3179.
- Dong, L. F., Sobey, M. N., Smith, C. J., Rusmana, I., Phillips, W., Stott, A., et al. (2011). Dissimilatory reduction of nitrate to ammonium, not denitrification or anammox, dominates benthic nitrate reduction in tropical estuaries. *Limnology and Oceanography*, *56*(1), 279–291.
- Erisman, J. W., Galloway, J., Seitzinger, S., Bleeker, A., & Butterbach-Bahl, K. (2011). Reactive nitrogen in the environment and its effect on climate change. *Current Opinion in Environmental Sustainability*, *3*(5), 281–290.
- Foley, J., de Haas, D., Yuan, Z., & Lant, P. (2010). Nitrous oxide generation in full-scale biological nutrient removal wastewater treatment plants. *Water Research*, *44*(3), 831–844.
- Gal, G., Imberger, J., Zohary, T., Antenucci, J., Anis, A., & Rosenberg, T. (2003). Simulating the thermal dynamics of Lake Kinneret. *Ecological Modelling*, *162*(1), 69–86.
- Galloway, J. N. (2004). Nitrogen cycles: Past, present, and future. *Biogeochemistry*, *70*, 153–226.
- Gardner, W. S., & McCarthy, M. J. (2009). Nitrogen dynamics at the sediment-water interface in shallow, sub-tropical Florida Bay: Why denitrification efficiency may decrease with increased eutrophication. *Biogeochemistry*, *95*(2–3), 185–198.
- Gardner, W. S., McCarthy, M. J., An, S., Sobolev, D., Sell, K. S., & Brock, D. (2006). Nitrogen fixation and dissimilatory nitrate reduction to ammonium (DNRA) support nitrogen dynamics in Texas estuaries. *Limnology and Oceanography*, *51*(1), 558–568.
- Glew, J. (1991). Miniature gravity corer for recovering short sediment cores. *Journal of Paleolimnology*, *5*(3), 285–287.
- Greaver, T., Clark, C., Compton, J., Vallano, D., Talhelm, A., Weaver, C., et al. (2016). Key ecological responses to nitrogen are altered by climate change. *Nature Climate Change*, *6*(9), 836–843.
- Groffman, P. M., Altabet, M. A., Bohlke, J. K., Butterbach-Bahl, K., David, M. B., Firestone, M. K., et al. (2006). Methods for measuring denitrification: Diverse approaches to a difficult problem. *Ecological Applications*, *16*(6), 2091–2122.
- Groffman, P. M., Butterbach-Bahl, K., Fulweiler, R. W., Gold, A. J., Morse, J. L., Stander, E. K., et al. (2009). Challenges to incorporating spatially and temporally explicit phenomena (hotspots and hot moments) in denitrification models. *Biogeochemistry*, *93*(1–2), 49–77.
- Gross-Wittke, A., Gunkel, G., & Hoffmann, A. (2010). Temperature effects on bank filtration: Redox conditions and physical-chemical parameters of pore water at Lake Tegel, Berlin, Germany. *Journal of Water and Climate Change*, *1*(1), 55–66.
- Gruber, N., & Galloway, J. N. (2008). An Earth-system perspective of the global nitrogen cycle. *Nature*, *451*(7176), 293–296.
- Hall, E. K., Neuhauser, C., & Cotner, J. B. (2008). Toward a mechanistic understanding of how natural bacterial communities respond to changes in temperature in aquatic ecosystems. *The ISME Journal*, *2*(5), 471–481.
- Hall, E. K., Singer, G. A., Kainz, M. J., & Lennon, J. T. (2010). Evidence for a temperature acclimation mechanism in bacteria: An empirical test of a membrane-mediated trade-off. *Functional Ecology*, *24*(4), 898–908.

- Heiri, O., Lotter, A. F., & Lemcke, G. (2001). Loss on ignition as a method for estimating organic and carbonate content in sediments: Reproducibility and comparability of results. *Journal of Paleolimnology*, 25(1), 101–110.
- Herbert, R. A., & Nedwell, D. B. (1990). Role of environmental factors in regulating nitrate respiration in intertidal sediments. In N. P. Revsbech & J. Sørensen (Eds.), *Denitrification in soil and sediment* (pp. 77–90). New York, NY: Springer.
- Holmes, R. M., Jones, J. B., Fisher, S. G., & Grimm, N. B. (1996). Denitrification in a nitrogen-limited stream ecosystem. *Biogeochemistry*, 33(2), 125–146.
- Holtgrieve, G. W., Schindler, D. E., Hobbs, W. O., Leavitt, P. R., Ward, E. J., Bunting, L., et al. (2011). A coherent signature of anthropogenic nitrogen deposition to remote watersheds of the Northern Hemisphere. *Science*, 334(6062), 1545–1548.
- Hynes, R. K., & Knowles, R. (1978). Inhibition by acetylene of ammonia oxidation in *Nitrosomonas europaea*. *FEMS Microbiology Letters*, 4(6), 319–321.
- Jørgensen, C. J., Jacobsen, O. S., Elberling, B., & Aamand, J. (2009). Microbial oxidation of pyrite coupled to nitrate reduction in anoxic groundwater sediment. *Environmental Science & Technology*, 43(13), 4851–4857.
- Jørgensen, K. S. (1989). Annual pattern of denitrification and nitrate ammonification in estuarine sediment. *Applied and Environmental Microbiology*, 55(7), 1841–1847.
- King, D., & Nedwell, D. B. (1984). Changes in the nitrate-reducing community of an anaerobic saltmarsh sediment in response to seasonal selection by temperature. *Microbiology*, 130(11), 2935–2941.
- King, D., & Nedwell, D. B. (1985). The influence of nitrate concentration upon the end-products of nitrate dissimilation by bacteria in anaerobic salt marsh sediment. *FEMS Microbiology Letters*, 31(1), 23–28.
- King, D., & Nedwell, D. B. (1987). The adaptation of nitrate-reducing bacterial communities in estuarine sediments in response to overlying nitrate load. *FEMS Microbiology Ecology*, 3(1), 15–20.
- Kraft, B., Tegetmeyer, H. E., Sharma, R., Klotz, M. G., Ferdelman, T. G., Hettich, R. L., et al. (2014). The environmental controls that govern the end product of bacterial nitrate respiration. *Science*, 345(6197), 676–679.
- Laverman, A. M., Van Cappellen, P., van Rotterdam-Los, D., Pallud, C., & Abell, J. (2006). Potential rates and pathways of microbial nitrate reduction in coastal sediments. *FEMS Microbiology Ecology*, 58(2), 179–192.
- Lorenzen, J., Larsen, L. H., Kjaer, T., & Revsbech, N. P. (1998). Biosensor determination of the microscale distribution of nitrate, nitrate assimilation, nitrification, and denitrification in a diatom-inhabited freshwater sediment. *Applied and Environmental Microbiology*, 64(9), 3264–3269.
- Luque-Almagro, V. M., Gates, A. J., Moreno-Vivian, C., Ferguson, S. J., Richardson, D. J., & Dolores Roldan, M. (2011). Bacterial nitrate assimilation: Gene distribution and regulation. *Biochemical Society Transactions*, 39, 1838–1843.
- MacFarlane, G., & Herbert, R. (1982). Nitrate dissimilation by *Vibrio* spp. isolated from estuarine sediments. *Microbiology*, 128(10), 2463–2468.
- Mania, D., Heylen, K., van Spanning, R. J. M., & Frostegard, A. (2014). The nitrate-ammonifying and nosZ-carrying bacterium *Bacillus vireti* is a potent source and sink for nitric and nitrous oxide under high nitrate conditions. *Environmental Microbiology*, 16(10), 3196–3210.
- Mazerolle, M. J. (2016). *AICcmodavg: Model selection and multimodel inference based on (Q) AIC (c)*. R package version 2.0–4. Retrieved from <http://CRAN.R-project.org/package=AICcmodavg>
- McClain, M. E., Boyer, E. W., Dent, C. L., Gergel, S. E., Grimm, N. B., Groffman, P. M., et al. (2003). Biogeochemical hot spots and hot moments at the interface of terrestrial and aquatic ecosystems. *Ecosystems*, 6(4), 301–312.
- McCrackin, M. L., & Elser, J. J. (2010). Atmospheric nitrogen deposition influences denitrification and nitrous oxide production in lakes. *Ecology*, 91(2), 528–539.
- McCrackin, M. L., & Elser, J. J. (2012). Denitrification kinetics and denitrifier abundances in sediments of lakes receiving atmospheric nitrogen deposition (Colorado, USA). *Biogeochemistry*, 108(1), 39–54.
- Messer, J. J., & Brezonik, P. L. (1984). Laboratory evaluation of kinetic-parameters for lake sediment denitrification models. *Ecological Modelling*, 21(4), 277–286.
- Myrstener, M., Jonsson, A., & Bergstrom, A. K. (2016). The effects of temperature and resource availability on denitrification and relative N₂O production in boreal lake sediments. *Journal of Environmental Sciences*, 47, 82–90.
- Nizzoli, D., Carraro, E., Nigro, V., & Viaroli, P. (2010). Effect of organic enrichment and thermal regime on denitrification and dissimilatory nitrate reduction to ammonium (DNRA) in hypolimnetic sediments of two lowland lakes. *Water Research*, 44(9), 2715–2724.
- Nogaro, G., & Burgin, A. J. (2014). Influence of bioturbation on denitrification and dissimilatory nitrate reduction to ammonium (DNRA) in freshwater sediments. *Biogeochemistry*, 120(1–3), 279–294.
- Ogilvie, B., Rutter, M., & Nedwell, D. (1997). Selection by temperature of nitrate-reducing bacteria from estuarine sediments: Species composition and competition for nitrate. *FEMS Microbiology Ecology*, 23(1), 11–22.
- Parkin, T. B. (1987). Soil microsites as a source of denitrification variability. *Soil Science Society of America Journal*, 51(5), 1194–1199.
- Pattinson, S. N., Garcia-Ruiz, R., & Whitton, B. A. (1998). Spatial and seasonal variation in denitrification in the Swale-Ouse system, a river continuum. *Science of the Total Environment*, 210(1–6), 289–305.
- Pfenning, K., & McMahon, P. (1997). Effect of nitrate, organic carbon, and temperature on potential denitrification rates in nitrate-rich riverbed sediments. *Journal of Hydrology*, 187(3), 283–295.
- Piña-Ochoa, E., & Alvarez-Cobelas, M. (2006). Denitrification in aquatic environments: A cross-system analysis. *Biogeochemistry*, 81(1), 111–130.
- Pinheiro, J., Bates, DebRoy, D. S., & Sarkar, D. (2007). *Linear and nonlinear mixed effects models*, R package version (p. 57).
- Pinheiro, J. C., & Bates, D. M. (1978). *Mixed-effects models in S and S-plus* (528 pp.). New York, NY: Springer.
- R Development Core Team. (2016). *R: A language and environment for statistical computing*. Retrieved from <http://www.r-project.org>
- Rockstrom, J., Steffen, W., Noone, K., Persson, A., Chapin, F. S., 3rd, Lambin, E. F., et al. (2009). A safe operating space for humanity. *Nature*, 461(7263), 472–475.
- Rysgaard, S., Glud, R. N., Risgaard-Petersen, N., & Dalsgaard, T. (2004). Denitrification and anammox activity in Arctic marine sediments. *Limnology and Oceanography*, 49(5), 1493–1502.
- Schreiber, F., Wunderlin, P., Udert, K. M., & Wells, G. F. (2012). Nitric oxide and nitrous oxide turnover in natural and engineered microbial communities: Biological pathways, chemical reactions, and novel technologies. *Frontiers in Microbiology*, 3, 372.
- Seitzinger, S., Harrison, J. A., Bohlke, J. K., Bouwman, A. F., Lowrance, R., Peterson, B., et al. (2006). Denitrification across landscapes and waterscapes: A synthesis. *Ecological Applications*, 16(6), 2064–2090.
- Seitzinger, S. P. (1988). Denitrification in fresh-water and coastal marine ecosystems: Ecological and geochemical significance. *Limnology and Oceanography*, 33(4), 702–724.
- Sheibley, R. W., Jackman, A. P., Duff, J. H., & Triska, F. J. (2003). Numerical modeling of coupled nitrification–denitrification in sediment perfluorocarbon cores from the hyporheic zone of the Shingobee River, MN. *Advances in Water Resources*, 26(9), 977–987.

- Silvennoinen, H., Liikainen, A., Torssonen, J., Stange, C. F., & Martikainen, P. J. (2008). Denitrification and N₂O effluxes in the Bothnian Bay (northern Baltic Sea) river sediments as affected by temperature under different oxygen concentrations. *Biogeochemistry*, 88(1), 63–72.
- Smith, C., DeLaune, R., & Patrick, W. (1982). Nitrate reduction in *Spartina alterniflora* marsh soil. *Soil Science Society of America Journal*, 46(4), 748–750.
- Smol, J. P. (2012). A planet in flux: How is life on Earth reacting to climate change? *Nature*, 483, S12–S15.
- Stoddard, J. L. (1994). Long-term changes in watershed retention of nitrogen. Its causes and aquatic consequences. In L. A. Baker (Ed.), *Environmental chemistry of lakes and reservoirs* (pp. 223–284). Washington, DC: American Chemical Society.
- Strohm, T. O., Griffin, B., Zumft, W. G., & Schink, B. (2007). Growth yields in bacterial denitrification and nitrate ammonification. *Applied and Environmental Microbiology*, 73(5), 1420–1424.
- Tiedje, J. M. (1988). Ecology of denitrification and dissimilatory nitrate reduction to ammonium. In A. J. B. Zehnder (Ed.), *Biology of anaerobic microorganisms* (pp. 179–244). New York, NY: John Wiley.
- Tiedje, J. M., Sextone, A. J., Myrold, D. D., & Robinson, J. A. (1982). Denitrification: Ecological niches, competition and survival. *Antonie van Leeuwenhoek*, 48(6), 569–583.
- Veraart, A. J., de Klein, J. J. M., & Scheffer, M. (2011). Warming can boost denitrification disproportionately due to altered oxygen dynamics. *PLoS ONE*, 6(3), e18508.
- Vila-Costa, M., Bartrons, M., Catalan, J., & Casamayor, E. O. (2014). Nitrogen-cycling genes in epilithic biofilms of oligotrophic high-altitude lakes (Central Pyrenees, Spain). *Microbial Ecology*, 68(1), 60–69.
- Vila-Costa, M., Pulido, C., Chappuis, E., Calviño, A., Casamayor, E. O., & Gacia, E. (2016). Macrophyte landscape modulates lake ecosystem-level nitrogen losses through tightly coupled plant-microbe interactions. *Limnology and Oceanography*, 61, 78–88.
- Wallenstein, M. D., Myrold, D. D., Firestone, M., & Voytek, M. (2006). Environmental controls on denitrifying communities and denitrification rates: Insights from molecular methods. *Ecological Applications*, 16(6), 2143–2152.
- Warneke, S., Schipper, L. A., Bruesewitz, D. A., McDonald, I., & Cameron, S. (2011). Rates, controls and potential adverse effects of nitrate removal in a denitrification bed. *Ecological Engineering*, 37(3), 511–522.
- Weiss, R. F., & Price, B. A. (1980). Nitrous oxide solubility in water and seawater. *Marine Chemistry*, 8(4), 347–359.
- Westermann, P., & Ahring, B. K. (1987). Dynamics of methane production, sulfate reduction, and denitrification in a permanently water-logged alder swamp. *Applied and Environmental Microbiology*, 53(10), 2554–2559.
- Yoon, S., Cruz-Garcia, C., Sanford, R., Ritalahti, K. M., & Löffler, F. E. (2015). Denitrification versus respiratory ammonification: Environmental controls of two competing dissimilatory NO₃/NO₂ reduction pathways in *Shewanella loihica* strain PV-4. *The ISME Journal*, 9(5), 1093–1104.
- Yoshinari, T., & Knowles, R. (1976). Acetylene inhibition of nitrous-oxide reduction by denitrifying bacteria. *Biochemical and Biophysical Research Communications*, 69(3), 705–710.
- Zhu-Barker, X., Cavazos, A., Ostrom, N., Horwath, W., & Glass, J. (2015). The importance of abiotic reactions for nitrous oxide production. *Biogeochemistry*, 126(3), 251–267.
- Zuur, A., Ieno, Walker, E., Saveliev, N. A., & Smith, G. (2009). *Mixed effects models and extensions in ecology with R* (574 pp.). New York, NY: Springer.

Denitrification temperature dependence in remote, cold and N-poor lake sediments**Carlos Palacin-Lizarbe^{1,2}, Lluís Camarero², and Jordi Catalan¹**

¹ CREAM, Campus UAB, Edifici C, E-08193 Cerdanyola del Vallès, Spain, ² Center for Advanced Studies of Blanes, (CEAB–CSIC), C/ d'accés a la Cala St. Francesc 14, E-17300 Blanes, Girona, Spain, ³ CSIC, E-08193 Cerdanyola del Vallès, Spain

Contents of this file

Table S1. Experimental results.

Table S2. Studies on the temperature dependence of the denitrification rates in aquatic ecosystems

Supporting information. Alternative regression models relating the DEN E_a (kJ mol^{-1}) to the inverse of the nitrate concentration ($[\text{NO}_3^-]^{-1}$) (μM) in the overlying water of the lake sediments

References

Table S2. Studies on the temperature dependence of the denitrification rates in aquatic ecosystems

Study reference	T range	Ecosystem	Habitat	Experimental device	Method	NO ₃ ⁻ <i>in situ</i> (μM)	NO ₃ ⁻ added (μM)	Q ₁₀	E _a (kJ mol ⁻¹)	E _a (eV)	E _a change (%)	Experimental T (°C)	<i>In situ</i> T (°C)
This study (experimental)	Complete	Lake (N-poor)	Sediment	Sediment core	Acetylene inhibition	5.1 (0.8-9.3)	7	3.6 (1.4-9.3)	76 (22-149)	0.79 (0.23-1.54)		10 (5-15)	5
This study (experimental)	Complete	Lake (N-poor)	Sediment	Sediment core	Acetylene inhibition	5.1 (0.8-9.3)	14	3.1 (1.6-5.6)	70 (31-114)	0.73 (0.32-1.18)		10 (5-15)	5
This study (experimental)	Complete	Lake (N-poor)	Sediment	Sediment core	Acetylene inhibition	5.1 (0.8-9.3)	28	2.5 (1.5-3.9)	58 (26-91)	0.6 (0.27-0.94)		10 (5-15)	5
This study (experimental) ^a	Complete	Lake (N-poor)	Sediment	Sediment core	Acetylene inhibition	5.3 (5.1-5.9)	28	2.2 (1.9-2.4)	51 (42-59)	0.53 (0.44-0.61)	51	10 (5-15)	5
This study (experimental) ^a	<i>In situ</i>	Lake (N-poor)	Sediment	Sediment core	Acetylene inhibition	5.3 (5.1-5.9)	28	3.3 (2.8-4.1)	77 (68-92)	0.8 (0.71-0.95)	51	7.5 (5-10)	5
Messer and Brezonik [1984]	Complete	Lake	Sediment	Slurries	Acetylene inhibition	-	12500	2.6	70	0.73		25 (14-36)	25 ^b
Myrsten et al. [2016]	Complete	Lake (N-poor)	Sediment	Slurries	Acetylene inhibition	5	62.7	1.77	47	0.49	13	14.5 (4-25)	4
Myrsten et al. [2016]	<i>In situ</i>	Lake (N-poor)	Sediment	Slurries	Acetylene inhibition	5	62.7	NA	53	0.55	13	7 (4-10)	4
Cavari and Phelps [1977]	Complete	Lake	<i>P. aeruginosa</i> culture	Culture	Nitrate removal	(7-107)	143	1.4	26	0.27	23	22.5 (15-30)	16 (16-30) ^c
Cavari and Phelps [1977]	<i>In situ</i>	Lake	<i>P. aeruginosa</i> culture	Culture	Nitrate removal	(7-107)	143	1.6	32	0.33	23	18.5 (15-22)	16 (16-30) ^c
Veraart et al. [2011]	Complete	Pond	Sediment	Microcosms	¹⁵ N-Tracer	-	119	8.6	179	1.86		18 (11-25)	17.5
Veraart et al. [2011]	Complete	Pond	Sediment	Ditch enclosure	¹⁵ N-Tracer	-	50	11.8	155	1.61		14 (8-20)	14 ^d
Boulétreau et al. [2012]	Complete	Stream	River biofilm	Slurries	Acetylene inhibition	85.7	1714	7 (4.2-9.8)	137 (91-183)	1.42 (0.94-1.9)	-69	16 (1-31)	7.2
Boulétreau et al. [2012]	<i>In situ</i>	Stream	River biofilm	Slurries	Acetylene inhibition	85.7	1714	NA	43	0.45	-69	6.5 (1-12)	7.2
Holmes et al. [1996]	Complete	Stream	Sediment (Parafilm)	Slurries	Acetylene inhibition	5.1	14286	3.5	88	0.91		17 (10-24)	23 (17-29)
Pfennig and McMahon [1997]	Complete	River (eutrophic)	Sediment	Slurries	Acetylene inhibition	-	357	1.8	41	0.43		13 (4-22)	10 (2-18.1)
Silvenoinen et al. [2008]	Complete	River (eutrophic)	Sediment	Sediment core	¹⁵ N-Tracer	-	30	3.1	82	0.85		12.5 (5-20)	17
Pattinson et al. [1998]	Complete	River (eutrophic)	Sediment	Sediment core	Acetylene inhibition	2300	814	2.2	48	0.5	167	12.5 (5-20)	5
Pattinson et al. [1998]	<i>In situ</i>	River (eutrophic)	Sediment	Sediment core	Acetylene inhibition	2300	814	7.1	128	1.33	167	7.5 (5-10)	5

Study reference	T range	Ecosystem	Microbial assemblage	Sample	Method	NO ₃ ⁻ <i>in situ</i> (μM)	NO ₃ ⁻ added (μM)	Q ₁₀	E _a (kJ mol ⁻¹)	E _a (eV)	E _a change (%)	Estimation (°C)	<i>In situ</i> T (°C)
<i>Puttinson et al.</i> [1998]	Complete	River (eutrophic)	Sediment	Sediment core	Acetylene inhibition	2300	1528	2	45	0.47	109	12.5 (5-20)	5
<i>Puttinson et al.</i> [1998]	<i>In situ</i>	River (eutrophic)	Sediment	Sediment core	Acetylene inhibition	2300	1528	4.2	94	0.97	109	7.5 (5-10)	5
<i>Puttinson et al.</i> [1998]	Complete	River (eutrophic)	Sediment	Sediment core	Acetylene inhibition	2300	2242	1.7	33	0.34	115	12.5 (5-20)	5
<i>Puttinson et al.</i> [1998]	<i>In situ</i>	River (eutrophic)	Sediment	Sediment core	Acetylene inhibition	2300	2242	2.9	71	0.74	115	7.5 (5-10)	5
<i>Puttinson et al.</i> [1998]	Complete	River (eutrophic)	Sediment	Sediment core	Acetylene inhibition	2300	2957	1.6	29	0.3	110	12.5 (5-20)	5
<i>Puttinson et al.</i> [1998]	<i>In situ</i>	River (eutrophic)	Sediment	Sediment core	Acetylene inhibition	2300	2957	2.5	61	0.63	110	7.5 (5-10)	5
<i>Shebley et al.</i> [2003]	Complete	Hyporheic zone	Sediment	Sediment core	Nitrate removal	0.14	no add	5.3	101	1.05		15 (8-22)	15 ^d
<i>Jørgensen et al.</i> [2009]	Complete	Groundwater aquifer	Sediment	Slurries	Nitrate removal	-	521	1.9	42	0.44	69	19 (9-29)	9
<i>Jørgensen et al.</i> [2009]	<i>In situ</i>	Groundwater aquifer	Sediment	Slurries	Nitrate removal	-	521	2.7	71	0.74	69	11.5 (9-14)	9
<i>Ambus [1993]</i>	Complete	Riparian (stream-land)	Soil (riparian, stream side)	Slurries	Acetylene inhibition	-	14286	2.9	65	0.67	18	12.5 (2-23)	7.5 (0-15)
<i>Ambus [1993]</i>	<i>In situ</i>	Riparian (stream-land)	Soil (riparian, stream side)	Slurries	Acetylene inhibition	-	14286	NA	77	0.8	18	8.5 (2-15)	7.5 (0-15)
<i>Westermann and Ahrling [1987]</i>	Complete	Swamp	Sediment Alder swamp	Slurries	Acetylene inhibition	12.5	1000	2.9 (2.8-3.0)	73 (70-76)	0.76 (0.73-0.79)	32	13.5 (2-25)	7.5 (0-15)
<i>Westermann and Ahrling [1987]</i>	<i>In situ</i>	Swamp	Sediment Alder swamp	Slurries	Acetylene inhibition	12.5	1000	NA	96	1	32	6 (2-10)	7.5 (0-15)
<i>King and Nedwell [1984]</i>	Complete	Wetland (Salt-marsh)	Culture dominated by <i>Pseudomonas</i> spp.	Culture	Nitrate removal	-	1000	NA	98	1.02		8 (3-13)	15 (0-20) ^e
<i>King and Nedwell [1984]</i>	Complete	Wetland (Salt-marsh)	Culture dominated by <i>Vibrio</i> spp.	Culture	Nitrate removal	-	1000	NA	60	0.62		18.5 (6-31)	15 (0-20) ^f
<i>Brin et al.</i> [2017]	Complete	Estuary (June)	Sediment	Slurries	Acetylene inhibition	1.1 (0.6-2.1) ^h	100 ⁱ	NA	36 ^k	0.37	25	17 (3-31)	16
<i>Brin et al.</i> [2017]	<i>In situ</i>	Estuary (June)	Sediment	Slurries	Acetylene inhibition	1.1 (0.6-2.1) ^h	100 ⁱ	NA	45	0.46	25	16 (12-20)	16
<i>Brin et al.</i> [2017]	Complete	Estuary (August)	Sediment	Slurries	Acetylene inhibition	1.1 (0.6-2.1) ^h	100 ⁱ	NA	46 ^k	0.48	78	15 (3-27)	22
<i>Brin et al.</i> [2017]	<i>In situ</i>	Estuary (August)	Sediment	Slurries	Acetylene inhibition	1.1 (0.6-2.1) ^h	100 ⁱ	NA	82	0.85	78	21.5 (18-25)	22
<i>Brin et al.</i> [2017]	Complete	Estuary (January)	Sediment	Slurries	Acetylene inhibition	1.1	100 ⁱ	NA	53 ^k	0.55	56	15	6

Study reference	T range	Ecosystem	Microbial assemblage	Sample	Method	NO ₃ ⁻ in situ (μM)	(0.6-2.1) ^h	NO ₃ ⁻ added (μM)	Q ₁₀	E _a (kJ mol ⁻¹)	E _a (eV)	E _a change (%)	Estimation T (°C)	In situ T (°C)
<i>Brin et al. [2017]</i>	<i>In situ</i>	Estuary (January)	Sediment	Slurries	Acetylene inhibition	1.1 (0.6-2.1) ^h		100 ⁱ	NA	83	0.86	56	6.5 (3-10)	6
<i>Brin et al. [2017]</i>	Complete	Marine, temperate (January)	Sediment (continental shelf)	Slurries	Acetylene inhibition	1.5 (1.0-4.0) ^h		100 ⁱ	NA	60 ^k	0.63	9	19 (3-35)	6
<i>Brin et al. [2017]</i>	<i>In situ</i>	Marine, temperate (January)	Sediment (continental shelf)	Slurries	Acetylene inhibition	1.5 (1.0-4.0) ^h		100 ⁱ	NA	66	0.69	9	6.5 (3-10)	6
<i>Brin et al. [2017]</i>	Complete	Marine, temperate (June)	Sediment (continental shelf)	Slurries	Acetylene inhibition	1.5 (1.0-4.0) ^h		100 ⁱ	NA	44 ^k	0.45	70	15 (3-27)	11
<i>Brin et al. [2017]</i>	<i>In situ</i>	Marine, temperate (June)	Sediment (continental shelf)	Slurries	Acetylene inhibition	1.5 (1.0-4.0) ^h		100 ⁱ	NA	74	0.77	70	11 (8-14)	11
<i>Brin et al. [2017]</i>	Complete	Marine, temperate (July)	Sediment (continental shelf)	Slurries	Acetylene inhibition	1.5 (1.0-4.0) ^h		100 ⁱ	NA	51 ^k	0.52	-65	15 (3-27)	16
<i>Brin et al. [2017]</i>	<i>In situ</i>	Marine, temperate (July)	Sediment (continental shelf)	Slurries	Acetylene inhibition	1.5 (1.0-4.0) ^h		100 ⁱ	NA	18	0.18	-65	16 (12-20)	16
<i>Brin et al. [2017]</i>	Complete	Marine, temperate (September)	Sediment (continental shelf)	Slurries	Acetylene inhibition	1.5 (1.0-4.0) ^h		100 ⁱ	NA	39 ^k	0.4	-17	13.5 (3-24)	17
<i>Brin et al. [2017]</i>	<i>In situ</i>	Marine, temperate (September)	Sediment (continental shelf)	Slurries	Acetylene inhibition	1.5 (1.0-4.0) ^h		100 ⁱ	NA	32	0.33	-17	17.5 (14-21)	17
<i>Brin et al. [2017]</i>	Complete	Marine, temperate (March)	Sediment (continental shelf)	Slurries	Acetylene inhibition	1.5 (1.0-4.0) ^h		100 ⁱ	NA	44 ^k	0.45	6	13.5 (3-24)	7
<i>Brin et al. [2017]</i>	<i>In situ</i>	Marine, temperate (March)	Sediment (continental shelf)	Slurries	Acetylene inhibition	1.5 (1.0-4.0) ^h		100 ⁱ	NA	46	0.48	6	6.5 (3-10)	7
<i>Brin et al. [2017]</i>	Complete	Marine, temperate (March)	Sediment (microcosm at 4°C, 2 weeks)	Slurries	Acetylene inhibition	-		100 ⁱ	NA	41 ^k	0.43		12.5 (3-22)	4 ⁱ
<i>Brin et al. [2017]</i>	Complete	Marine, temperate (March)	Sediment (microcosm at 4°C, 12 weeks)	Slurries	Acetylene inhibition	-		100 ⁱ	NA	40 ^k	0.42		12.5 (3-22)	4 ⁱ
<i>Brin et al. [2017]</i>	Complete	Marine, temperate (March)	Sediment (microcosm at 4°C + C, 12 weeks)	Slurries	Acetylene inhibition	-		100 ⁱ	NA	37 ^k	0.38		12.5 (3-22)	4 ⁱ
<i>Brin et al. [2017]</i>	Complete	Marine, temperate (March)	Sediment (microcosm at 17°C, 12 weeks)	Slurries	Acetylene inhibition	-		100 ⁱ	NA	44 ^k	0.46		12.5 (3-22)	17 ⁱ
<i>Brin et al. [2017]</i>	Complete	Marine, temperate (March)	Sediment (microcosm at 17°C + C, 12 weeks)	Slurries	Acetylene inhibition	-		100 ⁱ	NA	46 ^k	0.48		12.5 (3-22)	17 ⁱ
<i>Canion et al. [2014]</i>	Complete	Marine, temperate (March)	Sediment (Near shore, permeable)	Slurries	¹⁵ N-Tracer	53.9		100	2.5	74	0.77	41	13 (0-26)	5.6
<i>Canion et al. [2014]</i>	<i>In situ</i>	Marine, temperate (March)	Sediment (Near shore, permeable)	Slurries	¹⁵ N-Tracer	53.9		100	NA	104	1.08	41	5 (0-10)	5.6
<i>Canion et al. [2014]</i>	Complete	Marine, temperate (June)	Sediment (Near shore, permeable)	Slurries	¹⁵ N-Tracer	0.8		100	2	54	0.56	-26	13 (0-26)	17.9

Canion et al. [2014]	<i>In situ</i>	Marine, temperate (June)	Sediment (Near shore, permeable)	Slurries	¹⁵ N-Tracer	0.8	100	NA	40	0.41	-26	18 (17-19)	17.9
Study reference	T range	Ecosystem	Microbial assemblage	Sample	Method	NO₃⁻ <i>in situ</i> (μM)	NO₃⁻ added (μM)	Q₁₀	E_a (kJ mol⁻¹)	E_a (eV)	E_a change (%)	Estimationl T (°C)	<i>In situ</i> T (°C)
Kraft et al. [2014]	Complete	Marine, temperate	Bact. com. isolation (sandy tidal flat)	Culture	¹⁵ N-Tracer	-	1000	1.4	22	0.23	18	20 (10-30)	11 (2-19)
Kraft et al. [2014]	<i>In situ</i>	Marine, temperate	Bact. com. isolation (sandy tidal flat)	Culture	¹⁵ N-Tracer	-	1000	NA	26	0.27	18	12.5 (10-15)	11 (2-19)
Rysgaard et al. [2004]	Complete	Marine, polar	Sediment (polar 40 m water depth)	Slurries	¹⁵ N-Tracer	3.8	50	NA	61	0.63	110	11.5 (-2.25)	0 (-0.5-4)
Rysgaard et al. [2004]	<i>In situ</i>	Marine, polar	Sediment (polar 40 m water depth)	Slurries	¹⁵ N-Tracer	3.8	50	NA	128	1.33	110	-0.8 (-2.0-5)	0 (-0.5-4)
Canion et al. [2014]	Complete	Marine, polar	Sediment (Near shore, permeable)	Slurries	¹⁵ N-Tracer	0.5	100	2.3	61	0.63	34	10 (-1-21)	6.8
Canion et al. [2014]	<i>In situ</i>	Marine, polar	Sediment (Near shore, permeable)	Slurries	¹⁵ N-Tracer	0.5	100	NA	82	0.85	34	7.5 (6-9)	6.8
Canion et al. [2014]	Complete	Marine, subtropical gulf	Sediment (Near shore, permeable)	Slurries	¹⁵ N-Tracer	1.7	100	3.8	100	1.04	30	17.5 (-1-36)	29.9
Canion et al. [2014]	<i>In situ</i>	Marine, subtropical gulf	Sediment (Near shore, permeable)	Slurries	¹⁵ N-Tracer	1.7	100	NA	130	1.35	30	29.5 (27-32)	29.9
Canion et al. [2014]	Complete	Marine, subtropical bay	Sediment (Near shore, permeable)	Slurries	¹⁵ N-Tracer	2.2	100	5	121	1.25	47	19 (3-35)	31.8
Canion et al. [2014]	<i>In situ</i>	Marine, subtropical bay	Sediment (Near shore, permeable)	Slurries	¹⁵ N-Tracer	2.2	100	NA	191	1.98	47	32 (30-34)	31.8
Canion et al. [2014]	Complete	Artificial	DEN bed (sawdust (Pinus radiata))	DEN bed	Nitrate removal	-	10714	2.4	63	0.65		19 (14-24)	19 ^d
Warneke et al. [2011]	Complete	Artificial	DEN bed (wood chips and sawdust of <i>P. radiata</i>)	DEN bed	Nitrate removal	-	8929	2.1	53	0.54		19.5 (15-24)	19.5 ^d
Cameron and Schipper [2010]	Complete	Artificial	DEN bed (woodchips of <i>Pinus radiata</i>)	DEN bed	Nitrate removal	-	10714	1.9	45	0.47		19 (14-24)	19 ^d
Cameron and Schipper [2010]	Complete	Artificial	DEN bed (woodchips of <i>Eucalyptus</i>)	DEN bed	Nitrate removal	-	10714	2	50	0.52		19 (14-24)	19 ^d
Cameron and Schipper [2010]	Complete	Artificial	DEN bed (maize cobs)	DEN bed	Nitrate removal	-	10714	1.3	16	0.17		19 (14-24)	19 ^d
Cameron and Schipper [2010]	Complete	Artificial	DEN bed (wheat straw)	DEN bed	Nitrate removal	-	10714	1.2	14	0.15		19 (14-24)	19 ^d
Cameron and Schipper [2010]	Complete	Artificial	DEN bed (green waste)	DEN bed	Nitrate removal	-	10714	1.2	11	0.12		19 (14-24)	19 ^d

Notes (Table S2):

Numerical values in parenthesis indicate the range, minimum and maximum values.

Temperature (T) range: “complete” refers to the full experimental temperature range in the paper; “*in situ*” refers to a shorter range closer to the *in situ* temperature.

Q_{10} calculation: $Q_{10} = \frac{r_{dj}}{r_{di}} \left(\frac{10}{T_j - T_i} \right)$, where r_d is the denitrification rate and T the absolute temperature.

E_a (kJ mol⁻¹) calculation from: $\frac{r_{dj}}{r_{di}} = \exp\left[\frac{E_a}{R} \left(\frac{1}{T_i} - \frac{1}{T_j}\right)\right]$. Where R is the gas constant (8.314 J K⁻¹ mol⁻¹), T the absolute temperature and r_d the denitrification rate.

E_a (eV) from E_a (kJ mol⁻¹) data: E_a (eV) = 0.01037 * E_a (kJ mol⁻¹).

E_a change (%) = $\left(\frac{E_a \text{ in situ } T \text{ range} - E_a \text{ complete } T \text{ range}}{E_a \text{ complete } T \text{ range}} \right) * 100$.

^a Lake Redon, field campaign 3rd September 2013 (see Table S1).

^b Annual mean temperature (air) (<http://www.worldclim.org>).

^c Lake Kinneret water temperature: hypolimnion 16°C (constant), epilimnion 16-30°C [*Gal et al.*, 2003].

^d Experimental mean temperature.

^e Culture isolated at 10°C.

^f Culture isolated at 25°C.

^h Nitrate *in situ* is mean porewater nitrate (μM) data from *Brin et al.* [2014].

ⁱ Nitrate added: 100 nmol NO₃⁻N mL sediment⁻¹.

^j Sediments collected in the field at 7°C.

^k Mean E_a values of 45, 48 and 42 kJ mol⁻¹ for estuary, continental shelf and microcosms samples, respectively [*Brin et al.*, 2017], used in Fig. 3 plot.

Regression models relating the DEN E_a (kJ mol^{-1}) to the inverse of the nitrate concentration ($[\text{NO}_3^-]^{-1}$) (μM):

In this section, we provide a brief introduction of the linear mixed-effects models and detailed information about the performed alternative regression models relating the DEN E_a (kJ mol^{-1}) to the inverse of the nitrate concentration ($[\text{NO}_3^-]^{-1}$) (μM). The aim is to clarify and complement the information in the main manuscript (section 3.1 and Table 2).

Many common statistical models can be expressed as linear models that incorporate both fixed effects, which are parameters associated with an entire population or with certain repeatable levels of experimental factors, and random effects, which are associated with individual experimental units drawn at random from a population. A model with both fixed effects and random effects is called a mixed-effects model [Pinheiro and Bates, 1978]. All the performed regression models in this study have the same fixed part with the inverse of the nitrate concentration ($[\text{NO}_3^-]^{-1}$) (μM) in the overlying water of the lake sediments (Table 2).

Mixed-effects models are primarily used to describe relationships between a response variable and some covariates in data that are grouped according to one or more classification factors. Examples of such grouped data include longitudinal data, repeated measures data, multilevel data, and block designs. By associating common random effects to observations sharing the same level of a classification factor, mixed-effects models flexibly represent the covariance structure induced by the grouping of the data [Pinheiro and Bates, 1978].

The model 0 and 1 are simple linear regression models, without any random effects, they differ in the function used to fit the model. In model 0 is used the *lm* function from the R package *stats*, the design was inspired by the *S* function of the same name described in Chambers [1992]. Model 1 uses the *gls* function, from the R package *nlme* [Pinheiro et al., 2007], which fits linear models using generalized least squares. Both models are identical, have the same coefficient and intercept. We develop the model 1 to compare it with model 2, which incorporate the temporal autocorrelation intrinsic to sequential experimental additions, i.e., if it is the first, second or third addition in the core sample. Model 2 uses the same *gls* function to fit the model but incorporates an auto-regressive model of order 1 (corAR1) accounting for auto-correlation (see further details in Zuur et al. [2009] section 6.1). We conclude that temporal-autocorrelation was not interfering with the results as model 2 does not improve model 1. The two models explain the same fixed and global variance, and an ANOVA comparing the models showed that the more complex model 2 did not improve significantly ($p=0.56$) model 1. Models 3-10 are all mixed-effects models with the same fixed part with the inverse of the nitrate concentration and different composition of the random part. Models 3, 4 and 5 account for the sensor particular performance (#1, #2, #3, #4 or #5, see Table S1). Model 4 just modify the slope, not the intercept. Models 5 (nested in the sensor), 6 and 7 consider the core (sample) effect. Model 8 takes into account the three nitrate enrichment levels, and model 9 the addition order (first, second and third). Finally, model 10 takes into account the lake effect. Models with more than 1 factor crossed in the random part (not shown) were built with the *lmer* function within the *lme4* R package [Bates et al., 2015], these models did not improve model 1, 3 or 4 ($p(>0.05)$ in ANOVAs and have higher AICc values). As we mention in the manuscript (Results 3.1), the models accounting for the sensor effects (model 3 and 4 in Table 2) showed the lower AICc values, explained more variance and were the only ones that improved the initial model 1, which did not have the random part (ANOVA p-values of 0.047 and

0.008 for model 3 and 4, respectively). We selected model 4 as the best estimation because it is simpler than 3.

References:

- Ambus, P. (1993), Control of denitrification enzyme-activity in a streamside soil, *FEMS Microbiol. Ecol.*, 102(3-4), 225-234.
- Bates, D., M. Mächler, B. Bolker, and S. Walker (2015), Fitting linear mixed-effects models using lme4, *J. Stat. Softw.*, 67(1), 1-48.
- Boulêtreau, S., E. Salvo, E. Lyautey, S. Mastrorillo, and F. Garabetian (2012), Temperature dependence of denitrification in phototrophic river biofilms, *Sci. Total Environ.*, 416, 323-328.
- Brin, L. D., A. E. Giblin, and J. J. Rich (2014), Environmental controls of anammox and denitrification in southern New England estuarine and shelf sediments, *Limnol. Oceanogr.*, 59(3), 851-860.
- Brin, L. D., A. E. Giblin, and J. J. Rich (2017), Similar temperature responses suggest future climate warming will not alter partitioning between denitrification and anammox in temperate marine sediments, *Glob. Chang. Biol.*, 23, 331-340.
- Cameron, S. G., and L. A. Schipper (2010), Nitrate removal and hydraulic performance of organic carbon for use in denitrification beds, *Ecol. Eng.*, 36(11), 1588-1595.
- Canion, A., J. Kostka, T. Gihring, M. Huettel, J. Van Beusekom, H. Gao, G. Lavik, and M. Kuypers (2014), Temperature response of denitrification and anammox reveals the adaptation of microbial communities to in situ temperatures in permeable marine sediments that span 50° in latitude, *Biogeosciences*, 11(2), 309-320.
- Cavari, B. Z., and G. Phelps (1977), Denitrification in lake Kinneret in presence of oxygen, *Freshwater Biol.*, 7(4), 385-391.
- Chambers, J. M. (1992), *Linear models*, Wadsworth & Brooks/Cole, Pacific Grove, California.
- Gal, G., J. Imberger, T. Zohary, J. Antenucci, A. Anis, and T. Rosenberg (2003), Simulating the thermal dynamics of Lake Kinneret, *Ecol. Model.*, 162(1), 69-86.
- Holmes, R. M., J. B. Jones, S. G. Fisher, and N. B. Grimm (1996), Denitrification in a nitrogen-limited stream ecosystem, *Biogeochemistry*, 33(2), 125-146.
- Jørgensen, C. J., O. S. Jacobsen, B. Elberling, and J. Aamand (2009), Microbial Oxidation of Pyrite Coupled to Nitrate Reduction in Anoxic Groundwater Sediment, *Environ. Sci. Technol.*, 43(13), 4851-4857.
- King, D., and D. B. Nedwell (1984), Changes in the nitrate-reducing community of an anaerobic saltmarsh sediment in response to seasonal selection by temperature, *Microbiology*, 130(11), 2935-2941.
- Kraft, B., H. E. Tegetmeyer, R. Sharma, M. G. Klotz, T. G. Ferdelman, R. L. Hettich, J. S. Geelhoed, and M. Strous (2014), The environmental controls that govern the end product of bacterial nitrate respiration, *Science*, 345(6197), 676-679.
- Messer, J. J., and P. L. Brezonik (1984), Laboratory evaluation of kinetic-parameters for lake sediment denitrification models, *Ecol. Model.*, 21(4), 277-286.
- Myrstener, M., A. Jonsson, and A. K. Bergstrom (2016), The effects of temperature and resource availability on denitrification and relative N₂O production in boreal lake sediments, *J. Environ. Sci.*, 47, 82-90.
- Pattinson, S. N., R. Garcia-Ruiz, and B. A. Whitton (1998), Spatial and seasonal variation in denitrification in the Swale-Ouse system, a river continuum, *Sci. Total Environ.*, 210(1-6), 289-305.

- Pfenning, K., and P. McMahon (1997), Effect of nitrate, organic carbon, and temperature on potential denitrification rates in nitrate-rich riverbed sediments, *J. Hydrol.*, 187(3), 283-295.
- Pinheiro, J., D. Bates, S. DebRoy, and D. Sarkar (2007), Linear and nonlinear mixed effects models, in *R package version*, edited, p. 57.
- Pinheiro, J. C., and D. M. Bates (1978), *Mixed-Effects Models in S and S-plus*, 528 pp., Springer, New York, NY.
- Rysgaard, S., R. N. Glud, N. Risgaard-Petersen, and T. Dalsgaard (2004), Denitrification and anammox activity in Arctic marine sediments, *Limnol. Oceanogr.*, 49(5), 1493-1502.
- Sheibley, R. W., A. P. Jackman, J. H. Duff, and F. J. Triska (2003), Numerical modeling of coupled nitrification–denitrification in sediment perfusion cores from the hyporheic zone of the Shingobee River USA, *Adv. Water. Resour.*, 26(9), 977-987.
- Silvennoinen, H., A. Liikanen, J. Torssonen, C. F. Stange, and P. J. Martikainen (2008), Denitrification and N₂O effluxes in the Bothnian Bay (northern Baltic Sea) river sediments as affected by temperature under different oxygen concentrations, *Biogeochemistry*, 88(1), 63-72.
- Veraart, A. J., W. J. de Bruijne, J. J. de Klein, E. T. Peeters, and M. Scheffer (2011), Effects of aquatic vegetation type on denitrification, *Biogeochemistry*, 104(1-3), 267-274.
- Warneke, S., L. A. Schipper, D. A. Bruesewitz, I. McDonald, and S. Cameron (2011), Rates, controls and potential adverse effects of nitrate removal in a denitrification bed, *Ecol. Eng.*, 37(3), 511-522.
- Westermann, P., and B. K. Ahring (1987), Dynamics of methane production, sulfate reduction, and denitrification in a permanently waterlogged alder swamp, *Appl. Environ. Microbiol.*, 53(10), 2554-2559.
- Zuur, A., E. Ieno, N. Walker, A. Saveliev, and G. Smith (2009), *Mixed effects models and extensions in ecology with R.*, 574 pp., Springer-Verlag New York, New York, NY.

